2024

Green strategies to extract and formulate natural-based pigments: from red to blue hues

Ana Nunes Nunes

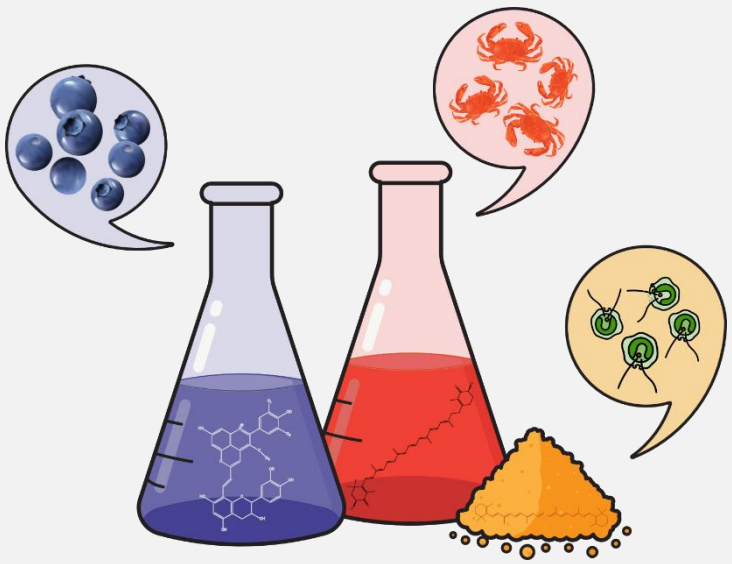

Thesis presented to obtain the **Ph.D. degree in**

Sustainable Chemistry

Oeiras, March, 2024

INSTITUTO DE TECNOLOGIA QUÍMICA E BIOLÓGICA ANTÓNIO XAVIER | UNIVERSIDADE NOVA DE LISBOA

Green strategies to extract and formulate natural-based pigments: from red to blue hues

Ana Nunes Nunes

Thesis presented to obtain the Ph.D. degree in

Sustainable Chemistry

Instituto de Tecnologia Química e Biológica António Xavier | Universidade Nova de Lisboa

Oeiras, March 2024

Cover Image

Designed by Ana Nunes Nunes

First Edition, March 2024

Supervisor Ana Alexandra Figueiredo Matias, Ph.D.
Invited Researcher
Food & Health Division, iBET - Instituto de Biologia Experimental e Tecnológica, Portugal

Co-supervisors Maria do Rosário Beja Gonzaga Bronze, Ph.D.
Associate Professor, Faculdade de Farmácia, Universidade de Lisboa
Senior Scientific Advisor
Head of Natural Bioactives and Nutraceuticals Characterization Lab, Food & Health Division, iBET - Instituto de Biologia Experimental e Tecnológica, Portugal

Joana Alexandra da Silva Oliveira Pinto da Silva, Ph.D.
Researcher Associate at REQUIMTE, Laboratório Associado para a Química Verde, Departamento de Química e Bioquímica, Faculdade de Ciências, Universidade do Porto, Portugal

Acknowledgments

To my supervisors, Doctor Ana Matias, Doctor Rosário Bronze, and Doctor Joana Oliveira, I want to express my profound gratitude for all the support and scientific guidance throughout my Ph.D. journey.

Ana, first and foremost, I want to express my heartfelt gratitude for encouraging and motivating me to embark on my Ph.D. journey. Furthermore, I deeply appreciate the support and resources you provided, enabling the successful development of this study. Your attention, guidance, and friendship throughout the process have been truly valuable.

Rosário, I am sincerely grateful for your guidance, support, and input in analytical chemistry. Your expertise and insights have significantly enhanced the quality of this work, and your consistent encouragement has been a constant source of inspiration. Furthermore, I am deeply appreciative for providing me with the necessary conditions that enable the successful development of this work.

Joana, I am deeply thankful for your support and for creating the necessary conditions during my stay in the Food Polyphenol Lab of REQUIMTE at FCUP, which played a crucial role in the development of this work. Your expertise and insights into anthocyanins and their derivatives have significantly enriched the quality of this research. Additionally, your consistent availability, encouraging words, and constant appreciation of my dedication have been truly appreciated.

To the members of my thesis committee, Doctor Alexandre Paiva and Doctor Ana Faria, I want to express my gratitude for the generous investment of your time and for the valuable insights, comments, and suggestions you provided that have enabled me to improve this work.

To Doctor Luis Gouveia, I want to express my gratitude for the valuable support and guidance in the statistical aspects of this research. Your enthusiasm, positivity, and expertise in the field have been fundamental in shaping the quantitative aspects of this work.

To all my current and previous colleagues and friends I have had the privilege of collaborating with throughout these years at NBPT, NBNC, and NBNF Lab of the Food & Health Division at iBET, I want to express my profound gratitude for the incredible journey we have shared over these years of research. The collaboration and team spirit I have experienced in this group have been valuable to the success of this Ph.D. project.

Cátia, a special thanks for your constant support and companionship, which began during my master and continued despite the distance. Your presence has been a steady source of strength and encouragement.

Agostinho and Liliana, my “supercritical” colleagues, a particular thanks for all the brainstorming sessions and valuable suggestions. Your dedication and assistance, even after leaving the iBET, were fundamental to the success of this research.

Ana Roda, sincere gratitude for being my right hand during the supercritical astaxanthin assays. Additionally, you have been a colleague and friend who consistently supported me, even after moving to FCT.

Viktoriya and Miguel, my “CPC” colleagues, a special thanks for your appreciated support and friendship. Together, we embarked on a learning journey to master this technique. I want to extend special recognition to Viktoriya, who was my right hand during this specific subchapter of CPC.

António Ferreira, Ana Bárbara, Beatriz, Marta, Leonor, and Rita a sincere thanks for your valuable support in the chemical characterization work, particularly in the HPLC analysis.

To the remaining team members, Ana Bernardo, Daniela, João, Maha, Maria João, Martim, Melanie, Naiara, Sara, Sofia, Teresa, and to all those who have crossed my path and contributed in some way, thank you for everything!

To my colleagues at the Food Polyphenols Lab of REQUIMTE at FCUP, with a special mention to Rita Pereira and Alexandra Borges, I want to express my gratitude for making me feel at home and for generously sharing your knowledge with me during my stay in Porto.

My gratitude to the funding entities that made this work possible Fundação para a Ciência e a Tecnologia/Ministério da Educação e Ciência (through SFRH/BD/144592/2019 Ph.D. Research Studentship; MultiBiorefinery (POCI-01-0145-FEDER-016403); the iNOVA4Health (UIDB/04462/2020 and UIDP/04462/2020), the Associate Laboratory LS4FUTURE (LA/P/0087/2020) and Associated Laboratory for Sustainable Chemistry, Clean Processes, and Technologies LAQV (UIDB/50 0 06/2020 and UIDP/50 0 06/2020) programmes); European Union (through D-Factory (613870) project) and Agência Nacional de Inovação (through INTERFACE programme).

To my family, particularly my grandmother, dad, mother, and sisters, as well as my lifelong friends, I want to express my heartfelt gratitude for always being there, providing words of encouragement, and celebrating every step with me, even when you did not fully understand what it was all about.

CONTENTS

Green strategies to extract and formulate natural-based pigments: from red to blue hues

ABSTRACT

Color plays a crucial role in shaping consumer food preferences, acceptability, and subsequent, selection. Despite the growing popularity of natural pigments in the food industry, several challenges hinder their widespread acceptance, namely regulatory restrictions, cost, and technical issues. These technical issues represent difficulties for industries aiming to replace synthetic colorants with natural options while meeting consumer demands.

Within this context, the main goal of this Ph.D. thesis was to develop suitable strategies to address the technological demands and challenges associated with the use of natural colorants in the food industry. The work aimed to efficiently utilize agricultural and food processing waste, aligning with specific goals related to (1) overcoming the scarcity of natural blue colorants, (2) addressing the limited availability of natural astaxanthin, and (3) managing the conditioned solubility of carotenoids. To achieve these objectives, a range of technologies were employed: centrifugal partition chromatography (CPC) and compressed fluid-based extraction were used for the preparative-scale downstream purification of bluish portisins derived from blueberry surplus anthocyanins; microwave (MW) pretreatment and supercritical fluid extraction (SFE) were applied for the recovery of astaxanthin from crab shell residues; and emulsification and spray drying were used for the formulation of carotenoids recovered from microalgae biomass, namely *Dunaliella salina*.

Depending on the process, an attempt was made to maximize the process yield and efficiency, by studying the impact of different process parameters on the pigment recovery/encapsulation:

(i) CPC downstream isolation process was applied for the recovery of bluish pigments from blueberry surplus extract after portisins hemi-synthesis, by selecting the two-phase solvent system consisted of tert-butyl-methyl ether, n-butanol, acetonitrile, and water (volume ratio 2:2:1:5) acidified with 0.1 vol.% of HCl, and varying conditions of sample load (100-500 mg/100 mL of column volume), mobile phase flow rate (10-20 mL/min), and rotation speed (1000-1600 rpm);

(ii) Portisins were isolated from blueberry surplus extract after portisins hemi-synthesis using compressed fluid-based extraction, and the operating conditions studied included pressure (100-500 bar), temperature (40-60°C), and ethanol content in the compressed fluid mixture (20-50 wt.%);

(iii) ASX was extracted from crab shell wastes, integrating MW pretreatment and SFE. MW pretreatment operating conditions applied included different solvent systems (hydroalcoholic mixtures with 0-50 vol.% of water) at different temperatures (40-140°C). SFE operating conditions explored included pressure (200-500 bar), temperature (40-60°C), ethanol content in the supercritical CO_2 (8-13 wt.%), and equilibration time (0-30 min);

(iv) And finally, carotenoids from *Dunaliella salina* were encapsulated using spray drying of emulsions, by varying conditions of oil phase concentration in the emulsion (3-37 wt.%), stirring speed (6500-21500 rpm), and inlet air temperature (110-220°C).

Results presented throughout the chapters of this thesis have shown that each strategy studied allowed a successful recovery/formulation of the target pigments, enabling the attainment of different products with interesting color properties, namely (i) and (ii) bluish portisins-rich extracts;

(iii) reddish astaxanthin-rich extracts; and (iv) orange hydrosoluble carotenoid-rich powder.

Results also showed that the optimal CPC conditions enabled a 5-fold increase purification of portisins. In contrast, the two-step compressed fluid extraction process led to a 1.5-fold increase in portisin content. In general, the proposed protocols provide alternative approaches for producing bluish portisin pigments, contributing to the sustainable utilization of blueberry residues towards a circular economy.

Additionally, the results demonstrated that under the optimized conditions, the maximum extractable astaxanthin was recovered within 30 min of extraction, and the astaxanthin concentration in the extract was improved compared to other extraction strategies. As a result, the proposed protocol for recovering astaxanthin from an alternative source was demonstrated to be an effective and suitable strategy for enhancing selective astaxanthin extraction, contributing to the sustainable utilization of marine crustacean waste streams.

Finally, the optimum conditions for encapsulating carotenoids led to an encapsulation yield of 39 wt.% and an efficiency of 74 wt.%. Furthermore, the resulting particles present interesting properties for use as food ingredients, such as their intense orange color and good water dispersibility. Consequently, encapsulation based on natural polysaccharides by spray drying emulsion can be considered a viable strategy for developing hydrosoluble forms of liposoluble pigment to enhance their dispersibility in aqueous-based products.

Overall, this research suggests that the strategies developed during this Ph.D. thesis for addressing the identified challenges may offer alternative methods

for natural pigments extraction, downstream purification, and encapsulation, emphasizing sustainable resource utilization, thus aligning with circular economy principles, and providing more environmentally friendly solutions for the food industry.

RESUMO

A cor tem um papel determinante nas escolhas do consumidor relativamente à aceitação e seleção dos alimentos. Apesar da crescente popularidade dos pigmentos naturais na indústria alimentar, existem vários desafios que impedem a sua aceitação generalizada, nomeadamente restrições regulamentares, custos e questões técnicas. As questões técnicas relacionam-se com as dificuldades que a indústria alimentar enfrenta quando pretende substituir corantes sintéticos por opções naturais, para responder às exigências dos consumidores.

Dentro deste contexto, o principal objetivo desta tese de doutoramento consistiu em desenvolver estratégias adequadas para ultrapassar os desafios tecnológicos associados à utilização de corantes naturais na indústria alimentar. O trabalho visou a valorização de resíduos agrícolas e de processamento de alimentos, alinhando-se com objetivos específicos relacionados com (1) contribuir com soluções naturais alternativas aos corantes azuis sintéticos, (2) a procura de novas fontes naturais do pigmento astaxantina e (3) aumentar a solubilidade aquosa de carotenoides. Para alcançar esses objetivos, foram utilizadas várias técnicas: cromatografia de partição centrífuga (CPC) e fluidos comprimidos para a purificação em larga escala de portisinas derivadas de antocianinas presentes nos excedentes de produção de mirtilos; pré-tratamento por micro-ondas (MW) combinado com a extração com fluidos supercríticos (SFE) para a recuperação da astaxantina a partir de resíduos de processamento de sapateira; e emulsificação combinado com *spray drying* para a formulação de carotenoides recuperados a partir de microalgas, nomeadamente *Dunaliella salina*, para aumento da sua solubilidade em matrizes aquosas.

Dependendo do processo, teve-se como objetivo maximizar/intensificar o rendimento e a eficiência, estudando o impacto de diferentes parâmetros do processo na recuperação/encapsulação do pigmento:

(i) O processo de separação de CPC foi aplicado para a recuperação de pigmentos azuis a partir de extrato de excedente de mirtilo após a hemi-síntese de portisinas, selecionando o sistema de solvente bifásico que inclui o éter metil terc-butílico, n-butanol, acetonitrilo e água (razão de volume 2:2:1:5) acidificado com 0.1% de HCl, e variando as seguintes condições: quantidade de amostra injetada (100-500 mg/100 mL do volume da coluna), fluxo da fase móvel (10-20 mL/min) e velocidade de rotação (1000-1600 rpm);

(ii) As portisinas foram isoladas do extrato de excedente de mirtilo após hemi-síntese utilizando extração com fluidos comprimidos, e as condições operacionais estudadas incluíram pressão (100-500 bar), temperatura (40-60°C) e teor de etanol na mistura de fluidos comprimidos (20-50% m/m);

(iii) A astaxantina foi extraída de resíduos de processamento da sapateira, integrando o pré-tratamento por MW e SFE. As condições operacionais do pré-tratamento por MW incluíram diferentes sistemas de solventes (misturas hidroalcoólicas com 0-50% de água) a diferentes temperaturas (40-140 °C). As condições operacionais de SFE exploradas incluíram pressão (200-500 bar), temperatura (40-60°C), teor de etanol no CO_2 supercrítico (8-13% m/m) e tempo de equilíbrio (0-30min);

(iv) Os carotenoides de *Dunaliella salina* foram encapsulados integrando a emulsificação e a secagem utilizando *spray drying*, variando as condições de concentração da fase oleosa da emulsão (3-37% m/m), velocidade de

agitação (6500-21500 rpm) e temperatura da alimentação do *spray drying* (110-220 °C).

Os resultados apresentados ao longo dos capítulos desta tese mostraram que cada estratégia estudada permitiu uma recuperação/formulação bem-sucedida dos pigmentos alvo, possibilitando a obtenção de diferentes produtos com propriedades de cor interessantes, nomeadamente (i) e (ii) extratos azuis ricos em portisinas; (iii) extratos avermelhados ricos em astaxantina; e (iv) pó alaranjado rico em carotenoides hidrossolúveis.

Os resultados também mostraram que as condições ótimas da CPC permitiram um aumento de 5 vezes no rendimento do processo de purificação de portinas. Por outro lado, o processo de extração com fluidos comprimidos em dois passos levou a um aumento de 1,5 vezes no teor de portisinas. Em geral, os protocolos propostos fornecem abordagens alternativas para a produção de pigmentos azuis, contribuindo para a utilização sustentável de resíduos de mirtilo numa perspetiva de economia circular.

Os resultados demostraram também que, sob condições otimizadas, a astaxantina máxima extraível foi recuperada em 30 de minutos de extração, e a concentração de astaxantina no extrato final foi aumentada em comparação com outras estratégias de extração. Como resultado, o protocolo proposto para a recuperação da astaxantina mostrou ser uma estratégia eficaz e adequada para a extração seletiva do pigmento, contribuindo para a utilização sustentável de resíduos de crustáceos marinhos.

Finalmente, as condições ótimas para a encapsulação de carotenoides resultaram num rendimento de encapsulação de 39 % e uma eficiência de

74%. Além disso, as partículas resultantes apresentam propriedades interessantes para serem utilizadas como corantes alimentares, nomeadamente a sua cor laranja intensa e boa dispersibilidade em água. Consequentemente, a encapsulação em polissacarídeos naturais via secagem por *spray drying* de emulsões pode ser considerada uma estratégia viável para desenvolver formulas hidrossolúveis de pigmentos lipossolúveis para melhorar a sua dispersão em produtos à base de água.

Em suma, as estratégias desenvolvidas durante esta tese de doutoramento sugerem métodos alternativos para a extração, purificação e subsequente encapsulação de pigmentos naturais, realçando a utilização de recursos sustentáveis, alinhando-se assim com os princípios da economia circular e fornecendo soluções mais sustentáveis para a indústria alimentar.

LIST OF PUBLICATIONS

Papers published in international peer-reviewed scientific journals (4)

Nunes, A.N., Roda, A., Gouveia, L.F., Fernández, N., Bronze, M.R., Matias, A.A. (2021) Astaxanthin Extraction from Marine Crustacean Waste Streams: An Integrated Approach between Microwaves and Supercritical Fluids. ACS Sustainable Chemistry & Engineering, 9(8), 3050-3059.
Doi: 10.1021/acssuschemeng.0c06534.

Nunes, A.N., Borges, A., Matias, A.A., Bronze, M.R., Oliveira, J. (2022) Alternative Extraction and Downstream Purification Processes for Anthocyanins. Molecules, 27(2), 368.
Doi: 10.3390/molecules27020368.

Nunes, A.N., Ivasiv, V., Gouveia, L.F., Fernández, N., Oliveira, J., Bronze, M.R., Matias, A.A. (2023) Isolation of Bluish Anthocyanin-derived Pigments from Blueberry Residues using Centrifugal Partition Chromatography. Journal of Chromatography A, 464150.
Doi: 10.1016/j.chroma.2023.464150.

Nunes, A.N., Monte, J., Rodríguez-Rojo, S., Nogueira, I., Gouveia, L.F., Brazinha, C., Matias, A.A. Development of a Carotenoid-Rich Microalgae Colorant by Microencapsulation. Colorants 2024, 3(1), 39-52.
Doi: 10.3390/colorants3010003.

Papers submitted to international peer-reviewed scientific journals (1)

Nunes, A.N., Oliveira, J., Bronze, M.R., Matias, A.A. Compressed fluid-based technologies for downstream isolation of Bluish Anthocyanin-derived Pigments obtained from Blueberry Surplus. Food and Function RSC.

Oral presentations (6)

Nunes, A.N., Oliveira, J., Bronze, M.R., Matias, A.A. (2022) Green strategies to extract and formulate natural pigments: from red to blue hues. 12th ITQB NOVA Ph.D. students' Meeting, Oeiras, Portugal.

Nunes, A.N., Roda, A., Gouveia, L.F., Fernández, N., Matias, A.A. (2020) Integrated microwave and supercritical carbon dioxide extraction processes for astaxanthin recovery from brown crab residues. 1st Iberian Meeting on Supercritical Fluids, Santiago de Compostela, Spain.

Nunes, A.N., Roda, A., Matias, A.A (2019) Recovery of astaxanthin pigments from marine crustacean waste streams using supercritical fluid technology. The European Summer School in High Pressure Technology 2019, Maribor/Graz, Slovenia/Austria.

Fernández, N., Abdallah, M., Rodríguez, L., Nunes, A.N., Batista, M., Matias, A.A. (2019) Sustainable extraction of bioactives from marine biomass at iBET. Business2Sea: Fórum do Mar 2019, Porto, Portugal.

Nunes, A.N., Monte, J., Rodríguez-Rojo, S., Nogueira, I., Brazinha, C., Gouveia, L.F., Matias, A.A. (2018) Microencapsulation of carotenoid pigments from *Dunaliella salina* into natural polysaccharides as potential food coloring ingredient. Food Bioactives and Health, 26-28 September 2018, Lisbon, Portugal.

Nunes, A.N., Monte, J., Rodríguez-Rojo, S., Nogueira, I., Brazinha, C., Crespo, J.G., Matias, A.A. (2018) Microencapsulation of carotenoid pigments from *Dunaliella salina* into natural polysaccharides as potential food coloring ingredient. Biocolours Conference 2018, Breda, Netherlands.

Posters in international scientific meetings (4)

Nunes, A.N., Ivasiv, V., Gouveia, L.F., Fernández, N., Oliveira, J., Bronze, M.R., Matias, A.A. (2023) Centrifugal partition chromatography for downstream isolation of bluish anthocyanin-derived pigments obtained from blueberry surplus. 4th International Conference on Food Bioactives and Health, Prague, Czech Republic.

Nunes, A.N., Roda, A., Monte, J., Rodríguez-Rojo, S., Nogueira, I., Gouveia, L.F, Brazinha, C., Matias, A.A. (2020) Valorization of carotenoid pigments as natural colorants. 10th ITQB NOVA Ph.D. students' Meeting, Oeiras, Portugal.

Nunes, A.N., Roda, A., Matias, A.A. (2018) Recovery of natural-based pigments from marine crustacean waste streams using Supercritical Fluid Technology. 12th International Symposium on Supercritical Fluids, Antibes-Juan-Les-Pins, France.

Roda, A., Nunes, A.N., Matias, A.A. (2018) Extraction of carotenoid pigment from brown crab residues using high pressure technology. 13th International Chemical and Biological Engineering Conference, Aveiro, Portugal.

CHAPTER 1

Introduction

CHAPTER 1

CONTENTS

This chapter contains excerpts from the author's publication: Nunes, A.N., Borges, A., Matias, A.A., Bronze, M.R., Oliveira, J. (2022) Alternative Extraction and Downstream Purification Processes for Anthocyanins. Molecules, 27(2), 368. DOI: 10.3390/molecules27020368.

The author was involved in the literature search, the structure outline, and the preparation of the original manuscript except for the anthocyanin introduction and deep eutectic solvent section, which was performed at FCUP by A. Borges supervised by J. Oliveira. Revision of the manuscript for submission was performed by the remaining authors.

1. ENVIRONMENTAL SUSTAINABILITY

Environmental Social and Governance (ESG) and Sustainable Development Goals (SDS) are vital frameworks that reflect a growing recognition of the need for sustainable and responsible practices in business and society. Both frameworks are used to assess and promote sustainability and responsible business practices, and both play a crucial role in guiding and evaluating a project's impact and sustainability.

ESG and SDS both focus on addressing pressing global challenges, such as climate change, inequality, poverty, and resource depletion. Focusing on sustainability often drives innovation within organizations. Companies are forced to develop new products, services, and processes that are more resource-efficient and environmentally friendly. This can lead to cost savings and improved competitiveness.

In particular, Environmental (E) from ESG is related to:

(i) Resource Efficiency: ESG emphasizes the responsible use of resources being crucial to consider how efficiently we use raw materials, energy, and water in production. Aim to minimize waste and reduce the environmental footprint.
(ii) Eco-Friendly Processes: We should ensure that the processes are environmentally friendly, using green chemistry principles and minimizing emissions and pollutants.
(iii) Biodiversity Conservation: Evaluate the impact of your raw material sourcing on local ecosystems and biodiversity. Sustainable practices may involve protecting or restoring natural habitats.

Moreover, the SDS framework, established by the United Nations, promotes global collaboration and partnerships to achieve its 17 goals. This encourages

governments, businesses, and civil society to work together on a global scale to address shared challenges (Figure 1).

Figure 1. 17th sustainable development goals [1].

Alignment of this Ph.D. Thesis with SDGs:

Goal 3 (Good Health and Well-being): SDG 3 by promoting natural alternatives to synthetic colorants, which can potentially benefit human health and well-being.

Goal 12 (Responsible Consumption and Production): SDG 12 by promoting sustainable consumption and production patterns through the use of natural colorants as alternatives to synthetic ones.

Goal 15 (Life on Land): SDG 15 by aiming to protect and restore terrestrial ecosystems.

Goal 8 (Decent Work and Economic Growth): Aim to create decent job opportunities in the areas where you operate, aligning with SDG 8.

By integrating ESG principles and aligning with relevant SDGs, the raw materials valorization can not only contribute to the development of natural colorants but also serve as a model for sustainable and responsible business practices, ultimately benefiting both the environment and society. This approach is important to ensure the project's long-term viability in an increasingly sustainability-conscious market.

2. FOOD ADDITIVES

The pressing need to respond to an expanding world population, coupled with increased consumer awareness and expectations, has driven significant advancements in food production systems, as well as the methods and products employed within the food industry [2]. Currently, food production involves the manufacturing of food in specialized facilities and then the distribution to various markets, at times over long distances. To ensure that food products remain in good condition during transportation to the consumer, significant amounts of energy are required for refrigeration, controlled packaging, and the use of additives to prevent spoilage and maintain freshness [3]. With an increasingly competitive global market, the food industry is driven to prioritize cost-effective strategies for food preservation, often turning to the utilization of additives [2,3].

Food additives comprise a diverse array of functional categories, including antioxidants, thickeners, stabilizers, emulsifiers, flavoring, sweeteners, nutritional additives, and colorants. These vital ingredients are added to food to perform useful functions, modifying appearance, preserving flavor, and/or

improving taste, among others. Consequently, food quality, safety, and appearance during the life cycle of processing to consumption are enhanced, thus meeting the increasingly challenging market demands and legal requirements [3,4].

In Europe, food additives are designated with a specific code known as E-number. This code consists of the letter “E” followed by three or four numbers. To ensure consumer safety, the amount of additive added to food is meticulously determined based on the type of food product, ensuring it does not exceed the acceptable daily intake [2].

Food additives should only be used when their technological benefits are necessary and cannot be achieved through other feasible methods. Furthermore, these ingredients should not pose health risks to consumers at the proposed level of use [2]. Major regulatory bodies, such as the European Food Safety Authority (EFSA) in the European Union, the Food and Drug Administration (FDA) in the United States, the Joint Expert Committee on Food Additives (JECFA) of the Food and Agriculture Organization (FAO)/World Health Organization (WHO), and the Codex Alimentarius, play key roles in legislating, standardization and evaluating the safety of food additives [2,4]. While the establishment of a global consensus on food additive legislation remains an ongoing challenge, there is a notable renewal in the pursuit of safe, natural, and sustainable alternatives [4]. The focus is on developing additives that align with consumers' preferences for clean labels and healthier food options, while also considering the ecological impact on their production and usage.

3. COLORANTS

Colorants are a class of additives that are specifically defined by the FDA as “any dye, pigment or substance which when added or applied to food, drug or cosmetic, or the human body, is capable (alone or through reactions with other substances) of imparting color” [5]. Color is the first and most impactful sensory attribute that largely determines the consumer's food preferences, acceptability, and subsequent, selection [2,6–8]. Studies have demonstrated that color is responsible for the shaping of consumers' assessments, accounting for a substantial 62-90 % of their overall perception and evaluation, having an important role in the market success of a product [9,10]. The significance of color in the food industry has created a lucrative market for experts in food colorants. Specifically, market research companies have projected a global food colors market size of USD 2.97 billion by 2025 [9].

Consumers frequently rely on color as a trustworthy indicator to assess various attributes of a food product, including its taste, and safety [7,10,11]. Recognizing the significance of color in consumers' perception, food manufacturing companies have identified this as a crucial marketing strategy [9,11]. As a result, color additives are widely used to standardize raw ingredients colors, provide identity to colorless foods, and compensate for color loss during processing and storage, thus making the food more attractive to the eye of the consumer [8,10,12].

Food colorants can be classified into three main categories based on their origin and production method. The first group consists of natural colorants, which are derived from living organisms through processes or modifications. Nature-identical colorants from the second group, and although they are

synthesized in industries, they closely mimic the natural pigments found in nature. The third group includes artificial or synthetic colorants, which are entirely man-made and not found in nature [2,3,11,13]. These three groups can further be categorized based on different criteria, including their solubility (soluble and insoluble), hiding power (transparent and opaque), and whether they are organic or inorganic [2]. However, the most used classification is based on their origin, distinguishing between natural, nature-identical, and synthetic colors.

The evolution of food colorants has seen significant changes over time. The practice of coloring food dates to around 1500 BCE, as evidenced by ancient Egyptian writings referencing the coloring of drugs, and the Romans describing the coloring of wine around 400 BCE [10]. From that time on, food coloring ingredients were derived from natural sources. Saffron, paprika, turmeric, and various flowers were popular substances used [10,14]. As the development of human civilization progressed and the population expanded, there was an increasing demand for colorants that could provide a wide range of consistent colors, with great tinctorial strength, in sufficient quantities, at low cost, with high stability, and without conveying flavor to products [12,15–17]. The use of natural colorants remained prevalent until the mid-nineteenth century when William Henry Perkin synthesized the first colorant, mauveine (also known as mauve or aniline purple), in 1856. This discovery marked a turning point in the history of colorants [10,11,16]. The synthesis of mauveine opened the doors to the production of numerous other synthetic colorants, which quickly gained popularity due to their cost-effectiveness, purity, superior stability, high coloring capacity, brightness expanded range of shades, and ease of use [2,16,17].

Nonetheless, synthetic colorants have been associated with various health issues, including hypersensitive, allergenic responses, asthma attacks, and carcinogenic potential [6,7,17]. Also, the environment is being seriously damaged due to the widespread use of synthetic dyes at the industrial scale [11]. These findings have raised concerns among regulatory authorities and health organizations, leading to stricter monitoring and regulation of the use of these additives to ensure compliance with good manufacturing practices and consumer safety [2,12,17]. Although current synthetic colorants undergo rigorous safety evaluation and comply with strict regulations, the industry is actively exploring new options to meet the changing demands of the market and adhere to evolving regulatory restrictions [10].

Consumers become more conscious and discerning about the food, seeking products that are perceived as natural and minimally processed. Consequently, there is a growing preference for natural additives in the 21st century [18]. This shift towards natural colorants is in line with the “clean label” trend, as is closely linked to the perception of good quality, safety, and health in food products [3]. Consumers now associate these attributes with products that use natural ingredients, including natural colorants. This perception has posed a significant new challenge for food research institutions and food industries [18].

One of the driving forces behind the expanding interest in natural colorants is the increasing awareness of environmental sustainability and potential side effects associated with the chemicals used in the synthesis of artificial food colors [19]. Natural colorants are recognized as safer alternatives by consumers and are appreciated for their health-promoting and eco-friendly properties [7,18]. Moreover, natural colorants can provide technological bioactive functionalities to food, delivering additional value-added properties

that distinguish them from their synthetic counterparts, thus enhancing their desirability in the market [3,20]. As a result, the market for natural colorants has been experiencing significant growth. In 2017, the market value of natural colorants reached 3.71 trillion dollars. This growth trend is expected to continue with a projected compound annual rate of 5.7% from 2017 to 2023 [8]. Artificial food colorants account for only 16% of the overall portfolio of food colorants in the EU, while in North America, they comprise 29% of the total food colorants used [9].

The use of both natural and synthetic colorants in the food industry is subjected to strict legislation and regulation to ensure consumer safety and proper use in food products. In the EU, the Council Regulation (EC) 1333/2008 (formerly 94/36/EC) regulates the use of colorants, specifying the approved colorants, the colorant sources, purity levels, permitted food addition, and maximum levels of integration into specific food products [13,19]. Food additives that are permitted for use in food are listed in Annex II of this Regulation [12]. Consequently, legal restrictions have significantly reduced the available color palette for the food industry [18].

To be approved as a food colorant additive, the new substances must be capable of restoring the original food appearance which may have experienced color changes from processing to distribution process [7]. Also, characteristics including toxicity, solubility, stability, and regulatory issues must be evaluated, along with consumer acceptance. Environmental sustainability, productivity, and production cost are also important considerations for commercial use [4].

4. NATURAL PIGMENTS

Nature produces a palette of color, covering the entire visible spectrum, which can be used as food colorants [18,21,22]. These pigments are obtained from various naturally occurring sources, including microorganisms, fungi, animals, plants, and even minerals [6,13,23]. They play essential functions in various biological processes, such as metabolism, photosynthesis, blood oxygen transport, protection from predators and UV radiation, and attraction of animals for pollination [6,24].

Naturally occurring pigments comprise a broad spectrum of compounds with varying structures. Based on the molecular polarity and chemical and physical characteristics, these pigments can be categorized into two main groups: water-soluble (hydrophilic) and lipid-soluble (lipophilic) molecules. Anthocyanins, which exhibit shades of red, purple, and blue, along with red betalains, fall into the water-soluble category. On the other hand, lipid-soluble pigments include green chlorophylls and yellow-orange-red carotenoids [13,15,20]. Consequently, these pigments are responsible for the appealing hues of red, orange, yellow, and green in many food products (Figure 2) [25,26].

Regulated natural colorants (Table 1), as specified in Regulation (EC) No 1129/2011, comprise a variety of pigments derived from natural sources (classified from E-100 to E-199). These colorants include curcumin (E-100), chlorophyll and chlorophyllin (E-140 and E-141), carotenoids (E-160), including carotenes (E-160a), lycopene (E-160d), lutein (E-161b), canthaxanthin (E-161g), betanin (E-162), and anthocyanins (E-163) [3,7].

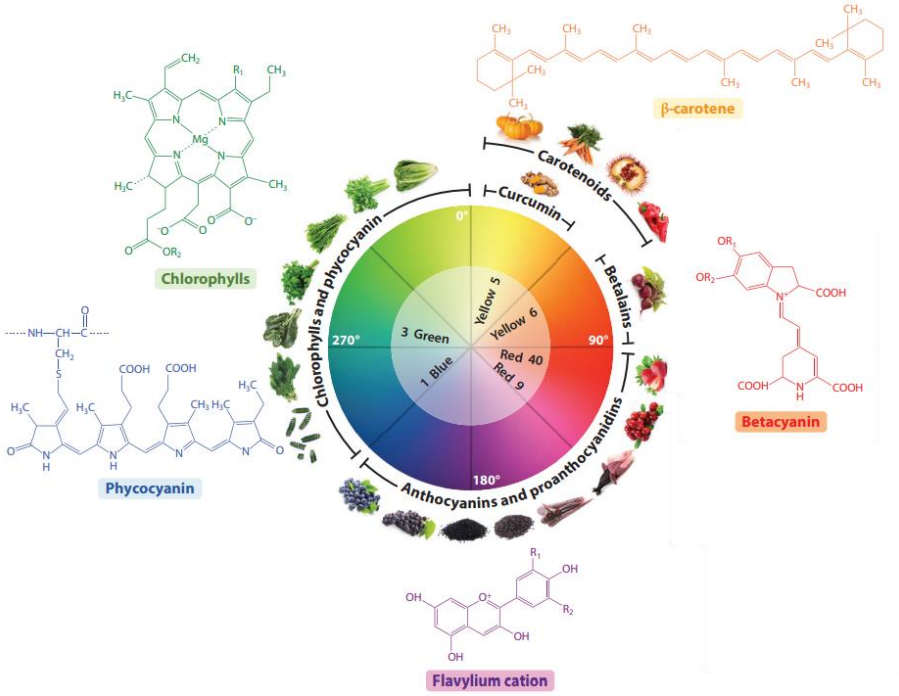

Figure 2. Chemical structures and colors of different representative natural pigments [27].

Despite the use of natural pigments in the food industry has gained popularity, there are several challenges associated with the widespread use of natural colorants. Regulatory restrictions and technical issues hinder the availability of a wide variety of commercially viable natural colorants. This limitation makes it difficult for industries to replace synthetic colorants with natural alternatives and meet consumer demand [22,27].

Table 1. Summary of examples of natural colorants of a wide range of colors with their corresponding color, approbation status, E-number, and primary sources. Adapted from [22].

Colorant	Color obtained	Approbation status	E-number	Primary source	Solubility
Curcumin	Yellow	Approved with combined maximum limit	E-100	*Curcuma longa* (rhizome)	Oil soluble
Riboflavin	Yellow	Approved at *quantum satis*	E-101	Some plants, animals, and microorganisms	Oil soluble
Carminic acid pH < 5	Orange	Approved with combined maximum limit	E-120	Coccus cacti L.	Water soluble
Carminic acid 7 < pH < 5	Red				
Carminic acid pH > 7	Violet				
Chloropyll	Green	Approved at *quantum satis*	E-140	Can be extracted from a range of green leaves, but usually grass, nettles or alfalfa is used	Oil soluble
Caramel	Caramel	Approved at *quantum satis*	E 150a	Sugar	Water soluble
Carbon black	Black	Approved at *quantum satis*	E-153	Derived from vegetable material, usually peat, by complete combustion to the insoluble carbon	Oil soluble
β-carontene	Yellow	Approved with combined maximum limit	E-160a	Extracted from several sources including algae, carrots, and palm oil	Oil soluble
Norbixin	Orange	Approved with combined maximum limit	E-160b	*Bixa orellana* (Seeds) (formed in alkaline hydrolysis)	Water soluble

Table 1. Cont. Summary of examples of natural colorants of a wide range of colors with their corresponding color, approbation status, E-number, and primary sources. Adapted from [22].

Colorant	Color obtained	Approbation status	E-number	Primary source	Solubility
Bixin	Orange	Approved with combined maximum limit	E-160b	*Bixa orellana* (Seeds)	Oil soluble
Paprika	Reddish orange	Approved at *quantum satis*	E-160c	*Capsicum annum*	Oil soluble
Crocin	Yellow	Approved at *quantum satis*	E-160c	*Gardenia*	Water soluble
Lutein	Yellow and orange	Approved with combined maximum limit	E-161b	*Calendula*	Oil soluble
Betanin	Pink or red	Approved at *quantum satis*	E-162	*Beta vulgaris*, *Hylocereus polyrhizus*, and red dragon fruit	Water soluble
Anthocyanin pH 1	Red	Approved at *quantum satis*	E-163	Grapes, redcurrants and blackcurrants, raspberries, strawberries, apples, cherries, red cabbages, purple sweet potatoes, and eggplant	Water soluble
Anthocyanin pH 4	Purple				
Anthocyanin pH 8	Green				
Anthocyanin pH 12	Yellow				

While perceived as healthier, natural food colors may not be as bright and stable as synthetic, particularly under neutral and high pH conditions. This instability creates challenges in maintaining the desired color intensity and appearance of products during storage [22,27]. Also, the cost of natural pigments is generally higher compared to synthetic pigments. The higher concentrations of natural pigments are often required to achieve the same color intensity, which can increase production costs. Furthermore, the range of hue that can be achieved with natural pigments is narrower compared to

synthetic alternatives [25]. Finding reliable sources of stable green, blue, and red natural colorants, especially at high pH levels, remains a critical need for the industry [10,27]. Additionally, the lack of uniformity in the production process of natural colorants presents a challenge. Since natural additives are derived from various raw materials, variations in color and stability can occur, making it difficult to standardize the final product color [22].

Overall, the limitations of natural pigments, including regulatory restrictions, cost, limited color range, and stability issues, present significant challenges for food industries looking to replace synthetic colorants with natural alternatives. Researchers and manufacturers are continually seeking technological advancements to improve the functional characteristics and stability of existing natural colorants and explore new and more reliable sources of natural colorants. Anthocyanins, anthocyanin derivatives, and carotenoids were the natural pigments studied in the present thesis and the ones that will be further described.

4.1. ANTHOCYANINS AND THEIR DERIVATIVES

Anthocyanins are water-soluble pigments that belong to the flavonoid group and play a crucial role when dealing with natural colorants, as they present an extensive range of vibrant natural colors, including red, orange, violet, and blue [28,29]. Anthocyanins are commonly found in leaves, flowers, fruits, vegetables, and other plant sources. These pigments play a vital function in plant coloration, environmental adaptation, and defense mechanisms [18]. Diverse structures and colors make anthocyanins a highly complex and interesting group of phytochemicals.

Anthocyanins are glycosylated derivatives of anthocyanidins, which are the aglycon form of these pigments [20]. Anthocyanins present different hydroxylation and methoxylation patterns contributing to the high diversity of these pigments in nature (Table 2). The most common anthocyanidins found in nature are cyanidin, malvidin, delphinidin, pelargonidin, and petunidin [19]. The composition and color of anthocyanins are influenced by the number and position of hydroxyl groups, the degree of glycosylation, and the presence of acylation with aliphatic or aromatic acids [25]. The pH also plays a role in the color of anthocyanins, with acidic conditions resulting in red colors and alkaline conditions leading to blue-purple hues [18]. As food colorants, anthocyanins present challenges due to their low physical stability and potential interaction with the food matrix, leading to color changes [22,30].

Table 2. Structures of the major anthocyanidins. Adapted from [31].

Anthocyanin	R1	R2
Delphinidin	OH	OH
Petunidin	OH	OCH_3
Malvidin	OCH_3	OCH_3
Cyanidin	OH	H
Peonidin	OCH_3	H
Pelargonidin	H	H

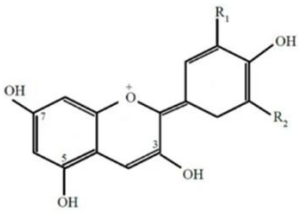

Despite their challenges, anthocyanins are already listed as a natural colorant by EU legislation as a product E-163 (Table 1) and are considered bioactive compounds with potential health benefits [2,3,22]. Anthocyanins present antioxidant, anti-allergic, anti-inflammatory, antiviral, antimicrobial, and anti-tumor properties [22]. Also, anthocyanins have been associated with a low

prevalence of certain disorders, such as cancer, cardiovascular diseases, diabetes, and obesity [22]. In the food industry, anthocyanins find applications in various products, including beverages, dairy products, confectionary items, and fruit preparations [2,3]. While the stability of anthocyanins presents challenges for their application as food colorants, the chemical transformation of anthocyanins that yield new pigments with different and unique colors hue appears to be both challenging and profitable [32].

Finding a natural blue pigment to replace synthetic blue colorants has proven to be a particularly challenging task due to limited natural sources [22,33]. Consequently, there is enormous industrial interest in investigating new sources. The availability of reliable sources of natural blue pigment would fill a crucial gap in the spectrum of industrially utilized natural colors [26]. Several years ago, researchers identified bluish anthocyanin-derived pigments, known as portisins, in fortified red wine [30,34]. These pigments display a distinct bluish color in acidic conditions, with a maximum absorption wavelength of around 570 nm. The structure of this group of pigments comprises a pyranoanthocyanin linked to a flavanol through a vinyl linkage. The process to obtain portisins involves two steps: first, the reaction of anthocyanins with pyruvic acid yielding anthocyanin-pyruvic acid adducts, and then, the anthocyanin-pyruvic acid adducts react with flavanols in the presence of acetaldehyde (Figure 3) [35], resulting in an extended π-electrons conjugation that imparts high stability and unique bluish color. Furthermore, the molar extinction coefficient of these bluish pigments is significantly higher compared to their anthocyanin precursors [34].

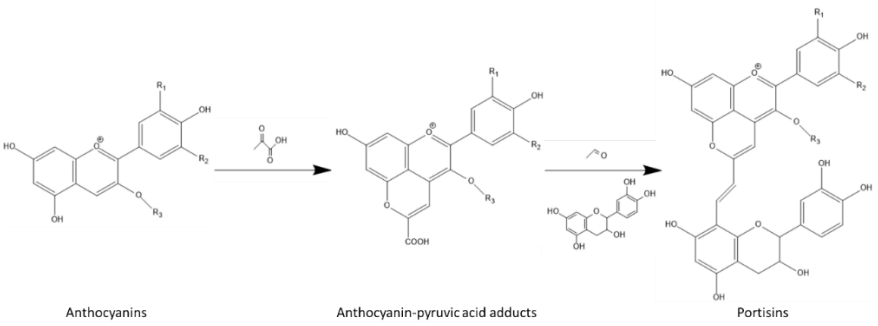

Figure 3. General scheme for portisins hemi-synthesis [36].

The chromatic properties and stability of portisins make them potential candidates as natural blue colorants for use in the food sector. However, portisins were found to occur in wines at very low levels, so an alternative pathway for commercial production had to be investigated [37]. Researchers have explored the hemi-synthesis of these anthocyanin-derived pigments by using various red fruit extracts as natural sources of anthocyanins to produce these bluish pigments [35].

Considering the complex chemical composition of natural products, efficient separation of target compounds is vital. Traditionally, portisins have been isolated from Port red wine or red fruit extracts after hemi-synthesis, using reversed-phase liquid chromatography (RP-LC) [34,38–41]. However, few information is available regarding the efficiency and throughput of the process, as well as the amount of solvent required for obtaining purified portisins. Moreover, column chromatography-based methods present significant drawbacks in terms of scalability for industrial applications, such as extended separation time, extensive use of organic solvents, and reduced recovery rated due to solid support adsorption [42,43]. Consequently, there

is an urgent need to develop efficient and sustainable methodologies for isolating these blue pigments from complex mixtures.

4.2. CAROTENOIDS

Carotenoids are a group of lipid-soluble pigments widely distributed in nature, with colors ranging from yellow to orange and red. They are found in various organisms such as higher plants, bacteria, fungi, yeast, algae, and animals [10,18,25,44]. Chemically, carotenoids are tetraterpenoids composed of isoprenoid units joined in a head-to-tail pattern [10]. These pigments can be classified into two classes based on functional groups: carotenes and xanthophylls. Carotenes consist of polyunsaturated hydrocarbons and include α-carotene, β-carotene, and lycopene, while xanthophylls contain polyunsaturated hydrocarbons with functional groups containing oxygen such as astaxanthin, lutein, and zeaxanthin (Table 3) [20,25,27,44]. Apocarotenoids are a subgroup of carotenoids characterized by a shorter carbon chain, such as bixin and crocetin [25]. Carotenoids exist in different configurations, with the all-trans isomeric configurations being the most common and stable in nature [44].

The color of carotenoids is determined by the level of conjugation in their chemical structure. Conjugated carotenoid systems with delocalized π electrons along the entire chain are responsible for the absorbance in the visible spectrum [10,27]. Carotenoids with larger conjugated systems exhibit redder shades, while those with shorter chains and fewer double bonds show less intense colors [10,18]. For example, lycopene, β-carotene, and γ-carotene, despite having the same number of double bonds, exhibit red, orange, and red-orange colors, respectively, due to differences in cyclization [19].

Table 3. Common carotenoid structures.

Structures
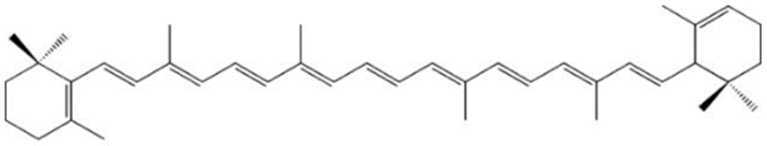
α-Carotene
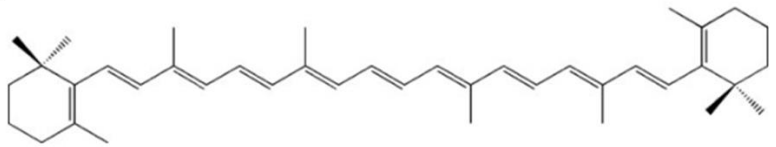
β-Carotene
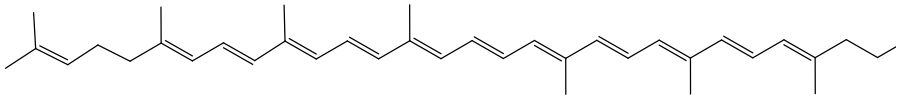
Lycopene
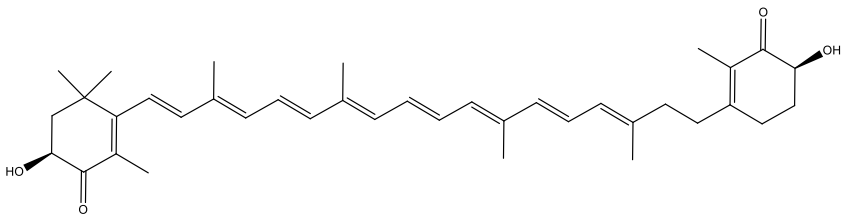
Astaxanthin
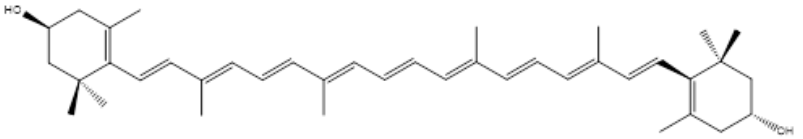
Lutein
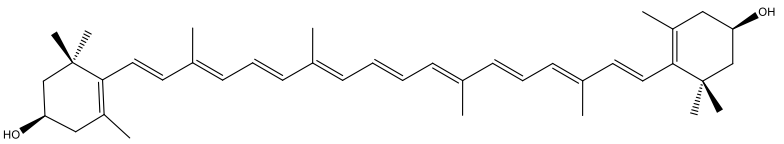
Zeaxanthin

Carotenoids are typically found within the membranes of organelles such as mitochondria, chloroplast, or endoplasmic reticulum. These pigments exhibit significant stability when present within the natural environment. However, when the cells are disrupted during the extraction procedures, carotenoids become more susceptible to degradation [18,25]. Therefore, it is important to select appropriate solvents and techniques to minimize their degradation and preserve their stability and color properties.

As carotenoids are hydrophobic compounds, the extraction of these pigments is primarily carried out using organic solvents. The selection of the appropriate solvent depends on the specific carotenoid and the natural source from which is extracted. The extraction of non-polar carotenes or esterified xanthophylls, which are hydrophobic in nature, often involves the use of organic solvents such as hexane, petroleum ether, or tetrahydrofuran. On the other hand, the extraction of more polar carotenoids, which have some degree of polarity, requires the use of solvents with intermediate polarity such as acetone, ethanol, and ethyl acetate [45].

Nevertheless, traditional organic solvent extraction methods for carotenoids have some limitations. Although these methods are scalable and efficient, high temperatures and long extraction times to achieve optimal yields are often required. In addition, the use of organic solvents raises concerns regarding the toxicity and the high energy costs associated with the solvent recovery after the extraction [6,8]. To address these issues, researchers have been exploring alternative solvents as potential substitutes. Vegetable oils, surfactants, deep eutectic solvents, ionic liquids, and pressurized or supercritical fluids have been proposed as alternative solvents for carotenoid extraction. These solvents offer advantages such as lower toxicity and improved sustainability [8,18,45].

To improve the extraction efficiency of carotenoids, pretreatment steps are often employed. These pretreatment methods involve various physical (*e.g.*, milling, cryogenic grinding, cooking, drying, ultrasound, osmotic shock), chemical (*e.g.*, liquid nitrogen, surfactants, acid, base), biological, or enzymatic processes. Also, the specific pretreatment steps employed depend on the characteristics of the source material and the selected carotenoid extraction method. By employing appropriate pretreatment and extraction methods, the extraction efficiency of carotenoids can be intensified [8,45].

Carotenoids are a suitable choice for food coloring purposes due to their nontoxicity, wide color spectrum, and relative stability compared to other natural pigments, enabling food manufacturers to create visually appealing and safe products [11]. Although some carotenoids are produced synthetically, many are obtained from natural sources. The food industry utilized powdered dried plant and liquid extracts obtained from sources such as paprika, annatto, tomato, and saffron. The European Union has approved specific carotenoids as food additives, which are assigned E-number E-160 and E-161 (Table 1) [7,18]. These are lutein, lycopene, zeaxanthin, β-carotene, bixin, norbixin, crocetin, and paprika [22,25].

The global carotenoid market size was estimated at USD 1.5 billion in 2019 and is projected to be USD 2.0 billion by 2026, displaying an annual growth rate of 4.2% [46]. These pigments find diverse technological applications in the food industry, including in sauces, marinades, spices blends, coating, beverages, dairy products, among others [2,3,22].

In addition to technological features (yellow, orange, and red color hues), these pigments present important health-related proprieties, being considered as functional ingredients [8,20]. Carotenoids are sources of provitamin A and have various biological functions, including solar light

absorption, oxygen transport, and antioxidant activity (singlet oxygen quenching) [7,27,47]. However, carotenoids are sensitive to oxidation and isomerization, particularly during food processing and storage, due to their electron-rich and highly unsaturated chemical structure [10,25,44].

Numerous factors can influence the oxidation of carotenoids, including light exposure, moisture, temperature, peroxides, metals, enzymes, lipids, and antioxidants. These factors can accelerate or inhibit the oxidation process, thereby impacting the stability and longevity of carotenoids in various systems [10,44]. In this context, the use of carotenoids as colorant additives and functional ingredients is challenging due to their low water solubility, and stability.

To address the aforementioned issues, microencapsulation techniques have emerged as an effective solution. Various techniques such as spray drying, freeze drying, coacervation, and inclusion complexes have been proposed as alternative approaches for encapsulating carotenoids [20,48]. These microencapsulation methods offer promising alternatives for ensuring the efficient delivery and application of carotenoids in various food applications.

5. RENEWABLE SOURCES OF NATURAL PIGMENTS

The exponential growth of the global population has led to a significant increase in the demand for food, both in its raw and processed forms. This demand has also resulted in a drastic rise in food waste across the entire food supply chain, from agricultural fields to processing facilities, retail stores, and consumer households [6]. Globally, an estimated 1.6 billion tons of food is wasted each year, with approximately 1.3-1.6 billion tons of edible food discarded, amounting to a staggering business value of USD 750 million.

Household waste has a significant impact, followed by processing, catering, primary production, and distribution [8,19]. Food waste mainly consists of meat and fish, vegetables, and dairy products, resulting in a substantial economic loss of approximately USD 27 billion [19].

The circular economy model presents an opportunity to effectively manage and unlock food waste potential as a valuable resource [7]. By implementing a comprehensive waste management system and optimizing resource utilization, the circular economy principles guide the management of food waste. This approach can be seen as a pyramid (Figure 4), which emphasizes prevention as the primary focus, followed by surplus food redistribution, animal feed production, and the recovery of high-value molecules such as natural colorants. Nutrient recycling, energy recovery, and waste disposal serve as the last resort in the hierarchy [19].

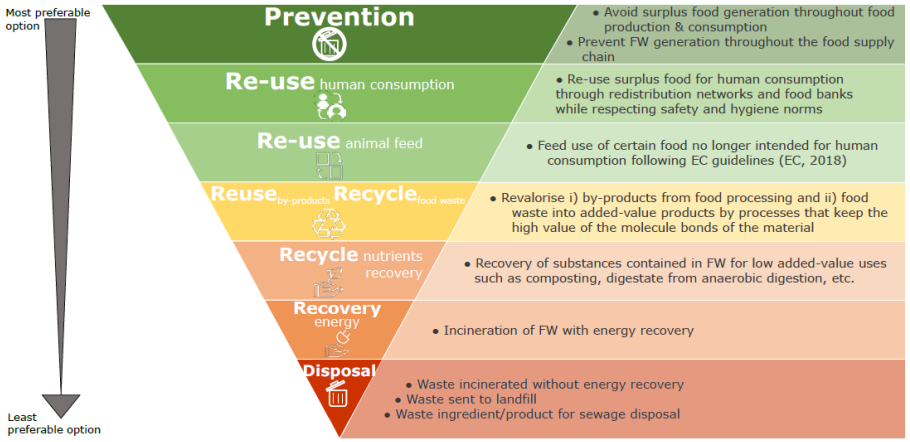

Figure 4. Practical application of the food waste hierarchy [49].

The key challenge lies in minimizing the environmental impact of waste while adhering to circular economy concepts. The exploitation of natural additives derived from food waste presents an innovative solution [8]. The industrial utilization of these additives has seen substantial growth due to increasing consumer demand for healthy and natural food options. By channeling the potential of food waste, valuable biomaterials, bioenergy, and high-value products, including natural pigments, can be produced, aligning with the principles of the circular economy [19].

The agro-food industry generates substantial amounts of by-products that contain compounds with high functionality and bioactivity. These by-products, often considered waste, represent an abundant and cost-effective source of natural compounds [6,7]. Fruit and vegetable waste, including seeds, peels, and pomaces, possess various bioactive functional ingredients such as pigments, dietary fiber, and polyunsaturated fatty acids. Exploiting these underutilized residuals' biomasses presents significant opportunities for innovation and the development of sustainable colorants [7,8].

To meet the increasing demand for natural colorants, alternative sources beyond the traditional plant-derived pigments have emerged. Microbial-derived pigments offer unique advantages. Microbial organisms, including bacteria, fungi, algae, and yeast, present opportunities for sustainable pigment production. The microbial fast growth, easier extraction, lower cost, and higher yields make them attractive sources for natural colorants [6,25].

Overall, the circular economy presents a promising framework for addressing the challenges posed by food waste and the demand for natural pigments. By utilizing food waste as a valuable resource, the production of sustainable natural colorants can be achieved. Exploiting alternatives sources, including by-products and microbial organisms, contributes to the development of

innovative and cost-effective processes, benefiting the food industry and the environment. Embracing circular economy principles and sustainable practices in the production of natural pigments is crucial for creating a greener and healthier future. Blueberry surplus, crab residues and microalgae *Dunaliella salina* were the sources of natural pigment studied in the present thesis and the ones that will be further described.

5.1. BLUEBERRY SURPLUS

Blueberry fruits (*Vaccinium* spp.) have gained global recognition and popularity due to their appealing blue color, unique flavor, and remarkable nutritional value [50–52]. These fruits have been recognized by the International Food and Agriculture Organization as one of the top five healthiest foods [53,54]. Blueberries are cultivated worldwide and are identified for their antioxidant, antitumor, anti-inflammatory, and anti-aging effects [28,55]. The increasing awareness of health benefits and consumer demand has led to a significant rise in blueberry production, with global production increasing from 622,900 tons in 2016 to 850,900 tons in 2020 [52,54]. However, this production growth also results in the generation of substantial agricultural waste during crop cultivation and harvesting [53].

These agricultural residues include blueberry leaves, branches, broken fruit debris, and surplus fruits that do not meet size and ripeness standards [53]. With the increasing emphasis on sustainability and the effective management of agricultural waste, there is a growing interest in investigating potential uses of the residues through bioprocessing techniques. The goal is to extract maximum value from the waste materials and generate value-added products within the framework of a circular economy.

Blueberries are not only known for their delicious taste but also their rich composition of organic acids, sugars, minerals, vitamins, fibers, pectin, and various phenolic compounds, especially anthocyanins [50]. Interestingly, these natural pigments are also present in blueberry agricultural residues, including skins, seeds, stems, and leaves, often in higher concentrations compared to the fruits [56]. Anthocyanins, in particular, contribute to up to 60% of the total polyphenolic content found in blueberries. Aligning with the principles of sustainable circular economy, the use of these residues as a source of natural pigments minimizes waste, efficiently utilizes resources, and adds value to agricultural by-products [7]. Such strategy contributes to the overall goal of achieving a more sustainable and environmentally friendly food production system.

5.2. CRAB RESIDUES

The crustacean processing industry has experienced significant growth in recent decades, resulting in the generation of large quantities of waste [57]. Each year, approximately 6 to 8 million tons of shell residues are produced globally, presenting a substantial opportunity for the conversion of these residues into valuable resources [58]. Crab shells are a natural and cost-effective source of various bioactive compounds and materials, including calcium carbonate, protein, chitin, lipids, and pigments such as astaxanthin [59–61]. As a result, there is a growing interest in developing extraction methodologies that efficiently isolate these natural ingredients and use this waste to contribute to a circular economy.

Astaxanthin is a carotenoid from the xanthophyll group, known for its attractive red-orange color. This liposoluble pigment naturally occurs in a

wide range of microorganisms and marine animals, including crabs and their processing waste [62–65]. Crustaceans are incapable of synthetizing carotenoids, so astaxanthin is formed through the oxidative transformation of ingested β-carotene or zeaxanthin obtained from feed microalgae [66]. Astaxanthin has been shown to offer numerous health benefits and is considered a powerful antioxidant [62,63,67]. Compared to other carotenoids, astaxanthin exhibits up to 10 times higher antioxidant capacity and is 100 times more effective than α-tocopherol [62,68].

The global market value of astaxanthin is estimated to be around USD 1 billion, and this pigment is widely used in the food, feed, nutraceutical, and pharmaceutical industries [62,69]. However, most of the commercially available astaxanthin is produced synthetically [70]. Consequently, there is a significant demand for natural astaxanthin from industries and a growing consumer preference for natural-derived products, leading to extensive efforts to enhance astaxanthin production from natural sources [62,71]. The production of astaxanthin from crab shells represents an opportunity to improve the economic viability of the crustacean processing industry, reduce the environmental impact of waste residues, replace synthetic astaxanthin, and meet market demand for this valuable pigment.

5.3. MICROALGAE

The marine environment is recognized as a valuable untapped source of bioactive compounds [72]. Microalgae, specifically eukaryotic photosynthetic microorganisms, have gained significant attention for their potential as viable resources for bioactive compound production [73]. Microalgae possess the ability to produce a diverse range of nutrients and biomolecules, including

carbohydrates, proteins, enzymes, fibers, vitamins, minerals, and pigments. These pigments are essential as they cannot be synthesized by humans or animals and must be obtained through diet [74].

One of the most notable classes of pigments synthesized by microalgae is carotenoids [75]. Among microalgae species, *Dunaliella salina* is known for the remarkable accumulation of β-carotene, reaching up to 14 % of its dry weight. Additionally, *Dunaliella salina* can also synthesize other carotenoids such as phytofluene, lutein, and zeaxanthin [76–78]. These carotenoids have found diverse applications as natural colorants and bioactive ingredients in various industries, including food, animal feed, nutraceuticals, pharmaceuticals, and cosmetics [79].

Due to the increasing market demand for carotenoids, *Dunaliella salina* has emerged as a promising and sustainable feedstock for commercial carotenoid production [76]. This microalgae species offers a high potential for large-scale cultivation as it is relatively easy and cost-effective to grow, can be cultivated using wastewater, absorbs carbon dioxide from the atmosphere, exhibits higher biomass productivity compared to traditional land plants, and does not compete with terrestrial crops for agricultural land [74,78,80–82]. Considering the ability to accumulate carotenoids and the carotenoids market demand, *Dunaliella salina* represents a compelling candidate for the sustainable production of carotenoids on a commercial scale.

6. ALTERNATIVE TECHNOLOGIES USED FOR THE EXTRACTION, DOWNSTREAM PURIFICATION, AND FORMULATION OF NATURAL PIGMENTS

6.1. EXTRACTION AND DOWNSTREAM PURIFICATION

Advancements in modern technologies have revolutionized the extraction, downstream purification, stabilization, and standardization of a wide range of natural colors. These innovative techniques have facilitated the production of diverse and vibrant natural colorants from various plant, microbial, and animal sources, providing exciting possibilities for the food industry [2].

To enhance the effectiveness and production of natural colorants, it is necessary to carefully choose appropriate procedures for extracting the natural pigments. The extraction of natural pigments is commonly carried out using conventional methods. In recent times, novel extraction techniques, often referred to as green extraction methods, have emerged as viable alternatives to the traditional approach due to their reduced solvent consumption and shorter extraction time. Also, these techniques can increase extraction yield, protect pigments from degradation, enhancing the quality of natural colorants. Classical techniques such as Soxhlet extraction, maceration, and hydrodistillation are straightforward, cost-effective methods that have been widely employed. Additionally, new technological approaches such as supercritical fluid extraction (SFE), pressurized liquid extraction (PLE), microwave-assisted extraction (MAE), ultrasound-assisted extraction (UAE), and pulsed electric field-assisted extraction (PEFE) have demonstrated exceptional efficiency in extracting and downstream isolating natural pigments [14,24,83]. Table 4 compares the advantages and limitations of these extraction methods.

Table 4. Advantages and limitations of different extraction methods commonly applied to natural pigments. Adapted from [83].

Extraction method	Solvent	Advantages	Limitations
Soxhlet extraction	Organic solvents (both polar and non-polar)	Easy to handle Low investment Automated system	Not suitable for heat-sensitive pigments Long extraction time Large solvent consumption
Maceration	Organic solvents (both polar and non-polar)	Automated system Easy to handle Low investment Applicable for heat-sensitive pigments	Very long extraction time Large solvent consumption Filtration step required
Hydrodistillation	Water	Easy to handle Low investment Automated system Moderate extraction time Applicable for heat-sensitive pigments	Non-automated system Repeated extraction may be required Not suitable for heat-sensitive pigments Long extraction time
SFE	CO_2 (non-polar) CO_2 with polar solvent	No use of toxic solvents	Required sophisticated safety controls High pressure leading to high capital and operating costs
PLE	Organic solvents (both polar and non-polar)	Automated system Fast extraction Reduced solvent consumption Automated system	Not suitable for heat-sensitive pigments High investment
MAE	Organic solvents (both polar and non-polar)	Fast extraction Easy to handle Moderate solvent consumption Moderate investment	Not suitable for heat-sensitive pigments Filtration step required Non-automated system
UAE	Organic solvents (both polar and non-polar)	Fast extraction Applicable for heat-sensitive pigments Simple Low investment	Large solvent consumption Filtration required Non-automated system
PEFE	Organic solvents (both polar and non-polar)	Fast extraction Applicable for heat- sensitive pigments Moderate investment	Large solvent consumption Filtration step required Non-automated system

Microwave (MW) pretreatment, SFE, PLE, and centrifugal partitional chromatography (CPC) downstream purification were the technologies used in the present thesis and the ones that will be further described.

6.1.1. MICROWAVE PRETREATMENT

MW pretreatment has emerged as a promising and innovative method for intensified extraction of both polar and nonpolar pigments [19]. The MW process involves applying different MW power levels along with suitable solvents (Figure 5) [16]. By using electromagnetic waves at specific frequencies (0.3-300 GHz), MW radiation induces rapid heating within the matrix cells [8]. This heating causes the expansion and breakdown of the matrix cell structure, facilitating the release of natural pigments into the solvent [19].

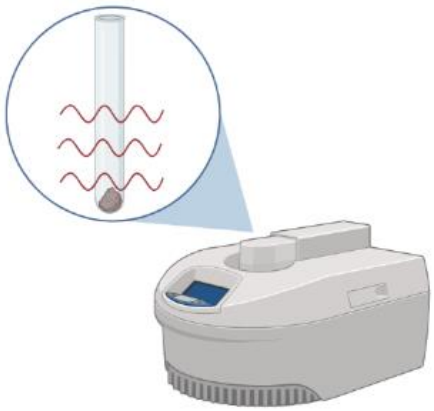

Figure 5. Schematic illustration of the MW pretreatment process. This figure was created using BioRender software (http://biorender.com, last accessed on 12 July 2023).

The use of MW radiation for extraction purposes was first reported in 1986. Due to its electromagnetic nature, MW presents perpendicular electric and

magnetic fields. The electric field is responsible for the induced heating via dipolar rotation and ionic conduction. Dipolar rotation is caused by the alignment of the molecules possessing a dipole moment on the electric field. This vibration produces collisions with surrounding molecules resulting in high heating rates. Accordingly, the larger the dielectric constant of the solvent, the greater the amount of thermal energy that will be produced. Consequently, MW heats the whole sample simultaneously and homogeneously when compared to conventional conductive heating. By disrupting hydrogen bonds, MW energy promotes the migration of dissolved ions from the sample matrix to the surrounding solvent, enhancing solvent penetration and extraction efficiency [15,44]. Polar solvents with high dielectric constants, such as water and ethanol, are commonly used due to their ability to absorb MW energy [44].

One of the key advantages of MW pretreatment is the ability to significantly reduce the extraction time and solvent consumption compared to conventional methods [16,44]. Furthermore, MW pretreatment is considered environmentally friendly as it requires less energy and promotes the efficient use of nontoxic solvents. Also, this rapid method is particularly useful for extracting thermally unstable compounds, as natural pigments [16,19,44]. The efficiency of MW pretreatment depends on several factors of optimization, including the selection of solvent, sample matrix, target compound, extraction time, temperature, and MW power [16].

However, it is important to note that the solvents used in the MW process are not highly selective, extracting a wide range of compounds with varying polarities [19]. To enhance selectivity, the MW process is often combined with other pretreatment (*e.g.* maceration, blanching, or cold soaking) or selective extraction processes [8]. This process integration helps to optimize

the extraction yield while maintaining the selectivity of the process and the stability of the extracted pigments.

6.1.2. COMPRESSED FLUID-BASED EXTRACTION AND DOWNSTREAM PURIFICATION

6.1.2.1. SUPERCRITICAL FLUID EXTRACTION

SFE is an environmentally friendly separation process based on the use of supercritical fluids as an alternative to organic solvents to extract target components from a solid matrix [84,85]. A supercritical fluid is defined as a substance above its critical temperature and pressure, exhibiting low viscosity and relatively high diffusivity, which provide appreciable penetrating power in the solid matrix with a rapid mass transfer rate [86–90]. Moreover, supercritical fluids have a density close to liquids that can be easily modified by tuning the pressure and the temperature [86,88–90]. Generally, the targeted compound solubility increases with the increase of the extraction pressure, which is directly a result of the increased solvent density [90,91]. The effect of extraction temperature is more complex and at constant pressure, an increase in temperature increases the targeted compound solubility in supercritical fluids due to solute vapor pressure enhancement. On the other hand, an increase in temperature also decreases the solvent density, reducing the solubility of the targeted compound in the supercritical fluid. This results in a phenomenon called the “crossover effect” where the targeted compound solubility is no longer dependent on the supercritical fluid density [91]. Therefore, these properties enable to fine-tune the solvent extracting power and selectivity of a supercritical fluid toward a target compound.

Although several fluids have been used for SFE, carbon dioxide (CO_2) is by far the most attractive and has been most widely used in food applications. CO_2 presents several advantages including mild critical conditions (31.1 °C and 73.8 bar) that are easily attainable, non-toxic, non-inflammable, non-explosive, relatively inert to several media, inexpensive, and readily available in pure form [86,88–93]. Due to these characteristics, the European Food Safety Authority and the United States Food and Drug Administration have assigned CO_2 as a generally recognized as safe (GRAS) solvent. In addition, the extraction processes using supercritical CO_2 preserve the bioactivity of the compounds due to the absence of light and oxygen in the system and low operating temperatures [94]. Moreover, the separation of compounds using supercritical CO_2 is clean with little-to-no residue as the solvent is gaseous at room temperature and pressure [88,89,91]. Furthermore, since CO_2 gas streams can be recycled, supercritical extraction using CO_2 can be regarded as an environmentally friendly process [87,90].

However, supercritical CO_2 is not suitable for the extraction of polar compounds due to its low polarity [91]. Hence, the addition of a modifier can significantly improve the extraction efficiency of polar substances. These polar co-solvents are added in small amounts to induce substantial changes in the solvent properties of pure supercritical CO_2 [87]. The target compound solubility in the supercritical CO_2 is enhanced as a consequence of positive hydrogen bonding interactions between co-solvent and polar solutes in the supercritical phase [86,89]. Within organic solvents, ethanol is the most environmentally favorable and healthy, being accepted as a “biosolvent” for food applications [93]. The primary limitations of direct industrial SFE application are the high investment cost and the need for qualified manpower. For this reason, SFE should be only considered for high added

value products or those that require compliance with strict environmental regulations [86,94].

SFE process is divided in two main steps (Figure 6): (1) dissolution of target compounds that are present on the solid matrix by the supercritical fluid and (2) separation of the extracted compounds from the supercritical fluid after the expansion [87,95]. During SFE, the supercritical fluid is pressurized and heated through a solvent pump and a heat exchange before entering the extractor. The desired extraction conditions are maintained by the operation of a back pressure regulating valve and temperature controllers attached to the extraction vessel [96]. The supercritical solvent is absorbed by the raw material, promoting the dilatation of the matrix structures, increasing the extraction rate. Simultaneously, the soluble compounds are dissolved by the supercritical solvent. Afterwards, the separation of the solute from the supercritical fluid is achieved in the separator by pressure reduction and/or temperature increase, yielding a solvent-free extract. The extract is consequently collected at the separator and the gas can be recycled or released to the atmosphere [95].

SFE represents an interesting alternative technique to conventional extraction for industrial applications. The first successful industrial application was the decaffeination of coffee beans using supercritical CO_2, patented in 1964. Currently, the use of supercritical fluids is widely applied in different industrial processes including the extraction of flavors, essential oils, algae, and biodiesel.

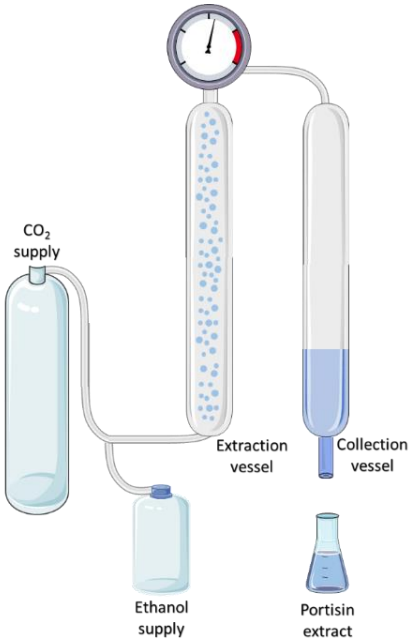

Figure 6. Schematic illustration of the compressed fluid-based extraction process. This figure was created with some free images available on the Smart Servier Medical Art website (https://smart.servier.com, last accessed on 22 December 2021).

6.1.2.2. PRESSURIZED LIQUID EXTRACTION

PLE, also known as accelerated solvent extraction in the analytical extraction area, pressurized fluid extraction, pressurized solvent extraction, or enhanced solvent extraction, is an alternative solid–liquid extraction process based on the use of organic solvents at elevated temperature and pressure (always below their critical point) for the recovery of bioactive compounds from natural matrices [85,97,98]. Subcritical extractions are carried out under high pressure to maintain the liquid state of the solvent, allowing extraction temperatures above its boiling point [99].

Elevating the temperatures of solvents above their atmospheric boiling points generally promotes higher target compound solubility by increasing both diffusion and mass transfer rate between the matrix and the solvent, coupled with the solvent ability to disrupt the target compound-matrix interactions [99]. Moreover, high temperatures reduce the viscosity and surface tension of the solvent and facilitate the extraction rate. On the other hand, high pressure forces solvent into matrix pores, allowing better contact between the solvent and the targeted compounds [83,99,100]. Therefore, the combined use of high pressures and temperatures provides a faster extraction process, reduced solvent consumption, and high extraction efficiencies with improved recovery rates compared to conventional techniques [97,99,101].

The solvent selection is based on the solubility characteristics of the target compound. Pressurized solvents present great flexibility due to the solvent physical–chemical properties, namely the viscosity, diffusivity, density, and dielectric constant. These properties can be tailored by adjusting the temperature and the pressure of the system [101]. The solvents most applied are water, ethanol, and their mixtures. Consequently, PLE shown to be effective when extracting both polar and moderately non-polar compounds from different matrices [98,102].

During the PLE process, the sample is placed into the extraction vessel, and the solvent is pressurized and heated until the desired combination of pressure and temperature variables is reached [96]. The extraction process can be accomplished in two modes: static or dynamic. In the static mode, after the extraction time, the system is rinsed with fresh solvent to transfer the extract to the collection vessel. In the dynamic mode, the fresh solvent is continuously pumped at a selected flow rate for a fixed period. During the

extraction process, extract fractions are collected in the collection vessel. In both operating modes, the mass transfer rates are accelerated according to Fick's law of diffusion [99].

PLE offers an alternative to conventional solvent extractions, due to the short time of extraction, and inert environment under high pressure and temperature [103]. Additionally, PLE is considered a potential alternative technique to SFE for the extraction of polar compounds. Moreover, owing to the limited use of organic solvents, PLE is considered a green extraction technique [104]. Therefore, PLE holds commercial interest as an alternative method for extracting bioactive compounds from natural sources.

6.1.3. CENTRIFUGAL PARTITION CHROMATOGRAPHY DOWNSTREAM PURIFICATION

Counter-current chromatography is a support-free liquid–liquid chromatography based on the differential partitioning of compounds between two immiscible liquid phases of a solvent system. One of the phases is applied as a liquid stationary phase while the other is a mobile liquid phase [105]. During counter-current chromatography separation, the stationary phase is maintained in the column without the use of any solid support, whereas the immiscible mobile phase is pumped through the stationary phase. The countercurrent chromatography column consists of a rotor containing a series of tubes or chambers connected by ducts, where the two immiscible liquid phases are repeatedly mixed and settled (Figure 7) [106]. The different constituents of the sample are partitioned between two phases and eluted from the column at different times, according to their partition coefficient (K) [107].

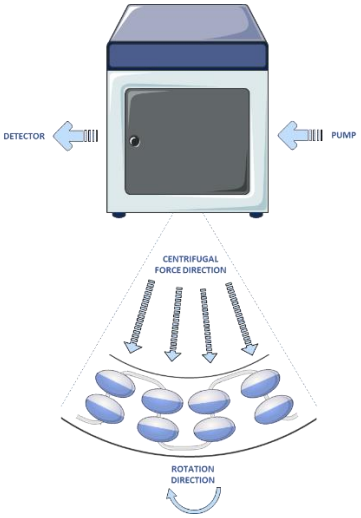

Figure 7. Schematic illustration of the counter-current chromatography process. This figure was made with some free images available on the Smart Servier Medical Art website (https://smart.servier.com, last accessed on 22 December 2021).

In the modern counter-current chromatography techniques, introduced in the 1980s, centrifugal force fields are used to maintain the stationary phase inside the column. According to the different principles of fluid mechanics, modern counter-current chromatography systems can be classified into hydrodynamic, such as high-speed counter-current chromatography (HSCCC) [108,109], or hydrostatic, such as CPC [110]. Hydrodynamic counter-current chromatography systems, pursued by Ito in the USA, are based on a variable centrifugal force field. The column contains one or several multilayer coils of open tubing mounted in a rotor that will induce a planetary rotation mode of the coils. The coils rotate around their axis which at the same time rotates around the central axis of the rotor [108]. Therefore, this technique is also known as multilayer coil countercurrent chromatography. In hydrostatic counter-current chromatography systems, pursued by Nunogaki in Japan, the

column retains the liquid stationary phase in small chambers working with a constant centrifugal force field produced by a single axis rotation mechanism. The column comprises a series of channels connected in cascade by ducts and aligned in cartridges or disks in a rotor [111].

Comparing both counter-current chromatography systems, HSCCC columns are more efficient due to the number of theoretical plates, providing sharper peaks [112]. However, the retention of biphasic solvent systems with slight density differences between the phases is low [105]. In contrast, CPC columns are usually more effective at retaining a broader range of biphasic solvent systems, particularly the aqueous two-phase solvent system or some very hydrophilic systems. Moreover, the retention of the stationary phase during the disruption of the equilibrium caused by high loadings and complex matrices is still high [112]. In addition, the CPC system allows working with faster mobile phase flow rates, reducing the separation time [105]. CPC apparatuses are easier to scale up without losing the chromatographic resolution. Nevertheless, CPC instrumentation is more expensive than HSCCC [111,113].

The liquid nature of the stationary phase presents several advantages when compared with the conventional chromatography techniques with a solid stationary phase. In the countercurrent chromatography column, the stationary phase available for interaction with the solute can be higher than 80%, while in HPLC is only 20% [114], giving higher sample loading capacity and limiting the column overloading [105,115]. Moreover, the sample loss caused by irreversible adsorption associated with the solid matrix is avoided. Therefore, counter-current chromatography is characterized by high sample recovery without chemical modifications or loss of biological activity [115]. In addition, a multiple choice of biphasic solvent systems can be used in

counter-current chromatography. This enables a large choice of solvents that can be employed with a varying polarity that can ensure the proper dissolution of the target compounds. Thus, the crude extract can be loaded into the system without any clean-up pretreatment [116,117]. Moreover, the liquid stationary phase is more stable in acidic or basic conditions than silica-based supports [118]. Although counter-current chromatography efficiency is lower than HPLC, the high selectivity and the high stationary to mobile phase ratio largely compensate once both have a positive effect on the resolution between the peaks [114]. From an economical point of view, counter-current chromatography has a relatively low cost of operation and maintenance by simplifying processing steps, decreasing solvent consumption (10 times less than for HPLC and dispensing expensive solid-support materials [111,117,119,120]. Once the initial investment in an instrument has been made, a set of coils would be expected to last the lifetime of the centrifuge. There are no column aging effects as a freshly filled column of solvents is used in each experiment [117,121].

Despite many advantages, counter-current chromatography presents challenges associated with the retention of the liquid stationary phase in the column. The stability of the stationary phase volume available to interact with the sample components is affected by the counter-current chromatography column characteristics (column volume, tube/chamber number, size, and shape), biphasic solvent system properties (density, viscosity, interfacial tension) and operating conditions (choice of mobile and stationary phases, mobile phase flow rate, rotational speed, and temperature) [122]. In fact, the separation efficiency and reproducibility are strongly dependent on the ability to retain the stationary phase. Consequently, optimization of the biphasic solvent system and operating conditions is required for a successful counter-current chromatography separation.

6.2. *FORMULATION*

To improve the stability and potential application of natural pigments, a deliberate selection of suitable encapsulation techniques is of crucial importance. The encapsulation of natural pigments has traditionally been done using conventional techniques. Coacervation, spray-drying, and emulsification are traditional methods recognized for their practicability, economic viability, and widespread implementation [20,48]. Table 5 compares the advantages and limitations of these encapsulation methods.

Table 5. Advantages and limitations of different encapsulation methods commonly applied to natural pigments. Adapted from [123].

Encapsulation method	Particle size (µm)	Advantages	Limitations
Coacervation	20-200	High encapsulation efficiency	Expensive method
		Efficient control of particle size	Aggregation of particles
		Simple	Hard scaling-up
		Versatile	Evaporation of volatiles
Spray drying	1-50	Low process cost	Particles no uniform
		Easy scaling-up technique	Low oil loading level
		Small droplets	Require further processing
		Narrow particle size distribution	Possibility of lost low-boiling point aromatics
Emulsification	0.1-100	Suitable for biodegradable and non-biodegradable polymeric micro-particles, and a wide range of liquid and solid core materials	Low encapsulation efficiency
			Production of high quantity residual solvent
			Expensive method

Spray drying of emulsions was the encapsulation technology used in the present thesis and the one that will be further described.

6.3. SPRAY-DRYING ENCAPSULATION

Spray drying is a widely used method in the food industry [124]. Although this technique is commonly known as a dehydration process, it is also widely recognized as a reliable method for microencapsulation [125]. In fact, microencapsulation by spray dryer is considered the oldest encapsulation method for food ingredients [126]. In 1930, spray drying was first employed to produce encapsulated flavors using acacia as wall material [127]. Since then, research papers focused on spray drying microencapsulation of bioactive compounds have substantially increased [128].

The key principle of the spray drying process involves covering the bioactive substances with a surrounding material, producing high-quality powders, easy to use, with excellent protection properties, stabilization, solubility, and controlled delivery of bioactive compounds [24,48,124,128]. Also, they present minimal transportation and storage costs due to the powdered form of the final product [126]. The resulting microstructures can be influenced by several factors, including the type of wall materials (e.g., polysaccharides, gums, and proteins), core material (e.g., hydrophilic and hydrophobic), and spray drying operating parameters (e.g., inlet and outlet temperatures, flow rate, and atomizer type) [124].

When selecting wall materials for food application, it is important to choose food-grade materials that are approved by regulatory authorities such as the FDA and EFSA or those certified as GRAS. Compared to pharmaceutical or cosmetic products, the options for wall materials in food products are more

limited due to the stricter regulations and lower profit margins for food additives. Even though, numerous commercially available materials can be used as wall materials for spray drying including gums, proteins, and polysaccharides [48,124].

The efficient wall material for spray drying microencapsulation in food applications should present excellent functional properties such as emulsifying, gel- and film-forming ability, high solubility, and low cost. Additionally, the wall material should meet specific criteria such as specific molecular weight, melting point, biodegradability, resistance to the gastrointestinal tract, ease of handling, low hygroscopicity, and the ability to form a protective barrier between the internal and external phases. This barrier is crucial to protect the core material from environmental conditions including moisture, heat, light, oxygen, pH, and other compounds [48,124].

The solubility of the core material, whether hydrophilic or hydrophobic, also plays an important role in the selection of the wall material. For hydrophilic compounds, the feed solution can be prepared simply by mixing the core material with dissolved wall material. On the other hand, for hydrophobic substances, the feed solution consists of mixtures of emulsified core material and dissolved wall materials [124,126]. The emulsification of core material in the feed solution utilizes emulsifiers to stabilize droplets by reducing the interfacial tension. Two common techniques used for this purpose are high-speed and high-pressure homogenization. High-speed homogenization applies mechanical forces, such as high shear forces, to break up larger droplets. On the other hand, high-pressure homogenization relies on the pressure to create turbulence and cavitation, leading to the breakdown of larger droplets [125,129].

To ensure the quality and prevent degradation of natural compounds, careful monitoring of the spray drying process conditions is crucial. Proper identification of the main objective and application of optimization methods are essential. Optimal process conditions in the encapsulation process by spray drying enhance encapsulation efficiency, minimize the loss of bioactive compounds, and reduce stickiness. Therefore, parameters such as feed solution flow rate, inlet and outlet air temperatures, airflow rate, and atomization conditions should be optimized [125].

As depicted in Figure 8, the spray drying process involves the use of spray drying equipment, which consists of components such as a feed pump, atomizer or spray nozzle, air heater, air dispenser, drying chamber, and system for exhaust air cleaning and powder recovery [126].

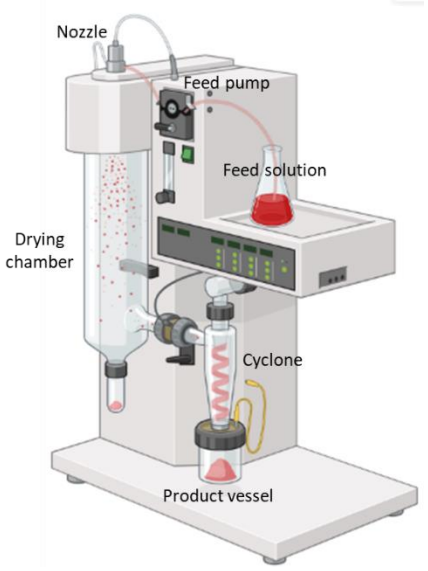

Figure 8. Schematic illustration of the spray drying process. This figure was created using BioRender software (http://biorender.com, last accessed on 12 July 2023).

This microencapsulation technique involves four main steps: (1) preparation of the feed solution to ensure the dissolution of the core and wall materials in water, (2) homogenization of the solution, dispersion or emulsion to guarantee uniform distribution of core and wall materials, (3) atomization of the feed solution into the drying chamber, where it comes in contact with a hot stream gas, and (4) dehydration of the atomized particles, where the droplets encounter the hot gas and the solvent rapidly evaporates, resulting in the production of dry solid particles [48,126].

Microencapsulation by spray drying is a commonly employed strategy to overcome the limitations faced when incorporating natural pigments into various functional food systems. These limitations include conditioned solubility, inferior thermal and chemical stability, unpleasant flavor, and limited bioaccessibility and bioavailability [24,128]. In comparison to other techniques, spray drying offers advantages such as ease of operation and cost-effectiveness. It is particularly suitable for encapsulating heat sensitive substances like natural pigments as the residence times of particles in the chamber are very short ensuring low particle temperature despite the contact with hot air [48]. Also, the evaporation of the solvent during the spray drying creates a cooling effect that prevents the temperature of the final powder from exceeding its wet bulb temperature [128]. Additionally, it offers large-scale production capacities, high encapsulation efficiency when operating parameters are adjusted properly, and the ability to use wall materials from different sources [130].

7. OBJECTIVES

The main goal of this thesis was to develop suitable strategies to address technological demands and challenges associated with the application of natural colorants in the food industry, as well as efficiently utilizing agricultural and food processing waste. This thesis was conducted in response to the specific demands and challenges: (1) limited availability of natural blue colorants, (2) scarcity of natural astaxanthin, and (3) conditioned solubility of carotenoids. The approach to overcome the challenges is highlighted in Table 6.

To achieve these goals the following specific objectives were accomplished:

1. Optimization of efficient and sustainable alternatives for the preparative-scale downstream purification of portisins:

(i) Selection of the feedstock, specifically blueberry surplus,

(ii) Extraction of anthocyanins,

(iii) Hemi-synthesis of portisins,

(iv) Downstream isolation of portisins using alternative technologies, such as CPC and compressed fluid-based extraction,

(v) Chemical characterization of the resulting bio-based products including identification and quantification of portisins,

(vi) Performance evaluation of the separation processes, considering factors such as throughput, efficiency, and environmental impact.

Table 6. Strategies to overcome specific demands and challenges associated with the application of natural colorants in the food industry.

Aim	Raw material	Natural pigment	Structure	Color
Develop a naturally derived blue pigment to meet the demand for a vibrant blue color	Blueberry surplus	Portisins	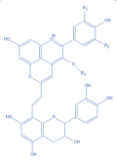	
Explore a new source of highly demanded astaxanthin	Crab residues	Astaxanthin	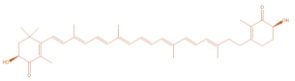	
Develop a hydrosoluble form of carotenoids to improve solubility in water-based food products	Microalgae	Carotenoids (β-carotene)		

2. Optimization of an effective process strategy to recover astaxanthin from alternative raw material, based on SFE using MW pretreatment:

(i) Selection of the biomass, specifically crustacean waste streams,

(ii) MW pretreatment of crab residues,

(iii) Isolation of astaxanthin using SFE,

(iv) Chemical characterization of the resulting bio-based products, including identification and quantification of astaxanthin.

3. Formulation of carotenoids recovered from microalgae biomass by emulsification followed by a spray drying step:

(i) Selection of the biomass, specifically *Dunaliella salina* extract,

(ii) Emulsification of carotenoid-rich extract,

(iii) Characterization of the resulting emulsions, including droplet size, morphology, and stability,

(iv) Spray drying of emulsions,

(v) Characterization of the resulting particles, including quantification of carotenoids, color properties, and particle size,

(vi) Incorporation of the resulting particles into a water-based food product.

8. OUTLINE

This thesis is divided into four chapters, as shown in Figure 9. The structure of the thesis follows the various stages of research conducted during the Ph.D. project.

Chapter 1 provides an overview of the current state-of-the-art, background information, and key concepts related to the scope of the thesis. Chapter 1 also presents the main objectives of the Ph.D. project.

Chapter 2 is divided into two parts and describes the development of alternative strategies for downstream isolation of bluish anthocyanin-derived pigments obtained from agricultural waste generated during blueberry crop production and harvesting.

Part I concerns the recovery of anthocyanins from blueberry surplus, hemi-synthesis of respective anthocyanin derivatives, and downstream isolation of portisins using CPC. This part provides the optimization of the separation conditions to improve the portisins content, process throughput, efficiency,

and environmental risk factor. Furthermore, Part I also contains a comparison between the proposed technique and conventional reverse-phase column chromatography.

Part II focuses on the separation of portisins using a compressed fluid-based extraction process. This part provides the optimization of the isolation conditions to increase the portisins content, process throughput, efficiency, and environmental risk factor. Additionally, Part II also includes a comparison of the explored technique with the different purification methods presented in Chapter 2 Part I.

Chapter 3 reports the isolation and formulation of orange carotenoid-derived pigments obtained from alternative marine sources.

Part I includes the extraction of astaxanthin pigments from crustacean waste streams, integrating MW pretreatment with SFE. This part provides the optimization of the pretreatment and extraction conditions to enhance the yield and content of astaxanthin. MW pretreatment was also tested in combination with conventional solvent extraction. Additionally, Part I also includes a comparison of the different extraction strategies explored.

Part II consists of the encapsulation of carotenoid pigments from microalgae biomass, integrating emulsification with spray drying. This part includes not only the investigation of the most favorable encapsulation conditions but also a detailed characterization of the emulsions and powders. Furthermore, Part II also contains a proof of concept: the incorporation of the developed water-soluble forms of carotenoids in an aqueous-based food product, namely jelly.

Chapter 4 provides an overview of the most relevant findings. The results are discussed in an integrated manner, highlighting the major advancements and

conclusions. Additionally, this chapter presents and discusses perspectives for future developments.

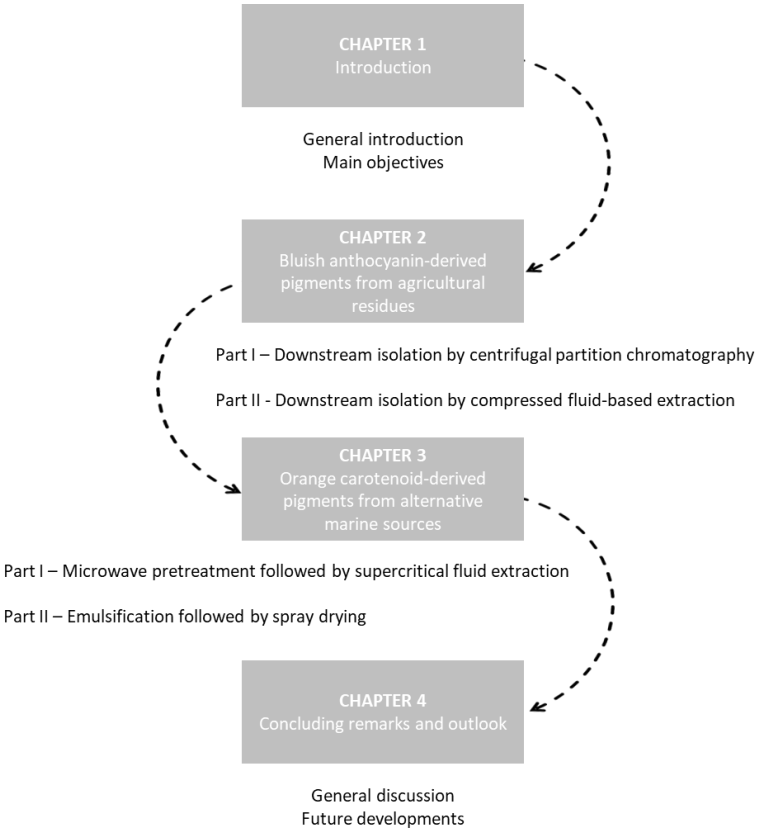

Figure 9. Schematic representation of the thesis layout.

According to Regulation n. º 377/2013, published in Diário da República on October 2, 2013, and considering that this Ph.D. thesis is based on scientific articles that have been published, submitted, or being prepared for publication, each chapter part (from Chapter 2 to Chapter 3) is structured as a manuscript format. This format includes an abstract summarizing the investigation performed, a brief review of the state-of-the-art, a materials

and methods section, a results and discussion section, significant conclusions, and the corresponding acknowledgments and references. It is important to note that this thesis does not include a comprehensive list of figures, tables, or abbreviations. Instead, all figure and table captions are accompanied by clear captions, and abbreviations and symbols are explicitly identified and explained within each chapter section. Abbreviations are defined within parenthesis the first time they are mentioned in the main text of each chapter section and are consistently used thereafter.

9. REFERENCES

[1] United Nations Sustainable Development, (n.d.). https://www.un.org/sustainabledevelopment/.

[2] C. Novais, A.K. Molina, R.M.V. Abreu, C. Santo-Buelga, I.C.F.R. Ferreira, C. Pereira, L. Barros, Natural Food Colorants and Preservatives: A Review, a Demand, and a Challenge, J. Agric. Food Chem. 70 (2022) 2789–2805. https://doi.org/10.1021/acs.jafc.1c07533.

[3] M. Carocho, P. Morales, I.C.F.R. Ferreira, Natural food additives: Quo vadis?, Trends Food Sci. Technol. 45 (2015) 284–295. https://doi.org/10.1016/j.tifs.2015.06.007.

[4] L. Sun, F. Xin, H.S. Alper, Bio-synthesis of food additives and colorants-a growing trend in future food, Biotechnol. Adv. 47 (2021) 107694. https://doi.org/10.1016/j.biotechadv.2020.107694.

[5] FDA, Overview of Food Ingredients, Additives & Colors, (2021). https://doi.org/https://www.fda.gov/food/food-ingredients-

packaging/overview-food-ingredients-additives-colors#foodadd.

[6] A.A.F. Zielinski, A. del P. Sanchez-Camargo, L. Benvenutti, D.M. Ferro, J.L. Dias, S.R.S. Ferreira, High-pressure fluid technologies: Recent approaches to the production of natural pigments for food and pharmaceutical applications, Trends Food Sci. Technol. 118 (2021) 850–869. https://doi.org/10.1016/j.tifs.2021.11.008.

[7] M. Faustino, M. Veiga, P. Sousa, E.M. Costa, S. Silva, M. Pintado, Agro-food byproducts as a new source of natural food additives, Molecules. 24 (2019) 1–23. https://doi.org/10.3390/molecules24061056.

[8] L. Cassani, N.E. Marcovich, A. Gomez-Zavaglia, Valorization of fruit and vegetables agro-wastes for the sustainable production of carotenoid-based colorants with enhanced bioavailability, Food Res. Int. 152 (2022) 110924. https://doi.org/10.1016/j.foodres.2021.110924.

[9] I. Viera, A. Pérez-Gálvez, M. Roca, Green natural colorants, Molecules. 24 (2019). https://doi.org/10.3390/molecules24010154.

[10] G.T. Sigurdson, P. Tang, M.M. Giusti, Natural Colorants: Food Colorants from Natural Sources, Annu. Rev. Food Sci. Technol. 8 (2017) 261–280. https://doi.org/10.1146/annurev-food-030216-025923.

[11] T. Singh, V.K. Pandey, K.K. Dash, S. Zanwar, R. Singh, Natural bio-colorant and pigments: Sources and applications in food processing, J. Agric. Food Res. 12 (2023) 100628. https://doi.org/10.1016/j.jafr.2023.100628.

[12] M. Oplatowska-Stachowiak, C.T. Elliott, Food colors: Existing and

emerging food safety concerns, Crit. Rev. Food Sci. Nutr. 57 (2017) 524–548. https://doi.org/10.1080/10408398.2014.889652.

[13] A.F. Vinha, F. Rodrigues, M.A. Nunes, M.B.P.P. Oliveira, Natural pigments and colorants in foods and beverages, Elsevier Inc., 2018. https://doi.org/10.1016/B978-0-12-813572-3.00011-7.

[14] M. Sharma, Z. Usmani, V.K. Gupta, R. Bhat, Valorization of fruits and vegetable wastes and by-products to produce natural pigments, Crit. Rev. Biotechnol. 41 (2021) 535–563. https://doi.org/10.1080/07388551.2021.1873240.

[15] M. Isabel Landim Neves, E. Keven Silva, M. Angela A. Meireles, Trends and Challenges in the Industrialization of Natural Colorants, Food Public Heal. 9 (2019) 33–44. https://doi.org/10.5923/j.fph.20190902.01.

[16] S. Yadav, K.S. Tiwari, C. Gupta, M.K. Tiwari, A. Khan, S.P. Sonkar, A brief review on natural dyes, pigments: Recent advances and future perspectives, Results Chem. 5 (2023) 100733. https://doi.org/10.1016/j.rechem.2022.100733.

[17] L. de Boer, Biotechnological production of colorants, Adv. Biochem. Eng. Biotechnol. 143 (2013) 51–89. https://doi.org/10.1007/10_2013_241.

[18] J.A. Fernández-López, V. Fernández-Lledó, J.M. Angosto, New insights into red plant pigments: More than just natural colorants, RSC Adv. 10 (2020) 24669–24682. https://doi.org/10.1039/d0ra03514a.

[19] I. Benucci, C. Lombardelli, C. Mazzocchi, M. Esti, Natural colorants from vegetable food waste: Recovery, regulatory aspects, and

stability—A review, Compr. Rev. Food Sci. Food Saf. 21 (2022) 2715–2737. https://doi.org/10.1111/1541-4337.12951.

[20] I. Luzardo-Ocampo, A.K. Ramírez-Jiménez, J. Yañez, L. Mojica, D.A. Luna-Vital, Technological applications of natural colorants in food systems: A review, Foods. 10 (2021) 1–34. https://doi.org/10.3390/foods10030634.

[21] T. Coultate, R.S. Blackburn, Food colorants: their past, present and future, Color. Technol. 134 (2018) 165–186. https://doi.org/10.1111/cote.12334.

[22] M.I. Landim Neves, E.K. Silva, M.A.A. Meireles, Natural blue food colorants: Consumer acceptance, current alternatives, trends, challenges, and future strategies, Trends Food Sci. Technol. 112 (2021) 163–173. https://doi.org/10.1016/j.tifs.2021.03.023.

[23] T. Imchen, K.S. Singh, Marine algae colorants: Antioxidant, anti-diabetic properties and applications in food industry, Algal Res. 69 (2023) 102898. https://doi.org/10.1016/j.algal.2022.102898.

[24] S. Ghosh, T. Sarkar, A. Das, R. Chakraborty, Natural colorants from plant pigments and their encapsulation: An emerging window for the food industry, Lwt. 153 (2022) 112527. https://doi.org/10.1016/j.lwt.2021.112527.

[25] S. Jurić, M. Jurić, Ż. Król-Kilińska, K. Vlahoviček-Kahlina, M. Vinceković, V. Dragović-Uzelac, F. Donsì, Sources, stability, encapsulation and application of natural pigments in foods, Food Rev. Int. 38 (2022) 1735–1790. https://doi.org/10.1080/87559129.2020.1837862.

[26] M.C. dos Santos, J.L. Bicas, Natural blue pigments and bikaverin,

Microbiol. Res. 244 (2021) 126653. https://doi.org/10.1016/j.micres.2020.126653.

[27] E.G. De Mejia, Q. Zhang, K. Penta, A. Eroglu, M.A. Lila, The Colors of Health: Chemistry, Bioactivity, and Market Demand for Colorful Foods and Natural Food Sources of Colorants, Annu. Rev. Food Sci. Technol. 11 (2020) 145–182. https://doi.org/10.1146/annurev-food-032519-051729.

[28] W. Kalt, A. Cassidy, L.R. Howard, R. Krikorian, A.J. Stull, F. Tremblay, R. Zamora-Ros, Recent Research on the Health Benefits of Blueberries and Their Anthocyanins, Adv. Nutr. 11 (2020) 224–236. https://doi.org/10.1093/advances/nmz065.

[29] W. Yang, Y. Guo, M. Liu, X. Chen, X. Xiao, S. Wang, P. Gong, Y. Ma, F. Chen, Structure and function of blueberry anthocyanins: A review of recent advances, J. Funct. Foods. 88 (2022) 104864. https://doi.org/10.1016/j.jff.2021.104864.

[30] N. Mateus, A.M.S. Silva, J.C. Rivas-Gonzalo, C. Santos-Buelga, V. de Freitas, A New Class of Blue Anthocyanin-Derived Pigments Isolated from Red Wines, 40 (2003) 1919–1923. https://doi.org/10.1021/JF020943A.

[31] A.G. Tarone, C.B.B. Cazarin, M.R. Marostica Junior, Anthocyanins: New techniques and challenges in microencapsulation, Food Res. Int. 133 (2020). https://doi.org/10.1016/j.foodres.2020.109092.

[32] K. Gould, K.M. Davies, C. Winefield, Anthcyanins Biosynthesis, Functions and Applications, 2009. https://doi.org/10.1007/978-0-387-77335-3.

[33] F. Pina, N. Basílio, A.J. Parola, M.J. Melo, J. Oliveira, V. De Freitas, The Triumph of the Blue in Nature and in Anthropocene, Dye. Pigment. 210 (2023) 110925. https://doi.org/10.1016/j.dyepig.2022.110925.

[34] J. Oliveira, C. Santos-Buelga, A.M.S. Silva, V. De Freitas, N. Mateus, Chromatic and structural features of blue anthocyanin-derived pigments present in Port wine, Anal. Chim. Acta. 563 (2006) 2–9. https://doi.org/10.1016/j.aca.2005.11.027.

[35] N. Mateus, J. Oliveira, M. Haettich-Motta, V. de Freitas, New Family of Bluish Pyranoanthocyanins, J. Biomed. Biotechnol. 2004 (2004) 299–305. https://doi.org/10.1155/S1110724304404033.

[36] J. Oliveira, N. Mateus, V. De Freitas, Wine-Inspired Chemistry: Anthocyanin Transformations for a Portfolio of Natural Colors, Synlett. 28 (2017) 898–906. https://doi.org/10.1055/s-0036-1589937.

[37] A.G. Newsome, C.A. Culver, R.B. Van Breemen, Nature's palette: The search for natural blue colorants, J. Agric. Food Chem. 62 (2014) 6498–6511. https://doi.org/10.1021/jf501419q.

[38] N. Mateus, A.M.S. Silva, J.C. Rivas-Gonzalo, C. Santos-Buelga, V. De Freitas, A new class of blue anthocyanin-derived pigments isolated from red wines, J. Agric. Food Chem. 51 (2003) 1919–1923. https://doi.org/10.1021/jf020943a.

[39] J. Oliveira, V. De Freitas, A.M.S. Silva, N. Mateus, Reaction between hydroxycinnamic acids and anthocyanin-pyruvic acid adducts yielding new portisins, J. Agric. Food Chem. 55 (2007) 6349–6356. https://doi.org/10.1021/jf070968f.

[40] A. Faria, J. Oliveira, P. Neves, P. Gameiro, C. Santos-Buelga, V. De Freitas, N. Mateus, Antioxidant properties of prepared blueberry (Vaccinium myrtillus) extracts, J. Agric. Food Chem. 53 (2005) 6896–6902. https://doi.org/10.1021/jf0511300.

[41] A. Faria, D. Pestana, R. Monteiro, J. Oliveira, V. de Freitas, I. Azevedo, C. Calhau, N. Mateus, Influence of anthocyanins and derivative pigments from blueberry (*Vaccinium myrtillus*) extracts on MPP+ intestinal uptake: A structure-activity approach, Food Chem. 109 (2008) 587–594. https://doi.org/10.1016/j.foodchem.2008.01.009.

[42] Y. Xu, D. Hu, Y. Li, C. Sun, W. Chen, An effective method for preparation of high-purity pelargonidin-3-O-glucoside from strawberry and its protective effect on cellular oxidative stress, J. Chromatogr. B Anal. Technol. Biomed. Life Sci. 1072 (2018) 211–220. https://doi.org/10.1016/j.jchromb.2017.11.025.

[43] F. Qiu, J. Luo, S. Yao, L. Ma, L. Kong, Preparative isolation and purification of anthocyanins from purple sweet potato by high-speed counter-current chromatography, J. Sep. Sci. 32 (2009) 2146–2151. https://doi.org/10.1002/jssc.200900038.

[44] M. Manzoor, J. Singh, A. Gani, N. Noor, Valorization of natural colors as health-promoting bioactive compounds: Phytochemical profile, extraction techniques, and pharmacological perspectives, Food Chem. 362 (2021) 130141. https://doi.org/10.1016/j.foodchem.2021.130141.

[45] R.K. Saini, Y.-S. Keum, Carotenoid extraction methods: A review of recent developments, Food Chem. 240 (2018) 90–103. https://doi.org/10.1016/j.foodchem.2017.07.099.

[46] H. Papapostolou, V. Kachrimanidou, M. Alexandri, S. Plessas, A. Papadaki, N. Kopsahelis, Natural Carotenoids: Recent Advances on Separation from Microbial Biomass and Methods of Analysis, Antioxidants. 12 (2023). https://doi.org/10.3390/antiox12051030.

[47] S. Singh, V. Aeri, V. Sharma, Encapsulated natural pigments: Techniques and applications, J. Food Process Eng. (2023) 1–19. https://doi.org/10.1111/jfpe.14311.

[48] M.A. González-Peña, A.E. Ortega-Regules, C. Anaya de Parrodi, J.D. Lozada-Ramírez, Chemistry, Occurrence, Properties, Applications, and Encapsulation of Carotenoids—A Review, Plants. 12 (2023) 1–22. https://doi.org/10.3390/plants12020313.

[49] J. Sanchez Lopez, C. Caldeira, V. Laurentiis, S. Sala, Brief on food waste in the European Union, (2020) 1–12.

[50] H. Xue, X. Zhu, J. Tan, L. Fan, Q. Li, J. Tang, X. Cai, Counter-current fractionation-assisted bioassay-guided separation of active compound from blueberry and the interaction between the active compound and α-glucosidase, Foods. 10 (2021). https://doi.org/10.3390/foods10030509.

[51] S. Silva, E.M. Costa, M. Veiga, R.M. Morais, C. Calhau, M. Pintado, Health promoting properties of blueberries: a review, Crit. Rev. Food Sci. Nutr. 60 (2020) 181–200. https://doi.org/10.1080/10408398.2018.1518895.

[52] H. Yang, Y. Wu, C. Zhang, W. Wu, L. Lyu, W. Li, Growth and physiological characteristics of four blueberry cultivars under different high soil pH treatments, Environ. Exp. Bot. 197 (2022) 104842. https://doi.org/10.1016/j.envexpbot.2022.104842.

[53] H. Liu, S. Qin, R. Sirohi, V. Ahluwalia, Y. Zhou, R. Sindhu, P. Binod, R. Rani Singhnia, A. Kumar Patel, A. Juneja, D. Kumar, Z. Zhang, J. Kumar, M.J. Taherzadeh, M. Kumar Awasthi, Sustainable blueberry waste recycling towards biorefinery strategy and circular bioeconomy: A review, Bioresour. Technol. 332 (2021) 125181. https://doi.org/10.1016/j.biortech.2021.125181.

[54] Y. Duan, A. Tarafdar, D. Chaurasia, A. Singh, P.C. Bhargava, J. Yang, Z. Li, X. Ni, Y. Tian, H. Li, M.K. Awasthi, Blueberry fruit valorization and valuable constituents: A review, Int. J. Food Microbiol. 381 (2022) 109890. https://doi.org/10.1016/j.ijfoodmicro.2022.109890.

[55] A.M. Mustafa, S. Angeloni, D. Abouelenein, L. Acquaticci, J. Xiao, G. Sagratini, F. Maggi, S. Vittori, G. Caprioli, A new HPLC-MS/MS method for the simultaneous determination of 36 polyphenols in blueberry, strawberry and their commercial products and determination of antioxidant activity, Food Chem. 367 (2022) 130743. https://doi.org/10.1016/j.foodchem.2021.130743.

[56] C. Bas-Bellver, C. Andrés, L. Seguí, C. Barrera, N. Jiménez-Hernández, A. Artacho, N. Betoret, M.J. Gosalbes, Valorization of Persimmon and Blueberry Byproducts to Obtain Functional Powders: In Vitro Digestion and Fermentation by Gut Microbiota, J. Agric. Food Chem. 68 (2020) 8080–8090. https://doi.org/10.1021/acs.jafc.0c02088.

[57] F. Ozogul, I. Hamed, Y. Ozogul, J.M. Regenstein, Crustacean By-products, Encycl. Food Chem. (2019) 33–38. https://doi.org/10.1016/B978-0-08-100596-5.21690-9.

[58] FAO, Food and Agriculture Organization of the United Nations., State World Fish. Aquac. (2014).

[59] M.J. Hülsey, Shell biorefinery: A comprehensive introduction, Green Energy Environ. 3 (2018) 318–327. https://doi.org/10.1016/j.gee.2018.07.007.

[60] F.M. Kerton, Y. Liu, K.W. Omari, K. Hawboldt, Green chemistry and the ocean-based biorefinery, Green Chem. 15 (2013) 860–871. https://doi.org/10.1039/c3gc36994c.

[61] T. Maschmeyer, R. Luque, M. Selva, Upgrading of marine (fish and crustaceans) biowaste for high added-value molecules and bio(nano)-materials, Chem. Soc. Rev. 49 (2020) 4527–4563. https://doi.org/10.1039/c9cs00653b.

[62] R.R. Ambati, P.S. Moi, S. Ravi, R.G. Aswathanarayana, Astaxanthin: Sources, extraction, stability, biological activities and its commercial applications - A review, Mar. Drugs. 12 (2014) 128–152. https://doi.org/10.3390/md12010128.

[63] T. Zhao, X. Yan, L. Sun, T. Yang, X. Hu, Z. He, F. Liu, X. Liu, Research progress on extraction, biological activities and delivery systems of natural astaxanthin, Trends Food Sci. Technol. 91 (2019) 354–361. https://doi.org/10.1016/j.tifs.2019.07.014.

[64] W. Routray, D. Dave, S.K. Cheema, V. V. Ramakrishnan, J. Pohling, Biorefinery approach and environment-friendly extraction for sustainable production of astaxanthin from marine wastes, Crit. Rev. Biotechnol. 39 (2019) 469–488. https://doi.org/10.1080/07388551.2019.1573798.

[65] R.K. Saini, S.H. Moon, Y.S. Keum, An updated review on use of tomato pomace and crustacean processing waste to recover commercially vital carotenoids, Food Res. Int. 108 (2018) 516–529.

https://doi.org/10.1016/j.foodres.2018.04.003.

[66] N. Martins, I.C.F.R. Ferreira, Wastes and by-products: Upcoming sources of carotenoids for biotechnological purposes and health-related applications, Trends Food Sci. Technol. 62 (2017) 33–48. https://doi.org/10.1016/j.tifs.2017.01.014.

[67] Y. Hou, A. Shavandi, A. Carne, A.A. Bekhit, T.B. Ng, R.C.F. Cheung, A.E. din A. Bekhit, Marine shells: Potential opportunities for extraction of functional and health-promoting materials, Crit. Rev. Environ. Sci. Technol. 46 (2016) 1047–1116. https://doi.org/10.1080/10643389.2016.1202669.

[68] F.A. Mohd Hatta, R. Othman, Carotenoids as potential biocolorants: A case study of astaxanthin recovered from shrimp waste, Elsevier Inc., 2020. https://doi.org/10.1016/b978-0-12-817067-0.00009-9.

[69] Industry Experts, Global Astaxanthin Market−Sources, Technologies and Applications, (2019) . https://www.reportlinker.com/ p02788641/Global-A. https://doi.org/. https://www.reportlinker.com/ p02788641/Global-Astaxanthin-Market-Sources-Technologies-and- Applications.html.

[70] A. Molino, J. Rimauro, P. Casella, A. Cerbone, V. Larocca, S. Chianese, D. Karatza, S. Mehariya, A. Ferraro, E. Hristoforou, D. Musmarra, Extraction of astaxanthin from microalga *Haematococcus pluvialis* in red phase by using generally recognized as safe solvents and accelerated extraction, J. Biotechnol. 283 (2018) 51–61. https://doi.org/10.1016/j.jbiotec.2018.07.010.

[71] M.N. Rammuni, T.U. Ariyadasa, P.H.V. Nimarshana, R.A. Attalage, Comparative assessment on the extraction of carotenoids from

microalgal sources: Astaxanthin from *H. pluvialis* and β-carotene from D. salina, Food Chem. 277 (2019) 128–134. https://doi.org/10.1016/j.foodchem.2018.10.066.

[72] M. Herrero, A. del P. Sánchez-Camargo, A. Cifuentes, E. Ibáñez, Plants, seaweeds, microalgae and food by-products as natural sources of functional ingredients obtained using pressurized liquid extraction and supercritical fluid extraction, TrAC - Trends Anal. Chem. 71 (2015) 26–38. https://doi.org/10.1016/j.trac.2015.01.018.

[73] S.R.P. Hosseini, O. Tavakoli, M.H. Sarrafzadeh, Experimental optimization of SC-CO_2 extraction of carotenoids from Dunaliella salina, J. Supercrit. Fluids. 121 (2017) 89–95. https://doi.org/10.1016/j.supflu.2016.11.006.

[74] H. Sovová, R.P. Stateva, New developments in the modelling of carotenoids extraction from microalgae with supercritical CO_2, J. Supercrit. Fluids. 148 (2019) 93–103. https://doi.org/10.1016/j.supflu.2019.03.002.

[75] P. Adadi, N.V. Barakova, E.F. Krivoshapkina, Selected Methods of Extracting Carotenoids, Characterization, and Health Concerns: A Review, J. Agric. Food Chem. 66 (2018) 5925–5947. https://doi.org/10.1021/acs.jafc.8b01407.

[76] M.N. Rammuni, T.U. Ariyadasa, P.H.V. Nimarshana, R.A. Attalage, Comparative assessment on the extraction of carotenoids from microalgal sources: Astaxanthin from *H. pluvialis* and β-carotene from D. salina, Food Chem. 277 (2019) 128–134. https://doi.org/10.1016/j.foodchem.2018.10.066.

[77] S. Pourkarimi, A. Hallajisani, A. Nouralishahi, A. Alizadehdakhel, A.

Golzary, Factors affecting production of beta-carotene from *Dunaliella salina* microalgae, Biocatal. Agric. Biotechnol. 29 (2020). https://doi.org/10.1016/j.bcab.2020.101771.

[78] R. Srinivasan, A. Chaitanyakumar, A. Mageswari, A. Gomathi, J.G.S. Pavan Kumar, M. Jayasindu, G. Bharath, J.S. Shravan, K.M. Gothandam, Oral administration of lyophilized Dunaliella salina, a carotenoid-rich marine alga, reduces tumor progression in mammary cancer induced rats, Food Funct. 8 (2017) 4517–4527. https://doi.org/10.1039/c7fo01328k.

[79] G.D. López, G. Álvarez-Rivera, C. Carazzone, E. Ibáñez, C. Leidy, A. Cifuentes, Bacterial Carotenoids: Extraction, Characterization, and Applications, Crit. Rev. Anal. Chem. 0 (2021) 1–24. https://doi.org/10.1080/10408347.2021.2016366.

[80] G. Di Lena, I. Casini, M. Lucarini, G. Lombardi-Boccia, Carotenoid profiling of five microalgae species from large-scale production, Food Res. Int. 120 (2019) 810–818. https://doi.org/10.1016/j.foodres.2018.11.043.

[81] A. Molino, S. Mehariya, G. Di Sanzo, V. Larocca, M. Martino, G.P. Leone, T. Marino, S. Chianese, R. Balducchi, D. Musmarra, Recent developments in supercritical fluid extraction of bioactive compounds from microalgae: Role of key parameters, technological achievements and challenges, J. CO2 Util. 36 (2020) 196–209. https://doi.org/10.1016/j.jcou.2019.11.014.

[82] A. Mouahid, C. Crampon, S.A.A. Toudji, E. Badens, Effects of high water content and drying pre-treatment on supercritical CO_2 extraction from *Dunaliella salina* microalgae: Experiments and

modelling, J. Supercrit. Fluids. 116 (2016) 271–280. https://doi.org/10.1016/j.supflu.2016.06.007.

[83] L. Ngamwonglumlert, S. Devahastin, N. Chiewchan, Natural colorants: Pigment stability and extraction yield enhancement via utilization of appropriate pretreatment and extraction methods, Crit. Rev. Food Sci. Nutr. 57 (2017) 3243–3259. https://doi.org/10.1080/10408398.2015.1109498.

[84] P. Wen, T.G. Hu, R.J. Linhardt, S.T. Liao, H. Wu, Y.X. Zou, Mulberry: A review of bioactive compounds and advanced processing technology, Trends Food Sci. Technol. 83 (2019) 138–158. https://doi.org/10.1016/j.tifs.2018.11.017.

[85] S. Silva, E.M. Costa, C. Calhau, R.M. Morais, M.E. Pintado, Anthocyanin extraction from plant tissues: A review, Crit. Rev. Food Sci. Nutr. 57 (2017) 3072–3083. https://doi.org/10.1080/10408398.2015.1087963.

[86] S. Yammine, S. Brianceau, S. Manteau, M. Turk, R. Ghidossi, E. Vorobiev, M. Mietton-Peuchot, Extraction and purification of high added value compounds from by-products of the winemaking chain using alternative/nonconventional processes/technologies, Crit. Rev. Food Sci. Nutr. 58 (2018) 1375–1390. https://doi.org/10.1080/10408398.2016.1259982.

[87] R.P.F.F. da Silva, T.A.P. Rocha-Santos, A.C. Duarte, Supercritical fluid extraction of bioactive compounds, TrAC - Trends Anal. Chem. 76 (2016) 40–51. https://doi.org/10.1016/j.trac.2015.11.013.

[88] B.A.S. Machado, C.G. Pereira, S.B. Nunes, F.F. Padilha, M.A. Umsza-Guez, Supercritical Fluid Extraction Using CO_2: Main Applications and

Future Perspectives, Sep. Sci. Technol. 48 (2013) 2741–2760. https://doi.org/10.1080/01496395.2013.811422.

[89] Y.H. Chai, S. Yusup, W.N.A. Kadir, C.Y. Wong, S.S. Rosli, M.S.H. Ruslan, B.L.F. Chin, C.L. Yiin, Valorization of tropical biomass waste by supercritical fluid extraction technology, Sustain. 13 (2021) 1–24. https://doi.org/10.3390/su13010233.

[90] K.Y. Khaw, M.O. Parat, P.N. Shaw, J.R. Falconer, Solvent supercritical fluid technologies to extract bioactive compounds from natural sources: A review, Molecules. 22 (2017). https://doi.org/10.3390/molecules22071186.

[91] M. Cvjetko Bubalo, S. Vidović, I. Radojčić Redovniković, S. Jokić, New perspective in extraction of plant biologically active compounds by green solvents, Food Bioprod. Process. 109 (2018) 52–73. https://doi.org/10.1016/j.fbp.2018.03.001.

[92] P. Ongkowijoyo, D.A. Luna-Vital, E. Gonzalez de Mejia, Extraction techniques and analysis of anthocyanins from food sources by mass spectrometry: An update, Food Chem. 250 (2018) 113–126. https://doi.org/10.1016/j.foodchem.2018.01.055.

[93] F.J. Barba, Z. Zhu, M. Koubaa, A.S. Sant'Ana, V. Orlien, Green alternative methods for the extraction of antioxidant bioactive compounds from winery wastes and by-products: A review, Trends Food Sci. Technol. 49 (2016) 96–109. https://doi.org/10.1016/j.tifs.2016.01.006.

[94] M.R.M. Junior, A.V. Leite, N.R.V. Dragano, Supercritical Fluid Extraction and Stabilization of Phenolic Compounds From Natural Sources – Review (Supercritical Extraction and Stabilization of

Phenolic Compounds), Open Chem. Eng. J. 4 (2010) 51–60. https://doi.org/10.2174/1874123101004010051.

[95] C.G. Pereira, M.A.A. Meireles, Supercritical fluid extraction of bioactive compounds: Fundamentals, applications and economic perspectives, Food Bioprocess Technol. 3 (2010) 340–372. https://doi.org/10.1007/s11947-009-0263-2.

[96] K. Ameer, H.M. Shahbaz, J.H. Kwon, Green Extraction Methods for Polyphenols from Plant Matrices and Their Byproducts: A Review, Compr. Rev. Food Sci. Food Saf. 16 (2017) 295–315. https://doi.org/10.1111/1541-4337.12253.

[97] M.J. Navas, A.M. Jiménez-Moreno, J.M. Bueno, P. Sáez-Plaza, A.G. Asuero, Analysis and Antioxidant Capacity of Anthocyanin Pigments. Part IV: Extraction of Anthocyanins, Crit. Rev. Anal. Chem. 42 (2012) 313–342. https://doi.org/10.1080/10408347.2012.680343.

[98] J. Azmir, I.S.M. Zaidul, M.M. Rahman, K.M. Sharif, A. Mohamed, F. Sahena, M.H.A. Jahurul, K. Ghafoor, N.A.N. Norulaini, A.K.M. Omar, Techniques for extraction of bioactive compounds from plant materials: A review, J. Food Eng. 117 (2013) 426–436. https://doi.org/10.1016/j.jfoodeng.2013.01.014.

[99] O. Sticher, Natural product isolation, Nat. Prod. Rep. 25 (2008) 517–554. https://doi.org/10.1039/b700306b.

[100] S. Farooq, M.A. Shah, M.W. Siddiqui, B.N. Dar, S.A. Mir, A. Ali, Recent trends in extraction techniques of anthocyanins from plant materials, J. Food Meas. Charact. 14 (2020) 3508–3519. https://doi.org/10.1007/s11694-020-00598-8.

[101] M.B. Soquetta, L. de M. Terra, C.P. Bastos, Green technologies for the extraction of bioactive compounds in fruits and vegetables, CYTA - J. Food. 16 (2018) 400–412. https://doi.org/10.1080/19476337.2017.1411978.

[102] R. Gallego, M. Bueno, M. Herrero, Sub- and supercritical fluid extraction of bioactive compounds from plants, food-by-products, seaweeds and microalgae – An update, TrAC - Trends Anal. Chem. 116 (2019) 198–213. https://doi.org/10.1016/j.trac.2019.04.030.

[103] G. Fomo, T.N. Madzimbamuto, T.V. Ojumu, Applications of nonconventional green extraction technologies in process industries: Challenges, limitations and perspectives, Sustain. 12 (2020) 1–21. https://doi.org/10.3390/su12135244.

[104] M. Herrero, A. del Pilar Sánchez-Camargo, A. Cifuentes, E. Ibáñez, Plants, seaweeds, microalgae and food by-products as natural sources of functional ingredients obtained using pressurized liquid extraction and supercritical fluid extraction, TrAC Trends Anal. Chem. 71 (2015) 1–13. https://doi.org/10.1016/j.trac.2015.01.018.

[105] A. Berthod, K. Faure, Separations with a Liquid Stationary Phase: Countercurrent Chromatography or Centrifugal Partition Chromatography, Anal. Sep. Sci. (2015) 1177–1206. https://doi.org/10.1002/9783527678129.assep046.

[106] J.P. Quirino, F.M. Alejandro, A.C. Bissember, Towards cleaner downstream processing of biomass waste chemical products by liquid chromatography: A review and recommendations, J. Clean. Prod. 253 (2020) 119937. https://doi.org/10.1016/j.jclepro.2019.119937.

[107] F. Das Neves Costa, G.G. Leitão, Strategies of solvent system selection

for the isolation of flavonoids by countercurrent chromatography, J. Sep. Sci. 33 (2010) 336–347. https://doi.org/10.1002/jssc.200900632.

[108] Y. Ito, Origin and evolution of the coil planet centrifuge: A personal reflection of My 40 Years of CCC research and development, Sep. Purif. Rev. 34 (2005) 131–154. https://doi.org/10.1080/15422110500322883.

[109] Y. Ito, J. Sandlin, High speed preparative counter-currrent chromatography with a coil plante centrifuge, J. Chromatogr. 244 (1982) 247–258. https://doi.org/10.1080/01483918508074123.

[110] W. Murayama, T. Kobayashi, Y. Kosuge, H. Yano, Y. Nunogaki, K. Nunogaki, A new centrifugal counter-current chromatograph and its application, J. Chromatogr. A. 239 (1982) 643–649. https://doi.org/10.1016/S0021-9673(00)82022-1.

[111] L. Marchal, J. Legrand, A. Foucault, Centrifugal partition chromatography: A survey of its history, and our recent advances in the field, Chem. Rec. 3 (2003) 133–143. https://doi.org/10.1002/tcr.10057.

[112] J.B. Friesen, J.B. McAlpine, S.N. Chen, G.F. Pauli, Countercurrent Separation of Natural Products: An Update, J. Nat. Prod. 78 (2015) 1765–1796. https://doi.org/10.1021/np501065h.

[113] M. Bojczuk, D. Żyżelewicz, P. Hodurek, Centrifugal partition chromatography – A review of recent applications and some classic references, J. Sep. Sci. 40 (2017) 1597–1609.

[114] A. Marston, K. Hostettmann, Developments in the application of counter-current chromatography to plant analysis, J. Chromatogr. A.

1112 (2006) 181–194. https://doi.org/10.1016/j.chroma.2005.10.018.

[115] R. Morley, M. Minceva, Operating mode selection for the separation of intermediately-eluting components with countercurrent and centrifugal partition chromatography, J. Chromatogr. A. 1594 (2019) 140–148. https://doi.org/10.1016/j.chroma.2019.02.020.

[116] X.Y. Huang, S. Ignatova, P. Hewitson, D.L. Di, An overview of recent progress in elution mode of counter current chromatography, TrAC - Trends Anal. Chem. 77 (2016) 214–225. https://doi.org/10.1016/j.trac.2015.08.006.

[117] K. Skalicka-Woźniak, I. Garrard, A comprehensive classification of solvent systems used for natural product purifications in countercurrent and centrifugal partition chromatography, Nat. Prod. Rep. 32 (2015) 1556–1561. https://doi.org/10.1039/c5np00061k.

[118] D. Thiébaut, R. Rosset, Hydrodynamic and hydrostatic high-speed countercurrent chromatography and its coupling with various kinds of detectors. Application to biochemical separations, J. Chromatogr. A. 626 (1992) 41–52. https://doi.org/10.1016/0021-9673(92)85327-P.

[119] R. Hu, Y. Pan, Recent trends in counter-current chromatography, TrAC - Trends Anal. Chem. 40 (2012) 15–27. https://doi.org/10.1016/j.trac.2012.07.018.

[120] A.P. Foucault, Enantioseparations in counter-current chromatography and centrifugal partition chromatography, J. Chromatogr. A. 906 (2001) 365–378. https://doi.org/10.1016/S0021-9673(00)00499-4.

[121] G.G. Leitão, F. Das Neves Costa, F. De Souza Figueiredo, Strategies of solvent system selection for the isolation of natural products by countercurrent chromatography, Med. Plants Biodivers. Drugs. (2012) 641–668. https://doi.org/10.1201/b12527-22.

[122] A. Berthod, T. Maryutina, B. Spivakov, O. Shpigun, I.A. Sutherland, Countercurrent chromatography in analytical chemistry (IUPAC technical report), Pure Appl. Chem. 81 (2009) 355–387. https://doi.org/10.1351/PAC-REP-08-06-05.

[123] I.T. Carvalho, B.N. Estevinho, L. Santos, Application of microencapsulated essential oils in cosmetic and personal healthcare products – a review, (2016) 109–119. https://doi.org/10.1111/ics.12232.

[124] S. Jafari, S. Mahdi, M. Ebrahimi, I. Kijpatanasilp, Food Hydrocolloids A decade overview and prospect of spray drying encapsulation of bioactives from fruit products : Characterization , food application and in vitro gastrointestinal digestion, 134 (2023).

[125] M. Homayoonfal, N. Malekjani, V. Baeghbali, E. Ansarifar, S. Hedayati, S.M. Jafari, Optimization of spray drying process parameters for the food bioactive ingredients, Crit. Rev. Food Sci. Nutr. 0 (2022) 1–41. https://doi.org/10.1080/10408398.2022.2156976.

[126] S. Kandasamy, R. Naveen, A review on the encapsulation of bioactive components using spray-drying and freeze-drying techniques, (2022) 1–14. https://doi.org/10.1111/jfpe.14059.

[127] A. Gharsallaoui, G. Roudaut, O. Chambin, A. Voilley, R. Saurel, Applications of spray-drying in microencapsulation of food ingredients: An overview, Food Res. Int. 40 (2007) 1107–1121.

https://doi.org/10.1016/j.foodres.2007.07.004.

[128] W. Lu, X. Yang, J. Shen, Z. Li, S. Tan, W. Liu, Z. Cheng, Choosing the appropriate wall materials for spray-drying microencapsulation of natural bioactive ingredients : Taking phenolic compounds as examples, Powder Technol. 394 (2021) 562–574. https://doi.org/10.1016/j.powtec.2021.08.082.

[129] T. Furuta, T.L. Neoh, Microencapsulation of food bioactive components by spray drying : A review, Dry. Technol. 39 (2021) 1800–1831. https://doi.org/10.1080/07373937.2020.1862181.

[130] S. Ribeiro, C.M. Veloso, Food Hydrocolloids Microencapsulation of natural dyes with biopolymers for application in food : A review, 112 (2021). https://doi.org/10.1016/j.foodhyd.2020.106374.

CHAPTER 2

Downstream isolation of bluish anthocyanin-derived pigments from blueberry surplus

CHAPTER 2

Part I – Centrifugal partition chromatography of portisins

CONTENTS

Adapted from:

Nunes, A.N., Ivasiv, V., Gouveia, L.F., Fernández, N., Matias, A.A., Oliveira, J., Bronze, M.R. (2023). Isolation of bluish anthocyanin-derived pigments obtained from blueberry surplus using centrifugal partition chromatography. Journal of Chromatography A, 464150, doi: 10.1016/j.chroma.2023.464150.

The author was involved in the conceptualization and design of all experiments. The experimental work was performed with the support of V. Ivasiv. The characterization of extracts by HPLC-DAD was acquired at iBET - Natural Bioactives and Nutraceuticals Characterization Lab supervised by M.R. Bronze. The characterization of extracts by HPLC-DAD–MS was acquired and interpreted at FCUP by J. Oliveira, and the statistical analysis was performed at iMed.ULisboa with the support of L. F. Gouveia. Data processing and interpretation, and results discussion were also performed by the author, as well as the preparation of the original manuscript.

1. ABSTRACT

Replacement of synthetic colorants with natural ones is a current marketing trend. Nevertheless, the naturally occurring blue colour is rare compared to other colours. In this work, centrifugal partition chromatography (CPC) process was developed as a more efficient and sustainable alternative to reversed phase column chromatography (RP-CC) for the preparative-scale purification of portisins. The strategy began with the extraction of anthocyanins from blueberry surplus and hemi-synthesis of respective portisins. Then, the CPC method development started with the biphasic solvent system selection followed by the optimization of the operating parameters and ended up with a comparison with RP-CC. Aiming at maximizing the the portisin content, process throughput, efficiency, and minimizing the environmental risk factor, the effect of sample load (100-500 mg/100 mL of column volume), mobile phase flow rate (10-20 mL/min), and rotation speed (1000-1600 rpm) was evaluated. The two-phase solvent system consisted of tert-butyl-methyl ether, n-butanol, acetonitrile, and water (volume ratio 2:2:1:5) acidified with 0.1 vol.% of HCl was selected. The best conditions were 464 mg of sample/100 mL of column volume, 20 mL/min of mobile phase flow rate, and 1600 rpm of rotation speed at reversed phase mode, allowing the purification of portisins by 5-fold. Compared to the RP-CC, the CPC process efficiency was 2.4 times higher, while the CPC process environmental risk factor was 5.5 times lower. Overall, this study suggests that CPC can be considered an effective, and sustainable alternative process for the preparative isolation of portisins. With this purification approach, the blueberry surplus has been valorized and a naturally derived product has been prepared, allowing its subsequent use as a natural blue colorant.

2. INTRODUCTION

The market of natural colors is growing at 10-15% annually and the global demand for natural colorants represents an important part of the total need for dyeing agents [1], with synthetic colorants being progressively substituted by natural ones. The reduced safety of synthetic dyes has been related to high levels of toxicity, allergic reactions, and behavioral and neurocognitive effects [2]. On the other hand, naturally derived pigments are associated with safety and health-promoting effects [2].

Among natural colors, blue is the biggest challenge since natural sources of blue are limited [3,4]. Portisins are a family of anthocyanin-derived pigments (also known as vinylpyranoanthocyanin–flavanols) found in aged Port red wines [5]. These compounds display unusual spectroscopic features, presenting a bluish color in acidic conditions with a visible λ_{max} at approximately 570 nm. This class of anthocyanin-derived pigments can be obtained through the reaction between anthocyanin-pyruvic acid adducts and flavanols in the presence of acetaldehyde (Figure 1) [5]. The resulting structure presents an extended π electrons conjugation conferring high stability to these molecules as well as the uncommon bluish color [6]. In addition, the molar extinction coefficient of these bluish pigments is significantly higher when compared to their anthocyanin precursors [7].

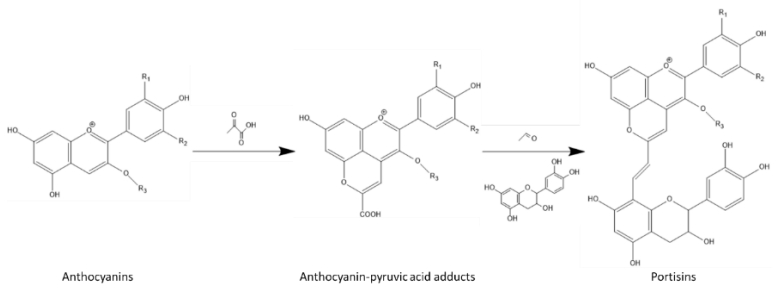

Figure 1. General scheme for portisins hemi-synthesis.

The portisins chromatic properties make this pigment a potential candidate as a naturally occurring blue colorant with applications in the nutraceutical and food sectors. However, the concentration of these pigments in Port wines are very low. Mateus and co-workers, study the hemi-synthesis of these anthocyanin-derived pigments found in red wines. The authors used several red fruit extracts as anthocyanin natural sources to produce these bluish pigments. The different red fruit anthocyanins yielded the respective anthocyanin-derived pigments [6]. Within anthocyanin-rich fruits (elderberry, blueberry, black currant, blackberry, and sweet cherry), both the total anthocyanin content and the type of anthocyanins present are quite variable. Elderberries present the highest anthocyanin content but only cyanidin is reported in this fruit. On the other hand, blueberries present higher anthocyanin content and also a more diverse anthocyanin profile (fifteen different anthocyanins) [8,9].

Blueberry fruits (*Vaccinium* spp.) present an attractive blue colour, unique taste, special fragrance, and high nutritional value [10–12]. The health-related benefits associated with the increasing health awareness and consumption trends have significantly increased the blueberry production. [12,13]. At the same time, a considerable amount of agricultural waste is generated during crop production and harvesting, including blueberry leaves and branches, broken blueberry fruits debris, and blueberry fruit that display unsatisfactory size and ripeness (blueberry surplus) [14]. Therefore, the production of portisins at a laboratory scale using blueberry surplus anthocyanins as precursors was identified as a promising alternative to obtain bluish colors.

The produced anthocyanin-derived extracts are complex systems comprising not only the portisins but also the remaining anthocyanins and

anthocyanin-pyruvic acid adducts. Traditionally, portisins isolation from Port red wine or the red fruit extracts after hemi-synthesis has been performed by RP-CC. Mateus and coworkers described the purification of portisins using a TSK Toyopearl HW-40 (S) gel column chromatography followed by semipreparative HPLC [5,7,9,15,16]. However, there is a lack of information regarding the throughput and efficiency of the process, as well as the solvent consumed to obtain the purified portisins. The main goal of these works was to characterize the new compounds rather than to evaluate the performance of the separation process. Additionally, column chromatography-based processes suffer from significant drawbacks when it comes to scalability in industrial settings. These drawbacks include prolonged separation time, extensive utilization of organic solvents, and diminished recovery rate due to irreversible adsorption of the solid support [17,18]. Therefore, there exists a pressing need to develop efficient and sustainable methodologies for the isolation of these bluish pigments from a complex mixture.

Centrifugal partition chromatography (CPC) is a viable alternative to conventional column chromatography. CPC is a liquid-liquid chromatography which does not require the use of a solid stationary phase. The separation principle is based on the fast-partitioning effects of the compounds between two immiscible liquid phases of a solvent system. During the separation process, centrifugal force keeps the stationary phase in the column, while the mobile phase, which is not miscible with the stationary phase, is pumped through the column. The partition coefficient (K) determines the elution order of the components from the column [19].

As a liquid-liquid chromatographic technique, CPC avoids the sample loss attributed to irreversible adsorption on the solid support, allowing excellent

sample recovery without chemical modifications or loss of bioactivity [20]. Also, CPC offers a larger surface area of the stationary phase for solute interaction compared to solid-liquid chromatography [20,21]. Apart from the initial investment, CPC provides the advantage of lower operational and maintenance costs. This is achieved by streamlining the processing steps, reducing solvent usage or even enabling the in-line eluent recycling, and dispensing expensive and pollutant solid-support materials [22–26]. As a result, CPC can significantly contribute to cost-effective and sustainable operations.

CPC has already demonstrated its efficacy in the isolation of anthocyanins from various sources, such as berry fruits [27–30], wine by-products [28,31,32], and flowers [33]. Du et al., described the preparative isolation of anthocyanins by high-speed counter-current chromatography (HSCCC) from a crude extract of blueberry (*Vaccinium myrtillus*) [34]. The authors explored the biphasic solvent system composed by tert-butyl-methyl ether, n-butanol, acetonitrile, and water (volume ratio 1:4:1:5) acidified with 1 vol.% of trifluoroacetic acid. The results demonstrated that preparative HSCCC separation was able to yield pure anthocyanins from a complex matrix of natural products. However, the performance of HSCCC was not evaluated. To date, there is no information in the existing literature regarding the utilization of CPC as a tool for the separation of portisins.

The objective of the present study was to establish a scalable and efficient process for selectively recovering portisins from the blueberry surplus, which was used as a source of anthocyanin for the portisin synthesis. For the first time, the feasibility of employing CPC for portisins purification was investigated. The proposed technique was compared to RP-CC. The portisin content in the obtained fractions, process throughput, efficiency, and

environmental risk factor were investigated to optimize the CPC operating conditions. The proposed approach represents a significant advancement in the challenging task of producing novel natural blue colorants for the nutraceutical and food industries, contributing to the valorization of this blueberry surplus.

3. MATERIALS AND METHODS

3.1. Raw material

Blueberry (*Vaccinium myrtillus*) surplus was kindly provided by Delícias do Tojal, CultiBaga, and Mirtilsul, Portugal. The raw material underwent dehydration using a Coolsafe Superior Touch 55-80 freeze-dryer (Labogene, Lillerød, Denmark) at a temperature of −55°C. Subsequently, the dried material was milled using a cutter-emulsifier CKE-8 (Sammic, Azkoitia, Spain). The processed biomass was protected from light and stored at a temperature of −20°C until subsequent analyses.

3.2. Chemicals

The chemicals employed for the extraction of anthocyanins and the hemi-synthesis of portisins included the following: methanol 99.8% from Fisher Scientific (Loughborough, UK), pyruvic acid 98% from Acros Organics (Geel, Belgium), ethanol absolute 99.9% from Carlo Herba (Val de Reuil, France), hydrochloric acid ≥37%, (+)-catechin hydrate ≥96.0% and acetaldehyde ≥99.0% from Sigma-Aldrich (St. Louis, Missouri, USA).

The specific chemicals used for various fractionation methodologies were as follows: methanol from 99.8% from Fisher Scientific (Loughborough, UK),

hydrochloric acid ≥37% from Sigma-Aldrich (St. Louis, Missouri, USA), tert-butyl-methyl ether 99.8% and acetonitrile 99.9% from Honeywell (Muskegon, USA), 1-butanol 99.8% and ethyl acetate 99.9% from Carlo Herba (Val de Reuil, France), Flash pure EcoFlex C18 12 g columns from Büchi Labortechnik (Flawil, Switzerland), LiChroprep RP-18 40-63 µm from Millipore (Massachusetts, USA).

The chemicals utilized for extract chemical characterization included the following: acetonitrile >99.9% from Chem Lab (Zedelgem, Bélgium), formic acid 99% from Carlo Herba (Val de Reuil, France), malvidin-3-glucoside for HPLC ≥95% from Extrasynthese (Genay, France) and vinylpyranomalvidin-3-O-glucoside-catechin used as standard for portisins quantification obtained as described by Mateus et al. [35].

3.3 Anthocyanins extraction from blueberry surplus

Anthocyanins were extracted and purified following the protocol described previously by Faria et al. [16] with slight modifications. The blueberry surplus was extracted with 50 vol.% aqueous methanol at pH 1.5 (adjusted with HCl) for 2 h at room temperature. Anthocyanins were exhaustively recovered from the residues by two extraction cycles of 10 mL per g of dry residue (ratio 10:1). The resulting extract was filtered, and the methanol was subsequently removed using a rotary evaporator at a temperature of 38°C under reduced pressure. The anthocyanin crude extract was then applied to a C-18 silica gel reversed phase previously conditioned with methanol and water. Firstly, deionized water was used to sugars and phenolic acids present in the extract. Then, anthocyanins were eluted with methanol at pH 1.5 (adjusted with HCl) and the solvent was evaporated

under reduced pressure at 38°C and the anthocyanin-rich extract was stored at −20°C in the absence of light, until further use.

3.4 Anthocyanin-pyruvic acid adducts synthesis

The synthesis of anthocyanin-pyruvic acid adducts was achieved through the reaction between the previously isolated anthocyanins with pyruvic acid (molar ratio pyruvic acid/anthocyanin of 400:1) in water at pH 2.6 (adjusted with NaOH) and at a temperature of 37°C following to the method outlined by Mateus et al. [36]. The reaction progress was monitored by high-performance liquid chromatography–diode array detector (HPLC-DAD) analysis at a wavelength 511 nm. The reaction was stopped by cooling the mixture after a maximum yield of anthocyanin-pyruvic acid adducts was reached (usually 7 days). Subsequently, the reaction mixture was applied to a C-18 silica gel reversed phase, and the anthocyanin-pyruvic acid adducts fraction was eluted using a mixture of 30 vol.% aqueous methanol pH 1.5 (adjusted with HCl). The methanol was evaporated at a temperature of 38°C under reduced pressure, and the resulting reaction mixture (RM1) was stored at a temperature of −20°C in the absence of light, until further use.

3.5 Portisins hemi-synthesis

Portisins were synthesized by subjecting the previously obtained anthocyanin-pyruvic acid adducts (RM1) to a reaction with (+)-catechin in the presence of acetaldehyde according to the methodology described by Mateus et al. [35]. The anthocyanin-pyruvic acid adducts were incubated with a mixture of 20 vol.% aqueous ethanol pH 1.5 (adjusted with HCl). The

reaction took place at a temperature of 37°C with (+)-catechin (molar ratio anthocyanin-pyruvic acid adducts/catechin 1:29) in the presence of acetaldehyde (molar ratio catechin/acetaldehyde 2:1). The reaction progress was monitored by HPLC-DAD analysis at a wavelength 570 nm. The reaction was stopped by cooling after a maximum yield of portisins was obtained (usually 8 days). The excess acetaldehyde was removed on the C-18 silica gel reversed phase. The bluish anthocyanin-derived compounds were eluted with methanol pH 1.5 (adjusted with HCl). The solvent was evaporated at a temperature of 38°C under reduced pressure and the reaction mixture (RM2) was stored at a temperature of −20°C in the absence of light, until further use.

3.6 Portisins separation procedures

3.6.1 Conventional reversed-phase liquid chromatography

Preparative RP-LC separations were conducted on a Sepacore® chromatography system X50 (Büchi Labortechnik, Flawil, Switzerland), which comprised of two C-605 pump modules, a C-620 control unit, a C-640 UV detector, and a C-660 fraction collector. This method was developed based on the purification procedure previously described for portisins isolation by Toyopearl gel column chromatography [16]. To prepare the sample solution, 100 mg of RM2 was dissolved in 20 mL of a 0.5 vol.% aqueous ethanol pH 1.5 (adjusted with HCl). The solution was filtered through a 0.45 µm membrane filter. The injection of the sample was carried out through a 6-way valve with a 20 mL loop. The sample was loaded on the flash C-18 cartridges (Flash pure EcoFlex C18 12 g) and a gradient elution with water/methanol pH 1.5 (adjusted with HCl) at a flow rate of 15 mL/min was performed. The eluent was monitored at 570 nm (portisins), 520 nm

(anthocyanins), 511 nm (anthocyanin-pyruvic acid adducts) and 280 nm (phenolic compounds). Fractions were collected every 50 mL automatically and subsequently grouped according to the color and the maximum absorption wavelength detected. The entire process, including method development, pumping, detection, fraction collection, equipment control, and data handling, was managed by SepacoreControl® 1.3 software.

3.6.2 Centrifugal partition chromatography

3.6.2.1 Apparatus

Preparative separations were carried out on a Fast Centrifugal Partition Chromatography (FCPC®) system A200 (Kromaton Rousselet Robatel, Annonay, France). The system's rotor had twin cells, giving a total column capacity of 265 mL, with 200 mL assigned to the cell volume. The solvent was pumped through the system using an analytical HPLC pump, while the sample was manually injected through a 20 mL sample loop. The FCPC® system was connected to a DAD detector capable of operating with four wavelengths simultaneously and performing continuous scans (200 - 800 nm). The fractions were easily collected with an automatic fraction collector. The whole process, including method development, pumping, detection, fraction collection, automated control of FCPC®, and data handling was managed by the Kromaflash integrated CPC-peripheral system, using the InterSoft® X software (version 10).

3.6.2.2 Biphasic solvent system selection

To assess the suitability of different two-phase solvent systems, HPLC-DAD analysis was conducted at a wavelength of 570 nm to determine the partition coefficient (K) value. The K was calculated as the ratio of the HPLC peak relative area percentage of individual portisins in the upper phase to that in the lower phase (Eq. 1).

K = peak area upper phase / peak area lower phase (Eq. 1)

Each biphasic solvent system was mixed with the RM2 (4 g/L) in a stoppered test tube. After the mixing, an equilibration step was implemented to facilitate the complete partition of anthocyanin derivatives. Both phases were collected to determine of the area of individual portisins. The K values were expressed as a mean of triplicates.

3.6.2.3 Biphasic solvent system and sample solution preparation

The CPC experiments were carried out using the biphasic system methyl t-butyl ether/n-butanol/acetonitrile/water (volume ratio 2:2:1:5). These solvents were gently mixed and settled, forming two distinct layers, the upper and lower phases. After phase separation, both phases were acidified by adding 0.1 vol.% of HCl. The preparation of the sample solution consisted of dissolving the dried RM2 in a mixture of the lower phase and upper phase, with a volume ratio of 9:1 [37].

3.6.2.4 Experimental procedure

3.6.2.4.1 Equilibration step

A homogeneous solvent equilibration on the rotor as achieved by loading the column with the organic stationary phase at a flow rate of 30 mL/min and a rotation speed of 600 rpm. The rotation speed was then tuned to the higher speed required for the retention of stationary phase. After establishing the working rotational speed, the aqueous mobile phase was pumped through the organic stationary phase until the hydrostatic equilibrium.

3.6.2.4.2 Injection step

The prepared sample solution was filtered through a 0.45 µm membrane filter to remove any precipitate. The filtered solution was then injected into the system via loop (100-500 mg/100 mL of column volume) after the hydrostatic equilibrium was reached.

3.6.2.4.3 Elution step

During the elution step, different rotation speed (1000-1600 rpm) and mobile phase flow rate (10-20 mL/min) were tested. These operating parameters were adjusted to enhance the stationary phase retention within the column while simultaneously reducing the separation time. The elution was performed in reversed phase mode (also known as descending mode), where the lower phase was used as the mobile phase. Compounds with lower K were eluted closer to the solvent front, while compounds with higher K were eluted later. The eluent was monitored at 570 nm (portisins),

520 nm (anthocyanins), 511 nm (anthocyanin-pyruvic acid adducts), and 280 nm (phenolic compounds). The fractions were collected every 25 mL automatically and subsequently grouped according to the color and the maximum absorption wavelength detected.

3.6.2.4.4 Extrusion step

The remaining sample components that were significantly retained on the column were rapidly eluted by pumping the organic stationary phase at a flow rate of 30 mL/min with the rotation speed set at 600 rpm. Each experiment resulted in four main fractions that were dried at a temperature of 38°C under reduced pressure and stored at a temperature of -20°C in the absence of light, for further analysis.

3.6.2.5 Stationary phase retention determination

The stationary phase retention Sf was calculated from Eq. 2:

$$Sf = Vc - (Vmp - Vx) / Vc \quad \text{(Eq. 2)}$$

where Vc is the column volume, Vmp is the mobile phase volume retained in the column and Vx is the extra column volume (injection loop, connecting tubing, and detection cell).

3.7. Anthocyanins and anthocyanin derivatives identification and quantification

3.7.1. High-Performance Liquid Chromatography-Diode Array Detector (HPLC-DAD)

The anthocyanin-rich extract and anthocyanin-pyruvic acid adducts fractions were analyzed in a Dionex UltiMate 3000 HPLC system equipped with a quaternary pump, autosampler, column compartment and coupled to an UltiMate 3000 Diode Array Detector (Thermo Scientific, Waltham, MA, USA) according to the method described by Oliveira et al. [7]. Chromatographic separation was performed on a Macherey-Nagel® RP-18 column (250 mm length, 4 mm width, and 5 μm particle size) maintained at 25°C. The eluents were A: H_2O/HCOOH (volume ratio 9:1), and B: CH_3CN/H_2O/HCOOH (volume ratio 3:6:1). The gradient consisted of 20-85% B for 70 min at a flow rate of 1.0 mL/min. The column was washed with 100% B for 10 min and then stabilized with the initial conditions for another 10 min [38]. The injection volume was 100 µL and the autosampler was held at 8°C. The photodiode array detector was programmed for scanning between 190 and 580 nm at a speed of 5 Hz with a bandwidth of 2 nm. The detection was monitored using four individual channels, 570 nm (portisins), 520 nm (anthocyanins), 511 nm (anthocyanin-pyruvic acid adducts), and 280 nm (phenolic compounds). For the acquisition and processing of data Chromeleon® software version 7.2 SR4 was used. The calibration curve for malvidin-3-glucoside was linear within the range of 0-100 ppm using acidified water pH 1.5 (adjusted with HCl) as solvent. Results for total anthocyanin content were presented as mg of malvidin-3-glucoside equivalents per g of extract and expressed as a mean of triplicates. The portisins fractions were also analyzed by HPLC-DAD using the same conditions but with a different eluent B: CH_3CN/H_2O/HCOOH (volume ratio

8:1.95:0.05). The calibration curve for vinylpyranomalvidin-3-O-glucoside-catechin was linear within the range of 0-80 ppm using 30 vol.% aqueous ethanol 0.1 M HCl as solvent. Results for portisin content were presented as mg of vinylpyranomalvidin-3-O-glucoside-catechin equivalents per g of extract and expressed as a mean of triplicates.

3.7.2. High-Performance Liquid Chromatography-Diode Array Detector – Mass Spectrometry (HPLC-DAD–MS)

The identity of anthocyanins and anthocyanin-derived compounds was determined by HPLC-DAD-MS analysis as previously described by Oliveira et al. [38]. A Finnigan Surveyor series liquid chromatograph, equipped with a LicroCART® reversed phase C18 column (150 mm length, 4.6 mm width, and 5 μm particle size) thermostatted at 25°C was used. Detection was carried out between 200 and 700 nm using a Finnigan Surveyor PDA Plus detector. The mass detection was carried out by a Finnigan LCQ DECA XP MAX (Finnigan Corp., San José, Calif., USA) mass detector with an API (Atmospheric Pressure Ionization) source of ionization and an ESI (ElectroSpray Ionization) interface. Eluents were A: H_2O/HCOOH (volume ratio 99:1), and B: CH_3CN/H_2O/HCOOH (volume ratio 30:69:1) for anthocyanins and anthocyanin-pyruvic acid adducts. For portisins, eluent B was: CH_3CN/HCOOH/H_2O (volume ratio 80:0.5:19.5). The HPLC gradient used was the same as reported above for the HPLC analysis except for the flow rate which was 0.5 ml/min. The capillary voltage was 4 V, and the capillary temperature was 325°C. Spectra were recorded in positive ion mode between *m/z* 150 and 2000. The mass spectrometer was programmed to do a series of three scans: a full mass, a zoom scan of the

most intense ion in the first scan, and a MS-MS of the most intense ion using a relative collision energy of 30 and 60 V.

3.8. Process throughput, process efficiency and environmental risk factor estimation

Process throughput (PT) was evaluated as a measure of mass processed per unit time:

$PT = m_{processed\ RM2} / t_{separation}$, mg processed RM2/h (Eq. 3)

where $m_{processed\ RM2}$ represents the mass of RM2 processed per run and $t_{separation}$ denotes the time taken for a single run.

Process efficiency (PE) was assessed as a metric for evaluating the production rate of one unit mass of the target compound:

$PE = m_{P\ recovered} / t_{separation}$, *mg portisins /h* (Eq. 4)

where $m_{P\ recovered}$ represents the mass of portisins recovered and $t_{separation}$ denotes the time consumed during the separation.

Process environmental risk factor (Er) was determined to assess the volume of waste solvent generated in the production of one unit mass of the target compound:

$Er = V_{total\ solvent} / m_{P\ recovered}$, *L solvent/g portisins* (Eq. 5)

where, $V_{total\ solvent}$ represents the total volume of solvent used and $m_{P\ recovered}$ denotes the mass of portisins recovered.

In the optimization of the CPC process, PT and PE were used as key indices, along together with the portisin content, to evaluate the performance of CPC. Additionally, the Er was determined to estimate of the environmental impact of the CPC process. These parameters (PT, PE and Er) were also determined for the RP-LC to compare and evaluate the performance and environmental impact of both methodologies.

3.9. Experimental design and statistical analysis

The impact of process factors on CPC fractionation was determined using a response surface technique. The program Modde® v.12 (Umetrics, Umea, Sweden) was used to evaluate the portisin content, process throughput, process efficiency, and environmental risk factor data obtained from tests conducted under experimental settings specified by a central composite face design. Adjustments to the design model and impacts of the variables were statistically significant whenever the resulting p-value was less than the predetermined = 0.05 (ANOVA and t-test).

4. RESULTS AND DISCUSSION

The objective of the present study was to establish a practical procedure to produce bluish anthocyanin-derived pigments known as portisins. The developed methodology involves three steps, namely (1) production of an extract rich in anthocyanins, (2) hemi-synthesis of anthocyanin-derived pigments, and (3) isolation of portisins using CPC.

4.1. Anthocyanins extraction from blueberry surplus

Conventional solid-liquid extraction with acidified water and methanol was performed to recover anthocyanins from the blueberry surplus. The blueberry surplus extract used to produce the blue pigments was analyzed in terms of the anthocyanin content by HPLC-DAD. The anthocyanin content was found to be 60 mg malvidin-3-glucoside equivalents/g extract. The identity of each anthocyanin present in the blueberry surplus extract was determined by HPLC-DAD-MS analyses, and the respective liquid chromatography chromatogram at 520 nm is presented in Figure 2.

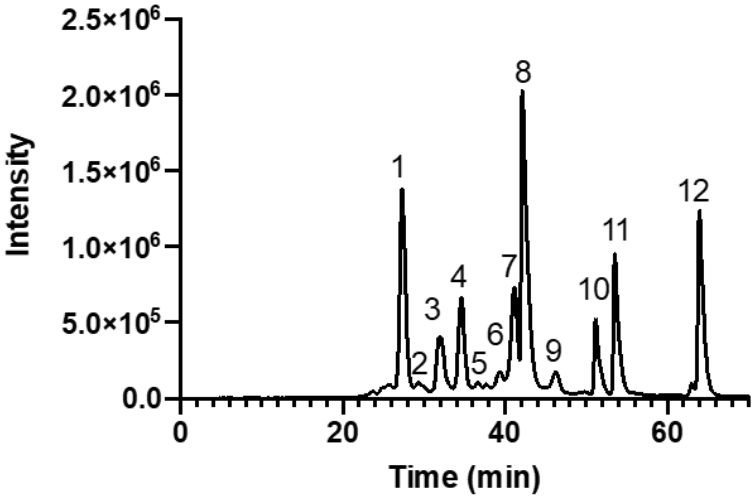

Figure 2. Chromatogram of the blueberry extract recorded at 520 nm. 1, delphinidin-3-galactoside; 2, delphinidin-3-glucoside; 3, cyanidin-3-galactoside and delphinidin-3-arabinoside; 4, petunidin-3-galactoside; 5, petunidin-3-glucoside; 6, petunidin-3-arabinoside; 7, malvidin-3-galactoside; 8, malvidin-3-glucoside; 9, malvidin-3-arabinoside; 10, cyanidin; 11, petunidin; 12, malvidin.

In a previous study, fifteen different anthocyanins corresponding to the galactoside, glucoside, and arabinoside derivatives of delphinidin, cyanidin,

petunidin, peonidin, and malvidin have been identified in a blueberry (*Vaccinium myrtillus)* extract [9]. It should be noticed that in the prepared extract, the peonidin-derivatives were not identified and that the presence of cyanidin, petunidin and malvidin aglycones was observed which could indicate a partial decomposition of anthocyanins present in the extract during the extraction and concentration process yielding to the hydrolysis of the ether bond.

4.2 Portisins hemi-synthesis

Portisins have been previously reported to result from the reaction between anthocyanin-pyruvic acid adducts and other compounds, namely flavanols, in the presence of acetaldehyde [6]. Considering this, the anthocyanin-pyruvic acid adducts were previously obtained through the reaction between blueberry anthocyanins with pyruvic acid as reported elsewhere [39]. To achieve a higher reaction yield and minimize the thermal degradation of anthocyanins and anthocyanin-pyruvic acid adducts, the reaction progress was monitored by HPLC-DAD. It was found that a mixture containing a high anthocyanin concentration (~500 mg/L) and a great excess of pyruvic acid (molar ratio 400:1 regarding anthocyanins) for 7 days yielded the highest conversion to anthocyanin-pyruvic acid adducts in aqueous solution at pH 2.6 and 37°C. Then, the production of portisin was assayed in a model solution of ethanol 20 vol.% pH 1.5 and 37°C, starting from anthocyanin-pyruvic acid adducts and (+)-catechin. From the results, the reaction of a high concentration (~150 mg/L) anthocyanin-pyruvic acid adducts with a great excess of (+)-catechin (molar ratio 1:29) in the presence of acetaldehyde (molar ratio catechin/acetaldehyde 2:1) for 8 days showed the highest reaction yield of portisin. The calculated reaction

yield for portisins was 99.2 wt.%. The chromatogram of the final reaction solution recorded at 570 nm (Figure 3) clearly showed the presence of several new peaks: vinylpyrano-delphinidin-3-galactose (or glucose)-catechin (peak 1), vinylpyrano-delphinidin-3-arabinose-catechin (peak 2), vinylpyrano-cyanidin-3-galactose (or glucose)-catechin (peak 3), vinylpyrano-petunidin-3-galactose (or glucose)-catechin (peak 4), vinylpyrano-cyanidin-3-galactose (or glucose)-catechin (peak 5), vinylpyrano-malvidin-3-galactose (or glucose)-catechin (peak 6), vinylpyrano-malvidin-3-galactose (or glucose)-catechin (peak 7), vinylpyrano-malvidin-3-arabinose-catechin (peak 8) (the chromatogram of the initial reaction solution recorded at 570 nm is provided in the Appendix page 248).

The identity of the portisins that were formed during the synthesis was performed by HPLC coupled with a mass detector. The most important peaks identified correspond to vinylpyrano-delphinidin-3-galactose (or glucose)-catechin (peak 1), vinylpyrano-petunidin-3-galactose (or glucose)-catechin (peak 4), vinylpyrano-malvidin-3-galactose (or glucose)-catechin (peak 7) and vinylpyrano-malvidin-3-arabinose-catechin (peak 8). By mass spectrometry, it was not possible to undoubtedly identify if the sugar moiety corresponds to glucose or galactose (as they are isomers) but according to the relative abundance of the respective anthocyanins in the precursor extract (Figure 2) it is possible to assume that peaks 1 and 4 should correspond to a galactoside derivative and peak 7 to a glucoside.

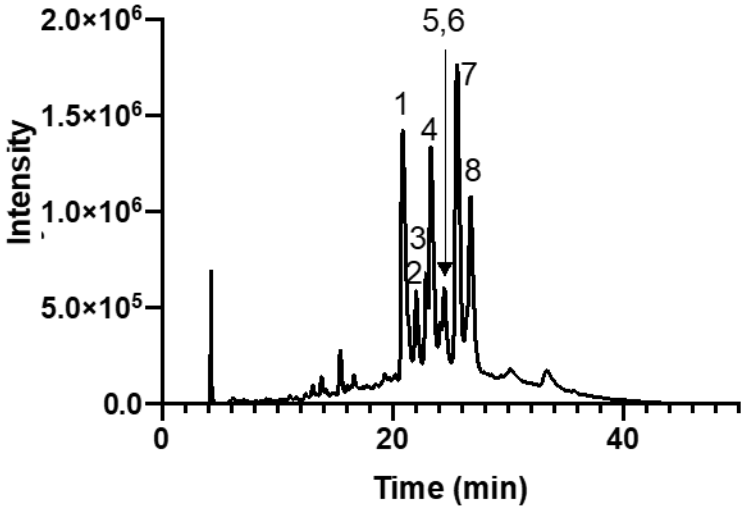

Figure 3. Chromatogram of the reaction mixture after 8 days showing the formation of portisins (peak 1-8) and the anthocyanin-pyruvic acid adducts precursors recorded at 570 nm. 1, vinylpyrano-delphinidin-3-galactose (or glucose)-catechin; 2, vinylpyrano-delphinidin-3-arabinose-Catechin; 3, vinylpyrano-cyanidin-3-galactose (or glucose)-catechin; 4, vinylpyrano-petunidin-3-galactose (or glucose)-catechin; 5, vinylpyrano-cyanidin-3-galactose (or glucose)-catechin; 6, vinylpyrano-malvidin-3-galactose (or glucose)-catechin; 7, vinylpyrano-malvidin-3-galactose (or glucose)-catechin; 8, vinylpyrano-malvidin-3-arabinose-catechin.

4.3 Centrifugal partition chromatography process optimization

The successful separation by CPC largely relies on various parameters, including the properties of the sample in the selected solvent system, physical properties of the solvent system itself, and operating parameters [40]. In fact, a crucial aspect for achieving an effective isolation in CPC is the ability to retain the stationary phase within the column chambers. Therefore, it is essential to optimize both the biphasic solvent system and the operating parameters to ensure efficient and reliable separation in CPC.

4.3.1. Biphasic solvent system selection

The initial optimization step in CPC separation involves the selection of suitable biphasic solvent system. This can be achieved by careful selection of solvents and their ratios to form a biphasic solvent system which, consequently, would adjust the K values of portisins. The K value is the ratio of the target compound concentration between the two solvent phases (Eq. 1). Ideally, the compound concentration should be equilibrated in the two immiscible solvent phases ($0.4 < K < 2.5$, ideally $K=1$) [41]. A compound with a smaller K value tends to elute closer to the solvent front with lower resolution, while compounds with higher K values exhibit higher resolution but longer elution time [42]. To achieve optimal separation, the K value should be adjusted to 1 by modifying the ratio of the components in the biphasic solvent system.

The RM2 contains a mixture of anthocyanin derivatives in a great range of quantities and polarities. To achieve efficient separation of portisins, which are medium polar compounds, organic-aqueous solvent systems were used. According to previous studies, several solvent systems have been commonly employed for the isolation of anthocyanin and anthocyanin-derivatives by counter-current chromatography. These solvent systems include (1) ethyl acetate, n-butanol, and water; and (2) tert-butyl-methyl ether, n-butanol, acetonitrile, and water [43]. Hence, different compositions of both biphasic solvent systems were investigated for the isolation of portisins. All the phases were acidified with HCl (pH 1.5) to preserve the pH-sensitive structure of anthocyanin-derived pigments. Also, adding the acid to the solvent system often substantially shortens the settling time, improving the retention of the stationary phase during the CPC separation [37].

Three different compositions for each biphasic solvent system were used and the respective range of K value of the target compounds are summarized in Table 1.

Table 1. The K value of portisins for different biphasic solvent systems.

Solvent system	Volume ratio	K range
EtOAc/BuOH/W	1:4:5	3.9 – 8.8
	2:3:5	4.0 – 11.1
	4:1:5	0.2 – 0.9
MtBE/BuOH/ACN/W	1:3:1:5	3.5 – 9.6
	2:2:1:5	1.5 – 6.3
	3:1:1:5	0.3 – 0.7

EtOAc: ethyl acetate, BuOH: n-butanol, W: water, MtBE: tert-butyl-methyl ether, ACN: acetonitrile.

The results demonstrated that the presence of a larger amount of n-butanol in the solvent system resulted in a greater K value of portisins. The observed phenomenon can be attributed to the increase in polarity of the organic phase in the solvent system. As the polarity of the organic phase increases, thereby improving the portisins dissolution. Among all the solvent systems, MtBE/BuOH/ACN/W in the volume ratio of 2:2:1:5 acidified with HCl (pH 1.5) exhibited a range of K value (1.5 – 6.3) closer to the sweet spot of K for optimal performance. Different K were obtained for each portisin. These observed differences may be associated with the different affinity between each portisin and mobile phase (e.g., hydrogen bonds). In this specific case, the elution of the first portisin from the CPC column will occur at a retention volume equal to the sum of the volume of mobile phase inside the column plus 1.5 times the column volume[37]. This ensures that the separation process of portisins might be performed by this solvent system within an acceptable timeframe, optimizing the efficiency

and productivity of the CPC system. Consequently, MtBE/BuOH/ACN/W (volume ratio 2:2:1:5) solvent system acidified with HCl (pH 1.5) was selected for portisins isolation by CPC.

4.3.2. Process parameters optimization

In CPC, once a suitable biphasic solvent system is adjusted for a specific separation, the adjustable operating parameters must be optimized. Considering the objectives and characteristics of the CPC process, a logical methodology capable of addressing the anticipated process parameters and complicated interactions. Also, the required high selectivity was necessary. The knowledge acquired from previous works [28–31,33,44], as well as some preliminary experimental results, simplified the task by keeping constant some factors (biphasic solvent system composition, sample solution preparation, injection mode, and operation mode), hence lowering the dimensions of the explorable space.

The preparation of the sample solution was fixed according to the K value of portisins. According to Ito [37], if K> 0.5, the sample solution should be prepared with the mobile phase. When K≤0.5, the stationary phase should be used as solvent in the preparation of the sample solution. In both cases, a small amount of the other phase should be added until two phases are formed. So, the sample solution was dissolved in a mixture of the mobile phase and stationary phase in a volume ratio of 9:1. The equilibrium mode was fixed, i.e., the sample was injected after the hydrostatic equilibrium was reached. This samples' injection mode is known to provide clear tracing of the elution curve and minimum carryover of the stationary phase [37].

The operating parameters and their ranges, sample load (100-500 mg/100 mL of column volume), mobile phase flow rate (10-20 mL/min), and rotation speed (1000-1600 rpm), were chosen under consideration of each effect and the maximum allowable pressure drop of 80 bar. A suitable balance was established between the number of needed experimental runs and the amount of acquired information. Considering the number of factors (3) and the predetermined objectives, a central composite face design consisting of a three-level full factorial design and star points put on the faces of the sides was chosen as an appropriate method for completing this task. To test the experimental variability and subsequently the uncertainty of the results as well as the adequacy of the underlying mathematical model, central duplicate points were added. Using response surface approach, the optimum conditions for portisins isolation by CPC were determined. Portisin content, process throughput, process efficiency, and environmental risk factor were examined as responses.

In this study, the elution-extrusion mode was fixed since this operation mode is known to extend the polarity range, being suitable for complex samples which contain solutes with a large range of K values. The extrusion step was used to collect all compounds that were retained on the CPC column after the portisins eluted, shortening the separation time.

The RM2 was fractionated by CPC yielding four main fractions (detailed information about each pool is provided in the SI). After being automatically collected every 25 mL, the fractions were subsequently grouped according to the color and the λ_{max} detected. In this sense, the initial fractions had an orange coloration and a λ_{max}~511 nm (which is a characteristic λ of anthocyanin-pyruvic acid adducts) and were therefore grouped into fraction 1 (F1). F1 contained the compounds that had the lowest K (0-0.9 ≤

K ≤ 1.0-3.3). The following fractions showed a blue/purple coloration and a λ_{max}~570 nm and were therefore grouped into fraction 2 (F2). F2 comprised the compounds that had values of K in the range 1.0-3.3 ≤ K ≤ 4.9-11. Fraction 3 (F3) is composed of weakly blue/purple-colored fractions, showing a λ_{max}~220 nm. These fractions were separated from F2 because other compounds in higher concentration started to elute with the portisins. The K of these fraction pool ranged from 4.9-11 to 5.1-19.5. Fraction 4 (F4) contained the highly retained compounds with λ_{max}~220 nm. These fractions were grouped separately from F3 since they had a dark reddish coloration. F4 contained the compounds that had the highest partition coefficient (4.2-12.6 ≤ K ≤ 6.2-23.6).

Typical chromatograms of the collected fractions by CPC are shown in Figure 4. From the results, it was possible to observed that the remaining anthocyanin-pyruvic acid adducts (λ_{max}~511 nm) were eluted in F1. These compounds have higher polarity compared to portisins and therefore have lower affinity for the stationary phase. As a result, they eluted earlier during the separation process. The separation of the more polar anthocyanin derivatives in the earlier fractions allows for a more selective isolation of the desired portisins in subsequent fractions.

The produced portisins (λ_{max}~570 nm) were subsequently eluted in F2 and F3. Among these fractions, F2 was found to be the richest fraction in portisins. However, it should be noted that F3 also contained some undesirable compounds (λ_{max}~220 nm) that co-eluted with remaining portisins. Based on HPLC analysis at 570 nm, the content of portisins in F1, F2, F3, and F4 of this representative CPC experiment was 0.1, 600.4, 40.7 and 1.4 mg/g, respectively (Figure 4). These results provide insights into the

distribution and concentration of portisins among the different fractions, with F2 being the most enriched fraction in terms of portisin content.

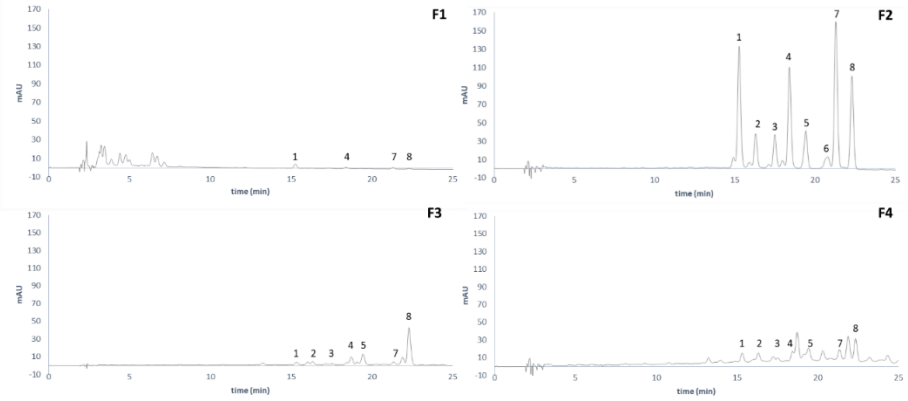

Figure 4. Chromatograms of portisins detected at 570 nm corresponding to (F1) fraction 1, (F2) fraction 2, (F3) fraction 3 and (F4) fraction 4. Fractions collected during the CPC experiment N5 (2 mg RM2/100 mL of column, 10 mL/min of mobile phase flow rate, and 1600 rpm of rotation speed).

Table 2 presents the details of the experimental conditions and outcomes for each CPC experiment. The results indicated that the tested CPC conditions were suitable for preserving the stationary phase retention (over 50%) throughout the separation procedure, allowing for efficient separation of the compounds. The fraction with the highest portisin content was obtained with a sample load of 100 mg/100 mL of column volume at 10 mL/min of mobile phase flow rate and 1600 rpm of rotation speed, which was 600 mg portisin/g (Table 2 - experiment N5).

Table 2. CPC conditions applied and respective stationary phase retention (Sf), portisin content (P content) in the obtained portisin-enriched fraction (F2), process throughput (PT), process efficiency (PE), and environmental risk factor (Er).

Exp Name	Load (mg RM2/100mL column)	Mobile phase flow rate (mL/min)	Rotation speed (rpm)	Separation time (h)	Sf (vol.%)	P content (mg P/g)	PT (mg RM2/h)	PE (mg P/h)	Er (L/g P)
N1	100	10	1000	3.3	79	595	60	4	223
N2	500	10	1000	4.0	79	478	248	17	55
N3	100	20	1000	2.7	68	503	75	6	278
N4	500	20	1000	2.5	66	373	391	19	83
N5	100	10	1600	3.5	79	600	57	4	221
N6	10	10	1600	3.7	80	465	265	20	46
N7	100	20	1600	3.1	67	591	64	4	417
N8.1	500	20	1600	2.2	69	483	458	29	48
N8.2	500	20	1600	2.1	72	459	480	35	38
N9	100	15	1300	2.8	73	559	71	4	310
N10.1	500	15	1300	1.9	72	404	522	26	38
N10.2	500	15	1300	1.8	75	436	545	37	25
N11	300	10	1300	3.5	80	587	170	13	70
N12	300	20	1300	2.5	72	468	234	16	95
N13	300	15	1000	3.0	72	539	195	12	108
N14	300	15	1600	3.0	75	425	197	13	96
N15	300	15	1300	3.4	71	494	176	11	120
N16	300	15	1300	3.0	74	496	197	15	83
N17	300	15	1300	3.4	69	585	176	12	114

Under these conditions, the process throughput, and the process efficiency of the experiment N5 were the lowest ones, 57 mg processed RM2/h and 4 mg portisin/h, respectively. Also, the environmental risk factor was higher (221 L solvent/g portisin). Whereas the highest process throughput and efficiency were 545 mg processed RM2/h and 37 mg portisin/h, respectively. These values were observed with a sample load of 500 mg RM2/100 mL at 15 mL/min of mobile phase flow rate and 1300 rpm of

rotation speed (Table 2 - experiment N10.2), corresponding to a portisin content of 436 mg portisin/g, a lower value compared with experiment N5. Under these conditions, the environmental risk factor was lower (25 L solvent/g portisin).

To obtain a selective separation (higher portisin content), the separation process takes more time. As a result, the process throughput and process efficiency decrease, and the environmental risk factor increases. However, the improvement in the CPC process might be in all four evaluated responses (portisin content, process throughput, process efficiency, and environmental risk factor). So, the influence of CPC process parameters on each response had to be evaluated. The sample load and mobile phase flow rate had significant effects on two of the four evaluated responses: portisin content and process throughput. The process efficiency and environmental risk factors were only significantly affected by the sample load. The application of different rotation speeds (1000-1600 rpm) resulted in no significant improvement in all the evaluated responses (model fit is provided in the Appendix page 253).

The goal was to optimize the isolation of portisins, maximizing the portisin content, process throughput, and process efficiency, minimizing the process environmental risk. To achieve that, a multiple linear regression approach with an automated optimizer (Modde® v.12) was used to predict one set of optimal conditions for all response variables. Twelve sets of optimal CPC conditions were proposed by the software. The output with the lowest overall distance to the target (log(D) = 1.16) was the following parameter-setting combination: sample load of 464 mg/100 mL of column volume, 20 mL/min of mobile phase flow rate, and 1600 rpm of rotation speed. Under these conditions, the fractionation of RM2 by CPC can result in optimal

portisins content (460 mg portisin/g), process throughput (474 mg processed RM2/h), process efficiency (30 mg portisin/h), and environmental risk factor (52 L/g portisin).

The comparison between the predicted results and the experimental results obtained using optimum isolation conditions is presented in Table 3. These findings reveal a strong agreement between the predicted and experimental outcomes, indicating that the response surface methodology model was successfully validated with a good correlation level. Also, it was possible to verify that the range of K calculated for F2 of the CPC experiment under the optimized conditions - K=1.6-6.5 (more details in the Appendix page 251) was close to the range of K determined in the shake flask test - K=1.5-4.1 (Table 1).

Table 3. Predicted and experimental values (n=2) of response variables under optimum CPC conditions and experimental values of response variables obtained by column chromatography (CC) experiment.

	Portisin content (mg P/g)	Process throughput (mg processed RM2/h/Vc*)	Process efficiency (mg P/h/Vc)	Environmental risk factor (L/g P)
CPC				
Predicted	460	2.4	0.15	52
Experimental	469 ± 46	2.06 ± 0.14	0.19 ± 0.03	30 ± 6
CC				
Experimental	396 ± 52	2.09 ± 0.02	0.08 ± 0.01	164 ± 38

*CPC column volume = 200 mL; RP-LC column volume = 12 mL

4.4. Reversed-phase liquid chromatography

RM2 was fractionated by gradient preparative RP-LC to compare with the separation performance of CPC. The operating parameters, namely sample load and mobile phase flow rate were selected considering the column manufacturer's specifications. The elution was carried out with aqueous ethanol with increasing percentage of ethanol up to 100 vol.% as adapted from Mateus and coworkers [5]. During the elution, 65 fractions were collected automatically and subsequently grouped into F1 and F2 according to the color and the maximum absorption wavelength detected. F1 contained the compounds that were eluted during the first 3h of the separation. This fraction presented an orange color (λ_{max}~511nm), which is characteristic of anthocyanin-pyruvic acid adducts. Portisins were subsequently collected in F2 during the last 43min of the separation process. Due to the presence of portisins, F2 exhibited a bluish/purple color (λ_{max}~570nm). Based on HPLC analysis at 570 nm, the portisins content in F1 and F2 of RP-LC experiments was 14.2 ± 0.1 mg/g, and 395.6 ± 51.9 mg/g, respectively.

There are two reports regarding the production portisins from a blueberry (*Vaccinium myrtillus*) extract [9,16]. The authors isolated portisins by Toyopearl gel column chromatography by elution with water/ethanol, following the same procedure previously described by Mateus and coworkers [5]. However, these works focused on the antioxidant properties [16] and MPP+ intestinal uptake [9] of the blueberry extract and two respective anthocyanin-derived reaction mixtures (anthocyanin pyruvic acid adducts and portisins). There is not enough data in the literature to allow a comparison of separation process performance.

4.5 Comparison of different purification methods

The use of CPC for portisins isolation from RM2 demonstrated significant advantages when compared to RP-LC, as evident from the results presented in Table 3. The comparison of portisin content in the fractions obtained by the two chromatographic techniques reveled similar selectivity toward portisins. Both methods yielded comparable values of portisin content and process throughput, indicating similar overall performance in terms of product concentration and processing capacity. However, notable differences were observed in terms of process efficiency and environmental risk factor. The process efficiency was significantly higher in CPC (2.4 times) compared to RP-LC. This suggests that CPC offers a more efficient and rapid process for the isolation of portisins. Furthermore, the environmental risk factor, was found to be lower in the CPC technique (5.5 times). These results indicate that CPC has a lower environmental impact, as it generates less waste solvent compared to RP-LC. Other studies available in the literature shown the same promising effect when comparing countercurrent chromatography with RP-HPLC [45,46]. Overall, the results highlight the irrefutable advantages of CPC over RP-LC for the isolation of portisins from the RM2 in terms of process efficiency and environmental sustainability.

5. CONCLUSIONS

The study reported emphasizes the potential of CPC for the separation of bluish anthocyanin derived pigments. The optimum CPC conditions for the isolation of portisins were identified using a graphical optimization technique that incorporate response surface methodology with a

desirability function, and the predicted values for all the analyzed responses were excellent agreement with the experimental ones. The optimum conditions include 464 mg of sample/100 mL of column volume, 20 mL/min of mobile phase flow rate, and 1600 rpm of rotation speed for the portisin content, process throughput, efficiency, and environmental risk factor of 469 mg portisin/g, 2.06 mg processed RM2/h/Vc, 0.19 mg portisin/h/Vc, and 30 L/g portisin, respectively. These conditions allowed the purification of portisins of 5-fold. The process efficiency was 2.4 times higher than the RP-LC process. The CPC process environmental risk factor was 5.5 times lower than in the conventional process. The key benefits of CPC technology include a substantial decrease in separation time and solvent usage, which improved the efficiency and environmental risk factor of the process in comparison to RP-LC. In conclusion, the results showed that the proposed protocol was an efficient and appropriate method for the production and isolation of blue portisin pigments with various application in the nutraceutical and food industries, thereby aiding in the sustainable use of these blueberry residues. As future work, it would be interesting to explore this technique for the separation of anthocyanin-pyruvic acid adducts prior to the portisins synthesis.

6. ACKNOWLEDGEMENTS

This work was funded by Fundação para a Ciência e Tecnologia/Ministério da Ciência, Tecnologia e Ensino Superior (FCT/MCTES, Portugal) through national funds to iNOVA4Health (UIDB/04462/2020 and UIDP/04462/2020), the Associate Laboratory LS4FUTURE (LA/P/0087/2020) and Associated Laboratory for Sustainable Chemistry, Clean Processes, and Technologies LAQV (UIDB/50006/2020 and UIDP/50006/2020). Funding from INTERFACE

Programme, through the Innovation, Technology and Circular Economy Fund (FITEC), is gratefully acknowledged. A.N.N. acknowledge FCT for the financial support received through SFRH/BD/144592/2019. J.O. acknowledge FCT her research contract (2022.00042.CEECIND/CP1724/CT0017). The authors also acknowledge Delícias do Tojal, CultiBaga, and Mirtilsul for kindly supplying the biomass.

7. REFERENCES

[1] R. Cortez, D.A. Luna-Vital, D. Margulis, E. Gonzalez de Mejia, Natural Pigments: Stabilization Methods of Anthocyanins for Food Applications, Compr. Rev. Food Sci. Food Saf. 00 (2016) 1–19. https://doi.org/10.1111/1541-4337.12244.

[2] M. Manzoor, J. Singh, A. Gani, N. Noor, Valorization of natural colors as health-promoting bioactive compounds: Phytochemical profile, extraction techniques, and pharmacological perspectives, Food Chem. 362 (2021) 130141. https://doi.org/10.1016/j.foodchem.2021.130141.

[3] M.I. Landim Neves, E.K. Silva, M.A.A. Meireles, Natural blue food colorants: Consumer acceptance, current alternatives, trends, challenges, and future strategies, Trends Food Sci. Technol. 112 (2021) 163–173. https://doi.org/10.1016/j.tifs.2021.03.023.

[4] F. Pina, N. Basílio, A.J. Parola, M.J. Melo, J. Oliveira, V. De Freitas, The Triumph of the Blue in Nature and in Anthropocene, Dye. Pigment. 210 (2023) 110925. https://doi.org/10.1016/j.dyepig.2022.110925.

[5] N. Mateus, A.M.S. Silva, J.C. Rivas-Gonzalo, C. Santos-Buelga, V. De Freitas, A new class of blue anthocyanin-derived pigments isolated from red wines, J. Agric. Food Chem. 51 (2003) 1919–1923. https://doi.org/10.1021/jf020943a.

[6] N. Mateus, J. Oliveira, M. Haettich-Motta, V. de Freitas, New Family of Bluish Pyranoanthocyanins, J. Biomed. Biotechnol. 2004 (2004) 299–305. https://doi.org/10.1155/S1110724304404033.

[7] J. Oliveira, C. Santos-Buelga, A.M.S. Silva, V. De Freitas, N. Mateus, Chromatic and structural features of blue anthocyanin-derived pigments present in Port wine, Anal. Chim. Acta. 563 (2006) 2–9. https://doi.org/10.1016/j.aca.2005.11.027.

[8] X. Wu, G.R. Beecher, J.M. Holden, D.B. Haytowitz, S.E. Gebhardt, R.L. Prior, Concentrations of anthocyanins in common foods in the United States and estimation of normal consumption, J. Agric. Food Chem. 54 (2006) 4069–4075. https://doi.org/10.1021/jf060300l.

[9] A. Faria, D. Pestana, R. Monteiro, J. Oliveira, V. de Freitas, I. Azevedo, C. Calhau, N. Mateus, Influence of anthocyanins and derivative pigments from blueberry (Vaccinium myrtillus) extracts on MPP+ intestinal uptake: A structure-activity approach, Food Chem. 109 (2008) 587–594. https://doi.org/10.1016/j.foodchem.2008.01.009.

[10] H. Xue, X. Zhu, J. Tan, L. Fan, Q. Li, J. Tang, X. Cai, Counter-current fractionation-assisted bioassay-guided separation of active compound from blueberry and the interaction between the active compound and α-glucosidase, Foods. 10 (2021). https://doi.org/10.3390/foods10030509.

[11] S. Silva, E.M. Costa, M. Veiga, R.M. Morais, C. Calhau, M. Pintado, Health promoting properties of blueberries: a review, Crit. Rev. Food Sci. Nutr. 60 (2020) 181–200. https://doi.org/10.1080/10408398.2018.1518895.

[12] H. Yang, Y. Wu, C. Zhang, W. Wu, L. Lyu, W. Li, Growth and physiological characteristics of four blueberry cultivars under different high soil pH treatments, Environ. Exp. Bot. 197 (2022) 104842. https://doi.org/10.1016/j.envexpbot.2022.104842.

[13] Y. Duan, A. Tarafdar, D. Chaurasia, A. Singh, P.C. Bhargava, J. Yang, Z. Li, X. Ni, Y. Tian, H. Li, M.K. Awasthi, Blueberry fruit valorization and valuable constituents: A review, Int. J. Food Microbiol. 381 (2022) 109890. https://doi.org/10.1016/j.ijfoodmicro.2022.109890.

[14] H. Liu, S. Qin, R. Sirohi, V. Ahluwalia, Y. Zhou, R. Sindhu, P. Binod, R. Rani Singhnia, A. Kumar Patel, A. Juneja, D. Kumar, Z. Zhang, J. Kumar, M.J. Taherzadeh, M. Kumar Awasthi, Sustainable blueberry waste recycling towards biorefinery strategy and circular bioeconomy: A review, Bioresour. Technol. 332 (2021) 125181. https://doi.org/10.1016/j.biortech.2021.125181.

[15] J. Oliveira, V. De Freitas, A.M.S. Silva, N. Mateus, Reaction between hydroxycinnamic acids and anthocyanin-pyruvic acid adducts yielding new portisins, J. Agric. Food Chem. 55 (2007) 6349–6356. https://doi.org/10.1021/jf070968f.

[16] A. Faria, J. Oliveira, P. Neves, P. Gameiro, C. Santos-Buelga, V. De Freitas, N. Mateus, Antioxidant properties of prepared blueberry (Vaccinium myrtillus) extracts, J. Agric. Food Chem. 53 (2005) 6896–6902. https://doi.org/10.1021/jf0511300.

[17] Y. Xu, D. Hu, Y. Li, C. Sun, W. Chen, An effective method for preparation of high-purity pelargonidin-3-O-glucoside from strawberry and its protective effect on cellular oxidative stress, J. Chromatogr. B Anal. Technol. Biomed. Life Sci. 1072 (2018) 211–220. https://doi.org/10.1016/j.jchromb.2017.11.025.

[18] F. Qiu, J. Luo, S. Yao, L. Ma, L. Kong, Preparative isolation and purification of anthocyanins from purple sweet potato by high-speed counter-current chromatography, J. Sep. Sci. 32 (2009) 2146–2151. https://doi.org/10.1002/jssc.200900038.

[19] A. Berthod, K. Faure, Separations with a Liquid Stationary Phase: Countercurrent Chromatography or Centrifugal Partition Chromatography, Anal. Sep. Sci. (2015) 1177–1206. https://doi.org/10.1002/9783527678129.assep046.

[20] R. Morley, M. Minceva, Operating mode selection for the separation of intermediately-eluting components with countercurrent and centrifugal partition chromatography, J. Chromatogr. A. 1594 (2019) 140–148. https://doi.org/10.1016/j.chroma.2019.02.020.

[21] A. Marston, K. Hostettmann, Developments in the application of counter-current chromatography to plant analysis, J. Chromatogr. A. 1112 (2006) 181–194. https://doi.org/10.1016/j.chroma.2005.10.018.

[22] L. Marchal, J. Legrand, A. Foucault, Centrifugal partition chromatography: A survey of its history, and our recent advances in the field, Chem. Rec. 3 (2003) 133–143. https://doi.org/10.1002/tcr.10057.

[23] K. Skalicka-Woźniak, I. Garrard, A comprehensive classification of

solvent systems used for natural product purifications in countercurrent and centrifugal partition chromatography, Nat. Prod. Rep. 32 (2015) 1556–1561. https://doi.org/10.1039/c5np00061k.

[24] R. Hu, Y. Pan, Recent trends in counter-current chromatography, TrAC - Trends Anal. Chem. 40 (2012) 15–27. https://doi.org/10.1016/j.trac.2012.07.018.

[25] A.P. Foucault, Enantioseparations in counter-current chromatography and centrifugal partition chromatography, J. Chromatogr. A. 906 (2001) 365–378. https://doi.org/10.1016/S0021-9673(00)00499-4.

[26] L. Lorántfy, R. Örkenyi, D. Rutterschmid, D. Bakonyi, J. Faragó, G. Dargó, Á. Könczöl, Continuous industrial-scale centrifugal partition chromatography with automatic solvent system handling: Concept and instrumentation, Org. Process Res. Dev. 24 (2020) 2676–2688. https://doi.org/10.1021/acs.oprd.0c00338.

[27] L.E. Rojo, D. Ribnicky, S. Logendra, A. Poulev, P. Rojas-Silva, P. Kuhn, R. Dorn, M.H. Grace, M.A. Lila, I. Raskin, In vitro and in vivo anti-diabetic effects of anthocyanins from Maqui Berry (Aristotelia chilensis), Food Chem. 131 (2012) 387–396. https://doi.org/10.1016/j.foodchem.2011.08.066.

[28] J.H. Renault, P. Thépenier, M. Zèches-Hanrot, L. Le Men-Olivier, A. Durand, A. Foucault, R. Margraff, Preparative separation of anthocyanins by gradient elution centrifugal partition chromatograghy, J. Chromatogr. A. 763 (1997) 345–352. https://doi.org/10.1016/S0021-9673(96)00880-1.

[29] A. Ruiz, C. Mardones, C. Vergara, D. Von Baer, S. Gómez-Alonso,

M.V. Gómez, I. Hermosín-Gutiérrez, Isolation and structural elucidation of anthocyanidin 3,7-β-O- diglucosides and caffeoyl-glucaric acids from calafate berries, J. Agric. Food Chem. 62 (2014) 6918–6925. https://doi.org/10.1021/jf5012825.

[30] M.A. Paissoni, P. Waffo-Teguo, W. Ma, M. Jourdes, L. Rolle, P.L. Teissedre, Chemical and sensorial investigation of in-mouth sensory properties of grape anthocyanins, Sci. Rep. 8 (2018) 1–13. https://doi.org/10.1038/s41598-018-35355-x.

[31] J.H. Renault, P. Thepenier, M. Zeches-Hanrot, A.P. Foucault, Separation of the two major anthocyanins from champagne vintage by-products by gradient elution centrifugal partition chromatography, J. Liq. Chromatogr. 18 (1995) 1663–1670. https://doi.org/10.1080/10826079508009303.

[32] Á.S. Lima, B.S. de Oliveira, S.V. Shabudin, M. Almeida, M.G. Freire, K. Bica, Purification of anthocyanins from grape pomace by centrifugal partition chromatography, J. Mol. Liq. 326 (2021) 115324. https://doi.org/10.1016/j.molliq.2021.115324.

[33] Nor Syaidatul Akmal Mohd Yousof, Nikos Xynos, Evanthia Dina, Maizatul Hashima Omar, Choong Yew Keong, Mohd Isa Wasiman, Nektarios Aligiannis, Comparison of Standard Elution and Displacement Modes in Centrifugal Partition Chromatography for an Efficient Purification of Four Anthocyanins from Hibiscus sabdariffa L., J. Pharm. Pharmacol. 6 (2018) 701–711. https://doi.org/10.17265/2328-2150/2018.08.001.

[34] Q. Du, G. Jerz, P. Winterhalter, Isolation of two anthocyanin sambubiosides from bilberry (Vaccinium myrtillus) by high-speed

counter-current chromatography, J. Chromatogr. A. 1045 (2004) 59–63. https://doi.org/10.1016/j.chroma.2004.06.017.

[35] N. Mateus, J. Oliveira, C. Santos-Buelga, A.M.S. Silva, V. De Freitas, NMR structure characterization of a new vinylpyranoanthocyanin-catechin pigment (a portisin), Tetrahedron Lett. 45 (2004) 3455–3457. https://doi.org/10.1016/j.tetlet.2004.03.007.

[36] N. Mateus, J. Oliveira, A.M. González-Paramás, C. Santos-Buelga, V. De Freitas, Screening of portisins (vinylpyranoanthocyanin pigments) in Port wine by LC/DAD-MS, Food Sci. Technol. Int. 11 (2005) 353–358. https://doi.org/10.1177/1082013205057940.

[37] Y. Ito, Golden rules and pitfalls in selecting optimum conditions for high-speed counter-current chromatography, J. Chromatogr. A. 1065 (2005) 145–168. https://doi.org/10.1016/j.chroma.2004.12.044.

[38] J. Oliveira, M.A. Da Silva, A.J. Parola, N. Mateus, N.F. Brás, M.J. Ramos, V. De Freitas, Structural characterization of a A-type linked trimeric anthocyanin derived pigment occurring in a young Port wine, Food Chem. 141 (2013) 1987–1996. https://doi.org/10.1016/j.foodchem.2013.04.091.

[39] J. Oliveira, V. Fernandes, C. Miranda, C. Santos-Buelga, A. Silva, V. De Freitas, N. Mateus, Color properties of four cyanidin-pyruvic acid adducts, J. Agric. Food Chem. 54 (2006) 6894–6903. https://doi.org/10.1021/jf061085b.

[40] J.B. Friesen, G.F. Pauli, GUESSmix-guided optimization of elution-extrusion counter-current separations, J. Chromatogr. A. 1216 (2009) 4225–4231. https://doi.org/10.1016/j.chroma.2008.12.053.

[41] J.B. Friesen, G.F. Pauli, G.U.E.S.S. - A generally useful estimate of solvent systems in CCC, J. Liq. Chromatogr. Relat. Technol. 28 (2005) 2777–2806. https://doi.org/10.1080/10826070500225234.

[42] Y. Guo, S. Tong, K. Zhang, J. Yan, Recent progress in separation prediction of counter-current chromatography, J. Sep. Sci. 44 (2021) 6–16. https://doi.org/10.1002/jssc.202000473.

[43] A.N. Nunes, A. Borges, A.A. Matias, M.R. Bronze, J. Oliveira, Alternative Extraction and Downstream Purification Processes for Anthocyanins, Molecules. 27 (2022). https://doi.org/10.3390/molecules27020368.

[44] L.E. Rojo, D. Ribnicky, S. Logendra, A. Poulev, P. Rojas-Silva, P. Kuhn, R. Dorn, M.H. Grace, M.A. Lila, I. Raskin, In vitro and in vivo anti-diabetic effects of anthocyanins from Maqui Berry (Aristotelia chilensis), Food Chem. 131 (2012) 387–396. https://doi.org/10.1016/j.foodchem.2011.08.066.

[45] C. Deamicis, N.A. Edwards, M.B. Giles, G.H. Harris, P. Hewitson, L. Janaway, Comparison of preparative reversed phase liquid chromatography and countercurrent chromatography for the kilogram scale purification of crude spinetoram insecticide, J. Chromatogr. A. 1218 (2011) 6122–6127. https://doi.org/10.1016/j.chroma.2011.06.073.

[46] C. Deamicis, Q. Yang, C. Bright, N. Edwards, G. Harris, S. Kaur, P. Wood, P. Hewitson, S. Ignatova, Development of a Scalable and Sustainable High Performance CounterCurrent Chromatography (HPCCC) Purification for Spinosyn A and Spinosyn D from Spinosad, (2017). https://doi.org/10.1021/acs.oprd.7b00249.

CHAPTER 2

Part II – Compressed fluid-based extraction of portisins

CONTENTS

Adapted from:

Nunes, A.N., Bronze, M.R., Oliveira, J., Matias, A. A Compressed fluid-based technologies for downstream isolation of bluish anthocyanin-derived pigments obtained from blueberry surplus. Submitted to Food and Function RSC.

The author was involved in the conceptualization and design of the experiments and performed all experimental work, except the characterization of extracts by HPLC-DAD acquired at iBET - Natural Bioactives and Nutraceuticals Characterization Lab supervised by M.R. Bronze. Data processing and interpretation, and results discussion were also performed by the author, as well as the preparation of the original manuscript.

1. ABSTRACT

A dynamic compressed fluid-based separation process combining sub/supercritical carbon dioxide and ethanol was explored to isolate portisins previously hemi-synthetized from blueberry surplus anthocyanins. The influence of process parameters such as pressure (100-500 bar), temperature (40-60°C), and ethanol content in the compressed fluid mixture (20-50 wt.%) on extraction yield, portisins yield, and portisins content in the extract were investigated. The two-step isolation process includes (1) a first step at 100 bar, 60°C, and 20 wt.% ethanol content in the compressed fluid mixture to remove the low polarity compounds; and (2) a second step at 500 bar, 40°C, and 100 wt.% ethanol to recover portisins, resulting in a 1.5-fold increase in portisin content. The performance of the two-step separation process was compared with conventional reverse phase liquid chromatography and centrifugal partitional chromatography in terms of portisins content in the extract, process throughput, process efficiency, and environmental risk factors. The two-step separation process decreased the environmental risk factor, although with a decrease in the throughput and efficiency. Nevertheless, the best separation technology to be used depends on the portisins application. Overall, this study contributed to a scalable and more sustainable process for natural colorant production, specifically focusing on blue pigments, with several industrial applications.

2. INTRODUCTION

Blueberry fruits (*Vaccinium* spp.) have gained worldwide attention due to their attractive blue color, unique taste, special flavor, and high nutritional value [1–3]. In fact, blueberry has been certified by the International Food

and Agriculture Organization as one of the five healthiest foods [4,5]. The increasing health awareness and consumption trends have significantly boosted blueberry production, leading to its global production increasing from 622,900 tons in 2016 to 850,900 tons in 2020 [3,5]. Alongside this growth, a substantial amount of agricultural waste is produced during crop production and harvesting. These agricultural residues include blueberry leaves, blueberry branches, debris from broken blueberry fruits, and blueberry surplus that do not meet size and ripeness standards [4]. Consequently, there has been a growing interest in developing potential applications of these residues in bioprocessing to obtain value-added products, thereby contributing to the efficient valorization of agricultural waste in a sustainable circular bioeconomy.

Blueberries are a rich source of organic acids, sugar, minerals, vitamins, fibers, and phenolic compounds, particularly anthocyanins [1]. These bioactive compounds are also present in blueberry agricultural residues, often in higher proportions [6]. Among them, anthocyanins account for up to 60% of the total polyphenolics in blueberries [7,8]. Anthocyanins are a diverse class of water-soluble plant pigments derived from flavonoids, exhibiting a wide range of natural colors such as red, violet, and blue [8,9]. In response to consumer concerns regarding the potential adverse effects of synthetic colors, there has been a growing interest in exploring the potential use of anthocyanins as natural food colorants [9]. However, the application of anthocyanin pigments is limited due to their low stability. The anthocyanins color is highly dependent on their structure and is greatly influenced by factors such as pH, temperature, light, oxygen, ascorbic acid, enzymes, sugars, degradation products, and metal ions [9–11]. As a result, the food industry has been actively seeking new alternative pigments that exhibit a blue color.

Alternatively, anthocyanin-derived pigments, namely vinylpyranoanthocyanin–catechins, offer higher coloring capacity and stability compared to the original anthocyanins [12]. These pigments, also known as portisins, are naturally occurring blue pigments that were initially identified in aged Port red wines. These pigments can be directly obtained by reacting anthocyanin-pyruvic acid adducts with flavanols in the presence of acetaldehyde (**Figure 1**) [13]. Although portisins occur at very low levels in Port wine, attempts have been made to produce these bluish pigments using several red fruit extracts as sources of anthocyanin [14].

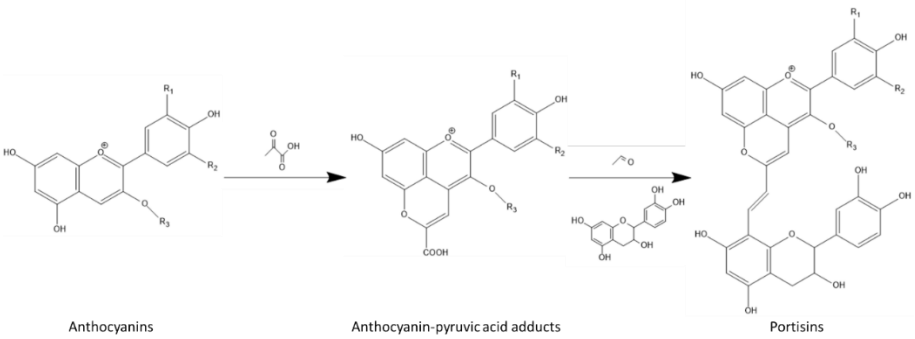

Figure 1. General scheme for portisins hemi-synthesis.

Portisins display an unusual bluish color under acidic conditions, with a visible λ_{max} at approximately 570 nm. The structural properties of these pigments, specifically the extended conjugated system of π-electrons, confer high stability and remarkable resistance to color bleaching by sulfur dioxide [15]. As a result, the increasing demand for natural blue colorants combined with the natural occurrence of these bluish anthocyanin-derived pigments in aged Port wine allow portisins to emerge as a promising alternative to synthetic Brilliant Blue FCF (E 133) [16].

Considering the complex chemical composition of natural products/extracts, which range from pigments to bioactive ingredients, the separation of target

compounds is essential. The isolation of portisins from wine or red fruit extracts after hemi-synthesis has traditionally been performed by C18 silica gel reverse phase liquid chromatography (RP-LC) [13,17,18]. However, this conventional method for portisins separation is time-consuming, requires a large volume of organic solvents, and results in low recovery rates due to irreversible adsorption to the solid support [19,20]. In an alternative approach, centrifugal partition chromatography (CPC) was employed for the preparative isolation of portisins semi-synthetized from blueberry surplus anthocyanin-derived extract [21]. This study concluded that the efficiency of the CPC process and the associated environmental risk factors were improved compared to the RP-LC process. Nevertheless, the recovery of portisin relied on organic solvents, which limits their subsequent use in food applications. Therefore, there is a current need to develop not only efficient and cost-effective technologies but also greener methodologies that employ biocompatible solvents for the isolation of these bluish pigments from a complex mixture.

Compressed fluid-based technologies, which include subcritical and supercritical fluid approaches, have been recognized as a promising process for the food, nutraceutical, pharma, and cosmetic industries. These technologies provide higher selectivity and avoid the need for toxic organic solvents [22]. Additionally, compressed fluid-based technologies can be particularly attractive for the extraction of portisins due to reduced process time and temperature, preserving the integrity of thermo-label compounds, and preventing oxidative reactions through the absence of light and oxygen [23,24].

While several fluids have been explored, carbon dioxide (CO_2) is by far the most attractive and has been widely used in food, nutraceutical, pharma, and

cosmetic applications. However, CO_2 is unsuitable for isolating polar compounds due to its nonpolar and lipophilic nature. Also, CO_2 exhibits a limited ability to extract high molecular weight compounds, which might limit the extraction performance of portisins (MW ≈ 800 g/mol). Therefore, the addition of a suitable modifier such as ethanol can significantly improve the solubility of medium polar/polar substances, increasing the selectivity of the process. Another strategy is the integration of compressed fluids: supercritical fluids combined with pressurized liquids [22,23].

Compressed fluids have been applied to isolate portisins precursors (anthocyanins) from different natural sources, including fruits [22,25,26] and fruit residues [23,27–31]. However, there is currently no information available in the literature regarding the application of compressed fluids for the efficient recovery of portisins.

The present study aimed to develop a greener process for the selective and efficient recovery of portisins from the blueberry surplus extract, which was used as the source of anthocyanin for the portisin hemi-synthesis. For the first time, the feasibility of applying compressed fluids to the purification of portisins was investigated. The extraction yield, portisins yield, and portisins content in the extract were analyzed to optimize the compressed fluid-based separation process conditions. Additionally, the process throughput, efficiency, and environmental risk factor of the proposed protocol were assessed and compared with the reported preparative chromatographic techniques (RP-LC and CPC) for portisins isolation. This separation approach represents a significant step in the challenging task of producing highly demanded blue colorants for the food, nutraceutical, pharma, and cosmetic industries, contributing to the sustainable utilization of blueberry surplus.

3. MATERIALS AND METHODS

3.1. Raw material

It is important to note that the crude portisin extract used in this study was the same material as employed in the study conducted by Nunes et al. [21]. To briefly recap, the blueberry surplus was initially extracted with 50 vol.% aqueous methanol solution at pH 1.5 (adjusted with HCl) for 2h at room temperature. Anthocyanins were recovered from the residues through two extraction cycles, using a 10:1 solvent-to-residue ratio. The resulting extract was filtered, and methanol was subsequently removed via rotary evaporation at 38 °C under reduced pressure. The anthocyanin crude extract was further processed on a C-18 silica gel reversed phase column, first with deionized water to remove sugars and phenolic acids and then with methanol at pH 1.5 (adjusted with HCl) to elute anthocyanins. The eluted solvent was evaporated under reduced pressure at 38°C. The identity of each anthocyanin present in the blueberry surplus extract and the quantification of total anthocyanin content were determined by HPLC-DAD-MS. The anthocyanin extract exhibited a total anthocyanin content of 60 mg malvidin-3-glucoside equivalents/g extract and the pigment profile consisted of 15 anthocyanins. The respective chromatogram at 520 nm is provided in the Chapter 2 Part I page 98.

After anthocyanin extract preparation, the crude portisin extract was obtained through the chemical reaction of blueberry surplus anthocyanin-rich extract with pyruvic acid and catechin, as previously described by Nunes et al. [21]. The reaction occurred in two steps: the initial formation of the anthocyanin-pyruvic acid adducts (reaction 1), followed by the synthesis of portisins (reaction 2). The identity of the portisins that were formed during the synthesis and the quantification of total portisins content were

performed by HPLC-DAD-MS. Reaction mixture 1 (RM1) was mainly comprised of anthocyanin-pyruvic acid adducts derived from the original anthocyanins present in the blueberry surplus, while reaction mixture 2 (RM2) predominantly contained the respective portisins along with the remaining anthocyanin-pyruvic acid adducts. The respective chromatogram of the RM1 and RM2 recorded at 570 nm is provided in the Chapter 2 Part I page 101. RM2 exhibited a total portisins content of 100 mg vinylpyranomalvidin-3-O-glucoside-catechin equivalents/g of extract. The RM2 was dried via rotary evaporation at 38°C under reduced pressure and was stored at a temperature of −20°C, in the absence of light, until used in this study.

3.2. Chemicals

The chemicals utilized for the compressed fluid-based separation process were as follows: CO_2 99.95% from Air Liquide (Lisbon, Portugal) and ethanol absolute 99.9% from Carlo Herba (Val de Reuil, France).

The chemicals employed for the chemical characterization of fractions were as follows: acetonitrile >99.9% from Chem Lab (Zedelgem, Bélgium), formic acid 99% from Carlo Herba (Val de Reuil, France), and vinylpyranomalvidin-3-O-glucoside-catechin, which was used as a standard for portisins quantification and obtained as described by Mateus et al. [32].

3.3. Portisins compressed fluid-based separation process

3.3.1. Compressed fluid-based separation process conditions optimization

The compressed fluid-based separation experiments were conducted in a supercritical fluid extraction system (Thar Technology, Pittsburgh, PA, U.S.A., model SFE-500F-2-C50) equipped with a 500 mL cylinder extraction cell and two different separators, each of them with 500 mL of capacity, with independent control of temperature and pressure. This apparatus was previously described by Nunes et al. [33]. The extraction vessel was filled with dried RM2 and glass beads to achieve a uniform distribution of the solvent flow. Based on previous works for portisins precursors [22,23,25–31] and preliminary experimental results, process variables, and their ranges, pressure (100-500 bar), temperature (40-60°C), and ethanol content in the compressed fluid mixture (10-40 wt.%), were chosen (Table 1). Other parameters have been fixed, such as the amount of RM2 (set at 100 mg), the CO_2+ethanol flow rate (set at 25 g/ min), and the extraction time (set at 35 min). Central replicate points were included to assess the experimental variability, uncertainty of results and the goodness of fit of the mathematical model. The extract was recovered in a flask placed in an ice bath. The extract was dried in a rotary evaporator at a temperature of 38 °C under reduced pressure and stored at temperature of −20°C in the absence of light until further use.

3.3.2. Two-step compressed fluid separation process

The two-step separation was conducted in previously mentioned extractor (Thar Technology, Pittsburgh, PA, USA, model SFE-500F-2-C50). A sequential extraction methodology was employed, comprising (1) a first step to remove low polarity compounds, including anthocyanin-pyruvic acid adducts, and (2) a second step to extract portisins, which are medium-polarity compounds. The operating conditions for each step were selected using a multiple linear

regression approach with an automated optimizer (Modde® v.12), based on the knowledge acquired from the optimization experiments conducted in the previous subsection 2.3.1. The selected conditions were as follows: (1) for the first step, 100 bar, 60°C and 20 wt.% ethanol content in the compressed fluid mixture, and (2) for the second step, 500 bar, 40°C and 40 wt.% ethanol content in the compressed fluid mixture. In addition to the conditions suggested by the Modde® software, an additional set of conditions, namely 500 bar, 40°C and 100 wt.% ethanol, was also evaluated in the second step to maximize the extraction of portisin after the recovery of the first fraction. Other parameters have been kept constant, such as the amount of RM2 (set at 100 mg) and the CO_2+ethanol flow rate (set at 25 g/ min). Two fractions were collected in a flask placed in an ice bath, with one fraction collected during each step of the separation process. The fractions were dried in a rotary evaporator at a temperature of 38°C under reduced pressure and stored at a temperature of −20°C in the absence of light until further use.

3.4. High-Performance Liquid Chromatography-Diode Array Detector (HPLC-DAD)

The anthocyanin-rich extract and anthocyanin-pyruvic acid adducts fractions were analyzed in a Dionex UltiMate 3000 HPLC system equipped with a quaternary pump, autosampler, column compartment and coupled to an UltiMate 3000 Diode Array Detector (Thermo Scientific, Waltham, MA, USA) according to the method described by Oliveira et al. [17]. Chromatographic separation was performed on a Macherey-Nagel® RP-18 column (250 mm length, 4 mm width, and 5 μm particle size) maintained at a temperature of 25°C. The eluents were A: H_2O/HCOOH (volume ratio 9:1), and B: CH_3CN/H_2O/HCOOH (volume ratio 3:6:1). The gradient consisted of 20-85% B

for 70 min at a flow rate of 1.0 mL/min. The column was washed with 100% B for 10 min and then stabilized with the initial conditions for another 10 min [34]. The injection volume was 100 µL and the autosampler was held at a temperature of 8°C. The photodiode array detector was programmed for scanning between 190 and 580 nm at a speed of 5 Hz with a bandwidth of 2 nm. The detection was monitored using four individual channels, 570 nm (portisins), 520 nm (anthocyanins), 511 nm (anthocyanin-pyruvic acid adducts), and 280 nm (phenolic compounds). For the acquisition and processing of data, Chromeleon® software version 7.2 SR4 was used. The calibration curve for malvidin-3-glucoside was linear within the range of 0-100 ppm using acidified water at pH 1.5 (adjusted with HCl) as solvent. Results for total anthocyanins content were presented as mg of malvidin-3-glucoside equivalents per g of fraction and expressed as a mean of triplicates. The portisins fractions were also analyzed by HPLC-DAD using the same conditions but with a different eluent B: CH_3CN/H_2O/HCOOH (volume ratio 8:1.95:0.05). The calibration curve for vinylpyranomalvidin-3-*O*-glucoside-catechin was linear within the range of 0-80 ppm using 30 vol.% aqueous ethanol 0.1 M HCl as solvent. Results for portisins content were presented as mg of vinylpyranomalvidin-3-*O*-glucoside-catechin equivalents per g of fraction.

3.5. Extraction yield and portisins yield estimation

Extraction yield (Y) was determined as a measure of mass recovered per mass of processed RM2:

$$Y = m_{\text{extract recovered}} / m_{\textit{processed RM2}} \text{ x100, wt.\%} \quad \text{(Eq. 1)}$$

Portisins yield (Y_P) was assessed as a measure of mass of portisins recovered per mass of processed RM2:

$$Y_P = m_{\text{P recovered}} / m_{processed\ RM2} \text{ x100, wt.\%} \quad \text{(Eq. 2)}$$

3.6. Process throughput, process efficiency, and environmental risk factor estimation

Process throughput (PT) was evaluated as a measure of mass processed per unit time:

$$PT = m_{processed\ RM2} / t_{extraction}, \text{ mg processed RM2/h} \quad \text{(Eq. 3)}$$

where $m_{processed\ RM2}$ represents the mass of RM2 processed per run and $t_{extration}$ denotes the time taken for a single run.

Process efficiency (PE) was assessed as a metric for evaluating the production rate of one unit mass of the target compound:

$$PE = m_{P\ recovered} / t_{extraction}, \textit{ mg portisins /h} \quad \text{(Eq. 4)}$$

where $m_{\ P\ recovered}$ represents the mass of portisins recovered and $t_{extraction}$ denotes the time consumed during the separation.

Process environmental risk factor (Er) was determined to assess the volume of waste solvent generated in the production of one unit mass of the target compound:

$$Er = V_{total\ solvent} / m_{P\ recovered}, \textit{ L /g portisins} \quad \text{(Eq. 5)}$$

where, $V_{total\ solvent}$ represents the total volume of solvent used (considering only the volume of ethanol, as CO_2 is automatically separated from the extract upon depressurization and potentially recycled) and $m_{P\ recovered}$ denotes the mass of portisins recovered.

PT and PE were used as key indices, along with the portisin content, to evaluate the performance of compressed fluid-based separation process. Additionally, the Er was determined to estimate the environmental impact of the separation process. These parameters (PT, PE and Er) were previously determined for the preparative RP-LC and CPC by Nunes et al. [21] and are available to compare and evaluate the performance and environmental impact of different methodologies applied. It is important to note that for meaningful comparisons, the results of PT and PE must be normalized by dividing them by the respective column/vessel of the separation equipment.

3.7. Experimental design and statistical analysis

The impact of process factors (pressure, temperature, and ethanol content in the compressed fluid mixture) on the compressed fluid-based separation was determined using a response surface technique. The program Modde® v.12 (Umetrics, Umea, Sweden) was used to evaluate the extraction yield, portisins yield, and portisins content in the extract obtained from tests conducted under experimental settings specified by a central composite face design. Adjustments to the design model and impacts of the variables were statistically significant whenever the resulting p-value was less than the predetermined $p = 0.05$ (ANOVA and t-test).

4. RESULTS AND DISCUSSION

4.1. Compressed fluid-based separation process optimization

The present study aimed to establish an alternative downstream isolation methodology for bluish anthocyanin-derived pigments. Considering the complex chemical composition of the blueberry extract after the hemi-

synthesis of portisins, the compressed fluid-based separation process was applied as a greener alternative for the isolation and recovery of portisins.

When compressed fluids are applied as a solvent, various experimental factors need to be considered and optimized for each investigated system. A systematic approach was necessary to effectively address the expected process factors, intricate interactions, and the desired high yield and content. Building upon previous studies on anthocyanins, which are the precursors for the formation of portisins, as well as preliminary experimental findings and instrumental limitations, some factors were kept constant (such as the amount of RM2, the CO_2+ethanol flow rate, and extraction time) to simplify the task and reduce the complexity of the parameter space explored.

The selection of operating parameters and their ranges, including pressure (100-500 bar) and temperature (40-60°C), was based on existing literature on the application of sub/supercritical fluids for anthocyanin recovery [22,23,25–31]. Also, to achieve efficient separation of portisins, which are medium polar compounds, a biocompatible polar co-solvent, namely ethanol, was added to the dense CO_2. Different ethanol concentrations in the compressed fluid mixture (10-40 wt.%) were investigated for the portisins separation.

To achieve the balance between the number of experimental runs and the acquired knowledge, a central composite face design was selected, which combined a full factorial design with star points placed on the faces of the sides. Central replicate points were included to assess the experimental variability, uncertainty of results, and the goodness of fit of the mathematical model. Response surface methodology was employed to determine the optimal conditions for the compressed fluid-based separation process of the portisin fraction from RM2.

The experimental conditions and corresponding outcomes for each compressed fluid-based separation experiment, as outlined in the central composite face design, are detailed in Table 1. Among the experiments, the highest extraction yield was 50 ± 11 wt.% (Table 1 - experiment N6). This yield was obtained at 40°C, 500 bar, and 40 wt.% ethanol content in the compressed fluid mixture. Under these conditions, portisins yield and portisins content in the collected fraction were among the highest, with yield at 5.0 ± 1.3 wt.% and content at 101 ± 19 mg portisins/g extract.

Table 1. Compressed fluid-based separation process conditions applied and respective extraction yield, portisins yield and portisins content in the extract. (Fixed parameters: 100 mg of RM2, 25 g/ min of CO_2+ethanol flow rate, and 35 min of extraction time)

Exp Name	Pressure (bar)	Temperature (°C)	Ethanol content (wt.%)	Extraction yield (wt.%)	Portisins yield (wt.%)	Portisins content (mg P/g extract)
N1	100	40	20	18.7	0.03	1.4
N2	500	40	20	11.4	0.07	6.0
N3	100	60	20	33.0	0.05	1.4
N4	500	60	20	1.6	0.04	23.9
N5	100	40	40	24.1	1.21	50.2
N6	500	40	40	49.9	5.04	101.0
N7	100	60	40	28.6	1.96	68.6
N8	500	60	40	38.2	0.22	5.7
N9	100	50	30	17.0	0.23	13.8
N10	500	50	30	31.9	2.41	75.7
N11	300	40	30	20.5	0.38	18.7
N12	300	60	30	26.4	0.55	20.9
N13	300	50	20	18.3	0.03	1.7
N14	300	50	40	38.9	4.10	105.5
N15	300	50	30	24.8	0.52	20.8
N16	300	50	30	11.2	0.32	29.0
N17	300	50	30	17.7	0.53	29.8

In this study, the ethanol content in the compressed fluid mixture was found to have a significant effect ($p < 0.05$) on the three evaluated responses: extraction yield, portisins yield, and portisins content in the extract. In addition, the extraction yield was significantly affected ($p < 0.05$) by some interactions between factors, specifically pressure with temperature and pressure with ethanol content in the compressed fluid mixture. Also, the interaction between pressure and ethanol content in the compressed fluid mixture significantly affected ($p < 0.05$) the portisins content in the extract (the model fit is provided in the Appendix page 260). Contour plots representing the extraction yield, portisins yield and portisins content in the extract as a function of the extraction temperature, pressure, and ethanol content in the compressed fluid mixture are presented in Figure 2.

From Figure 2, when a high content of ethanol in the compressed fluid mixture is used, by increasing the pressure, an increase of the extraction yield and portisins yield was observed. This can be attributed to the higher density of the mixture at increased pressure (the density is provided in the Appendix page 260), which enhances the solvating power of the compressed fluid mixture, improving the solubility of target compounds. Conversely, portisins content in the extract showed an opposite trend, which could be explained by the decrease in process selectivity due to the increased extraction of other compounds.

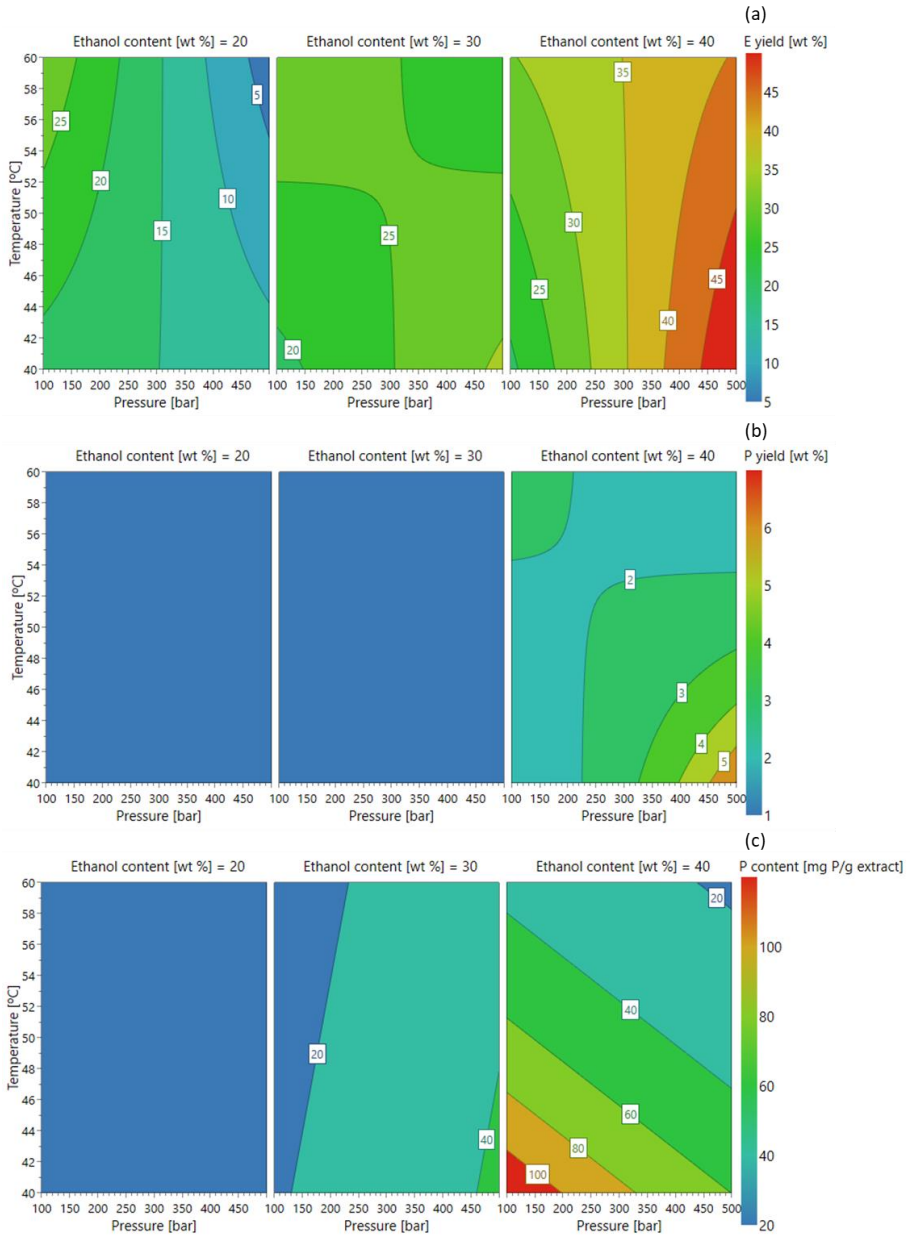

Figure 2. Contour plots of the effects of different temperatures, pressure, and ethanol content in the compressed fluid mixture on (Figure 2a) extraction yield, (Figure 2b) portisins yield, and (Figure 2c) portisins content in the extract.

When higher temperatures were applied to RM2, the extraction yield increased while portisins yield and content in the extract decreased, as depicted in Figure 2. Higher temperatures can lead to an accelerated thermal degradation rate of portisins or affect the interaction between portisins and ethanol, weakening their hydrogen bonds and thereby reducing portisins yield and content in the extract. Therefore, portisins solubility was found to be strongly dependent on the density of the mixture, with greater solubility observed at increasing density. This allowed for the avoidance of higher temperatures, which could lead to thermal degradation.

Previous studies have also demonstrated the influence of the density of the mixture on the solubility of anthocyanins (portisins precursors) in compressed CO_2 + ethanol mixtures, although specific results regarding the influence of pressure and temperature vary [22,23,31]. These variations can be attributed not only to the solubility of the substances in the compressed fluid mixture but also to the composition of the sample matrix, which introduces different mass transfer resistances [31].

The composition of the compressed fluid mixture was identified as the most crucial factor affecting portisins isolation. As shown in Figure 2, increasing the ethanol content in the compressed fluid mixture significantly improved the extraction yield, portisins yield, and portisins content in the extract. Supercritical CO_2, being nonpolar, has a limited capacity to extract medium polar compounds such as portisins. However, the addition of ethanol enhances the polarity of the fluid mixture and promotes the formation of hydrogen bonds between portisins and ethanol present in the CO_2 stream, thereby increasing the solubility of portisins. Previous studies by other researchers have also demonstrated that the solubility of anthocyanins

(portisins precursors) in compressed CO_2 + ethanol mixture is influenced by their polarity [22,23,25,28].

These findings indicate that using a relatively low temperature (40°C) with high pressure (500 bar) and significant ethanol content in the compressed fluid mixture (40 wt.%) resulted in the highest portisins yield but also the highest extraction of other compounds (extraction yield). It should be noted that this combination of parameters compromised the process selectivity, which is directly proportional to the final content of the target compound in the collected fraction. Consequently, a two-step compressed fluid isolation process was investigated, involving an initial step to remove low polarity compounds (including anthocyanin-pyruvic acid adducts) followed by a second step to recover portisins.

4.2. Two-step compressed fluid separation process

As demonstrated, operating pressure, temperature, and the ethanol content in the compressed fluid mixture have different effects on each evaluated response variable. Additionally, other compounds present in RM2 were co-extracted or negatively interfered with the purification of portisins, resulting in decreased portisins yield and content. Therefore, the goal was to optimize the isolation of portisins by maximizing portisins content in the extract, and portisins yield while minimizing the co-extraction of other compounds (extraction yield).

To achieve this, a two-step fractionation methodology was employed. The operating conditions for each step were selected using a multiple linear regression approach with an automated optimizer (Modde® v.12). Based on the knowledge acquired from the optimization experiments, the software

proposed 12 sets of optimal separation conditions for each step, and the output with the lowest probability of failure was chosen.

The first step (Table 2 – experiment N18 1st step) involved operating at 100 bar, 60°C and 20 wt.% ethanol content in the compressed fluid mixture for 60 min, which were the same conditions as experiment N3, but with extended extraction time. This extended time was necessary to ensure that no more compounds were being collected under those conditions, reaching a point where no further color was being extracted. The purpose of this step was to remove the low polarity compounds present in the RM2 before proceeding to the portisins recovery step.

The second step (Table 2 – experiment N18 2nd step) involved operating at 500 bar, 40°C and 40 wt.% ethanol content in the compressed fluid mixture for 75 min, which were the same conditions as experiment N6, but with extended extraction time. Similarly, the prolonged time was crucial to ensure that the collection reached a point where no more compounds were being extracted under those conditions. The objective of this step was to subsequently isolate portisins after the initial separation step of low polarity compounds.

The extraction yield, portisins yield, and portisins content in the extract obtained from the two-step isolation process are presented in Table 2. It is evident that the first step, which targeted the extraction of low polarity substances, resulted in lower values of extraction yield (22 ± 2 wt.%) and portisins yield (0.071 ± 0.002 wt.%). This fraction exhibited a yellow color and had a lower portisins content (3.3 ± 0.4 mg portisins/g extract).

Table 2. Two-step compressed fluid separation process conditions applied and respective extraction yield, portisins yield and portisins content in the extract. (Fixed parameters: 100 mg of RM2 and 25 g/ min of CO_2+ethanol flow rate)

Exp Name	Pressure (bar)	Temperature (°C)	Ethanol content (wt.%)	Extraction time (min)	Extraction yield (wt.%)	Portisins yield (wt.%)	Portisins content (mg P/g extract)
N18							
1st step	100	60	20	60	21.7	0.07	3.3
2nd step	500	40	40	75	41.8	4.62	110.9
N19							
1st step	100	60	20	60	22.5	0.08	3.4
2nd step	500	40	100	30	59.4	8.66	145.8

After collecting the first fraction, the operating conditions were set up for the second step. As can be seen from Table 2, this modification led to higher values of extraction yield (41.8 ± 1.9 wt.%) and portisins yield (4.62 ± 0.12 wt.%). The resulting fraction contained the medium polarity compounds found in RM2 and exhibited a distinct blue-purple color. However, the increase in portisins content in this fraction (111 ± 8. mg portisins/g extract) was only 11 wt.% compared to its initial value in the RM2. As a result, alternative conditions were tested for the second step of the two-step separation process (Table 2 – experiment N19).

Considering the significant improvement observed in portisins yield and content in the extract by increasing the ethanol content in the compressed fluid mixture, a second step (Table 2 – experiment N19 2nd step) was conducted at 500 bar and 40°C with compressed ethanol (100 wt.%) for 30 min. The goal was to maximize the extraction of portisins after the recovery of the first fraction (Table 2 – experiment N19 1st step). The results demonstrate that this modification resulted in a significantly higher portisins yield (8.7 ± 0.2 wt.%) portisins content in the extract (146 ± 5 mg portisins/g

extract). The portisins yield and content in the extract were 1.9 and 1.3 times higher, respectively, compared to the values obtained using compressed CO_2 with 40 wt.% of ethanol. The increase in portisins content in this fraction was 15 wt.% compared to its initial value in the RM2.

The results presented above demonstrated that employing a two-step isolation process yielded the highest portisins yield and selectivity. In the first step, supercritical CO_2 extraction was conducted at 100 bar, 60°C, and 20 wt.% ethanol content in the compressed fluid mixture for a duration of 60 min. This initial step effectively removed low-polarity compounds. Subsequently, in the second step, a pressurized liquid extraction was performed at 500 bar, 40°C with 100 wt.% ethanol for a duration of 30 min. This combination of conditions resulted in not only the highest yield of portisins but also the highest portisins content in the extract, highlighting the effectiveness of the chosen extraction conditions.

4.3. Comparison with the reported chromatographic methods

Despite the importance of process selectivity and biocompatibility, the cost-effectiveness of the applied methodology is equally crucial. To access this aspect, a comparison of process throughput, efficiency and environmental risk factor was conducted between the two-step compressed fluid separation, preparative CPC, and preparative RP-LC. The results of this comparison, which were normalized by dividing the PT and PE by the respective column volume (Vc) of the separation equipment, are presented in Table 3.

Table 3. Experimental values (n=2) of portisin content, process throughput, process efficiency and environmental risk factor under selected conditions of

two-step compressed fluid separation (CFS), preparative CPC, and preparative RP-LC.

	Portisins content (mg P/g extract)	Process throughput (mg processed extract/h/Vc)	Process efficiency (mg P/h/Vc)	Environmental risk factor (L/g P)
CFS*	146 ± 5	0.34 ± 0.00	0.03 ± 0.00	92 ± 2
CPC [21]	469 ± 46	2.06 ± 0.14	0.19 ± 0.03	30 ± 6
RP-LC [21]	396 ± 52	2.09 ± 0.02	0.08 ± 0.01	164 ± 38

*Conditions - 1st step: 100 bar, 60°C, 20 wt.% ethanol content, and 60 min; 2nd step: 500 bar, 40°C, 100 wt.% ethanol content, and 30 min.

Conventionally, the purification of portisins from Port red wine or the red fruit extracts after hemi-synthesis involves C18 silica gel reverse phase liquid chromatography [13,17,18]. However, the industrial scale implementation of column chromatography-based processes is hindered by certain limitations. In our previous work [21], CPC was successfully applied for the preparative isolation of portisins from RM2. The CPC separation employed a biphasic solvent system comprising tert-butyl-methyl ether, n-butanol, acetonitrile, and water in a volume ratio of 2:2:1:5, with 0.1% hydrochloric acid. Optimized conditions of 464 mg sample/100 mL of column volume, 20 mL/min of mobile phase flow rate, and 1600 rpm of rotation speed at descending mode, enabled the purification of portisins by 5-fold. Compared to conventional RP-LC, the CPC process exhibited improved efficiency (2.4 times) and reduce environmental risk factor were improved (5.5 times) as shown in Table 3. However, the recovery of portisin using organic solvents limits their suitability for certain application, particularly in the food industry. Tert-butyl-methyl ether is rarely used due to safety and quality concerns, while n-butanol can be applied in compliance with strict regulations, and acetonitrile is tightly controlled due to toxicity concerns in the food industry, emphasizing the

need to consider the purpose for which solvents are used, whether for analysis or processing, with careful to safety and regulatory guidelines [35].

In this work, the two-step compressed fluid separation process achieved a 1.5-fold purification of portisins. A comparison with conventional RP-LC revealed that the compressed fluid separation process had lower throughput, efficiency, and environmental risk factor (6.2, 2.8, and 1.8 times, respectively – Table 3). Although the compressed fluid separation strategy utilized environmental-friendly and food/pharmaceutical-accepted solvents, the process efficiency and selectivity towards portisins was lower. However, it is important to note that the environmental risk factor used in this comparison, which is based on the volume of waste solvent generated in the production of one unit mass of target compound, provides valuable insights. Nonetheless, this factor does not consider toxicity and environmental information, which are key factors that need to be considered to select compressed fluid-based separation over other processes. Nevertheless, this fractionation strategy provided the advantage of increasing solvent polarity by adjusting the CO_2 and ethanol ratio, without the need for undesired toxic organic solvents. As a result, two fractions were obtained, with the first fraction containing anthocyanin-pyruvic acid adducts (orange pigments), which can be also exploited as a secondary product toward a circular economy.

The portisins-rich fraction obtained through both alternative separation technologies exhibited a distinct blue-purple color and varied portisin content. Therefore, the selection of the suitable separation technology depends on the intended application of the resulting bluish fraction. CPC is suitable for applications that demand a high concentration of portisin and yield. On the other hand, if the use of biocompatible solvents is a critical

requirement, the two-step compressed fluid separation process can be employed.

5. CONCLUSIONS

In this work, a fractionation strategy using compressed fluids is proposed for the recovery of highly demanded blue pigments, portisins, which are semi-synthetized from blueberry surplus anthocyanin extract. The compressed fluid-based separation process conditions were determined using a graphical optimization method, combining response surface methodology with a desirability function. The proposed separation process consisted of two steps. First, supercritical CO_2 extraction was conducted at 100 bar, 60°C and 20 wt.% ethanol content in the compressed fluid mixture for a duration of 60 min to remove the low and medium polarity compounds. Subsequently, a pressurized liquid extraction was performed at 500 bar, 40°C with 100 wt.% ethanol for a duration of 30 min to recover portisins. This two-step compressed fluid separation process resulted in not only the highest yield of portisins but also the portisin content. These conditions resulted in a 1.5-fold purification of portisins. Comparing the two-step compressed fluid separation process to conventional preparative RP-LC, the process throughput and efficiency were 6.2 and 2.8 times lower, respectively. However, the two-step compressed fluid process offers the advantage of reduced ethanol consumption compared with preparative RP-LC, resulting in a lower environmental risk factor (1.8 times). Hence, the choice of the most suitable separation technology for portisins isolation depends on the intended application of the resulting bluish extract. Both alternative technologies have distinct advantages and considerations. Preparative CPC is ideal for applications requiring high portisin content, and efficient recovery.

On the other hand, the two-step compressed fluid separation process is beneficial when the use of biocompatible solvents is a critical requirement. Overall, the proposed protocol provides an alternative approach for producing bluish portisin pigments with potential application in the food, pharma, nutraceutical. and cosmetic industries. Also, it contributed to the sustainable utilization of blueberry residues towards a circular economy, offering a more environmentally friendly method for portisins extraction and purification.

6. ACKNOWLEDGEMENTS

This work was funded by Fundação para a Ciência e Tecnologia/Ministério da Ciência, Tecnologia e Ensino Superior (FCT/MCTES, Portugal) through national funds to iNOVA4Health (UIDB/04462/2020 and UIDP/04462/2020), the Associate Laboratory LS4FUTURE (LA/P/0087/2020) and Associated Laboratory for Sustainable Chemistry, Clean Processes, and Technologies LAQV (UIDB/50006/2020 and UIDP/50006/2020). Funding from INTERFACE Programme, through the Innovation, Technology and Circular Economy Fund (FITEC), is gratefully acknowledged. A.N.N. acknowledge FCT for the financial support received through SFRH/BD/144592/2019. J.O. acknowledge FCT her research contract (2022.00042.CEECIND_CP1724_CT0017). Ana A. Matias thanks for the IF Starting Grant – GRAPHYT (IF/00723/2014).

7. REFERENCES

[1] H. Xue, X. Zhu, J. Tan, L. Fan, Q. Li, J. Tang, X. Cai, Counter-current fractionation-assisted bioassay-guided separation of active compound from blueberry and the interaction between the active

compound and α-glucosidase, Foods. 10 (2021). https://doi.org/10.3390/foods10030509.

[2] S. Silva, E.M. Costa, M. Veiga, R.M. Morais, C. Calhau, M. Pintado, Health promoting properties of blueberries: a review, Crit. Rev. Food Sci. Nutr. 60 (2020) 181–200. https://doi.org/10.1080/10408398.2018.1518895.

[3] H. Yang, Y. Wu, C. Zhang, W. Wu, L. Lyu, W. Li, Growth and physiological characteristics of four blueberry cultivars under different high soil pH treatments, Environ. Exp. Bot. 197 (2022) 104842. https://doi.org/10.1016/j.envexpbot.2022.104842.

[4] H. Liu, S. Qin, R. Sirohi, V. Ahluwalia, Y. Zhou, R. Sindhu, P. Binod, R. Rani Singhnia, A. Kumar Patel, A. Juneja, D. Kumar, Z. Zhang, J. Kumar, M.J. Taherzadeh, M. Kumar Awasthi, Sustainable blueberry waste recycling towards biorefinery strategy and circular bioeconomy: A review, Bioresour. Technol. 332 (2021) 125181. https://doi.org/10.1016/j.biortech.2021.125181.

[5] Y. Duan, A. Tarafdar, D. Chaurasia, A. Singh, P.C. Bhargava, J. Yang, Z. Li, X. Ni, Y. Tian, H. Li, M.K. Awasthi, Blueberry fruit valorization and valuable constituents: A review, Int. J. Food Microbiol. 381 (2022) 109890. https://doi.org/10.1016/j.ijfoodmicro.2022.109890.

[6] C. Bas-Bellver, C. Andrés, L. Seguí, C. Barrera, N. Jiménez-Hernández, A. Artacho, N. Betoret, M.J. Gosalbes, Valorization of Persimmon and Blueberry Byproducts to Obtain Functional Powders: In Vitro Digestion and Fermentation by Gut Microbiota, J. Agric. Food Chem. 68 (2020) 8080–8090. https://doi.org/10.1021/acs.jafc.0c02088.

[7] A.M. Mustafa, S. Angeloni, D. Abouelenein, L. Acquaticci, J. Xiao, G.

Sagratini, F. Maggi, S. Vittori, G. Caprioli, A new HPLC-MS/MS method for the simultaneous determination of 36 polyphenols in blueberry, strawberry and their commercial products and determination of antioxidant activity, Food Chem. 367 (2022) 130743. https://doi.org/10.1016/j.foodchem.2021.130743.

[8] W. Kalt, A. Cassidy, L.R. Howard, R. Krikorian, A.J. Stull, F. Tremblay, R. Zamora-Ros, Recent Research on the Health Benefits of Blueberries and Their Anthocyanins, Adv. Nutr. 11 (2020) 224–236. https://doi.org/10.1093/advances/nmz065.

[9] W. Yang, Y. Guo, M. Liu, X. Chen, X. Xiao, S. Wang, P. Gong, Y. Ma, F. Chen, Structure and function of blueberry anthocyanins: A review of recent advances, J. Funct. Foods. 88 (2022) 104864. https://doi.org/10.1016/j.jff.2021.104864.

[10] J. Oliveira, A. Fernandes, V. De Freitas, Synthesis and structural characterization by LC-MS and NMR of a new semi-natural blue amino-based pyranoanthocyanin compound, Tetrahedron Lett. 57 (2016) 1277–1281. https://doi.org/10.1016/j.tetlet.2016.02.026.

[11] D.M. Jiménez-Aguilar, a. E. Ortega-Regules, J.D. Lozada-Ramírez, M.C.I. Pérez-Pérez, E.J. Vernon-Carter, J. Welti-Chanes, Color and chemical stability of spray-dried blueberry extract using mesquite gum as wall material, J. Food Compos. Anal. 24 (2011) 889–894. https://doi.org/10.1016/j.jfca.2011.04.012.

[12] V. De Freitas, N. Mateus, Formation of pyranoanthocyanins in red wines: A new and diverse class of anthocyanin derivatives, Anal. Bioanal. Chem. 401 (2011) 1467–1477. https://doi.org/10.1007/s00216-010-4479-9.

[13] N. Mateus, A.M.S. Silva, J.C. Rivas-Gonzalo, C. Santos-Buelga, V. De Freitas, A new class of blue anthocyanin-derived pigments isolated from red wines, J. Agric. Food Chem. 51 (2003) 1919–1923. https://doi.org/10.1021/jf020943a.

[14] N. Mateus, J. Oliveira, M. Haettich-Motta, V. de Freitas, New Family of Bluish Pyranoanthocyanins, J. Biomed. Biotechnol. 2004 (2004) 299–305. https://doi.org/10.1155/S1110724304404033.

[15] J. Oliveira, C. Santos-Buelga, A.M.S. Silva, V. De Freitas, N. Mateus, Chromatic and structural features of blue anthocyanin-derived pigments present in Port wine, Anal. Chim. Acta. 563 (2006) 2–9. https://doi.org/10.1016/j.aca.2005.11.027.

[16] F. Pina, N. Basílio, A.J. Parola, M.J. Melo, J. Oliveira, V. De Freitas, The Triumph of the Blue in Nature and in Anthropocene, Dye. Pigment. 210 (2023) 110925. https://doi.org/10.1016/j.dyepig.2022.110925.

[17] J. Oliveira, C. Santos-Buelga, A.M.S. Silva, V. De Freitas, N. Mateus, Chromatic and structural features of blue anthocyanin-derived pigments present in Port wine, Anal. Chim. Acta. 563 (2006) 2–9. https://doi.org/10.1016/j.aca.2005.11.027.

[18] J. Oliveira, V. De Freitas, A.M.S. Silva, N. Mateus, Reaction between hydroxycinnamic acids and anthocyanin-pyruvic acid adducts yielding new portisins, J. Agric. Food Chem. 55 (2007) 6349–6356. https://doi.org/10.1021/jf070968f.

[19] Y. Xu, D. Hu, Y. Li, C. Sun, W. Chen, An effective method for preparation of high-purity pelargonidin-3-O-glucoside from strawberry and its protective effect on cellular oxidative stress, J. Chromatogr. B Anal. Technol. Biomed. Life Sci. 1072 (2018) 211–220.

https://doi.org/10.1016/j.jchromb.2017.11.025.

[20] F. Qiu, J. Luo, S. Yao, L. Ma, L. Kong, Preparative isolation and purification of anthocyanins from purple sweet potato by high-speed counter-current chromatography, J. Sep. Sci. 32 (2009) 2146–2151. https://doi.org/10.1002/jssc.200900038.

[21] A.N. Nunes, V. Ivasiv, F. Gouveia, J. Oliveira, M. Ros, A.A. Matias, J. Oliveira, M. Ros, Isolation of Bluish Anthocyanin-derived Pigments obtained from Blueberry Surplus using Centrifugal Partition Chromatography, J. Chromatogr. A. (2023). https://doi.org/10.1016/j.chroma.2023.464150.

[22] A.T. Serra, I.J. Seabra, M.E.M. Braga, M.R. Bronze, H.C. De Sousa, C.M.M. Duarte, Processing cherries (Prunus avium) using supercritical fluid technology. Part 1: Recovery of extract fractions rich in bioactive compounds, J. Supercrit. Fluids. 55 (2010) 184–191. https://doi.org/10.1016/j.supflu.2010.06.005.

[23] I.J. Seabra, M.E.M. Braga, M.T. Batista, H.C. De Sousa, Effect of solvent (CO2/ethanol/H2O) on the fractionated enhanced solvent extraction of anthocyanins from elderberry pomace, J. Supercrit. Fluids. 54 (2010) 145–152. https://doi.org/10.1016/j.supflu.2010.05.001.

[24] A.L.B. Dias, A.C. de Aguiar, M.A. Rostagno, Extraction of natural products using supercritical fluids and pressurized liquids assisted by ultrasound: Current status and trends, Ultrason. Sonochem. 74 (2021) 105584. https://doi.org/10.1016/j.ultsonch.2021.105584.

[25] A. Sainz Martinez, C. Kornpointner, C. Haselmair-Gosch, M. Mikulic-Petkovsek, K. Schröder, H. Halbwirth, Dynamic streamlined extraction of iridoids, anthocyanins and lipids from haskap berries, Lwt. 138

(2021). https://doi.org/10.1016/j.lwt.2020.110633.

[26] S. Kühn, F. Temelli, Recovery of bioactive compounds from cranberry pomace using ternary mixtures of CO2 + ethanol + water, J. Supercrit. Fluids. 130 (2017) 147–155. https://doi.org/10.1016/j.supflu.2017.07.028.

[27] M. del P. Garcia-Mendoza, F.A. Espinosa-Pardo, A.M. Baseggio, G.F. Barbero, M.R. Maróstica Junior, M.A. Rostagno, J. Martínez, Extraction of phenolic compounds and anthocyanins from juçara (Euterpe edulis Mart.) residues using pressurized liquids and supercritical fluids, J. Supercrit. Fluids. 119 (2017) 9–16. https://doi.org/10.1016/j.supflu.2016.08.014.

[28] J. Paes, R. Dotta, G.F. Barbero, J. Martínez, Extraction of phenolic compounds and anthocyanins from blueberry (Vaccinium myrtillus L.) residues using supercritical CO2 and pressurized liquids, J. Supercrit. Fluids. 95 (2014) 8–16. https://doi.org/10.1016/j.supflu.2014.07.025.

[29] M.J. Otero-Pareja, L. Casas, M.T. Fernández-Ponce, C. Mantell, E.J.M. De La Ossa, Green extraction of antioxidants from different varieties of red grape pomace, Molecules. 20 (2015) 9686–9702. https://doi.org/10.3390/molecules20069686.

[30] O. Babova, A. Occhipinti, A. Capuzzo, M.E. Maffei, Extraction of bilberry (Vaccinium myrtillus) antioxidants using supercritical/subcritical CO2 and ethanol as co-solvent, J. Supercrit. Fluids. 107 (2016) 358–363. https://doi.org/10.1016/j.supflu.2015.09.029.

[31] L. Tamkutė, R. Liepuoniūtė, M. Pukalskienė, P.R. Venskutonis, Recovery of valuable lipophilic and polyphenolic fractions from

cranberry pomace by consecutive supercritical CO2 and pressurized liquid extraction, J. Supercrit. Fluids. 159 (2020). https://doi.org/10.1016/j.supflu.2020.104755.

[32] N. Mateus, J. Oliveira, C. Santos-Buelga, A.M.S. Silva, V. De Freitas, NMR structure characterization of a new vinylpyranoanthocyanin-catechin pigment (a portisin), Tetrahedron Lett. 45 (2004) 3455–3457. https://doi.org/10.1016/j.tetlet.2004.03.007.

[33] A.N. Nunes, C. Saldanha do Carmo, C.M.M. Duarte, Production of a natural red pigment derived from Opuntia spp. using a novel high pressure CO_2 assisted-process, RSC Adv. 5 (2015) 83106–83114. https://doi.org/10.1039/C5RA14998C.

[34] J. Oliveira, M.A. Da Silva, A.J. Parola, N. Mateus, N.F. Brás, M.J. Ramos, V. De Freitas, Structural characterization of a A-type linked trimeric anthocyanin derived pigment occurring in a young Port wine, Food Chem. 141 (2013) 1987–1996. https://doi.org/10.1016/j.foodchem.2013.04.091.

[35] FDA, CDER, CBER, Q3C — Tables and List Guidance for Industry, (2017). https://www.fda.gov/media/71737/download.

CHAPTER 3

Extraction and formulation of orange carotenoid-derived pigments from marine sources

CHAPTER 3

Part I – Intensified astaxanthin extraction from crustacean waste streams

CONTENTS

Adapted from:

Nunes, A.N., Roda, A., Gouveia, L.F., Fernández, N., Bronze, M.R., Matias, A.A. (2021) Astaxanthin Extraction from Marine Crustacean Waste Streams: An Integrated Approach between Microwaves and Supercritical Fluids. ACS Sustainable Chemistry & Engineering, 9 (8), 3050-3059. Doi: 10.1021/acssuschemeng.0c06534.

The author was involved in the conceptualization and design of all experiments. The experimental work was performed with the support of A. Roda. The characterization of extracts by HPLC-DAD was acquired with the support of J. Monte and R. Valério supervised by C. Brazinha. The statistical analysis was performed at iMed.ULisboa with the support of L. F. Gouveia. Data processing and interpretation, and results discussion were also performed by the author, as well as the preparation of the original manuscript.

1. ABSTRACT

Marine crustacean waste streams, in particular crab wastes, are promising alternative sources of astaxanthin (ASX), a high-demand carotenoid with a strong antioxidant capacity currently very used for nutraceutical and functional food formulations. However, the composition and rigid structure of the crab exoskeleton constitute a critical bottleneck for ASX recovery from these residues. In this work, an extraction strategy is proposed for obtaining an ASX-rich extract from crab shell wastes, integrating microwave (MW) pretreatment and supercritical fluid extraction (SFE). The multivariate nature of the processes involved is expected to lead to a non-additive contribution of the individual effect of factors on the extract quality and quantity. As such, the design of experiment approaches was used to screen and optimize both processes. MW pretreatment with different solvent systems (hydroalcoholic mixtures with 0-50 vol.% of water) at different temperatures (40-140°C) was applied followed by conventional solvent extraction (CSE) for disruption of crab shell structure. Different SFE conditions, namely pressure (200-500 bar), temperature (40-60°C), ethanol content in the supercritical CO_2 (8-13 wt.%), and equilibration time (0-30 min) were also explored to selectively recover ASX. Optimized operating conditions of each process individually were selected and ASX extraction efficiency through the integrated MW pretreatment and SFE strategy was assessed. All the extractable ASX was selectively recovered 12 times faster than traditional Soxhlet (SOX) extraction, demonstrating that the proposed extraction approach significantly improves the extraction efficiency. This study suggests that the integration of MW pretreatment with SFE can be considered a good strategy for intensification of ASX extraction from crab residues. With this extraction approach, not only marine crustacean waste streams have been valorized,

but also a high added value natural ingredient has also been isolated, allowing its subsequent use.

2. INTRODUCTION

The crustacean processing industry has expanded significantly during the past decades, generating vast amounts of waste [1]. Annually, around 6 to 8 million tons of shell residues are produced worldwide and its current underutilization provides a significant opportunity to convert them into valuable resources [2]. In fact, crab shells represent a natural and cheap source of several bioactive compounds and materials, including calcium carbonate, protein, chitin, lipids, and pigments (e.g. ASX) [3–5]. Consequently, there has been considerable interest in developing potential applications for an efficient valorization of this waste towards a circular economy.

ASX is a liposoluble carotenoid belonging to the xanthophyll group, which presents an attractive red-orange color and naturally occurs in a wide variety of microorganisms and marine animals [6–8]. It is the major carotenoid found in crabs, including in their processing waste [9]. In fact, crustaceans are unable to synthesize carotenoids, therefore ASX is derived through the oxidative transformation of ingested *β*-carotene or zeaxanthin from feed microalgae [10]. It has been reported that ASX has several health benefits and it is considered as a “super antioxidant” [6,7,11]. This pigment exhibits up to 10-fold higher antioxidant capacity than other carotenoids such as zeaxanthin, lutein, cantaxanthin, and *β*-carotene, and is 100-fold better than *α*-tocopherol [6,12]. Currently, ASX with an estimated global market value of about US$ 1 billion [13] finds important applications in the food, feed,

nutraceutical, and pharmaceutical industries [6]. However, almost all commercially available ASX is produced synthetically [14]. Therefore, the great demand for ASX generated by industries combined with the growing consumer interest in natural-derived products instead of synthetic ones has promoted major efforts to improve ASX production from natural sources [6,15]. In this line, new strategies should be attempted to produce ASX from crab shells in order to improve the economy of the crustacean processing industry, reduce the environmental impact caused by these residues, replace synthetic ASX, and guarantee its supply according to the market demand.

Traditionally, ASX recovery from natural sources has been performed by solid-liquid extraction using a broad range of organic solvents. However, this is a time-consuming methodology that involves the use of large volumes of organic solvents and high temperatures that are not suitable for the recovery of thermolabile substances such as ASX [10]. These shortcomings have stimulated the interest in developing new green strategies with suitable solvents.

SFE has emerged as an alternative to conventional organic solvent extraction. This technology is tunable and then potentially quite selective. In fact, advanced extraction with supercritical CO_2 can reduce the demand for food-grade solvents, increase the selectivity toward target compounds, and preserve their bioactivity due to the absence of oxygen in the system and low operating temperatures [16]. Also, the physicochemical properties of supercritical CO_2 show low viscosity, high diffusivity, and high density that enhance the penetration into biomass structure and the solubilization of the target compound [17]. Although the SFE technique has many advantages, some shortcomings are also displayed. Owing to the low solubility of ASX in supercritical CO_2, long extraction times and ultra-high extraction pressures

(≥1000 bar) are required for efficient pigment recovery, unless a co-solvent is added [18]. The addition of a modifier, such as ethanol, can significantly improve extraction efficiency, by enhancing the solute solubility and/or decreasing its interactions with the matrix [19]. Within organic solvents, ethanol is the most environmental and health favorable, being accepted as 'bio-solvent' for food, pharma and cosmetic applications [20]. Furthermore, the complexity of crab shells and the stable complex formed between ASX and proteins (carotenoproteins), also contribute to lower extraction rates of ASX [3,9]. The rigid structure of crab shells is constituted by extensive covalent and hydrogen-bonding between chitin and protein together with embedded calcium carbonate [3]. Therefore, crab shell waste requires an appropriate pretreatment before the SFE to detach ASX from proteins and minerals, increasing the subsequent extractability of the pigment.

MW radiation offers an alternative green pretreatment method for disruption of the solid structure of biomass making the target molecules more available for subsequent extraction. The main advantages of using MW pretreatment are the shortening of the extraction time and the reduction in the amount of solvent used, representing an excellent choice for reducing the environmental impact of the whole process [21]. Up to date, there is no information in the available literature on the application of MW radiation as a pretreatment prior to the SFE process for ASX recovery.

The objective of the present work was to develop a promising strategy to extract ASX selectively and efficiently from crab residues. For the first time, the feasibility of integrating MW pretreatment with SFE process on the extractability of ASX from crustacean residues was investigated. The efficiency of the proposed extraction protocol was compared to Soxhlet extraction (SOX) with acetone, CSE with ethanol and SFE without

pretreatment. The ASX yield and ASX content in the final extract were analyzed to optimize pretreatment and extraction conditions. This intensification strategy is proposed as a step further in the challenging task of processing crab waste valorization.

3. MATERIALS AND METHODS

3.1. Raw material

Brown crab (*Cancer pagurus*) processing waste was kindly provided by Tejo Ribeirinho, Lda., Portugal. Since more efficient extraction of carotenoids could be achieved with samples with low moisture content [11], crab shells were dehydrated in a Coolsafe Superior Touch 55-80 freeze dryer (Scanvac) at -55°C. Further, this conservation method allowed to quickly preserve the residues while increasing their durability by avoiding sample degradation due to heat, light, or oxygen [22]. After freeze-drying, the residues were milled using a cutter-emulsifier CKE-8 (Sammic, Azkoitia, Spain), and the particle size of the ground material was determined using an AS 200 basic vertical vibratory sieve shaker (Retsch, Haan, Germany), with a measuring range between 250 and 710 μm. The residual moisture content of 4 wt.% was determined as described in European Pharmacopeia 10.0. The processed biomass was protected from light and stored at -20°C until the day of the experiments.

3.2. Chemicals

The chemicals used for different extraction methodologies and chemical characterization of extracts were carbon dioxide 99.95% from Air Liquide (Lisbon, Portugal), ethanol absolute 99.9% from Carlo Herba (Val de Reuil,

France), acetone from Fisher Chemical (Loughborough, United Kingdom) and ASX from *Blakeslea trispora* ≥97% from Sigma-Aldrich (St. Quentin Fallavier, France).

3.3. Microwave pretreatment (MW)

Crab shells were pretreated with MW radiation using a Discover SP-CEM MW system (CEM Co., USA). The solvent system (hydroalcoholic mixtures with 0-50 vol.% of water) was added to the crab residues in a sealed borosilicate glass tube (1 mL per g of residue). After 30 s of pre-stirring, the mixture was irradiated with MW up to 300 W for different times (30-90 s), to achieve pretreatment temperatures of 41-140°C. After MW irradiation, the pretreated residues were quickly cooled down to 40°C in an ice bath, and process continued with the CSE or SFE.

3.4. Scanning electron microscopy (SEM)

To determine the extent of MW pretreatment on crab shell morphology, crab shells before and after the treatment were examined by scanning electron microscopy (FEG-SEM) (Jeol, JSM-5310 model, Japan) at 20/25 kV. The samples were coated with approximately 300 Å gold under an argon atmosphere.

3.5. Astaxanthin extraction procedures

3.5.1. Soxhlet extraction (SOX)

To quantify the maximum amount of extractable ASX from crab residues, a complete extraction of ASX was conducted by SOX. The extractions were performed following the procedure described by Rodrigues and co-workers [23]. Briefly, crab residues were extracted with acetone (33 mL per g of dry residue) for 6h, using a Soxhlet apparatus. The ASX-rich extracts were concentrated in a rotary evaporator at 40°C under reduced pressure for the quantification of ASX by UV-vis spectroscopy. After ASX determination, the extracts were completely dried and stored at -20°C in the absence of light.

3.5.2. Conventional solvent extraction (CSE)

Crab residues, without or with MW pretreatment, were extracted with ethanol (1 mL per g of dry residue) for 30 min at 40°C under magnetic stirring. The ASX-rich extracts were filtered, dried in a rotary evaporator at 40°C under reduced pressure and stored at -20°C in the absence of light. CSE process parameters were chosen based on prior experimental results.

3.5.3. Supercritical fluid extraction (SFE)

The SFE experiments were carried out in a supercritical fluid extraction system (Thar Technology, Pittsburgh, PA, USA, model SFE-500F-2-C50) comprising a 500 mL cylinder extraction cell and two different separators, each of them with 500 mL of capacity, with independent control of temperature and pressure. This apparatus was previously described by Nunes and co-workers [24]. The extraction vessel was filled with dried crab

residues, without or with MW pretreatment, and glass beads to achieve a uniform distribution of the solvent flow. The CO_2 flow rate for extraction was maintained at an average level of 16.5 g/min.

Based on previous works [25–28] and preliminary experimental results, process variables and their ranges, equilibration time (0-30 min), extraction pressure (200-500 bar), extraction temperature (40-60°C) and ethanol content in supercritical fluid mixture (8-13 wt.%), were chosen. Other parameters have been fixed, such as the amount of biomass (set at 25 g) and extraction time (set at 180 min). Extracts were recovered in a flask placed in an ice bath. The ASX-rich extracts were dried in a rotary evaporator at 40°C under reduced pressure and stored at -20°C in the absence of light.

3.6. Astaxanthin quantification

3.6.1. UV-vis spectrometry

ASX-rich extracts from each extraction protocol were analyzed by UV-vis spectroscopy to determine the ASX content. The samples were quantified based on the absorbance obtained at the maximum wavelength (476 nm for acetone and 474 nm for ethanol) and on linear correlation equations. Results were presented as μg of ASX per g of dry residues and μg of ASX per g of dry extract and expressed as a mean of triplicates.

3.6.2. High performance liquid chromatography (HPLC)

The carotenoid profile of the extract considered as the most representative was determined through HPLC. An Alliance e2695 HPLC model (Waters, Massachusetts, USA), equipped with a degasser, autosampler and a PDA

detector was used for the carotenoids analysis. Chromatographic separation was carried out with a YMC 30 Carotenoid Column (Classical Analytical HPLC Column S-5µm, 250 x 4.6 mm, YMC) coupled with a Guard Cartridges YMC C30 pre-column (5μm, 10x4.0mm, YMC) with a mobile phase of methanol:MTBE (80:20) at 25°C. The detection wavelength was set to 450 nm and the flow rate was 1 mL/min. All samples were previously dissolved in MTBE, centrifuged, and filtered through a 0.45 µm HLPC filter. The run time for the assay was 45 minutes and the retention time for all-trans astaxanthin, lutein, zeaxanthin, α-carotene, all-trans β-carotene, and 9-cis-β-carotene was 6.4, 6.7, 8.3, 20.5, 26 and 30 minutes respectively. Typical chromatogram is provided in the Appendix (page 265).

3.7. Experimental design and statistical analysis

A response surface methodology was used to evaluate the influence of process conditions on: (a) MW pretreatment followed by CSE and (b) SFE. The ASX yield and ASX content data resulting from the experiments performed according to the experimental conditions defined by: (a) central composite circumscribed design for MW pretreatment and (b) full factorial design for SFE, were analyzed by using the Modde v.12 (Umetrics, Umeå, Sweden) software. ANOVA one-way or two-way with replication for the average ASX yield and content were used to assess the significance of the contribution of the experimental factors and interactions. ANOVA Post-hoc groups comparison test was performed by computing the Dixon's test. The statistical tests, including the adjustments of the design model and factors effects, were considered to be significant when the resulting *p*-value was lower than the predefined $\alpha = 0.05$.

4. RESULTS AND DISCUSSION

4.1. Determination of the maximum extractable Astaxanthin

SOX extraction is known as a conventional technique which provides the highest recovery of carotenoids [29]. In order to determine the efficiency of SFE without or with MW pretreatment, the total amount of ASX in the crab residues was determined using SOX extraction. Ruen-ngam and co-workers [30] studied the effect of solvent in different extraction methods for the recovery of ASX from *Haematococcus pluvialis*. The results showed that the highest ASX yield for all extraction methods was achieved with acetone. From the studied solvents, acetone presents the most appropriate polarity ($\mathcal{E}'$ = 20.7) to dissolve the liposoluble ASX. Therefore, acetone was chosen as the solvent for SOX extractions. The maximum extractable ASX from crab residues obtained for the studied batches presented a high deviation: 9.7 ± 0.7 $\mu g_{ASX}/g_{dry\ residues}$ [23] and 3.7 ± 0.2 $\mu g_{ASX}/g_{dry\ residues}$. Since the crab specie, extraction methodology and storage conditions were the same, this difference can be attributed to the harvesting season and site [23,31]. Also, the ASX selectivity obtained using each batch was different probably due to the ASX availability in each biomass. In fact, ASX can be found in natural sources in esterified, carotenoprotein, and free form [32].

4.2. Microwave pretreatment process optimization

Crab shells have a complex and robust exoskeleton which constitute an obstacle to the entry of solvent. Therefore, a structure disruption treatment in the first step of extraction is required to improve the extractability of ASX [3,9]. Ruen-ngam and co-workers [30] extracted ASX from *Haematococcus pluvialis* using MW assisted extraction at 75°C for 5 min. However, these microalgae present different compositions and structural organization from

the crab exoskeleton. Also, the authors recovered ASX using organic solvents, limiting the subsequent application in nutraceutical formulations and functional food.

There are some limitations that restrict the implementation of MW assisted extraction process at industrial scale. The main disadvantage is its low penetration depth that turns impossible to uniformly irradiate a large vessel and consequently, only the external parts will be irradiated [33]. Therefore, in this work, a short MW pretreatment is proposed as an easy scale-up alternative for ASX extraction instead of a full time MW assisted extraction process. The energy absorbed by the biomass during an intense but short MW pretreatment will be equivalent to the energy absorbed during a MW assisted extraction [33]. Up to date, there are no studies in the available literature on the application of MW radiation as pretreatment to enhance the subsequent extraction of ASX from crustacean waste. In this context, MW radiation was applied to crab residues before the CSE.

When MW radiation is applied as a pretreatment, several experimental factors need to be considered and addressed for each system under investigation. The solvent system composition is one of the main variables affecting MW pretreatment performance and its selection is determined by the solubility of the target compound, the interaction between solvent and raw material, and MW absorbing properties of the solvent [34]. The solvent capacity to absorb MW energy and convert it to heat depends on its dissipation factor (tan δ): $\tan \delta = \varepsilon' / \varepsilon''$, where ε' represents the dielectric constant of the solvent, reflecting the solvent ability to be polarized by an electric field, and ε'' is the dielectric loss factor associated to the efficient conversion of electromagnetic energy into heat. Accordingly, the higher the dissipation factor, the greater the amount of thermal energy that will be

produced.[35] In this way, polar solvents such as water are usually applied due to their high dielectric constant (ε'_{water} = 78.3 > $\varepsilon'_{ethanol}$ = 24.3 [30]). However, ASX water solubility is low. Since MW applications can also involve the use of mixtures of nonpolar–polar solvents and water, hydroalcoholic mixtures with biocompatible solvents were tested to ensure a polar media.

Another key variable in the MW pretreatment is the treatment time and MW power. Zhao and co-workers [36] studied the effect of MW radiation on the stability of (all-E)-astaxanthin. Results showed that MW induced the isomerization of (all-E)-astaxanthin to its Z analogs, preferentially to (13Z)-astaxanthin, and the percentage of the isomerization increased with increasing both treatment time and MW power. In this way, the use of MW as a pretreatment was tested at lower MW power (226-288 W) for shorter periods (30-90 s) than MW assisted extraction process, corresponding to MW-induced temperature from 41 to 140°C. The appropriate combination of MW power and irradiation time allowed to achieve a desired preset temperature, thus turning two raw factors into just one to be optimized. Therefore, the effect of the solvent system composition and temperature was assessed by using a two-dimensional response surface approach, based on a central composite circumscribed design with three-star points.

The experimental conditions and results for each MW pretreatment experiment are shown in Table 1. The highest ASX recovery was 3.38 ± 0.22 $\mu g_{ASX}/g_{dry\ residues}$ (MW+CSE-2 and MW+CSE-10), approximately 93 wt.% of the total amount of ASX determined by SOX extraction. These values were obtained for solvent systems with the lowest water content (0 and 8 vol.%), at higher temperatures (125 and 140°C), corresponding to an ASX extract concentration of 233 ± 6 $\mu g_{ASX}/g_{dry\ extract}$.

Table 1. Effect of different MW pretreatment conditions on the ASX yield and ASX content in the extracts obtained by CSE.

Exp. number	Solvent system water content (vol.%)	Temperature (°C)	Time (s)	Max. pressure (bar)	ASX yield ($\mu g/g_{dry\ residues}$)	ASX content ($\mu g/g_{dry\ extract}$)
MW+CSE-1	8	55	46	**4.4**	3.17	196
MW+CSE-2	8	125	89	6.7	3.38	233
MW+CSE-3	43	55	34	3.4	2.13	92
MW+CSE-4	43	125	73	6.55	2.14	110
MW+CSE-5	25	90	57	6.3	2.72	145
MW+CSE-6	25	90	59	5.8	3.04	135
MW+CSE-7	25	90	60	5.4	3.11	133
MW+CSE-8	25	41	29	2.3	2.73	125
MW+CSE-9	25	140	91	7.7	3.22	146
MW+CSE-10	0	90	75	5.2	3.38	233
MW+CSE-11	50	90	55	5.4	2.04	86
MW+CSE-12	25	90	59	6.5	2.76	139
MW+CSE-13	25	90	57	6.6	3.14	136
MW+CSE-14	25	90	57	6.6	2.91	132
Max extractable ASX determined by SOX					3.65	210

In this study, the solvent system composition and pretreatment temperature had a significant effect on the evaluated responses (model fit is provided in Appendix page 265). Contour plots illustrating the effects of different solvent systems and temperatures are shown in Figure 1. When higher MW temperatures were applied to crab residues, the ASX yield significantly increased (Figure 1a). A similar trend was observed for the ASX content in the extracts (Figure 1b). Since a close-vessel microwave system was used, the

rapid increase in the temperature lead to a pressurized effect (Table 1) that might induce crab shells structure disruption, making ASX more available.[16]

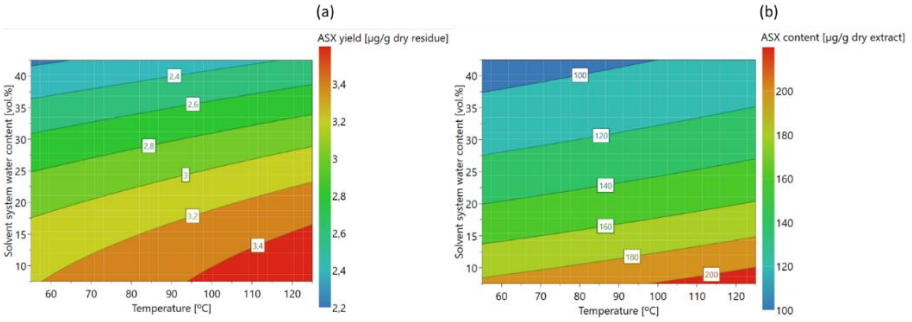

Figure 1. Contour plots of the effects of different solvent systems and temperature on (a) ASX yield and (b) ASX content.

To evaluate the extent of pretreatment on crab shell morphology, the residues before and after the different methodologies at the optimum conditions were examined by SEM (Figure 2). The crab exoskeleton is a natural composite consisting of highly mineralized chitin–protein fibers arranged in twisted plywood [3,5]. From Figure 2a, crab shells exhibited rough, porous, and thick surface morphology. After the quick MW pretreatment (Figure 2f), it was possible to clearly observe the nano-fiber structures with a fractured appearance. The impact of the short pretreatment on the shell structure was not so different from the impact promoted by the complete SFE process. As presented in Figure 2d, crab shells after SFE also showed a disarranged structure, presenting fractures and nanofibers. Nevertheless, by the overall SEM observation, the impact on the internal structure seemed to be much less extended than the promoted by

MW pretreatment. SEM images suggested that the sudden thermal stresses and the high localized pressures during the MW radiation affected the crab shell structure morphology, enhancing the mass-transfer rate, leading to subsequent increase of ASX extraction. Moreover, this pretreatment might break the ASX-protein complex, thereby increasing the ASX recovery since ASX is present in crab shells as a carotenoprotein [3,9].

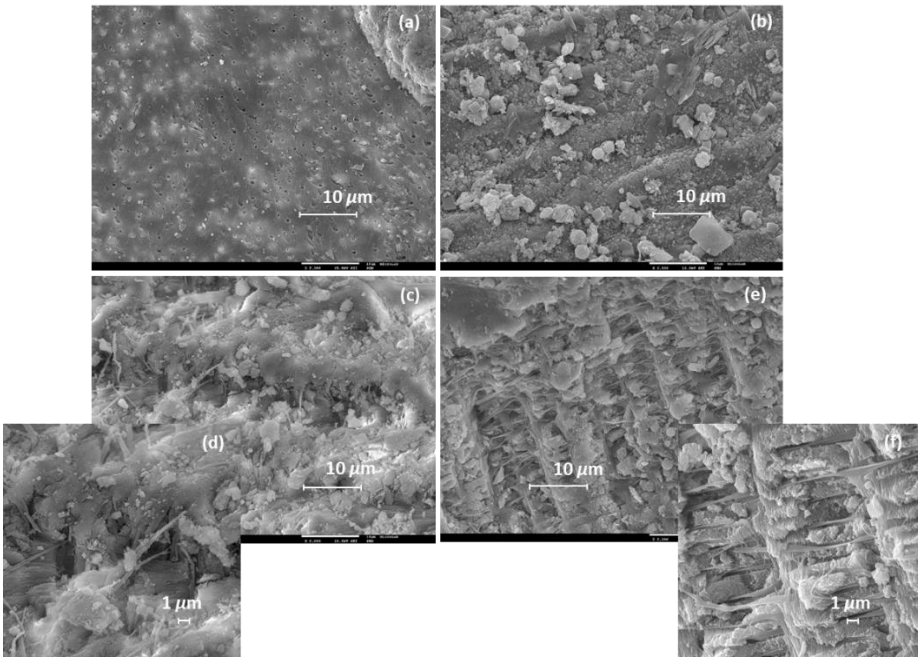

Figure 2. SEM images of freeze dried and milled crab shells (a) x2000, after CSE (b) x2000, after SFE (c) x2000 and (d) x4000, and after MW pretreatment (e) x2000 and (f) x4000.

Mezzomo and co-workers [37,38] studied different pretreatments of shrimp waste in order to make the carotenoid fraction available for the subsequent extraction procedures. The results showed that the cooking pretreatment significantly affected the extraction yield and total carotenoid content,

especially when combined with drying and milling processes. In fact, the authors also suggested that the proposed heating pretreatment could break the carotenoid-protein complex from the shrimp shells, increasing the extraction yield. However, in the present work, a heat treatment different from the classical conductive heating methods was performed, where MW heat the whole sample simultaneously and homogeneously.

Another important factor that affected MW pretreatment was the solvent system used. According to the results, the yield of ASX from crab residues was enhanced with the decrease of water content in the solvent system mixture (Figure 1a). The same influence was observed for the ASX content in the extract (Figure 1b). This trend could be explained not only by the lower water solubility of hydrophobic ASX [7] but also by the lower dielectric constant (ε') of ethanol compared with water ($\varepsilon'_{water} = 78.3 > \varepsilon'_{ethanol} = 24.3$) [30]. In fact, MW pretreatment usually imply the use of solvent systems with higher dielectric constant. Nevertheless, using a solvent with lower dielectric constant which absorbs MW energy at a lower level might be a way to prevent thermal degradation of ASX [39]. The results above suggest the use of pure ethanol as solvent system at MW induced temperature of 140°C.

4.3. Supercritical fluid extraction process optimization

SFE is known as an efficient method for the extraction of thermolabile compounds such as ASX. Moreover, the higher diffusion coefficient and lower viscosity of supercritical CO_2 allow for rapid penetration into the pores of biomass, thus enhancing ASX extraction efficiency [29]. Supercritical CO_2 has already been used as a solvent for ASX recovery from other crustaceans [25–28,40,41] and microalgae [14,42–48]. The authors have reported optimized

extraction parameters to maximize the ASX yield. Nevertheless, literature results are variable and even discordant probably due to the type of extractor used, biomass composition, moisture content in the sample, and pretreatment applied to biomass. Therefore, optimization of the extraction conditions is required for each case. For these reasons, SFE conditions were optimized as an alternative to CSE to recover ASX from crab residues.

Taking into consideration the goals and the nature of the SFE process, it was necessary to follow a rational approach, able to deal with the expected process factors and complex interactions as well as the desired high selectivity and yield. The knowledge acquired from previous experiments, as well as some instrumental limitations, simplified the task by keeping constant some factors, thus reducing the dimensionality of the space to be explored. A proper balance between the number of required experimental runs and the knowledge acquired was set. As such, taking into consideration the number of factors (4) and the goals defined, a two-level full factorial design was selected as a suitable approach to such task. Central replicate points were included to assess the experimental variability and consequently the uncertainty of the results as well as the goodness of fit of the underlying mathematical model. Response surface methodology was employed to determine the optimum conditions for SFE of the crab residues.

The experimental conditions and results for each SFE experiment are reported in Table 2. The highest ASX yield was 6.01 ± 0.29 $\mu g_{ASX}/g_{dry\ residues}$ (SFE-9). This ASX recovery was obtained at 40°C, 200 bar, 13 wt.% ethanol content in the supercritical fluid mixture and 180 min of extraction without equilibration time. The extract with the highest ASX content was obtained at 40°C, 500 bar, 13 wt.% ethanol content in the supercritical fluid mixture and

180 min of extraction with an equilibration time of 30 min, which was 1023 ± 71 $\mu g_{ASX}/g_{dry\ extract}$ (SFE-12).

Table 2. Effect of different SFE conditions on the ASX yield and ASX content in the obtained extracts.

Exp. number	Eq.time (min)	Pressure (bar)	Temperature (°C)	Ethanol (wt.%)	CO_2 density (kg/m^3)	ASX yield ($\mu g/g_{dry\ residues}$)	ASX content ($\mu g/g_{dry\ extract}$)
SFE-1	0	200	40	8	839.9	0.70	155
SFE-2	30	200	40	8	839.9	0.75	322
SFE-3	0	500	40	8	991.2	2.54	772
SFE-4	30	500	40	8	991.2	4.40	960
SFE-5	0	200	60	8	723.8	0.03	8
SFE-6	30	200	60	8	723.8	1.27	270
SFE-7	0	500	60	8	933.5	2.51	667
SFE-8	30	500	60	8	933.5	0.81	301
SFE-9	0	200	40	13	839.9	6.01	887
SFE-10	30	200	40	13	839.9	3.18	678
SFE-11	0	500	40	13	991.2	5.14	793
SFE-12	30	500	40	13	991.2	5.17	1023
SFE-13	0	200	60	13	723.8	1.87	395
SFE-14	30	200	60	13	723.8	2.26	490
SFE-15	0	500	60	13	933.5	5.34	782
SFE-16	30	500	60	13	933.5	4.37	730
SFE-17	15	350	50	11	899.4	5.10	897
SFE-18	15	350	50	11	899.4	4.63	793
SFE-19	15	350	50	11	899.4	4.80	803
Max extractable ASX determined by SOX						9.72	1300

The ASX yield and ASX content in the extract were significantly influenced (p<0.05) by three of the four operating parameters studied: temperature, pressure, and ethanol content in the supercritical fluid mixture. The

application of a static equilibration time of 15 or 30 min prior to dynamic extraction resulted in no significant improvement in the ASX yield and ASX concentration in the extract (model fit is provided in the Appendix page 269). No equilibration time was therefore used in subsequent experiments of MW pretreatment and SFE integration. Contour plots representing the ASX yield and ASX content as a function of the extraction temperature, pressure, and ethanol content in the supercritical mixture are presented in Figure 3.

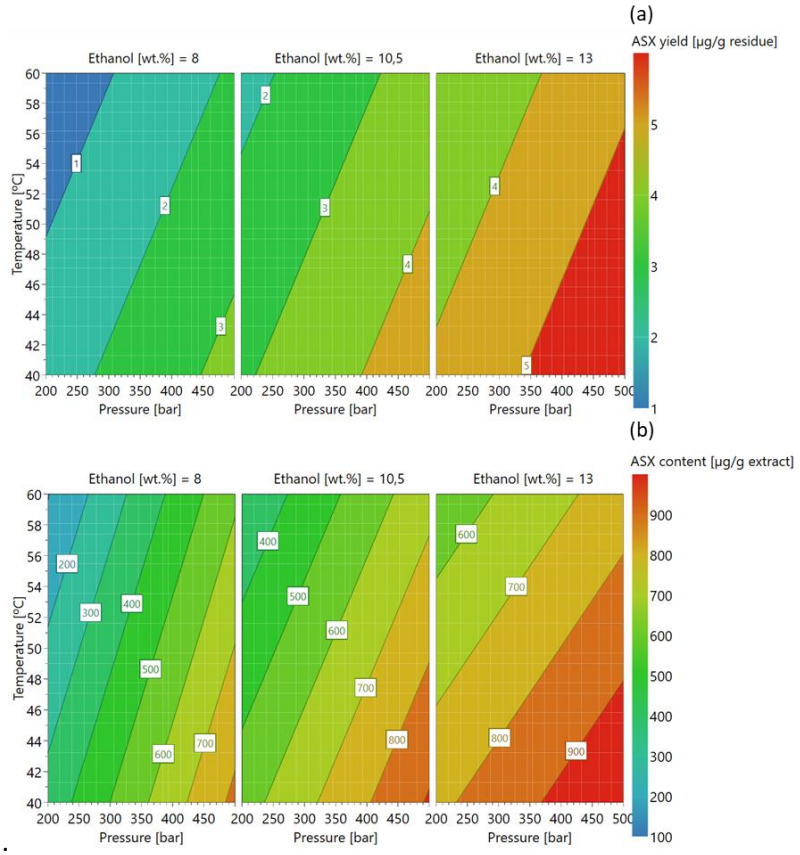

Figure 3. Contour plots of the effects of temperature and pressure on (a) ASX yield and (b) ASX content in the extracts.

From Figure 3, by increasing the pressure, an increase in the ASX yield from crab residues and the ASX content in the extracts was observed. This might

be explained by the increase of CO_2 density up to 1.3 times with increasing pressures (Table 2), which improves the solvating power for lipophilic compounds, thus enhancing the solubility of ASX [25]. In fact, Fuente and coworkers [49] and Youn and coworkers [50] measured the ASX solubility in supercritical CO_2 as a function of temperature and pressure. The authors found that the solubility of ASX increased with pressure and temperature. However, in this work, the opposite trend can be observed for the temperature, as the higher the temperature, the lower the ASX yield and ASX content. This can also be related to the density of supercritical CO_2 since it decreases up to 1.2 times with increasing temperatures (Table 2). Moreover, higher temperatures may increase the thermal degradation rate of ASX [25]. Furthermore, the temperature could affect the interaction between the ASX and ethanol, weakening their hydrogen bonds [45]. Therefore, ASX solubility was found to be strongly dependent on the fluid density, since greater solubility was observed with increasing solvent density, thus avoiding the use of higher temperatures, limiting thermal degradation.

The same behavior was also found by other authors. Mezzomo and coworkers [38] studied the effects of temperature (40-60°C) and pressure (100-300 bar) on carotenoid recovery. The authors observed that the carotenoid content strongly increased with solvent density. Parjikolaei and coworkers [51] evaluated the effects of temperature (35-55°C) and pressure (200-400 bar) on ASX recovered from shrimp waste. It was also found that the ASX yield increased as pressure increased. At the lowest pressure, increasing temperature negatively affected the ASX yield while at the highest pressure, the ASX yield increased with increasing temperature.

Figure 3 also shows the effect of ethanol content in the supercritical fluid mixture on the ASX yield and ASX content in the obtained extracts. An

increasing amount of ethanol resulted in an improvement in both evaluated responses. Supercritical CO_2 has a nonpolar character and presents a limited capacity to extract slightly polar compounds such as ASX. Sánchez-Camargo and coworkers [26] investigated the effect of ethanol addition to supercritical CO_2 on the extraction of ASX from shrimp waste. Similar results were observed, 10 wt.% ethanol in supercritical CO_2 conferred a significant improvement in the extraction yield and selectivity of ASX. The author suggested that the addition of ethanol could increase the polarity of supercritical CO_2 and promote the formation of hydrogen bonds between ASX and ethanol present in the CO_2 stream, increasing the ASX solubility. Moreover, introducing ethanol as a modifier could also help to swell the pores of crab shells, improving the interaction of the solvent with the internal structure of the matrix since the surface area increased.

The results above show that relatively low temperature (40°C) at high pressure (500 bar) with the addition of ethanol in the supercritical fluid mixture (13 wt.%) were the best extraction conditions within the studied range, to obtain not only the highest ASX yield but also the highest selectivity.

4.4. Microwave pretreatment and supercritical fluid extraction process integration

The effect of MW radiation on crab residues was also tested in combination with SFE. Therefore, the optimal MW pretreatment conditions found for CSE were applied to improve the performance of SFE and compared with the results achieved by the different extraction approaches studied. The applied SFE conditions were 500 bar, 40°C, and 13 wt.% ethanol content in the supercritical fluid mixture after an MW pretreatment where ethanol was

used as a solvent system at 140°C. It is well known that extraction processes carried out during long extraction times to obtain a higher yield can compromise the selectivity, i.e., the final content of the target compound in the extract. Bearing this in mind, ASX yield and ASX content in the extract were measured at different timepoints of SFE (Figure 4).

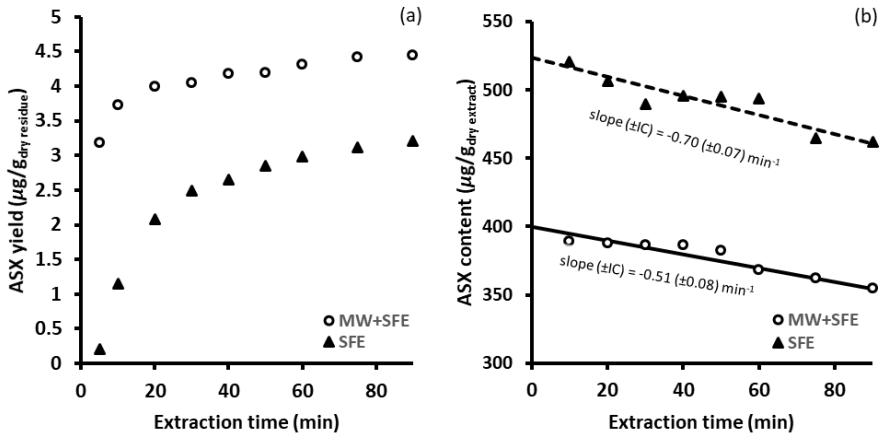

Figure 4. ASX yield (a) and ASX content in the extract (b) as a function of time, obtained for SFE and MW+SFE. [MW: ethanol as solvent system and 140°C MW temperature, during 90s. SFE: 500 bar, 40°C and 13 wt.% ethanol content in the supercritical fluid mixture, during 90 min]

Regarding the results of SFE with and without pretreatment (Figure 4a), an ASX yield plateau close to the maximum extractable ASX by each method was achieved upon 90 min of extraction. At that time point, the MW+SFE showed a yield increase of 1.4-fold with respect to the SFE alone. Further, the MW pretreatment accelerated the extraction rate of ASX as it could reach the maximum ASX yield obtained by SFE in only 10 min. From Figure 4b, the ASX content in the extract decreased with the extraction time at both studied strategies. Similar slopes can be observed, although the SFE was slightly

lower than the MW+SFE. This decrease in selectivity, regarding extraction time, was a consequence of the later extraction of other undesirable compounds. Different intercepts were observed and where no MW pretreatment was applied, the ASX content in the extract was significantly higher. The improvement in the ASX extraction process might be in the quantity extracted (ASX extraction yield) as well as in the quality of the extract (product richness - ASX content in the final extract). Final extract ASX richness is of crucial relevance for its commercialization since the higher the ASX richness, the more valuable the product is, or the less complex could be the further downstream process for its purification. Undesired substances (impurities) are obtained in the traditional extraction methodologies, depreciating the final product. Considering the acceleration of ASX extraction and the different extraction rates of other undesired compounds, an optimal extraction time of 30 min was selected for MW+SFE as a balance between the ASX yield and ASX extract concentration. As ASX is a thermolabile compound, the reduction of extraction time is advantageous for ASX stability [29]. Moreover, the shortening of extraction time reduced the amount of solvent used.

It should be noted that the batch used for the screening of SFE parameters presented a high amount of ASX (9.7 ± 0.7 $\mu g_{ASX}/g_{dry\ residues}$) compared to the batch used for this comparison of different extraction strategies (3.7 ± 0.2 $\mu g_{ASX}/g_{dry\ residues}$). The highly variable nature of the crab residues does not only affect the maximum extractable ASX content by SOX extraction but also the performance of SFE.

4.5. Comparison of different extraction strategies

MW pretreatment of crab residues was tested in combination with CSE (MW+CSE) and SFE (MW+SFE). A comparison of ASX yield obtained with MW+CSE, MW+SFE, SFE without pretreatment, and CSE without pretreatment, with respect to the maximum extractable ASX obtained by SOX extraction (3.65 ± 0.22 $\mu g_{ASX}/g_{dry\ residues}$), is shown in Figure 5. The results demonstrate that MW+CSE and MW+SFE were able to provide an ASX yield higher (p>0.05) than the one obtained by SOX extraction. In addition, the comparison of ASX content in the extracts obtained by the different extraction strategies showed that they presented different selectivity toward ASX. In fact, ASX content in the extracts obtained by SFE and MW+SFE was found to be significantly higher than SOX (see statistical differences in Appendix page 273).

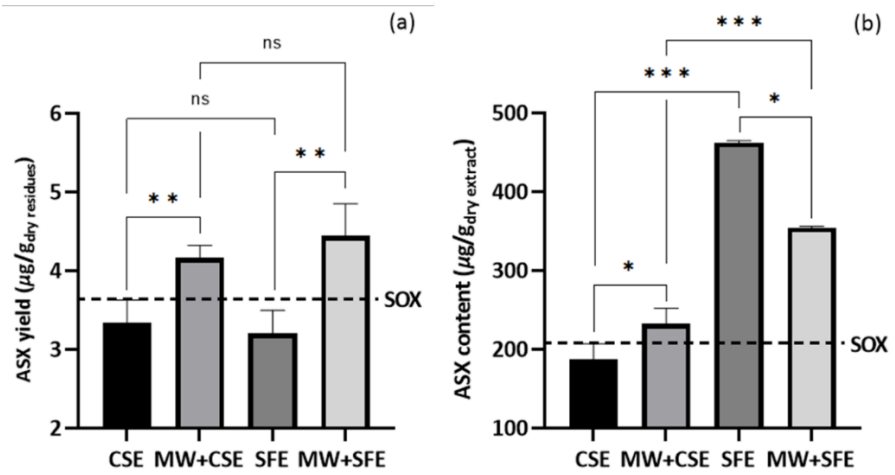

Figure 5. ASX yield (a) and ASX content in extracts (b) obtained from crab residues using different extraction strategies. The statistically significant differences are represented by asterisk (*). *p=0.037, **p=0.006, *** p<0.001, ns: not significant. [CSE: ethanol and 40°C. MW: ethanol as a solvent system and 140°C MW temperature, during 90 s. SFE: 500 bar, 40°C and 13 wt.% ethanol content in the supercritical fluid mixture, during 90 min]

The highest ASX yield 4.44 ± 0.41 $\mu g_{ASX}/g_{dry\ residues}$ was obtained with MW+SFE. The amount of ASX extracted by CSE, MW+CSE, and SFE was slightly lower (3.20 ± 0.30 to 4.16 ± 0.16 $\mu g_{ASX}/g_{dry\ residues}$). In fact, a significant difference was noted for the ASX yield when applying MW pretreatment before CSE and SFE (p=0.006). However, no significant difference (p=0.702) was observed regarding the ASX yield when using CSE or SFE. The promising effect of the use of MW+SFE for ASX extraction from crab residues seems irrefutable when the results obtained using this integrated strategy were compared to the ones obtained using other extraction methods. From Figure 5, comparing MW+CSE and MW+SFE it was possible to conclude that the SFE increased the selectivity toward ASX. A significant difference (p<0.001) was observed for ASX content when using SFE instead of CSE. In fact, the ASX content in the extract was a 1.5-fold increase while similar ASX recovery was observed. In addition, the results for SFE without pretreatment and MW+SFE confirm that MW pretreatment was crucial to enhancing the ASX yield. A significant difference (p=0.037) was noted for ASX content when applying MW pretreatment before the extraction process. Given the discussion above, integrated MW and SFE processes could be considered a promising strategy to recover ASX from crab residues.

5. CONCLUSIONS

An intensification strategy integrating MW pretreatment with SFE is proposed in this work for the first time to enhance ASX recovery from crab processing waste and to improve ASX concentration in the final extract/product. The best SFE conditions were achieved at 500 bar, 40°C, and

13 wt.% ethanol content in the supercritical fluid mixture after an MW pretreatment where ethanol was used as a solvent system, at 140°C and 300 W, during 90 s. Under these optimized conditions, the maximum extractable ASX was recovered within 30 min of extraction and the ASX concentration in the extract was improved in comparison to other extraction strategies. The key benefits of combining MW pretreatment with environmentally friendly SFE include a significant decrease in extraction time and solvent usage, contributing to the intensification of the process. The proposed protocol demonstrated to be an effective and suitable strategy for the enhancement of selective ASX extraction with potential application in the nutraceutical and food industry, contributing to the sustainable utilization of these marine crustacean waste streams.

6. ACKNOWLEDGEMENTS

The authors acknowledge the financial support received from the FCT through the POCI-01-0145-FEDER-016403 project. iNOVA4Health-ID/Multi/04462/2013, a program financially supported by FCT/Ministério da Educação e Ciência through national funds and co-funded by FEDER under the PT2020 Partnership Agreement and funding from INTERFACE Programme, through the Innovation, Technology and Circular Economy Fund (FITEC) are also acknowledged. A.N.N. acknowledges FCT for the financial support received through SFRH/BD/144592/2019.

7. REFERENCES

[1] F. Ozogul, I. Hamed, Y. Ozogul, J.M. Regenstein, Crustacean By-products, Encycl. Food Chem. (2019) 33–38.

https://doi.org/10.1016/B978-0-08-100596-5.21690-9.

[2] FAO, Food and Agriculture Organization of the United Nations., State World Fish. Aquac. (2014).

[3] M.J. Hülsey, Shell biorefinery: A comprehensive introduction, Green Energy Environ. 3 (2018) 318–327. https://doi.org/10.1016/j.gee.2018.07.007.

[4] F.M. Kerton, Y. Liu, K.W. Omari, K. Hawboldt, Green chemistry and the ocean-based biorefinery, Green Chem. 15 (2013) 860–871. https://doi.org/10.1039/c3gc36994c.

[5] T. Maschmeyer, R. Luque, M. Selva, Upgrading of marine (fish and crustaceans) biowaste for high added-value molecules and bio(nano)-materials, Chem. Soc. Rev. 49 (2020) 4527–4563. https://doi.org/10.1039/c9cs00653b.

[6] R.R. Ambati, P.S. Moi, S. Ravi, R.G. Aswathanarayana, Astaxanthin: Sources, extraction, stability, biological activities and its commercial applications - A review, Mar. Drugs. 12 (2014) 128–152. https://doi.org/10.3390/md12010128.

[7] T. Zhao, X. Yan, L. Sun, T. Yang, X. Hu, Z. He, F. Liu, X. Liu, Research progress on extraction, biological activities and delivery systems of natural astaxanthin, Trends Food Sci. Technol. 91 (2019) 354–361. https://doi.org/10.1016/j.tifs.2019.07.014.

[8] W. Routray, D. Dave, S.K. Cheema, V. V. Ramakrishnan, J. Pohling, Biorefinery approach and environment-friendly extraction for sustainable production of astaxanthin from marine wastes, Crit. Rev. Biotechnol. 39 (2019) 469–488.

https://doi.org/10.1080/07388551.2019.1573798.

[9] R.K. Saini, S.H. Moon, Y.S. Keum, An updated review on use of tomato pomace and crustacean processing waste to recover commercially vital carotenoids, Food Res. Int. 108 (2018) 516–529. https://doi.org/10.1016/j.foodres.2018.04.003.

[10] N. Martins, I.C.F.R. Ferreira, Wastes and by-products: Upcoming sources of carotenoids for biotechnological purposes and health-related applications, Trends Food Sci. Technol. 62 (2017) 33–48. https://doi.org/10.1016/j.tifs.2017.01.014.

[11] Y. Hou, A. Shavandi, A. Carne, A.A. Bekhit, T.B. Ng, R.C.F. Cheung, A.E. din A. Bekhit, Marine shells: Potential opportunities for extraction of functional and health-promoting materials, Crit. Rev. Environ. Sci. Technol. 46 (2016) 1047–1116. https://doi.org/10.1080/10643389.2016.1202669.

[12] F.A. Mohd Hatta, R. Othman, Carotenoids as potential biocolorants: A case study of astaxanthin recovered from shrimp waste, Elsevier Inc., 2020. https://doi.org/10.1016/b978-0-12-817067-0.00009-9.

[13] Industry Experts, Global Astaxanthin Market−Sources, Technologies and Applications, (2019) . https://www.reportlinker.com/ p02788641/Global-A. https://doi.org/. https://www.reportlinker.com/ p02788641/Global-Astaxanthin-Market-Sources-Technologies-and- Applications.html.

[14] A. Molino, J. Rimauro, P. Casella, A. Cerbone, V. Larocca, S. Chianese, D. Karatza, S. Mehariya, A. Ferraro, E. Hristoforou, D. Musmarra, Extraction of astaxanthin from microalga Haematococcus pluvialis in red phase by using generally recognized as safe solvents and

accelerated extraction, J. Biotechnol. 283 (2018) 51–61. https://doi.org/10.1016/j.jbiotec.2018.07.010.

[15] M.N. Rammuni, T.U. Ariyadasa, P.H.V. Nimarshana, R.A. Attalage, Comparative assessment on the extraction of carotenoids from microalgal sources: Astaxanthin from H. pluvialis and β-carotene from D. salina, Food Chem. 277 (2019) 128–134. https://doi.org/10.1016/j.foodchem.2018.10.066.

[16] S.F. Bruno, F.J.A.A. Ekorong, S.S. Karkal, M.S.B. Cathrine, T.G. Kudre, Green and innovative techniques for recovery of valuable compounds from seafood by-products and discards: A review, Trends Food Sci. Technol. 85 (2019) 10–22. https://doi.org/10.1016/j.tifs.2018.12.004.

[17] F. Al Khawli, M. Pateiro, R. Domínguez, J.M. Lorenzo, P. Gullón, K. Kousoulaki, E. Ferrer, H. Berrada, F.J. Barba, Innovative green technologies of intensification for valorization of seafood and their by-products, Mar. Drugs. 17 (2019) 1–20. https://doi.org/10.3390/md17120689.

[18] O. Catchpole, T. Moreno, F. Montañes, S. Tallon, Perspectives on processing of high value lipids using supercritical fluids, J. Supercrit. Fluids. 134 (2018) 260–268. https://doi.org/10.1016/j.supflu.2017.12.001.

[19] N. Mezzomo, S.R.S. Ferreira, Carotenoids functionality, sources, and processing by supercritical technology: A review, J. Chem. 2016 (2016). https://doi.org/10.1155/2016/3164312.

[20] C. Capello, U. Fischer, K. Hungerbühler, What is a green solvent? A comprehensive framework for the environmental assessment of solvents, Green Chem. 9 (2007) 927–93.

https://doi.org/10.1039/b617536h.

[21] M. Arshadi, T.M. Attard, R.M. Lukasik, M. Brncic, A.M. Da Costa Lopes, M. Finell, P. Geladi, L.N. Gerschenson, F. Gogus, M. Herrero, A.J. Hunt, E. Ibáñez, B. Kamm, I. Mateos-Aparicio, A. Matias, N.E. Mavroudis, E. Montoneri, A.R.C. Morais, C. Nilsson, E.H. Papaioannou, A. Richel, P. Rupérez, B. Škrbić, M.B. Solarov, J. Švarc-Gajić, K.W. Waldron, F.J. Yuste-Córdoba, Pre-treatment and extraction techniques for recovery of added value compounds from wastes throughout the agri-food chain, Green Chem. 18 (2016) 6160–6204. https://doi.org/10.1039/c6gc01389a.

[22] O. Catchpole, S. Tallon, P. Dyer, F. Montanes, T. Moreno, E. Vagi, W. Eltringham, J. Billakanti, Integrated supercritical fluid extraction and bioprocessing, Am. J. Biochem. Biotechnol. 8 (2012) 263–287. https://doi.org/10.3844/ajbbsp.2012.263.287.

[23] L.A. Rodrigues, C. V. Pereira, I.C. Leonardo, N. Fernández, F.B. Gaspar, J.M. Silva, R.L. Reis, A.R.C. Duarte, A. Paiva, A.A. Matias, Terpene-Based Natural Deep Eutectic Systems as Efficient Solvents to Recover Astaxanthin from Brown Crab Shell Residues, ACS Sustain. Chem. Eng. 8 (2020) 2246–2259. https://doi.org/10.1021/acssuschemeng.9b06283.

[24] A.N. Nunes, C. Saldanha do Carmo, C.M.M. Duarte, Production of a natural red pigment derived from Opuntia spp. using a novel high pressure CO_2 assisted-process, RSC Adv. 5 (2015) 83106–83114. https://doi.org/10.1039/C5RA14998C.

[25] A.P. Sánchez-camargo, H.A. Martinez-correa, L.C. Paviani, F.A. Cabral, The Journal of Supercritical Fluids Supercritical CO 2 extraction of

lipids and astaxanthin from Brazilian redspotted shrimp waste (Farfantepenaeus paulensis), 56 (2011) 164–173. https://doi.org/10.1016/j.supflu.2010.12.009.

[26] A.P. Sánchez-camargo, M.Â.A. Meireles, A.L.K. Ferreira, E. Saito, F.A. Cabral, The Journal of Supercritical Fluids Extraction of ω-3 fatty acids and astaxanthin from Brazilian redspotted shrimp waste using supercritical CO 2 + ethanol mixtures, J. Supercrit. Fluids. 61 (2012) 71–77. https://doi.org/10.1016/j.supflu.2011.09.017.

[27] S.A. Radzali, B.S. Baharin, R. Othman, M. Markom, R.A. Rahman, Co-solvent selection for supercritical fluid extraction of astaxanthin and other carotenoids from Penaeus monodon waste, J. Oleo Sci. 63 (2014) 769–777. https://doi.org/10.5650/jos.ess13184.

[28] L. Felix-valenzuela, I. Higuera-ciaparai, F. Goycoolea-valencia, Supercritical CO2/ethanol Extraction of Astaxanthin From Blue Crab (Callinectes Sapidus) Shell Waste, J. Food Process Eng. 24 (2000) 101–112.

[29] R.K. Saini, Y.-S. Keum, Carotenoid extraction methods: A review of recent developments, Food Chem. 240 (2018) 90–103. https://doi.org/10.1016/j.foodchem.2017.07.099.

[30] D. Ruen-ngam, A. Shotipruk, P. Pavasant, Comparison of extraction methods for recovery of astaxanthin from Haematococcus pluvialis, Sep. Sci. Technol. 46 (2011) 64–70. https://doi.org/10.1080/01496395.2010.493546.

[31] P. C, M. A, C. ML, B. I, Chemical Characterization of Cancer Pagurus, Maja Squinado, Necora Puber and Carcinus Maenas Shells, Poultry, Fish. Wildl. Sci. 05 (2017) 1–6. https://doi.org/10.4172/2375-

446X.1000181.

[32] S. Ahmadkelayeh, K. Hawboldt, Extraction of lipids and astaxanthin from crustacean by-products: A review on supercritical CO2 extraction, Trends Food Sci. Technol. 103 (2020) 94–108. https://doi.org/10.1016/j.tifs.2020.07.016.

[33] A. Álvarez, J. Poejo, A.A. Matias, C.M.M. Duarte, M.J. Cocero, R.B. Mato, Microwave pretreatment to improve extraction efficiency and polyphenol extract richness from grape pomace. Effect on antioxidant bioactivity, Food Bioprod. Process. 106 (2017) 162–170. https://doi.org/10.1016/j.fbp.2017.09.007.

[34] M. Llompart, C. Garcia-Jares, M. Celeiro, T. Dagnac, Extraction | Microwave-Assisted Extraction, 3rd ed., Elsevier Inc., 2019. https://doi.org/10.1016/B978-0-12-409547-2.14442-7.

[35] C. Grosso, P. Valentão, F. Ferreres, P.B. Andrade, Alternative and efficient extraction methods for marine-derived compounds, Mar. Drugs. 13 (2015) 3182–3230. https://doi.org/10.3390/md13053182.

[36] L. Zhao, G. Zhao, F. Chen, Z. Wang, J. Wu, X. Hu, Different effects of microwave and ultrasound on the stability of (all-E)-astaxanthin, J. Agric. Food Chem. 54 (2006) 8346–8351. https://doi.org/10.1021/jf061876d.

[37] N. Mezzomo, B. Maestri, R.L. Dos Santos, M. Maraschin, S.R.S. Ferreira, Pink shrimp (P. brasiliensis and P. paulensis) residue: Influence of extraction method on carotenoid concentration, Talanta. 85 (2011) 1383–1391. https://doi.org/10.1016/j.talanta.2011.06.018.

[38] N. Mezzomo, J. Martínez, M. Maraschin, S.R.S. Ferreira, Pink shrimp

(P. brasiliensis and P. paulensis) residue: Supercritical fluid extraction of carotenoid fraction, J. Supercrit. Fluids. 74 (2013) 22–33. https://doi.org/10.1016/j.supflu.2012.11.020.

[39] B. Hiranvarachat, S. Devahastin, N. Chiewchan, G.S. Vijaya Raghavan, Structural modification by different pretreatment methods to enhance microwave-assisted extraction of β-carotene from carrots, J. Food Eng. 115 (2013) 190–197. https://doi.org/10.1016/j.jfoodeng.2012.10.012.

[40] D.J. Charest, M.O. Balaban, M.R. Marshall, C.J. A., Astaxanthin Extraction from Crawfish Shells by Supercritical CO2 with Ethanol as Cosolvent, J. Aquat. Food Prod. Technol. 10 (2001) 81–96. https://doi.org/10.1300/J030v10n03_08.

[41] M. López, L. Arce, J. Garrido, A. Ríos, M. Valcárcel, Selective extraction of astaxanthin from crustaceans by use of supercritical carbon dioxide, Talanta. 64 (2004) 726–731. https://doi.org/10.1016/j.talanta.2004.03.048.

[42] J.O. Valderrama, M. Perrut, W. Majewski, Extraction of Astaxantine and phycocyanine from microalgae with supercritical carbon dioxide, J. Chem. Eng. Data. 48 (2003) 827–830. https://doi.org/10.1021/je020128r.

[43] L. Wang, B. Yang, B. Yan, X. Yao, Supercritical fluid extraction of astaxanthin from Haematococcus pluvialis and its antioxidant potential in sunflower oil, Innov. Food Sci. Emerg. Technol. 13 (2012) 120–127. https://doi.org/10.1016/j.ifset.2011.09.004.

[44] G. Di Sanzo, S. Mehariya, M. Martino, V. Larocca, P. Casella, S. Chianese, D. Musmarra, R. Balducchi, A. Molino, Supercritical carbon

dioxide extraction of astaxanthin, lutein, and fatty acids from haematococcus pluvialis microalgae, Mar. Drugs. 16 (2018). https://doi.org/10.3390/md16090334.

[45] B. Nobre, F. Marcelo, R. Passos, L. Beirão, A. Palavra, L. Gouveia, R. Mendes, Supercritical carbon dioxide extraction of astaxanthin and other carotenoids from the microalga Haematococcus pluvialis, Eur. Food Res. Technol. 223 (2006) 787–790. https://doi.org/10.1007/s00217-006-0270-8.

[46] F.A. Reyes, J.A. Mendiola, E. Ibañez, J.M. Del Valle, Astaxanthin extraction from Haematococcus pluvialis using CO2-expanded ethanol, J. Supercrit. Fluids. 92 (2014) 75–83. https://doi.org/10.1016/j.supflu.2014.05.013.

[47] S. Machmudah, A. Shotipruk, M. Goto, M. Sasaki, T. Hirose, Extraction of astaxanthin from Haematococcus pluvialis using supercritical CO2 and ethanol as entrainer, Ind. Eng. Chem. Res. 45 (2006) 3652–3657. https://doi.org/10.1021/ie051357k.

[48] K. Fujii, Process integration of supercritical carbon dioxide extraction and acid treatment for astaxanthin extraction from a vegetative microalga, Food Bioprod. Process. 90 (2012) 762–766. https://doi.org/10.1016/j.fbp.2012.01.006.

[49] J.C. de la Fuente, B. Oyarzún, N. Quezada, J.M. del Valle, Solubility of carotenoid pigments (lycopene and astaxanthin) in supercritical carbon dioxide, Fluid Phase Equilib. 247 (2006) 90–95. https://doi.org/10.1016/j.fluid.2006.05.031.

[50] H. Youn, M. Roh, A. Weber, G.T. Wilkinson, B. Chun, Solubility of astaxanthin in supercritical carbon dioxide, Korean J. Chem. Eng. 24

(2007) 831–834.

[51] B.R. Parjikolaei, R.B. El-houri, X.C. Fretté, K.V. Christensen, Influence of green solvent extraction on carotenoid yield from shrimp (Pandalus borealis) processing waste, J. Food Eng. 155 (2015) 22–28. https://doi.org/10.1016/j.jfoodeng.2015.01.009.

CHAPTER 3

Part II – Encapsulation of carotenoids from microalgae biomass

CONTENTS

Adapted from:

Nunes, A.N., Monte, J., Rodríguez-Rojo, S., Nogueira, I., Brazinha, C., Gouveia, L.F., Matias, A.A. (2023) Development of a Carotenoid-Rich Microalgae Colorant by Microencapsulation. Colorants 2024, 3(1), 39-52. Doi: 10.3390/colorants3010003.

The author was involved in the conceptualization and design of the experiments and performed all experimental work, except the characterization of particles by HPLC-DAD acquired at FCT-UNL with the support of J. Monte supervised by C. Brazinha, the particle size distribution by laser diffraction was acquired at BioEcoUVa by S. Rodríguez-Rojo, the particle morphology by SEM was acquired at CEFEMA by I. Nogueira, and the statistical analysis was performed at iMed.ULisboa with the support of L. F. Gouveia. Data processing and interpretation, and results discussion were also performed by the author, as well as the preparation of the original manuscript.

1. ABSTRACT

Dunaliella salina has been recognized as an excellent biomass source of carotenoid, which can be used as a natural orange coloring agent for food products. The most eco-friendly approach for extracting carotenoids is through supercritical carbon dioxide extraction, as it yields highly concentrated extracts while preventing pigment thermal degradation. However, there are limitations when a lipophilic extract is considered as a food ingredient, in particular very difficult handling, and low solubility in water-based products. This study aimed to develop a hydrosoluble form of a natural carotenoid-rich extract recovered from algae biomass within a biorefinery concept to be incorporated in aqueous-based food products. A two-step process was developed starting with the emulsification of the supercritical extract into a mixture of maltodextrin and arabic gum, using soya lecithin as emulsifier. The emulsification was followed by a spray drying step. The impact of process variables on the encapsulation yield, efficiency, emulsion properties, and particle characteristics was studied. The resulting particles exhibited an intense orange color and good water dispersibility, facilitating uniform yellow coloring when incorporated into an aqueous-based product. Overall, spray drying emulsions containing carotenoids derived from *Dunaliella salina* prove to be a promising strategy for the global market demand for natural colorants.

2. INTRODUCTION

The marine environment is widely recognized as a valuable and underexploited source of bioactive compounds [1]. Particularly, microalgae, which are photosynthetic eukaryotic microorganisms, have attracted

significant attention due to their potential as an industrially feasible feedstock of bioactive compounds [2]. Microalgae produce a wide spectrum of nutrients and biomolecules including carbohydrates, protein, enzymes, fibers, vitamins, minerals, and pigments. Importantly, many of these pigments are essential and cannot be synthesized by humans or animals, necessitating their acquisition through dietary sources [3]. Besides, the mass cultivation of microalgae offers several distinct advantages in terms of sustainability. Cultivating microalgae is a straightforward and cost-effective process that can utilize wastewater as a growth medium, and fix carbon dioxide from the atmosphere. Also, exhibit higher biomass productivity when compared to traditional terrestrial plants, and do not compete for agricultural land with conventional crops [3–7].

Carotenoids represent a category of naturally occurring pigmented compounds synthesized by plants and microorganisms [8]. Microalgae, in particular, emerge as highly productive producers of these lipid-soluble pigments [4]. Among various microalgae species, *Dunaliella salina* holds the distinction of accumulating the highest levels of *β*-carotene, reaching up to 14% of its dry weight. Additionally, this microalgae can synthesize other valuable carotenoids such as zeaxanthin, lutein, phytofluene, and phytoene [5,9,10]. These pigments have found diverse applications across various market segments as natural coloring agents and bioactive ingredients in the food, nutraceuticals, pharmaceuticals, and cosmetic industries [11]. Consequently, carotenoids have reached a strong and increasing demand in the market [9]. Indeed, the global carotenoid market, which was valued at 1.44 billion USD in 2019, is expected to grow to 1.84 billion USD in 2027, with a compound annual growth rate of 3.4% [12]. Given the remarkable carotenoid content of Dunaliella salina and the market demand, this

microalgae has emerged as a promising and sustainable feedstock for the commercial production of carotenoids [9].

Carotenoids are stored and protected within the cell wall of *Dunaliella salina*. While the FDA has designated Dunaliella salina Generally Recognized as Safe, incorporating the whole cells into food, nutraceutical, or cosmetic products may not be the most effective approach. These pigments are enclosed within a non-rigid cell wall structure, which potentially restricts their release and bioavailability [13]. In this context, carotenoid extraction plays a crucial step in pigment production. The most suitable sustainable solvent for carotenoid extraction is supercritical carbon dioxide, providing highly concentrated extracts and avoiding the thermal degradation of carotenoids [14]. The elevated pressures drive supercritical fluid into the microalgae cells. Since the diffusion rate of the supercritical fluid resembles that of a gas, mass transfer is significantly accelerated. Consequently, the extraction time can be considerably shorter compared to traditional solvent extraction methods [15]. However, there are limitations when considering a lipophilic extract as a food ingredient due to its poor physiochemical properties, notably its challenging handling and low water solubility [16].

Encapsulation techniques can help to overcome the above-mentioned issues. Encapsulation entraps a target ingredient in a wall material, to isolate the ingredient from the environment [17–19]. Among various encapsulating methods, spray drying emulsions represent a widely employed dehydration technique in the food industry due to its cost-effectiveness and ability to produce high-quality powders that offer excellent protection, stabilization solubility, and controlled release of lipophilic bioactive compounds [17,20]. To obtain these emulsions, lipophilic bioactive compounds are homogenized, forming droplets

dispersed within the aqueous phase. The process of spray-drying emulsions allows the encapsulation of the carotenoid-rich extract in a solid carrier, yielding a dispersible powder [21].

Several materials are accessible for commercial use as wall materials in spray dryer applications. These materials include both natural and modified polysaccharides, gums, lipids, proteins, and synthetic polymers. A suitable wall material for spray drying should exhibit functional characteristics such as emulsifying, gel, film-forming, high solubility, and low cost [22–24]. Maltodextrin offers good oxidative stability and high water solubility but tends to exhibit poor oil retention, emulsifying efficiency, and emulsion stability [16,22,25]. Conversely, gum arabic demonstrates a strong emulsifying capacity [16,26]. Mixing both materials has been shown to offer advantages, as the partial replacement of gum arabic with maltodextrin results in wall materials with enhanced solubility [16,27]. Also, soya lecithin is a natural emulsifier that stabilizes oil droplets during the incorporation of a lipophilic extract into oil-in-water emulsions, producing microcapsules with improved stability and water solubility [28].

Spray drying has been employed for drying microalgae suspensions, including *Dunaliella salina* biomass [29]. However, there is limited information available in the literature regarding the encapsulation of *Dunaliella salina* carotenoids through spray drying. The authors, instead of using carotenoid concentrated extract, encapsulated β-carotene-rich cells of *Dunaliella salina* within a polymer matrix [13,30,31]. In addition, no studies have explored the application of encapsulated carotenoid powders derived from *Dunaliella salina* for the purpose of coloring and/or enhancing the color of food products.

Within this context, the objective of this work was to explore the integration of encapsulation processes by (1) studying the emulsions containing carotenoid-rich extract from *Dunaliella salina* and (2) drying the emulsions using a spray dryer to produce particles that enhance the dispersibility of carotenoids in water-based products. This study marked the first attempt to assess the feasibility of applying a highly concentrated extract recovered from *Dunaliella salina* biomass. The research involved analyzing the yield of collected particles and encapsulation efficiency to optimize the encapsulation conditions. As a proof of concept, the incorporation of the developed water-soluble carotenoid forms was evaluated in an aqueous-based product. This approach represents a significant step forward in the challenging task of production of new natural carotenoid-rich colorants with improved dispersibility in water-based products, addressing the needs of the nutraceutical and food industries.

3. MATERIALS AND METHODS

3.1. Raw material

Dunaliella salina extract used as core material in the encapsulation experiments was provided by NATECO$_2$ (Wolnzach, Germany) within a European project framework: D-Factory, whose main goal was the development of a sustainable algae biorefinery. The microalga *Dunaliella salina* from Monzón Biotech S.L. (Monzón, Spain) presented a total carotenoid content of 8 wt.%. The carotenoid-rich extract, obtained by ultra-high-pressure extraction with supercritical carbon dioxide (up to 1000 bar) of freeze-dried biomass, presented a total carotenoid content of 28 wt.%.

3.2. Chemicals

The reagents employed in the spray drying emulsions methodology included the following: nitrogen (99.99% purity, Air Liquid, Lisbon, Portugal), gum arabic (Sigma-Aldrich, St. Louis, Missouri, EUA), maltodextrin DE 13.0-17.0 (Sigma-Aldrich, St. Louis, Missouri, EUA), soya lecithin (Solgar, Inc., Leonia, NJ, USA) and olive oil (Gallo, Abrantes, Portugal).

3.3. Carotenoids encapsulation by spray drying emulsion

3.3.1. Preparation of oil-in-water emulsion

A solution of maltodextrin and gum Arabic (50 wt.%) was prepared by dissolving both in distilled water at a concentration of 20 g/100mL. Soya lecithin, used as an emulsifier, was added at a ratio of 20 mg/g lipophilic extract in all samples. The soya lecithin was combined with the extract, which was previously diluted in olive oil (50 wt.%). Subsequently, the oil phase was added to the polymer aqueous phase, with varying concentrations relative to the total solids of the emulsion (3-37 wt.%). These concentrations were determined based on prior research [16] and preliminary experimental results. The oil-in-water (o/w) emulsions were prepared by subjecting the mixture to homogenization using an ultra-turrax blender (IKA-Werke GmbH & Co. KG, Staufen, Germany) for 5 min, at stirring speeds ranging from 6500 to21500 rpm. Then, the resulting emulsions were promptly subjected to the spray drying process.

3.3.2. Spray drying process optimization

O/w emulsions were dried using a laboratory scale spray dryer, Büchi Mini Spray Dryer B-290 (Büchi Labortechnik, Flawil, Switzerland), which was equipped with a nozzle featuring a 0.7 mm tip and a nozzle cap with a diameter of 1.4mm. The emulsions were fed into the system via a peristaltic pump. Based on previous works for other biomass [16,22,23,26,32,33] and preliminary experimental results, processing conditions, namely inlet air temperature of 110-220°C, aspirator flow rate of 36 m^3/h, compressed nitrogen flow rate of 439 L/h and feed flow rate of 4.5 mL/min, were selected. The collected particles were stored at 4°C and protected from light until further use.

The encapsulation yield was determined by calculating the ratio of the weight of the resulting powder collected in the vessel after spray drying to the weight of all solids present in the emulsion (including both wall and core material), expressed as a percentage. Encapsulation efficiency was assessed as the ratio of carotenoids extracted from the particles to the total carotenoid content in the initial feed solution, also expressed as a percentage.

3.4. Oil-in-water emulsion characterization

3.4.1. Emulsion droplet size

The emulsion droplet size distribution of o/w emulsions was assessed using a dynamic light scattering (DLS) with a Zetasizer Nano Zs instrument (Malvern Instruments, Worcestershire, UK). All measurements were conducted at room temperature. The instrument provides data on the mean diameter of the particle size distribution (Dv50) and the

polydispersity index (PDI). PDI values below 0.4 indicate a narrow particle size distribution.

3.4.2. Emulsion stability

The o/w emulsions were transferred into a glass tube with an internal diameter of 15 mm and height of 50 mm, filling it to a height of 20 mm. The tube was then tightly sealed with a plastic cap and stored at room temperature. Emulsions stability was assessed by observing phase separation at two time points: 15 min and 1 day after emulsion preparation. The degree of the creaming index was quantified using a creaming index (CI), which represents the percentage of the cream layer (HC) formed at the surface of the emulsion relative to the total volume of the emulsion in the tube (HE) [34]:

$$CI, vol.\% = HC/HE \ x\ 100 \qquad \text{(Eq. 1)}$$

3.4.3. Emulsion morphology

O/w emulsions were examined under a microscope to assess their respective microstructures. Right after their production, the emulsions were gently agitated using a magnetic stirrer to maintain uniformity. A droplet was then collected and placed onto a microscope slide, which was covered with a cover slip. An optical microscope, the Leica DM6 B (Leica Microsystems CMS GmbH, Wetzlar, Germany), was employed to analyze the microstructure of both the freshly prepared and reconstituted emulsions, using a x100 oil immersion objective. Digital image files were captured using Leica LAS X software.

3.4.4. Emulsion reconstitution

Dried particles were weighted (n=3) and mixed with distilled water to obtain reconstituted emulsion with the same dry matter content as before the drying process. After 1 h of continuous rotation at 500 rpm using an orbital mixer (Orbit 300, Labnet International, Inc., New Jersey, USA), samples were taken for the assessment of droplet size distribution, stability, and morphological characteristics, following the same procedure as described for fresh emulsions.

3.5. Spray dried particle characterization

3.5.1. Total Carotenoids Content (TCC)

The determination of TCC in the particles was carried out using high performance liquid chromatography (HPLC). For carotenoid analysis, an Alliance e2695 HPLC model (Waters, Massachusetts, USA), equipped with a degasser, autosampler, and a PDA detector was employed. Separation of carotenoids was achieved using a YMC 30 Carotenoid Column (Classical Analytical HPLC Column S-5µm, 250 x 4.6 mm, YMC) coupled with a Guard Cartridges YMC C30 pre-column (5µm, 10x4.0mm, YMC). The mobile phase consisted of methanol and MTBE (80:20) at 25°C. Detection of carotenoids was performed at a wavelength of 450 nm, and the flow rate was set to 1 mL/min.

Calibration curves for lutein and zeaxanthin were found to be linear in the concentration range of 0.5-100 mg/L, while for all-trans beta carotene, 9-cis β carotene and α-carotene linearity was observed in the range of 0.5-200 mg/L, using MTBE as the solvent. Prior to analysis, all the samples were

prepared by dissolving them in MTBE, followed by centrifugation, and filtration through a 0.45 μm HLPC filter. The total duration of the assay was 45 min, with retention times for lutein, zeaxanthin, α-carotene, all-trans beta carotene, and 9-cis-β-carotene recorded at 6.7, 7.9, 20.5, 26 and 30 min, respectively. A representative chromatogram is included in the Appendix (page 276).

3.5.2. Particle size distribution

The particle size of the samples was assessed using laser diffraction, employing a Malvern Mastersizer 2000. For measurements in at dry state, a Scirocco 2000 dry disperser (Malvern Instruments, Malvern, UK) was utilized. Particle size measurements are presented as volume distribution and defined as Dv50, which is derived as the average of three separated measurements. Additionally, the span value is reported, calculated as the ratio of Dv50 to (Dv90–Dv10). Span values close to 1 indicate a narrow particle size distribution.

3.5.3. Particle morphology

To examine the shape and structure of the particles, scanning electron microscopy (FEG-SEM) (Jeol, SM-5310 model, Tokyo, Japan) was employed, operating at a voltage of 20 to 25 kV. Prior to imaging, the samples were coated with a thin layer of gold approximately 300 Å thick, in an argon atmosphere.

3.5.4. Particle color properties

The color of particles was evaluated using the CIELab method with a Minolta Colorimeter CR-200, (Minolta, Osaka, Japan. This method utilizes three distinct attributes or characteristics of visual perception: tonality, luminosity, and chromatism.

The CIELab color space system is founded on the continuous Cartesian representation of three orthogonal axes: L*, a*, and b*. The L* coordinate L* signifies brightness, with L* = 0 representing black and L* = 100 representing colorless. The a* axis represents the green to red color component, where a* > 0 corresponds to red and a* < 0 corresponds to green. The b* axis signifies to the blue to yellow color component, where b* > 0 represents yellow and b* < 0 represents blue. The chroma (color purity) is denoted as C*, while the hue angle, represented by h°, indicates the sample's color (0° or 360° = red, 90° = yellow, 180° = green, and 270° = blue). The values of C* and h° were determined using the following expressions:

$$C^* = (a^* + b^{*2})^{1/2} \quad \text{(Eq. 2)}$$

$$\mathrm{h}^\circ = \arctan(\mathrm{b}^*/\mathrm{a}^*) \quad \text{(Eq. 3)}$$

Subsequently, these values were converted into RGB color values (representing red, green, and blue), using the OpenRGB software (Logicol, Trieste, Italy).

3.6. Incorporation of *Dunaliella salina* $scCO_2$ extract and spray dried particles in an aqueous-based product

The jelly solution was prepared using commercial jelly powder (Royal, Portugal). To prepare the solution, the jelly powder was dissolved in boiling water at a ratio of 1:50 (%, w/v). The *Dunaliella salina* $scCO_2$ extract and the produced colorant powder were then introduced into the mixture at a solid concentration of 0.001 wt.%. The resulting preparations were poured into plastic cups, sealed with screw caps, and stored in a refrigerator. Visual assessments were conducted to evaluate the uniformity of color distribution within the mixtures.

3.7. Experimental design and statistical analysis

Response surface methodology was employed to assess the influence of process conditions on the encapsulation process of *Dunaliella salina* $scCO_2$ extract. The data related to encapsulation yield and efficiency, obtained through experiments conducted under specific conditions set by a central composite circumscribed design, were analyzed using the Modde® v.12 software (Umetrics, Umeå, Sweden). The statistical significance of the design model and the effects of various factors were determined by evaluating the p-values. Any factor or model adjustment was considered statistically significant when the resulting p-value was less than the predefined α = 0.05. the assessment was carried out using ANOVA and t-test.

4. RESULTS AND DISCUSSION

Aiming at developing a hydrosoluble form of $scCO_2$ extract from *Dunaliella salina* a two-step encapsulation process was developed: (1) emulsifying step: o/w emulsion of the $scCO_2$ extract (lipophilic character) in an aqueous solution containing the wall material (maltodextrin and gum arabic); (2) spray drying step: drying step to develop hydrosoluble forms of carotenoid-rich extract derived from *Dunaliella salina.*

4.1. Encapsulation process optimization

When applying spray drying to dry emulsions, it is crucial to carefully consider and manage various experimental factors for each specific system being studied. To achieve the desired high encapsulation yield and efficiency while accounting for the expected process factors and complex interactions, a systematic and rational approach was necessary.

Utilizing the knowledge gained from prior research, along with preliminary experimental findings and awareness of instrumental constraints, certain factors were held constant. These include the composition of the emulsion aqueous phase, the composition of the emulsion oil phase, the spray dryer aspirator flow rate, the compressed nitrogen flow rate, and the feed flow rate. By maintaining these factors at fixed values, the complexity of the space to be explored was reduced, simplifying the research process. The remaining parameters and their ranges, such as the oil phase concentration in the emulsion (3-37 wt.%), the stirring speed (6500-21500 rpm), and the inlet air temperature (110-220°C), were chosen based on available information for other biomass [16,22,23,26,32,33].

An appropriate balance between the number of necessary experimental trials and the knowledge acquired was determined. Considering the three factors and the defined objectives, a central composite circumscribed design was chosen. This design encompasses a full factorial design and star points. Additionally, Central replicate points were integrated to evaluate experimental variability, result uncertainty, and the goodness of fit of the mathematical model employed. Using response surface methodology, the optimum conditions for encapsulating the *Dunaliella salina* $scCO_2$ extract were determined.

The experimental conditions and outcomes for each encapsulation trial are detailed in Table 1. The highest encapsulation yield was 69.0 ± 0.9 wt.% (Table 1 - experiment N11). This recovery was obtained at 3 wt.% oil phase concentration in the emulsion, 13500 rpm, and 165°C of inlet air temperature. This finding was consistent with previous reports. According to Durmaz *et al*., the encapsulation yield of 50.8-70.2 % was obtained for spray drying *Dunaliella salina* biomass using maltodextrin [13]. Bustos-Garza *et al*. reported a 49.4-50.9 % encapsulation yield for spray drying of astaxanthin derived from *Haematococcus pluvialis* in a mixture of gum arabic and maltodextrin [35].

The encapsulation experiment with the highest encapsulation efficiency was obtained at 30 wt.% oil phase concentration in the emulsion, 17500 rpm, and 130°C of inlet air temperature, which was 80.0 ± 13.3 wt.% (Table 1 - experiment N4). The obtained values were on par with encapsulation efficiency of 39.3-74.2% previously by Foo *et al.* for spray-dried fucoxanthin from *Chaetoceros calcitrans* in gum arabic and maltodextrin [36].

Table 1. Summary of experimental results for the encapsulation of $scCO_2$ extract from *Dunaliella salina*.

Encapsulation Process							Emulsion characterization						Particle characterization			
							Fresh			Reconstituted						
Exp.	Oil (wt.%)	Stirring (rpm)	Inlet T[a] (°C)	Outlet T[b] (°C)	EY[c] (wt.%)	EE[d] (wt.%)	Dv50[e] (μm)	PDI[f]	CI[g] 1day (vol.%)	Dv50 (μm)	PDI	CI 1day (vol.%)	Dv50 (μm)	Span	TCC[h] (wt.%)	RGB color
N1	10	9500	130	75	39	31	5.33	0.06	10.0	4.9	0.26	2.50	12	1.8	0.31	
N2	10	17500	130	85	57	4	4.32	0.26	2.5	4.8	0.11	0.05	8	2.0	0.04	
N3	30	9500	130	76	31	58	9.41	ND	10.0	8.9	ND	10.00	16	1.8	1.75	
N4	30	17500	130	76	25	80	5.22	0.26	5.0	1.4	0.34	5.00	14	7.1	2.40	
N5	10	9500	200	98	54	32	5.33	0.06	10.0	5.1	0.13	5.00	10	1.9	0.32	
N6	10	17500	200	105	58	4	4.32	0.22	2.5	4.7	0.13	0.05	9	2.0	0.04	
N7	30	9500	200	105	28	72	9.41	ND	10.0	10.5	ND	10.00	39	11.2	2.16	
N8	30	17500	200	110	39	74	5.22	0.26	5.0	8.2	0.42	5.00	21	16.7	2.22	
N9	20	13500	110	75	42	52	5.05	0.07	10.0	6.6	0.39	5.00	11	1.9	1.04	
N10	20	13500	220	115	48	27	5.05	0.07	10.0	5.0	0.11	5.00	13	2.0	0.54	
N11	3	13500	165	92	69	13	4.37	0.21	5.0	4.6	0.12	2.50	9	1.9	0.04	
N12	37	13500	165	98	16	79	10.00	ND	15.0	7.0	0.34	7.50	26	17.6	2.92	
N13	20	6500	165	90	40	37	16.87	ND	15.0	9.4	ND	7.50	14	1.9	0.74	
N14	20	21500	165	85	46	37	4.56	0.18	5.0	2.0	0.39	1.25	9	2.2	0.74	
N15	20	13500	165	88	42	34	5.05	0.07	10.0	2.3	0.45	5.00	10	1.7	0.67	
N16	20	13500	165	76	42	47	5.05	0.07	10.0	5.0	0.20	5.00	9	1.8	0.93	
N17	20	13500	165	88	43	44	5.05	0.07	10.0	2.1	0.45	5.00	10	1.7	0.88	

[a]Inlet air temperature; [b]Outlet air temperature; [c]Encapsulation yield; [d]Encapsulation efficiency; [e]Mean diameter of the particle size distribution; [f]Polydispersity index; [g]Creaming index; [h]Total carotenoids content.

ND - not detected for Dv50 values >9.4 μm

The oil phase concentration in the emulsion has a significant effect (p<0.05) on both evaluated responses: encapsulation yield and efficiency. In addition, the encapsulation efficiency was significantly affected (p<0.05) by some interactions between factors, namely oil concentration in the emulsion and stirring speed (the model fit is provided in the Appendix (page 276). Contour plots representing the encapsulation yield and efficiency as a function of the oil phase concentration in the emulsion, stirring speed during the emulsification step, and inlet air temperature of spray drying are presented in Figure 1.

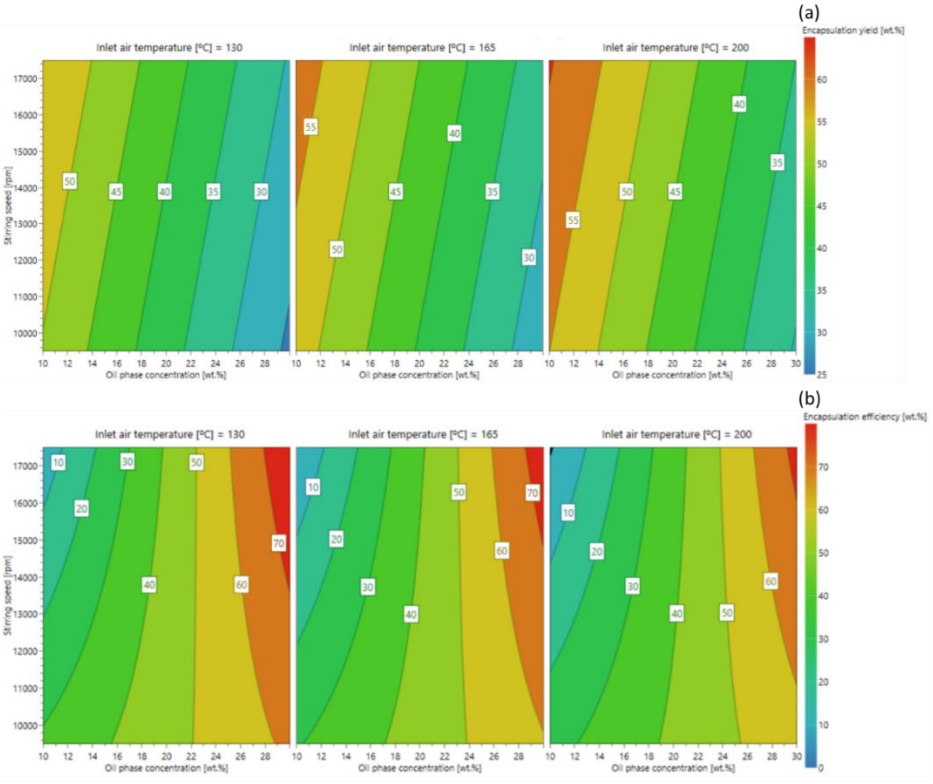

Figure 1. Contour plots of the effects of different emulsion oil phase concentration, emulsification stirring speed, and spray drying inlet air temperature on (a) encapsulation yield, and (b) encapsulation efficiency.

Figure 1a illustrates a significant impact (p<0.05) of oil phase concentration in the emulsion on the encapsulation yield. A decreasing amount of oil phase resulted in the improvement in encapsulation yield. This effect was more pronounced at higher inlet air temperatures (p=0.05) and higher stirring speeds (p=0.05). Insufficiently high inlet air temperature can lead to incomplete water vaporization resulting in inadequately dried powder that adheres to the drying chamber wall [26]. The process of water evaporation is more effective at higher inlet air temperatures due to the improved efficiency of heat and mass transfer between the chamber wall and the moving fluid, ultimately resulting in higher yields [26].

From Figure 1b, when high oil phase concentration in the emulsion was employed, an increase in the stirring speed led to a rise in encapsulation yield. This observation can be attributed to the smaller emulsion droplet size achieved, which promotes the retention of carotenoids during the spray drying process. This, in turn, makes it more challenging for the oil to diffuse to the drying surface of the particles [37,38]. Interestingly, higher inlet air temperatures were found to decrease the encapsulation efficiency (Figure 1b). This phenomenon may be associated with the carotenoid losses attributed to oxidation and/or degradation induced by the elevated temperatures [37].

The above results show that low oil phase concentration in the emulsion, and medium stirring speed at medium inlet air temperature were the best encapsulation conditions within the studied range, to obtain the highest yield. Whereas the greatest encapsulation efficiency was attained using a high concentration of the oil phase, and high stirring speed at lower inlet air temperature. Consequently, processing factors were demonstrated to have different effects on each response variable evaluated. The improvement in

the process of carotenoid encapsulation might be not only in the encapsulation yield but also in the encapsulation efficiency. In this way, the goal was to optimize the encapsulation of carotenoids, maximizing the encapsulation yield and efficiency. The operational parameters for emulsion spray drying were determined through a multiple linear regression approach employing an automated optimizer (Modde® v.12). The software generated twelve sets of optimal encapsulation conditions. Among these, the parameter-setting combination with the lowest probability of failure was identified as follows: 30 wt.% oil phase concentration in the emulsion, 17500 rpm stirring speed, and an inlet air temperature of 200°C (same conditions as experiment N8).

4.2. Oil-in-water emulsion characterization

In order to ensure the effective retention of carotenoid-rich extract during the spray-drying process, assessing emulsion properties such as droplet size, morphology, and stability is a critical step [37]. The mean diameters of the particle size distribution and creaming index for both freshly prepared and reconstituted emulsions are presented in Table 1.

The mean droplet diameters of the fresh emulsions ranged from 4.3 to 16.9 μm with a PDI<0.4, indicating that emulsions are monodisperse. Reducing the oil phase concentration in the emulsion and increasing the stirring speed resulted in a reduction in droplet size and narrowed the droplet distribution. The incorporation of carotenoids, being lipophilic compounds, into aqueous-based products necessitates the employment of emulsifiers. Emulsifiers, acting as surface-active agents, facilitate the rapid absorption of oil droplets at the o/w interface during the homogenization process, thus

preventing the dispersed-phase droplets in emulsions from clustering together [21,35,39]. Therefore, the reduction in droplet size could be explained by increasing the concentration of gum Arabic, which is known to have good emulsifying properties. Also, the reduction in droplet size as stirring speed increases can be attributed to the heightened local dissipation of energy within the emulsion-breaking zone, thus avoiding the droplet coalescence [40]. Lima and co-workers found higher values (from 40.9 to 52.3 μm) when producing carotenoid-enriched emulsions with gum arabic and similar homogenizing system (ultra-turrax blender) [21].

Microscopic examination was carried out on both freshly prepared and reconstituted emulsions to assess their respective microstructures. Figure 2a displays the microscopic images of fresh emulsions prepared with different oil phase concentrations at the same stirring speed. It is visually evident that an increase in the oil phase concentration in the emulsion resulted in larger droplet size, even at the same stirring speed. In Figure 2b, microscopic images of fresh emulsions prepared with different stirring speeds but with the same oil phase concentration are presented. It is noticeable that higher stirring speeds corresponded to smaller mean diameters of emulsion droplets. These visual observations align with the results obtained for emulsion droplet size.

Following the preparation of o/w emulsions, they underwent spray drying to directly obtain particles, which were subsequently re-suspended in water. The particles exhibited excellent solubility in water, due to the solubility properties conferred by maltodextrin. Figure 2c and Figure 2d show the microscopic images of reconstituted emulsions prepared with different oil phase concentrations and stirring speeds. The effects of both oil phase concentration and stirring speed on the droplet morphology of

the reconstituted emulsions mirrored the observation made for the freshly prepared emulsions. Notably, the processing of emulsions through spray drying led to a reduction in droplets sizes, although a non-negligible loss of droplets was observed.

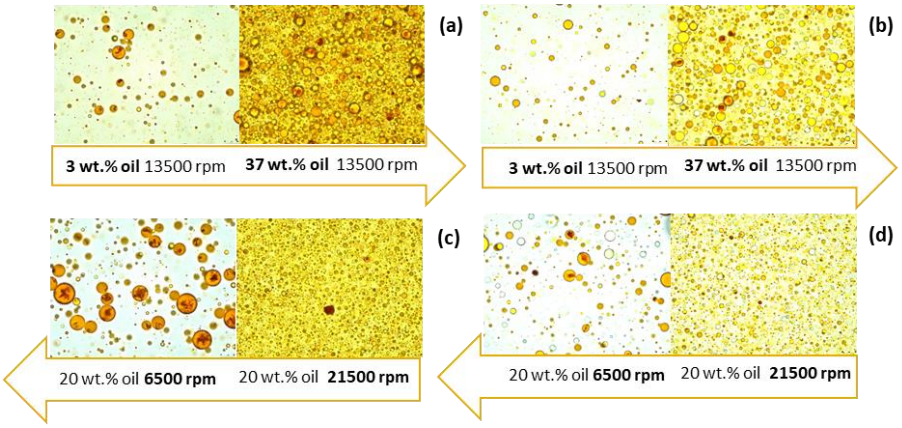

Figure 2. Effect of oil phase concentration on the droplet morphology of the fresh (a) and reconstituted emulsions (b). Effect of stirring speed on the droplet morphology of the fresh (c) and reconstituted emulsions (d). Optical microscopy through a x100 oil immersion objective.

The visual separation of an emulsion can be regarded as an indication of physical instability. When emulsions undergo instability, the oil phase tends to rise to the top while the denser aqueous phase settles at the bottom [41]. In this evaluation, the physical stability of the emulsions was assessed by analyzing the extent of the cream layer. The larger the creaming index, the greater the agglomeration of the emulsion droplets, which results in a less stable emulsion. According to the results presented in Table 1, all emulsions were stable 15 minutes after preparation, presenting an CI equal to 0 vol.%. This time was considered sufficient to ensure emulsion stability throughout the spray dryer experiment. After one day of preparation, the emulsions were physically unstable with CI varying between 2.5 and 15

vol.%. Since the presented strategy (spray drying of emulsions) is a continuous process, the physical stability of the emulsion during the entire experiment was ensured (<15 min).

4.3. Spray dried particle characterization

Yellow to orange, dry, easily dispersible powders were successfully produced by spray drying emulsions. The total carotenoid content, color properties, and particle size of the obtained particles are given in Table 1. Assessing these properties is of significance as they dictate the potential applications of these powders in the food industry [13].

The highest total carotenoid content was 2.9 ± 0.5 wt.% (Table 1 - experiment N12). This concentration was obtained at 37 wt.% oil phase concentration in the emulsion, 13500 rpm and 165°C of inlet air temperature. As expected, the total carotenoid content was highly affected by the oil phase concentration in the emulsion. This effect was more pronounced when applying higher stirring speed during the emulsion preparation. The particles produced in this study exhibited a notably higher carotenoid content compared to the findings of Leach and co-workers [30]. The authors studied the encapsulation of *Dunaliella salina* biomass through spray drying, employing maltodextrin and gum Arabic as the encapsulation matrix, resulting in a total carotenoid content ranging from 0.16 to 0.79 wt.%. The increased carotenoids level observed in the current study can primarily be attributed to the utilization of a highly concentrated extract of *Dunaliella salina*, rather than the entire biomass cell. Also, the addition of soya lecithin as an emulsifier may have effectively prevented the migration of the oil phase, which contains carotenoids, to the surface of particles.

Studies have indicated that the average particles size generated by a spray dryer for different biological materials can reach up to 50 μm [42]. Particle size is influenced not only by the parameters of the spray drying process but also by the emulsion properties, including solid content, size, and stability [37]. In Table 1, the particle size of the different powders obtained via spray drying emulsions at various inlet air temperatures are depicted. The mean particle sizes for the encapsulated carotenoid samples in this study ranged between 7.6 and 39.4 μm. Additionally, polydisperse particles were obtained with span values above 1. A decrease in particle size was observed with an increase in the concentration of wall material and stirring speed during emulsification step. It is noteworthy that larger particle sizes have been reported when applying the same encapsulation process to whole biomass instead of using a highly concentrated carotenoid extract [13]. In their study, the encapsulation of *Dunaliella salina* cells suspension with maltodextrin by spray drying resulted in the mean diameter ranging from 80.1 to 143.7 μm.

The carotenoid-rich particles were subjected to SEM analysis, and no non-encapsulated extract was detected in the product. Figure 3 displays SEM microphotograph of particles obtained under optimal conditions (Table 1 – experiment N8). All samples exhibited similar morphology characterized by spherical shape with extensive dented, smooth surfaces, and an absence of fractures. The surface irregularities observed on the particles are influenced by factors such as the composition of the feed solution, droplet size, and temperature during the spray drying process [35]. The spherical shape arises from the atomization of the feed solution, with the generated droplets solidifying as they cool [36]. The development of dents can be attributed to the rapid water evaporation and consequent particle shrinkage during the drying process [35]. These surface features can be

advantageous for enhancing particle dispersibility and rehydration during emulsion reconstitution [21]. The absence of fractures in the particles may be attributed to the film-forming properties imparted by gum Arabic, which enhances the retention and protection of the carotenoid-rich extract [22]. In contrast, Orset *et al.* applied a similar technique to dry a suspension of *Dunaliella salina* cells, resulting in a damaged cell structure with a porous surface. Consequently, carotenoids were more exposed to environmental risk factors such as oxygen and light. However, the morphology of the particles obtained in the present study aligns with previous research on carotenoid encapsulation from various sources using spray drying technique [21,22,35,36].

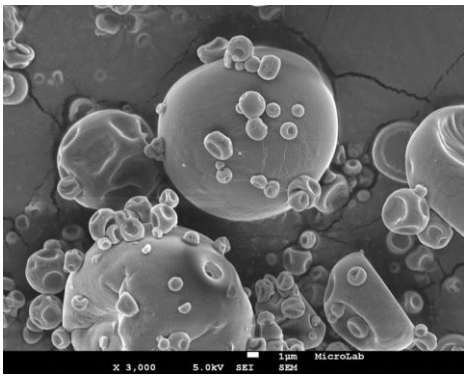

Figure 3. SEM microphotograph of the particles produced with an oil phase concentration of 30 wt.%, 17500 rpm od stirring speed during emulsification and at 200°C of inlet air temperature. SEM images captured with x3000 magnification.

Since *Dunaliella salina* $scCO_2$ extract has been suggested as a natural colorant due to its vibrant orange to yellow appearance, CIELab parameters were employed to assess its color characteristics. In the Appendix (page

281), these CIELab parameters, including L* (reflecting lightness), a* (representing redness-greenness), b* (indicating yellowness-blueness), C* (chroma) and h° (hue), are provided. These colorimetric parameters were subsequently converted to RGB, as presented in Table 1. The data obtained falls within the first quadrant of the CIELAB color chart. All particles exhibit distinctive colors associated with carotenoids, confirming that the pigment is encapsulated within the carriers. The lightness values ranged from the L* = 52.3 to the L* = 78.4. Notably, the L* values for spray dryer samples increased with an increase in maltodextrin and gum Arabic concentration in the feed solution. A higher concentration of the encapsulating agent resulted in a whitening effect on the powder. All the samples display positive a* values, consistent with their orange color, which ranged from a* = 5.0 to a* = 18.3. The a* value exhibited a direct correlation with the carotenoid content, decreasing as the number of encapsulation agents (aqueous phase) increased, leading to a decrease in the amount of extract (oil phase) decreased. Positive values of the b* parameter were observed, ranging from b* = 35.4 to b* = 59.2, indicating that the resulting particles had a yellowish color. The b* value was inversely proportional to the carotenoid content. Other studies have also reported a strong relationship between the total carotenoid content and color parameters a* and b* [21,35,36]. Minor variations were detected in the C* and hue angle h° parameters.

4.4. Incorporation of *Dunaliella salina* $scCO_2$ extract and particles in an aqueous-based food product

The *Dunaliella salina* $scCO_2$ extract and the resulting colorant powder were introduced into the jelly mixture at a concentration of 0.001 wt.%. Pictures

were captured after refrigeration, and these images are displayed in Figure 4. The images clearly illustrate the effective blending of the orange color into the product following the incorporation of water-soluble particles, in contract in contrast to the $scCO_2$ extract, which led to color segregation within the jelly.

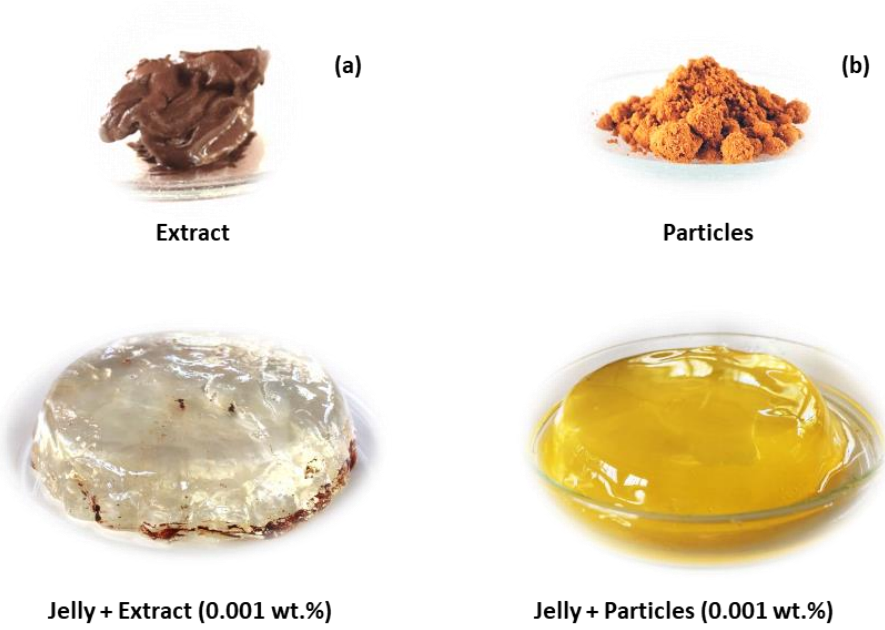

Figure 4. Incorporation of (a) $scCO_2$ extract and (b) particles in a water-based food product – Jelly.

5. CONCLUSIONS

The study reported herein highlights the potential of emulsification followed by spray drying for encapsulation as an effective method for encapsulating natural pigments derived from *Dunaliella salina*. The optimum conditions for carotenoid encapsulation include 30 wt.% emulsion

oil phase concentration, emulsification stirring speed of 17500 rpm, and a spray drying inlet air temperature of 200°C. Under these conditions, an encapsulation yield of 39 wt.% and an efficiency of 74 wt.% were obtained. Furthermore, the resulting particles exhibit desirable characteristics for utilization as food ingredients, as they present a vibrant orange hue and excellent water dispersibility. This feature enables uniform yellow color integration when incorporated into aqueous-based products. Notably, this study marks the first exploration of utilizing a concentrated extract derived from *Dunaliella salina* biomass, rather than the entire cell. This approach enables the attainment of higher carotenoid concentration in the final formulation. The results confirm that encapsulation of carotenoid pigments using natural polysaccharides through emulsion-based spray drying is a promising strategy for developing water-soluble forms of liposoluble pigments, thereby enhancing their dispersibility in aqueous-based products. These results are useful for broadening the utilization of healthy natural colorants derived from algal biomass in the fields of foods, pharmaceuticals, and cosmetics.

6. ACKNOWLEDGEMENTS

The authors would like to acknowledge NATECO2 (Wolnzach, Germany) for providing the supercritical carbon dioxide extract from *Dunaliella salina* and Monzón Biotech S.L. (Monzón, Spain) for providing the *Dunaliella salina* for the supercritical carbon dioxide extract. The authors are grateful to Mário Santos for the use of Minolta Colorimeter CR-200 at INIAV (Instituto Nacional de Investigação Agrária e Veterinária). Carla Brazinha (Post-Doctoral grant SFRH/BPD/79533/2011) acknowledges the grant support by Portuguese Fundação para a Ciência e a Tecnologia, Portugal. Ana A. Matias

thanks for the IF Starting Grant – GRAPHYT (IF/00723/2014). This work was supported by the Associate Laboratory for Green Chemistry LAQV [UID/QUI/50006/2013, POCI-01-0145-FEDER – 007265]; the European KBBE P7 project “D- Factory” [613870]; the Portuguese Fundação para a Ciência e Tecnologia (PEst-OE/EQB/LA0004/2011); the iNOVA4Health Research Unit (LISBOA-01-0145-FEDER-007344), which is cofunded by Fundação para a Ciência e Tecnologia / Ministério da Ciência e do Ensino Superior, through national funds and by FEDER under the PT2020 Partnership Agreement.

7. REFERENCES

[1] M. Herrero, A. del P. Sánchez-Camargo, A. Cifuentes, E. Ibáñez, Plants, seaweeds, microalgae and food by-products as natural sources of functional ingredients obtained using pressurized liquid extraction and supercritical fluid extraction, TrAC - Trends Anal. Chem. 71 (2015) 26–38. https://doi.org/10.1016/j.trac.2015.01.018.

[2] S.R.P. Hosseini, O. Tavakoli∗, M.H. Sarrafzadeh, Experimental optimization of SC-CO2 extraction of carotenoids from Dunaliella salina, J. Supercrit. Fluids. 121 (2017) 89–95. https://doi.org/10.1016/j.supflu.2016.11.006.

[3] H. Sovová, R.P. Stateva, New developments in the modelling of carotenoids extraction from microalgae with supercritical CO2, J. Supercrit. Fluids. 148 (2019) 93–103. https://doi.org/10.1016/j.supflu.2019.03.002.

[4] G. Di Lena, I. Casini, M. Lucarini, G. Lombardi-Boccia, Carotenoid profiling of five microalgae species from large-scale production, Food Res. Int. 120 (2019) 810–818.

https://doi.org/10.1016/j.foodres.2018.11.043.

[5] R. Srinivasan, A. Chaitanyakumar, A. Mageswari, A. Gomathi, J.G.S. Pavan Kumar, M. Jayasindu, G. Bharath, J.S. Shravan, K.M. Gothandam, Oral administration of lyophilized Dunaliella salina, a carotenoid-rich marine alga, reduces tumor progression in mammary cancer induced rats, Food Funct. 8 (2017) 4517–4527. https://doi.org/10.1039/c7fo01328k.

[6] A. Molino, S. Mehariya, G. Di Sanzo, V. Larocca, M. Martino, G.P. Leone, T. Marino, S. Chianese, R. Balducchi, D. Musmarra, Recent developments in supercritical fluid extraction of bioactive compounds from microalgae: Role of key parameters, technological achievements and challenges, J. CO2 Util. 36 (2020) 196–209. https://doi.org/10.1016/j.jcou.2019.11.014.

[7] A. Mouahid, C. Crampon, S.A.A. Toudji, E. Badens, Effects of high water content and drying pre-treatment on supercritical CO2 extraction from Dunaliella salina microalgae: Experiments and modelling, J. Supercrit. Fluids. 116 (2016) 271–280. https://doi.org/10.1016/j.supflu.2016.06.007.

[8] P. Adadi, N.V. Barakova, E.F. Krivoshapkina, Selected Methods of Extracting Carotenoids, Characterization, and Health Concerns: A Review, J. Agric. Food Chem. 66 (2018) 5925–5947. https://doi.org/10.1021/acs.jafc.8b01407.

[9] M.N. Rammuni, T.U. Ariyadasa, P.H.V. Nimarshana, R.A. Attalage, Comparative assessment on the extraction of carotenoids from microalgal sources: Astaxanthin from H. pluvialis and β-carotene from D. salina, Food Chem. 277 (2019) 128–134.

https://doi.org/10.1016/j.foodchem.2018.10.066.

[10] S. Pourkarimi, A. Hallajisani, A. Nouralishahi, A. Alizadehdakhel, A. Golzary, Factors affecting production of beta-carotene from Dunaliella salina microalgae, Biocatal. Agric. Biotechnol. 29 (2020). https://doi.org/10.1016/j.bcab.2020.101771.

[11] G.D. López, G. Álvarez-Rivera, C. Carazzone, E. Ibáñez, C. Leidy, A. Cifuentes, Bacterial Carotenoids: Extraction, Characterization, and Applications, Crit. Rev. Anal. Chem. 0 (2021) 1–24. https://doi.org/10.1080/10408347.2021.2016366.

[12] R.K. Saini, P. Prasad, V. Lokesh, X. Shang, J. Shin, Carotenoids : Dietary Sources , Extraction , Encapsulation , Bioavailability , and Health Benefits — A Review of Recent Advancements, (2022).

[13] D. Yaşar, N. Konar, B. Gurbuz, D.G. Polat, B. Mert, Spray-Drying Optimization for Dunaliella salina and Porphyridium cruentum Biomass, Res. Sq. (2023). https://doi.org/10.21203/rs.3.rs-2535537/v1.

[14] R.K. Saini, Y.-S. Keum, Carotenoid extraction methods: A review of recent developments, Food Chem. 240 (2018) 90–103. https://doi.org/10.1016/j.foodchem.2017.07.099.

[15] M. Gong, A. Bassi, Carotenoids from microalgae: A review of recent developments, Biotechnol. Adv. 34 (2016) 1396–1412. https://doi.org/10.1016/j.biotechadv.2016.10.005.

[16] P. Montero, M.M. Calvo, M.C. Gómez-Guillén, J. Gómez-Estaca, Microcapsules containing astaxanthin from shrimp waste as potential food coloring and functional ingredient: Characterization,

stability, and bioaccessibility, LWT - Food Sci. Technol. 70 (2016) 229–236. https://doi.org/10.1016/j.lwt.2016.02.040.

[17] A.S.L. Lim, Y.H. Roos, Spray drying of high hydrophilic solids emulsions with layered interface and trehalose-maltodextrin as glass formers for carotenoids stabilization, J. Food Eng. 171 (2016) 174–184. https://doi.org/10.1016/j.jfoodeng.2015.10.026.

[18] J. Loksuwan, Characteristics of microencapsulated ??-carotene formed by spray drying with modified tapioca starch, native tapioca starch and maltodextrin, Food Hydrocoll. 21 (2007) 928–935. https://doi.org/10.1016/j.foodhyd.2006.10.011.

[19] G.A. Rocha, C.S. Fávaro-Trindade, C.R.F. Grosso, Microencapsulation of lycopene by spray drying: Characterization, stability and application of microcapsules, Food Bioprod. Process. 90 (2012) 37–42. https://doi.org/10.1016/j.fbp.2011.01.001.

[20] T.C. Kha, M.H. Nguyen, P.D. Roach, C.E. Stathopoulos, Microencapsulation of Gac oil: Optimisation of spray drying conditions using response surface methodology, Powder Technol. 264 (2014) 298–309. https://doi.org/10.1016/j.powtec.2014.05.053.

[21] P.M. Lima, G.C. Dacanal, L.S. Pinho, L.J. Pérez-Córdoba, M. Thomazini, I.C.F. Moraes, C.S. Favaro-Trindade, Production of a rich-carotenoid colorant from pumpkin peels using oil-in-water emulsion followed by spray drying, Food Res. Int. 148 (2021). https://doi.org/10.1016/j.foodres.2021.110627.

[22] A.Y. Guadarrama-Lezama, L. Dorantes-Alvarez, M.E. Jaramillo-Flores, C. Pérez-Alonso, K. Niranjan, G.F. Gutiérrez-López, L. Alamilla-Beltrán, Preparation and characterization of non-aqueous extracts

from chilli (Capsicum annuum L.) and their microencapsulates obtained by spray-drying, J. Food Eng. 112 (2012) 29–37. https://doi.org/10.1016/j.jfoodeng.2012.03.032.

[23] M.P. Rascón, C.I. Beristain, H.S. García, M.A. Salgado, Carotenoid retention and storage stability of spray-dried encapsulated paprika oleoresin using gum Arabic and Soy protein isolate as wall materials, LWT - Food Sci. Technol. 44 (2011) 549–557. https://doi.org/10.1016/j.lwt.2010.08.021.

[24] R. Liang, Q. Huang, J. Ma, C.F. Shoemaker, F. Zhong, Effect of relative humidity on the store stability of spray-dried beta-carotene nanoemulsions, Food Hydrocoll. 33 (2013) 225–233. https://doi.org/10.1016/j.foodhyd.2013.03.015.

[25] C.P. Coronel-Aguilera, M.F. San Martín-González, Encapsulation of spray dried b-carotene emulsion by fluidized bed coating technology, LWT - Food Sci. Technol. 62 (2015) 187–193. https://doi.org/10.1016/j.lwt.2014.12.036.

[26] R. V. Tonon, C.R.F. Grosso, M.D. Hubinger, Influence of emulsion composition and inlet air temperature on the microencapsulation of flaxseed oil by spray drying, Food Res. Int. 44 (2011) 282–289. https://doi.org/10.1016/j.foodres.2010.10.018.

[27] E. Janiszewska-turak, N. Dellarosa, U. Tylewicz, L. Laghi, S. Romani, M. Dalla, D. Witrowa-rajchert, The influence of carrier material on some physical and structural properties of carrot juice microcapsules, Food Chem. 236 (2017) 134–141. https://doi.org/10.1016/j.foodchem.2017.03.134.

[28] D. Wu, J. Lu, S. Zhong, P. Schwarz, B. Chen, J. Rao, Effect of chitosan

coatings on physical stability, antifungal and mycotoxin inhibitory activities of lecithin stabilized cinnamon oil-in-water emulsions, Lwt. 106 (2019) 98–104. https://doi.org/10.1016/j.lwt.2019.02.029.

[29] S. Orset, G.C. Leach, R. Morais, a J. Young, Spray-drying of the microalga Dunaliella salina: effects on beta-carotene content and isomer composition., J. Agric. Food Chem. 47 (1999) 4782–4790. https://doi.org/10.1021/jf990571e.

[30] G. Leach, G. Oliveira, R. Morais, Spray-drying of Dunaliella salina to produce a ? -carotene rich powder, J. Ind. Microbiol. Biotechnol. 20 (1998) 82–85. https://doi.org/10.1038/sj.jim.2900485.

[31] M.H. Morowvat, Y. Ghasemi, Spray- Drying Microencapsulation of β -Carotene Contents in Powdered Dunaliella salina Biomass, 8 (2016) 1533–1536.

[32] E.G. Donhowe, F.P. Flores, W.L. Kerr, L. Wicker, F. Kong, Characterization and invitro bioavailability of β-carotene: Effects of microencapsulation method and food matrix, LWT - Food Sci. Technol. 57 (2014) 42–48. https://doi.org/10.1016/j.lwt.2013.12.037.

[33] E.C. Frascareli, V.M. Silva, R. V. Tonon, M.D. Hubinger, Effect of process conditions on the microencapsulation of coffee oil by spray drying, Food Bioprod. Process. 90 (2012) 413–424. https://doi.org/10.1016/j.fbp.2011.12.002.

[34] D.J. McClements, Food emulsions: principles, practice and techniques., Third Edit, Boca Raton: CRC Press., 1999.

[35] C. Bustos-Garza, J. Yáñez-Fernández, B.E. Barragán-Huerta, Thermal

and pH stability of spray-dried encapsulated astaxanthin oleoresin from Haematococcus pluvialis using several encapsulation wall materials, Food Res. Int. 54 (2013) 641–649. https://doi.org/10.1016/j.foodres.2013.07.061.

[36] S.C. Foo, N.M.H. Khong, F. Yusoff, Physicochemical , microstructure and antioxidant properties of microalgae- derived fucoxanthin rich microcapsules, Algal Res. 51 (2020) 102061. https://doi.org/10.1016/j.algal.2020.102061.

[37] A. Bustamante, L. Masson, J. Velasco, J.M. Del Valle, P. Robert, Microencapsulation of H. pluvialis oleoresins with different fatty acid composition: Kinetic stability of astaxanthin and alpha-tocopherol, Food Chem. 190 (2016) 1013–1021. https://doi.org/10.1016/j.foodchem.2015.06.062.

[38] A. Gharsallaoui, G. Roudaut, O. Chambin, A. Voilley, R. Saurel, Applications of spray-drying in microencapsulation of food ingredients: An overview, Food Res. Int. 40 (2007) 1107–1121. https://doi.org/10.1016/j.foodres.2007.07.004.

[39] D.J. McClements, Food emulsions: Principles, practice and techniques., 2nd Editio, Boca Raton: CRC Press., 2005.

[40] G. Chen, D. Tao, An experimental study of stability of oil – water emulsion, Fuel Process. Technol. 86 (2005) 499–508. https://doi.org/10.1016/j.fuproc.2004.03.010.

[41] C. Chung, D.J. Mcclements, C. Chung, D.J. Mcclements, Structure – function relationships in food emulsions : Improving food quality and sensory perception Structure – function relationships in food emulsions : Improving food quality and sensory perception, Food

Struct. 1 (2014) 106–126. https://doi.org/10.1016/j.foostr.2013.11.002.

[42] N. Konar, Y. Durmaz, D. Genc, P. Behic, Optimization of spray drying for Chlorella vulgaris by using RSM methodology and maltodextrin, (2022) 1–11. https://doi.org/10.1111/jfpp.16594.

CHAPTER 4

Concluding remarks and outlook

CHAPTER 4

CONTENTS

1. GENERAL DISCUSSION AND CONCLUSIONS

The increasing awareness of environmental sustainability and concerns about the potential side effects of synthetic food colorants have driven the growing interest in natural colorants. Consumers perceive natural colorants as safer alternatives, valuing their health-promoting attributes and eco-friendly nature. Additionally, natural colorants offer technological bioactive functionalities, providing extra value and setting them apart from synthetic counterparts, which boosts their market desirability [1–5]. Although promising, natural colorants still face some challenges and limitations.

The experimental work conducted during this Ph.D. thesis represents, therefore, an effort to establish a scientific basis for addressing crucial technological challenges in the application of natural colorants in the food industry, while simultaneously contributing to the sustainable utilization of agricultural and food processing waste. As consumers increasingly seek healthier and more sustainable food options, the demand for natural additives has escalated, prompting the industry to explore innovative methods. The present research aimed to link this demand by developing efficient strategies for extracting, downstream purifying, and encapsulating natural pigments, thereby replacing the synthetic colorants, and reducing the waste in alignment with the principles of biorefinery and the circular economy. In this way, the processes proposed in this research work aimed at valorizing these residues by producing colored extracts/powders using alternative technologies.

The motivations behind this work included addressing specific challenges/issues associated with the application of natural colorants in the food industry, namely the limited availability of natural blue colorants, scarcity of natural astaxanthin, and conditioned solubility of carotenoids.

Consequently, this research aims to connect these challenges by selecting processing units that could be readily scaled to an industrial level, ensuring the feasibility of upscaling the most promising approaches, and advancing a more sustainable food industry.

To achieve these objectives, a range of technologies were employed, including (i) MW pretreatment, which is already proposed as an easy scale-up alternative for intensified extraction of natural pigments [6], (ii) compressed fluid-based technology, which is a well-established technology and already widely applied in different industrial processes [7], (iii) CPC, which is an emerging separation technology in natural product purifications and already reached industrial-scale solutions [8], and (iv) spray drying emulsions, which is already widely used in industry because it is simple and relatively inexpensive [9].

Accordingly, (i) CPC and compressed fluid-based extraction were used for the preparative-scale downstream purification of bluish portisins derived from blueberry surplus anthocyanins; (ii) MW pretreatment and supercritical fluid extraction were applied for the recovery of astaxanthin from crab shell residues; and (iii) emulsification and spray drying were used for the formulation of carotenoids recovered from microalgae biomass, namely *Dunaliella salina*. Overall, each strategy studied allowed a successful recovery/formulation of the target pigments, enabling the attainment of different products with interesting color properties, namely (i) bluish portisins-rich extracts; (ii) reddish astaxanthin-rich extracts; and (iii) orange hydrosoluble carotenoid-rich powder.

The culmination of this research yielded valuable insights and alternative strategies across multiple studies, addressing the challenges of natural

colorants application, and demonstrating their potential to revolutionize the food industry.

Downstream isolation of bluish anthocyanin-derived pigments from blueberry surplus

(i) The first study focused on the development of a highly efficient CPC process for the preparative-scale purification of portisins from blueberry surplus anthocyanins. Optimal conditions were determined, resulting in a 5-fold increase in the purification of portisins with 2.4 times higher efficiency compared to the conventional preparative reverse phase liquid chromatography (RP-LC) process. The CPC process demonstrated a 5.5 times lower environmental risk factor, providing a sustainable alternative for the production and isolation of blue portisin pigments, effectively valorizing blueberry residues.

(ii) The second study introduced a dynamic separation process, employing compressed fluids, to recover portisins. This separation process, utilizing compressed CO_2 and ethanol, resulted in a 1.5-fold increase in portisins content and reduced environmental risk factors compared to preparative RP-LC. The choice between CPC and compressed fluid-based separation depends on the intended application of the bluish extract, offering an alternative method for downstream portisin isolation.

Extraction and formulation of orange carotenoid-derived pigments from marine sources

(iii) In the third study, an integrated MW pretreatment and SFE strategy enhanced astaxanthin recovery from crab shell waste. The optimized conditions yielded improved astaxanthin concentration in the extract, recovering all extractable astaxanthin 12 times faster than traditional Soxhlet

extraction. This intensified extraction approach demonstrated its potential for efficient astaxanthin extraction in the nutraceutical and food industry, valorizing marine crustacean waste streams.

(iv) The final study focused on the formulation of hydrosoluble forms of liposoluble pigment, specifically carotenoids from *Dunaliella salina* microalgae. Emulsification followed by spray drying resulted in orange-hued, water-dispersible particles, offering a promising strategy for natural colorant development with broader application potential in the food, pharmaceutical and cosmetic industries.

Overall, this research provides alternative strategies for addressing the identified challenges, offering alternative methods for natural pigments extraction, downstream purification, and encapsulation. The present work emphasizes sustainable resource utilization, aligning with circular economy principles and providing more environmentally friendly solutions for the food and related industries.

2. OUTLOOK

Although the outcomes achieved in this work are promising, the shift from the industry well-establish methods to novel and eco-friendly processes requires compelling evidence of their effectiveness. Consequently, several questions remain to be addressed prior to large-scale commercial implementation. Challenges related to availability, technical feasibility, costs, and regulatory constraints of natural colorants impose limitations on their widespread adoption.

(i) Toxicity

While the production methods for diverse natural colorants vary, a general trend suggests these additives exhibit improved safety profiles compared to their synthetic counterparts. Nevertheless, the significance of assessing potential toxicity remains unchanged. Ensuring the safety of these natural colorants requires comprehensive toxicological, carcinogenic, and safety evaluations. Rigorous studies are essential to preemptively verify their safety, mitigate potential concerns, and prevent risks.

(ii) Effectiveness

The effectiveness of natural colorants raises concerns, given the larger quantities required for incorporation into food products. Natural colorants often exhibit lower tinctorial strength, necessitating substantial quantities to achieve the desired color hue. This might lead to sensorial changes in the appearance, taste, and texture of food. Therefore, meticulous evaluation of their efficacy is vital, considering the potential need for larger amounts than synthetic additives, impacting cost-effectiveness and feasibility. Moreover, the affordability of natural colorants is a crucial factor that must align reasonably with the synthetic alternatives to remain competitive in the global market. Failing to meet this criterion could render these natural options less attractive for food applications.

(iii) Sources

The use of natural materials as sources for obtaining natural colorants presents challenges and considerations. The demand for substantial biomass quantities for extraction of each natural colorant unit pressures resource availability, necessitating sustainable practices to ensure long-term viability. Hence, the feasibility of the proposed methodologies must be evaluated

considering the quantity of raw materials produced. Addressing the inherent variability in the composition of these natural sources is also vital, warranting comprehensive seasonal and stability assessments to ensure consistent product quality during the processing, transportation, and storage.

(iv) Synergistic Effects

While natural compounds often exhibit remarkable synergistic interactions, compatibility issues can arise. Some natural colorants, typically used in the form of natural extracts rather than pure compounds, may engage in positive or negative synergies with other additives, natural or synthetic, and with inherent food components. These interactions can either enhance or inhibit the coloring function of the natural colorant. This challenge could limit their applicability, necessitating thorough testing and assessment for successful incorporation into food products, including pigment stabilization.

(v) Multiple Functions

Natural colorants extend beyond coloring capacity, offering diverse functions. Comprehensive characterization and functional properties evaluation could broaden their potential applications.

(vi) Process Scalability

Although research has been conducted at the laboratory scale on the different extraction, downstream purification, and encapsulation processes, upscaling and validation are essential. Beyond scalability, environmental sustainability, productivity, and production cost impact the commercial adoption of natural colorants. Integrating life cycle analysis and techno-economic analysis becomes crucial for a holistic assessment.

As future work, natural extract/powder toxicity assessment, stability studies, characterization, and functional proprieties evaluation are imperative. Additionally, process scalability studies, life cycle analysis, and techno-economic assessment will be essential to validate the viability of the proposed approaches.

The research conducted in this Ph.D. thesis contributes to the future development of natural colorants by addressing specific challenges associated with their applications within the food industry. It also represents an important step towards effectively valorizing of agricultural and food processing waste. Furthermore, by exploring microorganisms, namely microalgae, for natural pigment production, the risk of overharvesting plant sources is mitigated, safeguarding ecosystems. Overall, this research advances the knowledge and potential of natural colorants, forging the way for a more sustainable and vibrant future in the field.

3. REFERENCES

[1] J.A. Fernández-López, V. Fernández-Lledó, J.M. Angosto, New insights into red plant pigments: More than just natural colorants, RSC Adv. 10 (2020) 24669–24682. https://doi.org/10.1039/d0ra03514a.

[2] M. Faustino, M. Veiga, P. Sousa, E.M. Costa, S. Silva, M. Pintado, Agro-food byproducts as a new source of natural food additives, Molecules. 24 (2019) 1–23. https://doi.org/10.3390/molecules24061056.

[3] I. Benucci, C. Lombardelli, C. Mazzocchi, M. Esti, Natural colorants from vegetable food waste: Recovery, regulatory aspects, and stability—A review, Compr. Rev. Food Sci. Food Saf. 21 (2022) 2715–2737. https://doi.org/10.1111/1541-4337.12951.

[4] I. Luzardo-Ocampo, A.K. Ramírez-Jiménez, J. Yañez, L. Mojica, D.A. Luna-Vital, Technological applications of natural colorants in food systems: A review, Foods. 10 (2021) 1–34. https://doi.org/10.3390/foods10030634.

[5] M. Carocho, P. Morales, I.C.F.R. Ferreira, Natural food additives: Quo vadis?, Trends Food Sci. Technol. 45 (2015) 284–295. https://doi.org/10.1016/j.tifs.2015.06.007.

[6] A. Álvarez, J. Poejo, A.A. Matias, C.M.M. Duarte, M.J. Cocero, R.B. Mato, Microwave pretreatment to improve extraction efficiency and polyphenol extract richness from grape pomace. Effect on antioxidant bioactivity, Food Bioprod. Process. 106 (2017) 162–170. https://doi.org/10.1016/j.fbp.2017.09.007.

[7] Ž. Knez, M. Pantić, D. Cör, Z. Novak, M. Knez Hrnčič, Are supercritical fluids solvents for the future?, Chem. Eng. Process. - Process Intensif. 141 (2019). https://doi.org/10.1016/j.cep.2019.107532.

[8] L. Lorántfy, R. Örkenyi, D. Rutterschmid, D. Bakonyi, J. Faragó, G. Dargó, Á. Könczöl, Continuous industrial-scale centrifugal partition chromatography with automatic solvent system handling: Concept and instrumentation, Org. Process Res. Dev. 24 (2020) 2676–2688. https://doi.org/10.1021/acs.oprd.0c00338.

[9] F.Y. de Boer, A. Imhof, K.P. Velikov, Encapsulation of colorants by natural polymers for food applications, Color. Technol. 135 (2019) 183–194. https://doi.org/10.1111/cote.12393.

APPENDIX

APPENDIX A – Centrifugal partition chromatography of portisins

Anthocyanin-pyruvic acid adducts synthesis

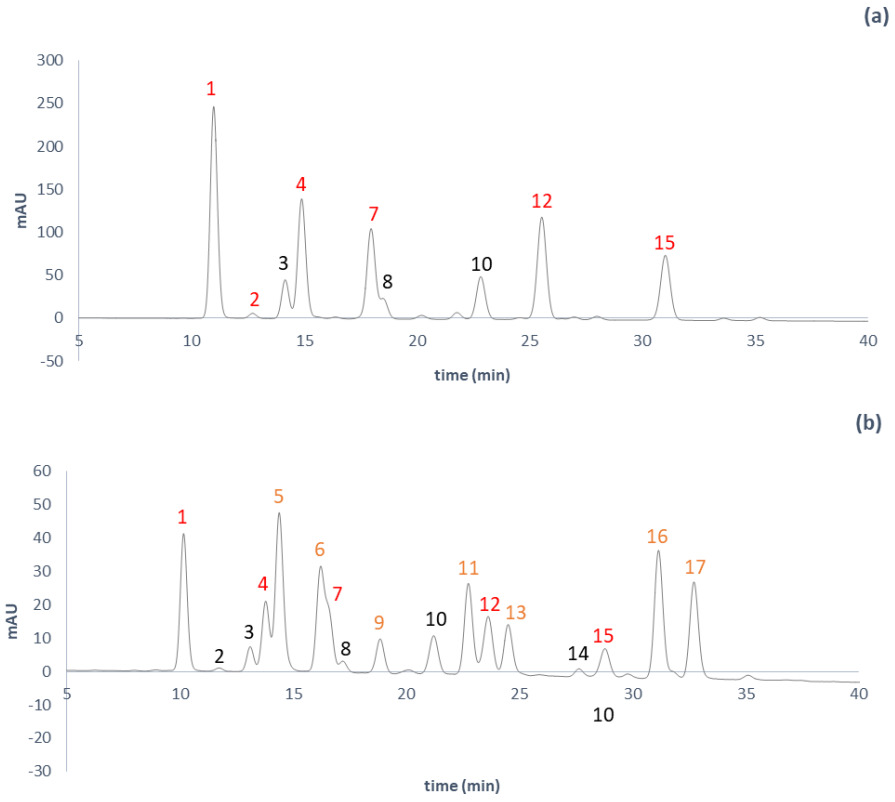

Figure A1. Chromatogram of the (a) initial and (b) final anthocyanin-pyruvic acid adducts reaction solution recorded at 511 nm. (1,4,7,12, 15 = λ_{max} ~520 nm; 5, 6, 9, 11, 13, 16, 17 = λ_{max} ~511 nm)

Portisins hemi-synthesis

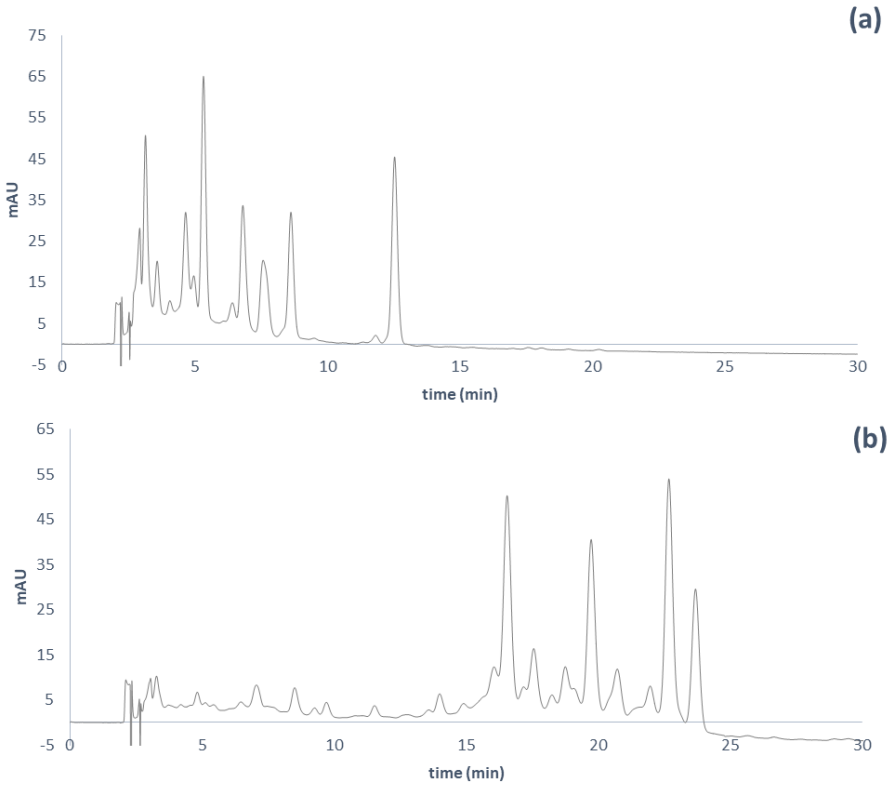

Figure A2. Chromatogram of the (a) initial and (b) final portisin reaction solution recorded at 570 nm. (tr 3-10 min = λ_{max} ~511 nm; tr 15-25 min = λ_{max} ~570 nm)

Portisins identification

Table A1. Identification by mass spectrometry in the positive ion mode of the pigments formed during the portisins hemi-synthesis reaction between blueberries anthocyanin-pyruvic acid adducts and (+)-catechin in the presence of acetaldehyde.

Retention time (min)	λ_{max}	$[M^+]$	MS^2	MS^3	Identity
20.88	568	803	641	489	vinylpyrano-delphinidin-3-galactose(or glucose)-Cat
22.02	571	773	641	489	vinylpyrano-delphinidin-3-arabinose-Cat
22.96	565	781	619	329	Delphinidin-3-galactose(or glucose)-ethyl-Cat
23.01	568	787	619	329	vinylpyrano-cyanidin-3-galactose(or glucose)-Cat
23.34	568	817	655	503	vinylpyrano-petunidin-3-galactose(or glucose)-Cat
23.36	568	787	655	503	vinylpyrano-petunidin-3-arabinose-Cat
24.19	568	781	619	329	Delphinidin-3-galactose(or glucose)-ethyl-Cat
24.30	571	787	619	329	vinylpyrano-cyanidin-3-galactose(or glucose)-Cat
25.60	571	831	669	517	vinylpyrano-malvidin-3-galactose(or glucose)-Cat
26.77	574	801	669	517	vinylpyrano-malvidin-3-arabinose-Cat

Table A2. Identification by mass spectrometry in the positive ion mode of the portisins detected in fraction CC-F2 5 after CPC.

Retention time (min)	λ_{max}	[M+]	MS2	MS3	Identity
20.99	568	803	641	489	vinylpyrano-delphinidin-3-galactose(or glucose)-Cat
22.22	571	773	641	489	vinylpyrano-delphinidin-3-arabinose-Cat
23.01	568	787	619	329	vinylpyrano-cyanidin-3-galactose(or glucose)-Cat
23.36	568	787	655	503	vinylpyrano-petunidin-3-arabinose-Cat
24.19	571	787	619	329	vinylpyrano-cyanidin-3-galactose(or glucose)-Cat
25.62	568	831	669	517	vinylpyrano-malvidin-3-galactose(or glucose)-Cat
26.86	568	801	669	517	vinylpyrano-malvidin-3-arabinose-Cat

Table A3. Summary of CPC experimental process conditions (flow rate and rotation speed) for each CPC step (loading, equilibration, elution, and extrusion) and respective solvent consumption.

	Loading			Equilibration			Elution			Extrusion			
Exp Name	SP Flow rate	Rotation speed	time	MP Flow rate	Rotation speed	time	MP Flow rate	Rotation speed	time	SP Flow rate	Rotation speed	time	Total solvent*
	mL/min	rpm	min	mL/min	Rpm	min	mL/min	rpm	min	mL/min	rpm	min	L
N1	30	600	20	10	1000	10	10	1000	140	30	600	30	3.0
N2	30	600	20	10	1000	10	10	1000	180	30	600	30	3.8
N3	30	600	20	10	1000	10	20	1000	100	30	600	30	4.2
N4	30	600	20	10	1000	10	20	1000	90	30	600	30	3.8
N5	30	600	20	10	1600	10	10	1600	150	30	600	30	3.2
N6	30	600	20	10	1600	10	10	1600	160	30	600	30	3.4
N7	30	600	20	10	1600	10	20	1600	125	30	600	30	5.2
N8.1	30	600	20	10	1600	10	20	1600	71	30	600	30	3.0
N8.2	30	600	20	10	1600	10	20	1600	65	30	600	30	2.8
N9	30	600	20	10	1300	10	15	1300	105	30	600	30	3.4
N10.1	30	600	20	10	1300	10	15	1300	55	30	600	30	1.9
N10.2	30	600	20	10	1300	10	15	1300	50	30	600	30	1.7
N11	30	600	20	10	1300	10	10	1300	150	30	600	30	3.2
N12	30	600	20	10	1300	10	20	1300	90	30	600	30	3.8
N13	30	600	20	10	1000	10	15	1000	120	30	600	30	3.8
N14	30	600	20	10	1600	10	15	1600	120	30	600	30	3.8
N15	30	600	20	10	1300	10	15	1300	145	30	600	30	4.6
N16	30	600	20	10	1300	10	15	1300	120	30	600	30	3.8
N17	30	600	20	10	1300	10	15	1300	145	30	600	30	4.6
OC	30	600	20	10	1600	10	20	1600	60	30	600	45	2.6

SP, stationary phase; MP, mobile phase; OC, optimized conditions.

*Include the solvent required for the loading, equilibration, elution, and extrusion steps. The amount of SP left over was also comprised.

Table A4. Summary of fraction grouping process information: retention time (tr_i and tr_f), elution volume (V_i and V_f), and coefficient partition (K_i and K_f) of each collected fraction (F1-F4).

	F1						F2						
Exp Name	**start-end time**	**tr_i**	**V_i**	**K_i**	**tr_f**	**V_f**	**K_f**	**start-end time**	**tr_i**	**V_i**	**K_i**	**tr_f**	**V_f**	**K_f**
	hh:mm:ss - hh:mm:ss	**min**	**mL**		**min**	**mL**		**hh:mm:ss - hh:mm:ss**	**min**	**mL**		**min**	**mL**	
N1	00:09:02-00:20:19	9.0	90	0.3	20.3	203	1.0	00:20:19-01:59:36	20.3	203	1.0	119.6	1196	7.8
N2	00:09:02-00:29:19	9.0	90	0.2	29.3	293	1.6	00:29:20-02:01:46	29.3	293	1.6	121.8	1218	8.0
N3	00:06:49-00:21:28	6.8	135	0.5	21.5	429	2.7	00:21:28-01:00:53	21.5	429	2.7	60.9	1218	8.5
N4	00:07:13-00:16:14	7.2	144	0.6	16.2	325	2.0	00:16:14-00:44:24	16.2	325	2.0	44.4	888	6.5
N5	00:09:04-00:51:56	9.1	91	0.2	51.4	514	3.3	00:51:56-02:13:08	51.4	514	3.3	133.1	1331	9.4
N6	00:04:32-00:33:52	4.5	45	0.0	33.9	339	2.0	00:33:52-02:10:53	33.9	339	2.0	130.9	1309	8.6
N7	00:01:38-00:13:41	1.6	33	0.0	13.7	274	1.5	00:13:41-00:57:23	13.7	274	1.5	57.4	1148	7.5
N8.1	00:07:37-00:18:10	7.6	152	0.6	18.2	363	2.4	00:18:10-01:00:23	18.2	363	2.4	60.4	1208	9.6
N8.2	00:09:28-00:17:00	9.5	189	0.9	17.0	340	2.1	00:17:00-00:51:39	17.0	340	2.1	51.7	1033	7.7
N9	00:07:49-00:28:55	7.8	117	0.4	28.9	434	2.8	00:28:55-01:15:37	28.9	434	2.8	75.6	1134	8.1
N10.1	00:06:30-00:16:39	6.5	98	0.2	16.7	250	1.4	00:16:39-00:51:33	16.7	250	1.4	51.6	773	5.5
N10.2	00:04:32-00:13:33	4.5	68	0.0	13.6	203	1.0	00:13:33-00:48:27	13.6	203	1.0	48.5	727	4.9
N11	00:09:03-00:31:36	9.1	91	0.3	31.6	316	1.8	00:31:36-01:52:49	31.6	316	1.8	112.8	1128	7.3
N12	00:06:57-00:13:42	7.0	139	0.5	13.7	274	1.6	00:13:42-00:55:22	13.7	274	1.6	55.4	1107	8.3
N13	00:07:57-00:21:30	8.0	119	0.4	21.5	323	2.0	00:21:30-01:11:15	21.5	323	2.0	71.3	1069	7.8
N14	00:07:41-00:19:46	7.7	115	0.3	19.8	297	1.7	00:19:46-01:12:59	19.8	297	1.7	73.0	1095	7.9
N15	00:07:44-00:21:18	7.7	116	0.3	21.3	320	2.0	00:21:18-01:12:32	21.3	320	2.0	72.5	1088	8.5
N16	00:07:35-00:19:38	7.6	114	0.2	19.6	295	1.8	00:19:38-01:28:57	19.8	297	1.9	89.0	1334	11.0
N17	00:07:36-00:22:40	7.6	114	0.2	22.7	340	2.3	00:22:40-01:16:54	22.7	340	2.3	76.9	1154	9.6
OC	00:05:40-00:13:33	5.7	113	0.3	13.6	271	1.6	00:13:33-00:43:57	13.6	271	1.6	44.0	879	6.5

Table A4. Cont. Fraction grouping process information: retention time (tr_i and tr_f), elution volume (V_i and V_f), and coefficient partition (K_i and K_f) of each collected fraction (F1-F4).

	F3							F4						
Exp Name	**start-end time**	**tr_i**	**Vr_i**	**K_i**	**tr_f**	**Vr_f**	**K_f**	**start-end time**	**tr_i**	**Vr_i**	**K_i**	**tr_f**	**Vr_f**	**K_f**
	hh:mm:ss - hh:mm:ss	**min**	**mL**		**min**	**mL**		**hh:mm:ss - hh:mm:ss**	**min**	**mL**		**min**	**mL**	
N1	01:59:36-02:19:44	119.6	1196	7.8	79.7	797	5.1	02:19:44-02:30:38	79.7	797	4.3	150.6	1506	9.9
N2	02:01:46-03:04:48	121.8	1218	8.0	184.8	1848	12.4	03:04:48-03:10:54	184.8	1848	10.7	190.6	1906	12.8
N3	01:00:53-01:40:07	60.9	1218	8.5	100.1	2002	14.4	01:40:07-01:46:14	100.1	2002	11.1	106.2	2125	15.3
N4	00:44:24-01:36:29	44.4	888	6.5	96.5	1930	14.8	01:36:29-01:41:03	96.5	1930	10.4	101.1	2021	15.6
N5	02:13:08-02:34:59	133.1	1331	9.4	155.0	1550	11.0	02:34:59-02:38:34	155.0	1550	10.1	158.6	1586	11.3
N6	02:10:53-02:44:42	130.9	1309	8.6	164.7	1647	11.0	02:44:42-02:51:34	164.7	1647	9.7	171.6	1716	11.5
N7	00:57:23-01:56:10	57.4	1148	7.5	116.2	2323	15.6	01:56:10-02:08:14	116.2	2323	12.4	128.2	2565	17.3
N8.1	01:00:23-01:19:21	60.4	1208	9.6	79.4	1587	12.9	01:19:21-01:22:23	79.4	1587	8.6	142.4	2848	23.6
N8.2	00:51:39-01:11:58	51.7	1033	7.7	72.0	1439	10.9	01:11:58-01:17:17	72.0	1439	7.8	77.3	1546	11.8
N9	01:15:37-01:45:17	75.6	1134	8.1	106.0	1590	11.6	01:45:17-01:56:50	106.0	1590	9.1	116.8	1753	12.9
N10.1	00:51:33-00:59:33	51.6	773	5.5	59.6	893	6.5	00:59:33-01:05:38	59.6	893	4.8	65.6	985	7.2
N10.2	00:48:27-00:53:32	48.5	727	4.9	53.5	803	5.5	00:53:32-01:00:24	53.5	803	4.2	60.4	906	6.2
N11	01:52:49-02:34:13	112.8	1128	7.3	154.2	1542	10.1	02:34:13-02:41:04	154.2	1542	9.0	161.1	1611	10.6
N12	00:55:22-01:35:32	55.4	1107	8.3	95.5	1911	14.8	01:35:32-01:40:52	95.5	1911	10.2	132.3	2646	20.7
N13	01:11:15-02:06:20	71.3	1069	7.8	126.3	1895	14.3	02:06:20-02:12:19	126.3	1895	10.5	132.3	1985	15.1
N14	01:12:59-02:04:45	73.0	1095	7.9	124.5	1868	13.9	02:04:45-02:10:52	124.5	1868	10.3	130.9	1963	14.7
N15	01:12:32-02:24:50	72.5	1088	8.5	124.8	1873	15.1	02:24:50-02:35:35	124.8	1873	10.4	155.6	2334	18.9
N16	01:28:57-02:04:52	89.0	1334	11.0	124.9	1873	15.8	02:04:52-02:10:11	124.9	1873	10.3	130.2	1953	16.5
N17	01:16:54-02:30:10	76.9	1154	9.6	150.2	2253	19.5	02:30:10-02:36:15	150.2	2253	12.6	156.3	2344	20.3
OC	00:43:57-01:00:32	44.0	879	6.5	60.5	1211	9.2	01:00:32-01:12:01	60.5	1211	6.4	72.0	1440	11.1

Experimental design and statistical analysis

Centrifugal Partition Chromatography (CPC) process parameters optimization

A response surface methodology was used to evaluate the influence of process conditions on CPC separation of portisins from a complex natural extract. Several factors are known to affect the total portisin content, as well as process throughput, efficiency, and environmental risk factor. Among all the potential factors, the effect of the sample load (0.2-1.0 g), mobile phase flow rate (10-20 mL/min), and rotation speed (1000-1600 rpm) in total portisin content, process throughput, efficiency and environmental risk factor were studied (Chapter 2 Part I Table 2). The factors included in the central composite face design (CCFD) were chosen based on literature, prior experimental results and under consideration of each effect and the maximum allowable pressure drop of 80 bar.

Portisin content, process throughput, efficiency and environmental risk factor data resulting from the experiments performed according to the experimental conditions defined by the CCFD were analyzed by using the Modde v.12 (Umetrics, Umeå, Sweden) software. The statistical tests, including the adjustments of the design model and factors effects, were significant when the resulting *p*-value was lower than the predefined α=0.05.

In this study, the sample load and mobile phase flow rate had significant effects on two of the four evaluated responses: portisin content, and process throughput. The process efficiency and environmental risk factor were only significantly affected by the sample load. The application of

different rotation speeds (1000-1600 rpm) resulted in no significant improvement in all the evaluated responses.

Contour plots illustrating the effects of different sample loads and mobile phase flow rates are shown in Figure A3. From Figure A3 (a), it is possible to observe that by increasing the sample load, a decrease in the portisins content in the collected fraction was observed. This might be explained because the solute–solute interactions become more prominent than solute-solvent interactions, lowering the peak resolution among the compounds [1]. The same influence was observed for the environmental risk factor (Figure A3 (d)). By increasing the sample load, a decrease in the amount of solvent needed to perform de CPC separation was observed, diminishing the environmental impact of wastes. Also, an increasing sample load resulted in the improvement of the process efficiency and throughput (Figure A3 (b) and (c)). This behavior could be related to the increase of the recovered portisin/processed extract in a shorter duration of the separation process.

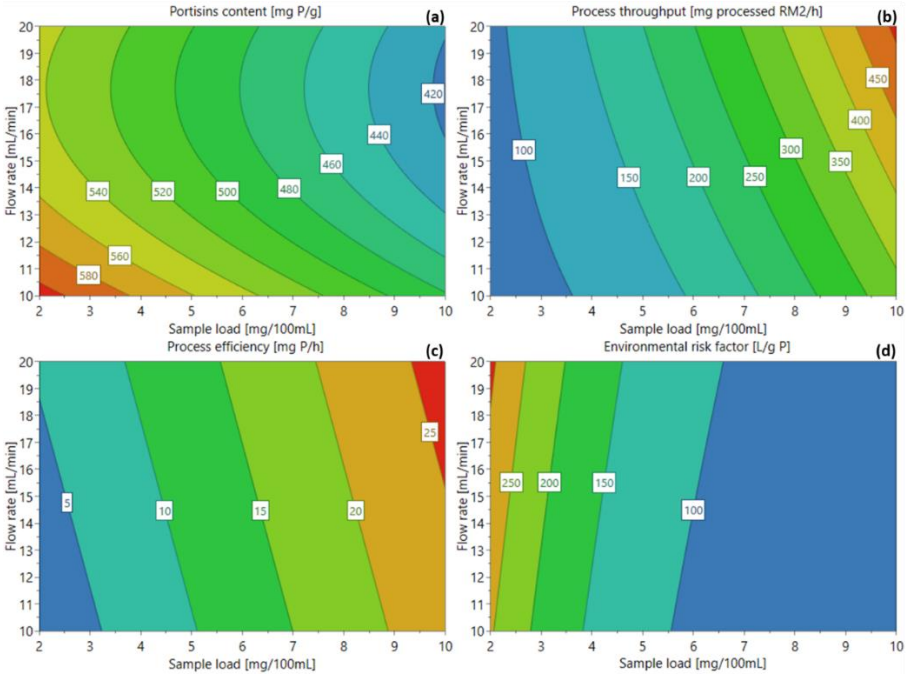

Figure A3. Contour plots of the effects of different sample load and mobile flow rate on (a) portisin content, (b) process throughput, (c) process efficiency, and (d) environmental risk factor.

Another important factor that affected CPC separation was the flow rate of the mobile phase applied. According to the results, the portisin content was significantly decreased with the increase in mobile phase flow rate (Figure A3 (a)). This trend could be explained by the decrease in the retention of the stationary phase with increasing mobile phase flow rates (Chapter 2 Part I Table 2) [2]. The retention of the stationary phase is the amount of the stationary phase maintained in the column during the separation process [3]. Since higher retention of the stationary phase provides a better peak resolution, a lower mobile phase flow rate produces better separation, but a higher separation time is needed. The opposite trend was observed for the process efficiency and throughput. An increasing mobile phase flow

rate resulted in the improvement of the process efficiency and throughput. This could be related to the decrease in the separation time with increasing mobile phase flow rates.

The underlying two factor polynomial models include linear, factor interactions as well as quadratic terms as depicted by Eq. A1. In this equation A, B and C represent the independent variables, i.e., the sample load, mobile phase flow rate and rotation speed.

$$Y = \mathrm{a} + b_1\mathrm{A} + b_2\mathrm{B} + b_3\mathrm{C} + +b_{12}\mathrm{AB} + b_{13}\mathrm{AC} + b_{23}\mathrm{BC} + c_1\mathrm{A}^2 + c_2\mathrm{B}^2 + c_3\mathrm{C}^2 \quad \text{(Eq. A1)}$$

The model coefficients (a, b_x and c_x) were estimated by multivariate linear regression and its significance assessed after performing the corresponding ANOVA (Table A5).

Table A5. Linear and quadratic effects and respective significance levels (p) of the tested variables [factors: sample load (A), mobile phase flow rate (B) and rotation speed (C)] and interactions on portisin content, process throughput, efficiency, and environmental risk factor.

	Portisins content		Process throughput		Process efficiency		Environmental risk factor	
	Coeff. SC	p value	Coeff. SC	p value	Coeff. SC	p value	Coeff. SC	p value
Constant	479		223		15.6		1.97	
A	-52	4.2E-05	146	3.3E-07	8.7	1.1E-06	-0.25	8.4E-08
B	-20	3.2E-02	40	1.5E-02	1.5	1.9E-01	0.03	1.8E-01
C	8	3.8E-01	5	7.3E-01	1.6	1.6E-01	-0.04	1.0E-01
A²			35	1.2E-01			0.07	2.9E-02
B²	18	1.2E-01						
C²			-18	3.6E-01				
AB			27	5.3E-02				
AC					1.5	1.4E-01	-0.05	2.7E-02
BC	17	4.2E-02						

The response surfaces fitted to the portisin content, process throughput, efficiency, and environmental risk factor (Figure A3) can be described using a polynomial models as a function of sample load (A), mobile phase flow rate (B) and rotation speed (C). In these response surface, the non-significant effects (Table A5) were removed from the complete model (Eq. A1) giving origin to the simplified models described in Eq. A2, Eq. A3, Eq. A4, and Eq. A5.

$$Portisin\ content, \frac{mg_{portisin}}{g} = 479 - 52\mathrm{A} - 20\mathrm{B} + 8\mathrm{C} + 17\mathrm{BC} + 18\mathrm{B}^2 \quad \text{(Eq. A2)}$$

$$Process\ throughput, \frac{mg_{processed\ RM2}}{h} = 223 + 146\mathrm{A} + 40\mathrm{B} + 5\mathrm{C} + 27AB + 35\mathrm{A}^2 - 18\mathrm{C}^2 \quad \text{(Eq. A3)}$$

$$Process\ efficiency, \frac{mg_{portisin}}{h} = 15.6 + 8.7\mathrm{A} + 1.5\mathrm{B} + 1.6\mathrm{C} + 1.5\mathrm{AC} \quad \text{(Eq. A4)}$$

$$Environmental\ risk, \frac{L_{solvent}}{h} = 1.97 - 0.25\mathrm{A} + 0.03\mathrm{B} - 0.04\mathrm{C} - 0.05\mathrm{AC} + 0.07\mathrm{A}^2 \quad \text{(Eq. A5)}$$

Table A6. ANOVA analysis for portisin content, process throughput, efficiency, and environmental risk factor using different CPC separation conditions.

Portisins content	**DF**	**SS**	**MS (variance)**	**F**	***p* value**	**SD**
Total	18	4534710	251928			
Constant	1	4455110	4455110			
Total corrected	17	79595	4682			68
Regression	5	65577	13115	11	0.00	115
Residual	12	14018	1168			34
Lack of Fit	9	13216	1468	5	0.09	38
(Model error)						
Pure error	3	802	267			16
(Replicate error)						
	N = 18	Q^2 =	0.651	Cond. no. =	3.0	
	DF = 12	R^2 =	0.824	RSD =	34.2	
	Comp. = 2	R^2 adj. =	0.751			
Process throughput	**DF**	**SS**	**MS (variance)**	**F**	*p* value	**SD**
Total	18	12057900	669881			
Constant	1	7896340	7896340			
Total corrected	17	4161520	244795			495
Regression	5	3856070	771215	30	0.00	878
Residual	12	305449	25454			160
Lack of Fit	9	255568	28396	2	0.36	169
(Model error)						
Pure error	3	49881	16627			129
(Replicate error)						
	N = 18	Q^2 =	0.864	Cond. no. =	4.0	
	DF = 12	R^2 =	0.927	RSD =	159.5	
	Comp. = 2	R^2 adj. =	0.896			
Process efficiency	**DF**	**SS**	**MS (variance)**	**F**	*p* value	**SD**
Total	18	47159	2620			
Constant	1	32343	32343			
Total corrected	17	14816	872			30
Regression	3	13220	4407	39	0.00	66

Residual	14	1597	114			11
Lack of Fit	11	660	60	0	0.98	8
(Model error)						
Pure error	3	937	312			18
(Replicate error)						
	N = 18	Q^2 =	0.816	Cond. no. =	1.2	
	DF = 14	R^2 =	0.892	RSD =	10.7	
	Comp. = 2	R^2 adj. =	0.869			
Environmental risk factor	**DF**	**SS**	**MS (variance)**	**F**	p value	**SD**
Total	18	40302	2239			
Constant	1	24642	24642			
Total corrected	17	15660	921			30
Regression	2	15382	7691	415	0.00	88
Residual	15	278	19			4
Lack of Fit	12	252	21	2	0.25	5
(Model error)						
Pure error	3	26	9			3
(Replicate error)						
	N = 18	Q^2 =	0.977	Cond. no. =	3.2	
	DF = 15	R^2 =	0.982	RSD =	4.3	
	Comp. = 2	R^2 adj. =	0.980			

The values for R^2 of these models suggest a good agreement between the experimental data and the values predicted by the model for the portisin content, process throughput, efficiency, and environmental risk factor. About 82%, 91%, 85%, and 92% of the observed overall variance concerning the portisin content, process throughput, efficiency, and environmental risk factor respectively, are explained by these models (Table A6). The reproducibility of the model to the portisin content, process throughput, efficiency and environmental risk factor was 94%, 76%, 92% and 99% respectively, considering the center points.

APPENDIX B – Compressed fluid-based separation of portisins

Compressed fluid-based separation process

Table B1. Compressed fluid-based separation process conditions applied and respective density of the CO_2 + ethanol binary systems.

Exp Name	Pressure (bar)	Temperature (°C)	Ethanol content (wt. %)	x CO_2	x EtOH	CO_2 + EtOH density (Kg/m^3)
N1	100	40	20	0.81	0.19	796 [5]
N2	500	40	20	0.81	0.19	~956[a] [6]
N3	100	60	20	0.81	0.19	~779[b] [6]
N4	500	60	20	0.81	0.19	~912[c] [6]
N5	100	40	40	0.61	0.39	827 [5] [6]
N6	500	40	40	0.61	0.39	nf
N7	100	60	40	0.61	0.39	nf
N8	500	60	40	0.61	0.39	nf
N9	100	50	30	0.71	0.29	760
N10	500	50	30	0.71	0.29	~922[d] [6]
N11	300	40	30	0.71	0.29	~914[e] [6]
N12	300	60	30	0.71	0.29	~855[f] [6]
N13	300	50	20	0.81	0.19	882 [7] [6]
N14	300	50	40	0.61	0.39	nf
N15	300	50	30	0.71	0.29	873 [7]
N16	300	50	30	0.71	0.29	873 [7]
N17	300	50	30	0.71	0.29	873 [7]

[a]x EtOH=0.203, 45 °C, 450 bar; [b]x EtOH=0.203, 65 °C, 150 bar; [c]x EtOH=0.203, 65 °C, 450 bar; [d]x EtOH=0.271, 55 °C, 450 bar; [e]x EtOH=0.271, 45 °C, 300 bar; [f]x EtOH=0.271, 65 °C, 300 bar; nf – not found

Experimental design and statistical analysis

Compressed fluid separation process parameters optimization

A response surface methodology was used to evaluate the influence of process conditions on compressed fluid separation process of portisins from a complex natural extract. Several factors are known to affect the portisins content, as well as extraction yield and portisins content. Among all the potential factors, the effect of the pressure (100-500 bar), temperature (40-60°C), and ethanol content in the compressed fluid mixture, in extraction

yield, portisins yield, and portisin content were studied (Chapter 2 Part II Table 1). The factors included in the central composite face design (CCFD) were chosen based on literature, prior experimental results, and some instrumental limitations.

Extraction yield, portisin yield and portisin content resulting from the experiments performed according to the experimental conditions defined by the CCFD were analyzed by using the Modde v.12 (Umetrics, Umeå, Sweden) software. The statistical tests, including the adjustments of the design model and factors effects, were considered to be significant when the resulting *p*-value was lower than the predefined α=0.05. It is worth noting that both portisin yield and portisin content presented positive skewness, which indicated the need for a log transformation prior to statistical analysis.

The underlying two factor polynomial models include linear, factor interactions as well as quadratic terms as depicted by Eq. B1. In this equation A, B and C represent the independent variables, i.e. the pressure, temperature, and ethanol content in the compressed fluid mixture.

$$Y = \mathrm{a} + b_1\mathrm{A} + b_2\mathrm{B} + b_3\mathrm{C} + +b_{12}\mathrm{AB} + b_{13}\mathrm{AC} + b_{23}\mathrm{BC} + c_1\mathrm{A}^2 + c_2\mathrm{B}^2 + c_3\mathrm{C}^2 \qquad \text{(Eq. B1)}$$

The model coefficients (a, b_x and c_x) were estimated by multivariate linear regression and its significance assessed after performing the corresponding ANOVA (Table B2).

Table B2. Linear and quadratic effects and respective significance levels (p) of the tested variables [factors: pressure (A), temperature (B), and ethanol content in the compressed fluid mixture (C)] and interactions on extraction yield, portisin yield, portisin content in the extract.

	Extraction yield		Portisin yield		Portisin content	
	Coeff. SC	**p value**	**Coeff. SC**	**p value**	**Coeff. SC**	**p value**
Constant	25.1	1.41E-09	-0.46	2.01E-04	1.41	3.57E-07
A	0.9	4.62E-01	0.08	4.18E-01	0.14	9.88E-02
B	0.3	8.37E-01	-0.08	3.95E-01	-0.04	6.54E-01
C	7.9	8.15E-05	0.63	1.60E-05	0.45	2.22E-04
AB	-3.4	1.41E-02	-0.16	7.05E-02		
AC	6.2	2.78E-04			-0.21	1.47E-02
BC					-0.13	8.55E-02
C²					-0.19	7.62E-02

The response surfaces fitted to the extraction yield, portisin yield, and portisin content (Chapter 2 Part II Figure 2) can be described using a polynomial model as a function of pressure (A), temperature (B) and ethanol content in the compressed fluid mixture (C). In these response surface, the non-significant effects (Table B2) were removed from the complete model (Eq. B1) giving origin to the simplified models described in Eq. B2, Eq. B3, and Eq. B4.

$$Extraction\ yield, wt.\% = 25.1 + 0.9\mathrm{A} + 0.3\mathrm{B} + 7.9C - 3.4AB + 6.2\mathrm{AC} \quad \text{(Eq. B2)}$$

$$Portisin\ yield, wt.\% = -0.46 + 0.08\mathrm{A} - 0.08\mathrm{B} + 0.63\mathrm{C} - 0.16\mathrm{AB} \quad \text{(Eq. B3)}$$

$$Portisin\ content, \frac{mg_{portisin}}{g_{extract}} = 1.41 \mp 0.14\mathrm{A} - 0.04\mathrm{B} + 0.45\mathrm{C} - 0.21\mathrm{AC} - 0.13\mathrm{BC} - 0.19\mathrm{C}^2 \quad \text{(Eq. B4)}$$

Table B3. ANOVA analysis for extraction yield, portisin yield, and portisin content using different compressed fluid separation conditions.

Extraction yield	**DF**	**SS**	**MS (variance)**	**F**	***p* value**	**SD**
Total	16	12119	757			
Constant	1	10050	10050			
Total corrected	15	2069	138			11.74
Regression	5	1839	368	15.96	0.000	19.18
Residual	10	230	23			4.80
Lack of Fit	9	205	23	0.90	0.679	4.78
(Model error)						
Pure error	1	25	25			5.02
(Replicate error)						
	N = 16	Q^2 =	0.627	Cond. no. =	1.1	
	DF = 10	R^2 =	0.889	RSD =	4.8	
	Comp. = 1	R^2 adj. =	0.833			

Portisin yield	**DF**	**SS**	**MS (variance)**	**F**	***p* value**	**SD**
Total	17	12.21	0.72			
Constant	1	3.63	3.63			
Total corrected	16	8.58	0.54			0.73
Regression	4	7.00	1.75	13.33	0.000	1.32
Residual	12	1.57	0.13			0.36
Lack of Fit	10	1.54	0.15	10.01	0.094	0.39
(Model error)						
Pure error	2	0.03	0.01			0.12
(Replicate error)						
	N = 17	Q^2 =	0.625	Cond. no. =	1.1	
	DF = 12	R^2 =	0.816	RSD =	0.4	
	Comp. = 1	R^2 adj. =	0.755			

Portisin content	**DF**	**SS**	**MS (variance)**	**F**	***p* value**	**SD**
Total	17	31.79	1.870			
Constant	1	25.61	25.609			
Total corrected	16	6.18	0.386			0.62
Regression	6	5.17	0.862	8,55132	0.002	0.93
Residual	10	1.01	0.101			0.32
Lack of Fit	8	0.99	0.124	16,414	0.059	0.35
(Model error)						
Pure error	2	0.01	0.007			0.09
(Replicate error)						
	N = 17	Q^2 =	0.512	Cond. no. =	2.8	
	DF = 10	R^2 =	0.837	RSD =	0.3	
	Comp. = 1	R^2 adj. =	0.739			

The values for R^2 of these models suggest a good agreement between the experimental data and the values predicted by the model for the extraction yield, portisin yield and portisin content. About 89%, 82%, and 84% of the observed overall variance concerning the extraction yield, portisin yield and portisin content respectively, are explained by these models (Table B3). The reproducibility of the model to the extraction yield, portisin yield and portisin content was 82%, 97%, and 98% respectively, considering the center points.

APPENDIX C – Intensified astaxanthin extraction from crustacean waste streams

High pressure liquid chromatography (HPLC)

To identify the presence of other carotenoids, an HPLC analysis of the SFE-12 extract was performed. The HPLC carotenoid profile is shown in Figure C1. This result confirms ASX as the major carotenoid in the extract. All-trans-ASX was the principal form of ASX identified (compound 3). Zeaxanthin was also identified (compound 5), in residual amount. Moreover, the compounds 2 and 4 may correspond to esterified forms of ASX. In this way, the interference of other carotenoids in the determination of ASX content by UV-vis spectrometry was not significant.

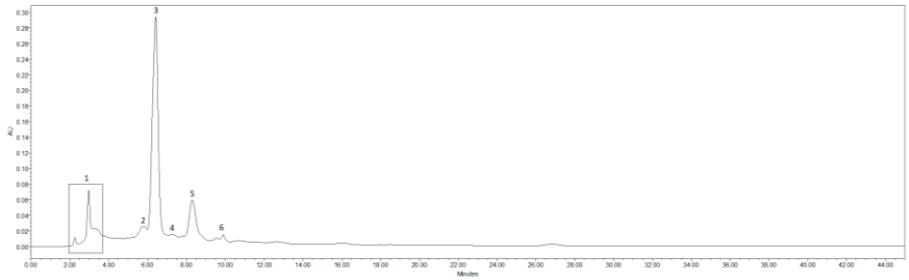

Figure C1. HPLC carotenoids profile at 450 nm of the SFE-12 extract obtained with 30 min of static equilibration time, at 500 bar, 40 °C and 13 wt.% addition of ethanol in the supercritical fluid mixture. [1- solvent signal; 2, 4 and 6- non identified forms of carotenoids; 3- all-trans astaxanthin; 5- zeaxanthin]

Experimental design and statistical analysis

MW pretreatment (MW) process optimization

A response surface methodology was used to evaluate the influence of process conditions on MW pretreatment followed by conventional solvent extraction (CSE) of astaxanthin (ASX) from crab residues. Several factors are

known to affect the ASX extract quantity and quality. Among all the potential factors, the effect of the solvent system water content (0-50 vol.%) and the MW temperature (41-140°C) in ASX yield and ASX content were studied (Chapter 3 Part I Table 1). The factors included in the central composite circumscribed design (CCCD) were chosen based on prior experimental results.

ASX yield and ASX content data resulting from the experiments performed according to the experimental conditions defined by the CCCD were analyzed by using the Modde v.12 (Umetrics, Umeå, Sweden) software. The statistical tests, including the adjustments of the design model and factors effects, were considered to be significant when the resulting *p*-value was lower than the predefined α=0.05.

The underlying two factor polynomial models include linear, factor interactions as well as quadratic terms as depicted by Eq. C1. In this equation A and B represent the independent variables, i.e., the solvent system water content and MW temperature.

$$Y = \mathrm{a} + b_1\mathrm{A} + b_2\mathrm{B} + b_{12}\mathrm{AB} + c_1A^2 + c_2B^2 \qquad \text{(Eq. C1)}$$

The model coefficients (a, b_x and c_x) were estimated by multivariate linear regression and its significance assessed after performing the corresponding ANOVA (Table C1).

Table C1. Linear and quadratic effects and respective significance levels (p) of the tested variables [factors: solvent system water content (A) and MW temperature (B)] and interactions on ASX yield and ASX content.

	ASX yield		ASX content	
	Coeff. SC	**p value**	**Coeff. SC**	**p value**
Constant	2.91	<0.0001	138.8	<0.0001
A	-0.52	0.0001	-54.5	5.3E-06
B	0.11	0.0897	10.6	0.0111
A^2	-0.13	0.0733	13.1	0.0068
B^2			1.3	0.6848

The contour plots fitted to the ASX yield and ASX content (Chapter 3 Part I Figure 1) can be described using a polynomial model as a function of solvent system water content (A) and MW temperature (B). In these response surface, the non-significant effects (Table C1) were removed from the complete model (Eq. C1) giving origin to the simplified models described in Eq. C2 and Eq. C3.

$$ASX\ yield, \mu g/g_{dry\ residue} = 2.91 - 0.52A + 0.11B - 0.13A^2 \quad \text{(Eq. C2)}$$

$$ASX\ content, \mu g/g_{dry\ extract} = 138 - 54.5A + 10.6B + 13.1A^2 + 1.3B^2 \quad \text{(Eq. C3)}$$

Table C2. ANOVA analysis for ASX yield and ASX content obtained from crab residues using different MW pretreatment conditions.

ASX yield	DF	SS	MS (variance)	F	*p*-value	SD
Total	12	98.1	8.18			
Constant	1	95.5	95.48			
Total corrected	11	2.6	0.24			0.49
Regression	5	2.5	0.50	19.4138	0.001	0.70
Residual	6	0.1	0.03			0.16
Lack of Fit	4	0.030	0.007	0.12013	0.962	0.09
(Model error)						
Pure error	2	0.12	0.06			0.25
(Replicate error)						
	N = 12			Cond. no. =	2.23	
	DF = 6	R^2 =	0.942	RSD =	0.16	
		R^2 adj. =	0.893			

ASX yield	DF	SS	MS (variance)	F	*p*-value	SD
Total	12	288962	24080			
Constant	1	262848	262848			
Total corrected	11	26114	2374			48.7
Regression	6	25825	4304	74.5	0.000	65.6
Residual	5	288.8	57.8			7.6
Lack of Fit	3	234.3	78.1	2.9	0.269	8.8
(Model error)						
Pure error	2	54.5	27.2			5.2
(Replicate error)						
	N = 12			Cond. no. =	3.2	
	DF = 5	R^2 =	0.989	RSD =	7.6	
		R^2 adj. =	0.976			

The values for R^2 of these models suggest a good agreement between the experimental data and the values predicted by the model for the ASX yield and ASX content. About 89% and 98% of the observed overall variance concerning the ASX yield and ASX content respectively, are explained by these models (Table C2). However, no optimum conditions were observed in the response surface for the CSE of ASX from the MW pretreated crab residues. Therefore, only the identification of the region of the studied experimental domain corresponding to the best response can be achieved. The reproducibility of the model to the ASX yield and ASX content was 79% and 98% respectively, considering the center points. The results above suggest the use of pure ethanol as solvent system at 140°C.

Supercritical fluid extraction (SFE) process optimization

A response surface methodology was used to evaluate the influence of process conditions on SFE of ASX from crab residues. Several factors are known to affect the ASX extract quantity and quality. Among all the potential factors, the effect of the equilibration time (0-30 min), extraction pressure (200-500 bar), extraction temperature (40-60°C) and ethanol content in supercritical fluid mixture (8-13 wt.%) in ASX yield and ASX content were studied (Chapter 3 Part I Table 2). The factors included in the two-level full factorial design (FFD) were chosen based on prior experimental results as well as on available literature.

ASX yield and ASX content data resulting from the experiments performed according to the experimental conditions defined by the FFD were analyzed by using the Modde v.12 (Umetrics, Umeå, Sweden) software. The statistical tests, including the adjustments of the design model and factors effects,

were considered to be significant when the resulting *p*-value was lower than the predefined α=0.05.

The underlying two factor polynomial models include linear, factor interactions as well as quadratic terms as depicted by Eq. C4. In this equation A, B, C and D represent the independent variables, i.e., the equilibration time, extraction pressure, extraction temperature and ethanol content in supercritical fluid mixture.

$$Y = \mathrm{a} + b_1\mathrm{A} + b_2\mathrm{B} + b_3\mathrm{C} + b_4\mathrm{D} + b_{12}\mathrm{AB} + b_{13}\mathrm{AC} + b_{14}\mathrm{AD} + b_{23}\mathrm{BC} + b_{24}\mathrm{BD} + b_{34}\mathrm{CD} + c_1\mathrm{A}^2 + c_2\mathrm{B}^2 + c_3\mathrm{C}^2 + c_4\mathrm{D}^2 \quad \text{(Eq. C4)}$$

The model coefficients (a, b_x and c_x) were estimated by multivariate linear regression and its significance assessed after performing the corresponding ANOVA (Table C3).

Table C3. Linear and quadratic effects and respective significance levels (p) of the tested variables [factors: equilibration time (A), extraction pressure (B), extraction temperature (C) and ethanol content in supercritical fluid mixture (D)] and interactions on ASX yield and ASX content.

	ASX yield		ASX content	
	Coeff. SC	***p* value**	**Coeff. SC**	***p* value**
Constant	4.95	<0.0001	818	<0.001
B	0.84	0.0026	166	0.0004
C	-0.57	0.0264	-115	0.0063
D	1.00	0.0008	123	0.0050
D^2	-1.85	0.0060	-212	0.0326

The contour plots fitted to the ASX yield and ASX content (Chapter 3 Part I Figure 3) can be described using a polynomial model as a function of extraction pressure (A), extraction temperature (B) and ethanol content in supercritical fluid mixture (C). In these response surface, the non-significant

effects (Table C3) were removed from the complete model (Eq. C4) giving origin to the simplified models described in Eq. C5 and Eq. C6.

$$ASX\ yield, \mu g/g_{dry\ residue} = 4.95 + 0.84A - 0.57B + C - 1.85C^2 \quad \text{(Eq. C5)}$$

$$ASX\ content, \mu g/g_{dry\ extract} = 818 + 166\text{A} - 115\text{B} + 123\text{C} - 212C^2 \quad \text{(Eq. C6)}$$

Table C4. ANOVA analysis for ASX yield and ASX content obtained from crab residues using different SFE conditions.

ASX yield	DF	SS	MS (variance)	F	*p*-value	SD
Total	19	261.5	13.7			
Constant	1	195.1	195.1			
Total corrected	18	66.4	3.7			1.9
Regression	4	53.3	13.3	14.1	0.00	3.6
Residual	14	13.2	0.9			1.0
Lack of Fit	12	13.1	1.1	19.2	0.05	1.0
(Model error)						
Pure error	2	0.11	0.06			0.2
(Replicate error)						
	N = 19			Cond. no. =	5.08	
	DF = 14	R^2 =	0.802	RSD =	0.97	
	Comp. = 2	R^2 adj. =	0.745			

ASX content	DF	SS	MS (variance)	F	*p*-value	SD
Total	19	8.8E6	462863			
Constant	1	7.2E6	7.2E6			
Total corrected	18	1.6E6	86533			294
Regression	4	1.2E6	308792	13.4	0.000	556
Residual	14	322432	23031			152
Lack of Fit	12	315848	26321	8.0	0.116	162
(Model error)						
Pure error	2	6584	3292			57
(Replicate error)						
	N = 19			Cond. no. =	5.08	
	DF = 14	R^2 =	0.793	RSD =	152	
	Comp. = 2	R^2 adj. =	0.734			

The values for R^2 of these models suggest a good agreement between the experimental data and the values predicted by the model for the ASX yield and ASX content. About 74% and 73% of the observed overall variance concerning the ASX yield and ASX content respectively, are explained by these models (Table C4). However, no optimum conditions were observed in the response surface for the SFE extraction of ASX from crab residues. Therefore, only the identification of the region of the studied experimental domain corresponding to the best response can be achieved. The reproducibility of the model to the ASX yield and ASX content was 98% and 96% respectively, considering the center points. These results above suggest the use of relatively low temperature (40°C), high pressure (500 bar), addition of ethanol in the supercritical fluid mixture (13 wt.%) without static equilibration time.

Comparison of different extraction strategies with Soxhlet extraction (SOX)

Table C5. ANOVA one-way with replication for the average ASX yield.

Source of variation	SS	DF	MS	F	*p*-value	F crit
Between	3.454	5	0.691	9.091	0.001	3.106
Within	0.912	12	0.076			
Total	4.366					

	Difference
|CSE - SOX|=	0.31
|MW+CSE - SOX|=	0.45*
|SFE - SOX|=	0.27
|MW+SFE - SOX|=	0.79*

Post-hoc comparisons against the control (SOX) have been performed and the following differences were found to be larger than the critical Difference (D=0.43), that is statistically significant (at a α=0.05 level):

|MW+CSE - SOX| = 0.45

|MW+SFE - SOX| = 0.79

Table C6. ANOVA one-way with replication for the average ASX content.

Source of variation	SS	DF	MS	F	*p*-value	F crit
Between	121780	5	24356	64.405	0.000	3.106
Within	4538	12	378			
Total	126318					

	Difference
|CSE - SOX|=	23
|MW+CSE - SOX|=	23
|SFE - SOX|=	181*
|MW+SFE - SOX|=	100*

Post-hoc comparisons against the control (SOX) have been performed and the following differences were larger than the critical Difference (D=30.3):

|SFE-SOX| = 181

|MW+SFE - SOX| = 100

Influence of MW pretreatment and extraction methodology

Table C7. ANOVA two-way with replication for the average ASX yield.

Source of variation	SS	DF	MS	F	*p*-value	F crit
Extraction methodology	0.00969	1	0.00969	0.169	0.702	7.709
MW	1.58224	1	1.58224	27.56	0.006	7.709
Interaction	0.00969	1	0.00969	0.169	0.702	7.709
Within	0.229636	4	0.057409			
Total	1.831255					

A significant difference (*p*=0.006) is noted for the average ASX yield due to MW pretreatment (larger ASX yields when using the MW pretreatment). No significant difference (*p*=0.702) is noted regarding the average ASX yield when using both extraction methodologies (CSE or SFE). The potential variable interaction is not significant (*p*=0.702).

Table C8. ANOVA two-way with replication for the average ASX content.

Source of variation	SS	DF	MS	F	*p*-value	F crit
Extraction methodology	78834	1	78834	380.5	<0.001	7.709
MW	1975	1	1975	9.5	0.037	7.709
Interaction	11574	1	11574	55.9	0.002	7.709
Within	829	4	207			
Total	93211	7				

A significant difference (p<0.001) is noted for the average ASX content due to the extraction methodology (larger for SFE), as well as for the MW pretreatment (p=0.037, larger ASX content when using the MW pretreatment). A significant variable interaction (p=0.002) is noted regarding the average content when using CSE or SFE with or without MW. This means that, based on the observed data, the effect of the MW or extraction methodology was not additive. As can be seen the average content when using MW pretreatment was larger for the CSE but lower in the case of SFE.

APPENDIX D – Encapsulation of carotenoids from microalgae biomass

High pressure liquid chromatography (HPLC)

To identify the presence of *Dunaliella salina* carotenoids, an HPLC analysis of the particles was performed. The typical HPLC carotenoid profile is shown in Figure D1. This result confirms β-carotene as the major carotenoid in the particles. 9-cis-β-carotene was the principal form of carotene identified (compound 5). Lutein, zeaxanthin, α-carotene, and all-trans beta carotene were also identified (compound 1, 2, 3 and 4, respectively), in residual amount.

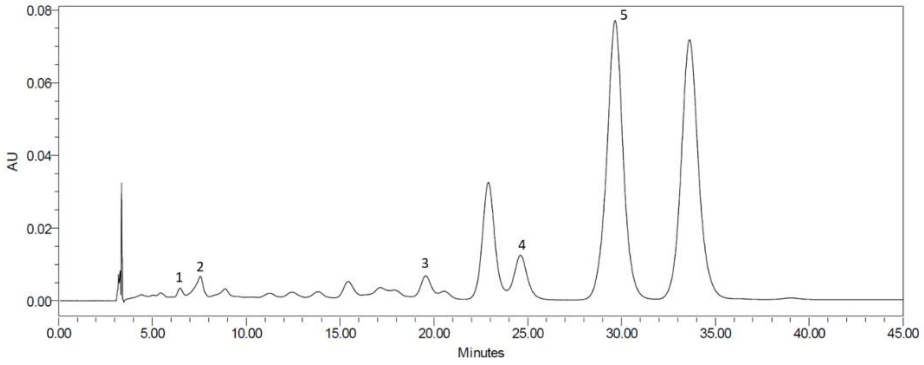

Figure D1. HPLC carotenoids profile at 450 nm of the particle produced with an emulsion oil concentration of 37 %, 13500 rpm of emulsification stirring seed and at 165°C of spray drying inlet air temperature. (1) lutein; (2) zeaxanthin; (3) α-carotene; (4) all-trans beta carotene and (5) 9-cis-β-carotene

Experimental design and statistical analysis

A response surface methodology was used to evaluate the influence of process conditions on the encapsulation of ultra-high supercritical carbon dioxide ($scCO_2$) extract from *Dunaliella salina* integrating the o/w

emulsification and spray drying. Several factors are known to affect some attributes of the intermediate products (fresh emulsion and dried particles) as well as some process related aspects. These factors are illustrated in Figure D2.

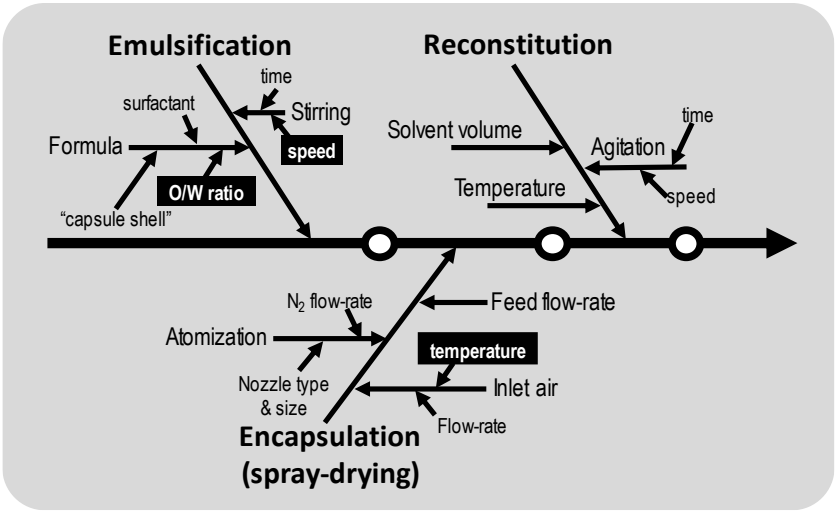

Figure D2. Ishikawa diagram displaying the variables impacting the reconstituted microcapsules dispersion attributes. The black shaded variables were included in the multifactorial optimization.

Among all the potential factors, the effect of the emulsion oil concentration with respect to total solids (3-37 wt.%), the emulsification stirring speed (6500-21500 rpm) and the spray drying inlet air temperature (110-220°C) in several attributes of the fresh emulsion, the particles and the reconstituted emulsion were studied (Chapter 3 Part II Table 1).

The encapsulation yield and efficiency data resulting from the experiments performed according to the experimental conditions defined by the CCD were analyzed by using the Modde v.12 (Umetrics, Umeå, Sweden)

software. The statistical tests, including the adjustments of the design model and factors effects, were considered to be significant when the resulting *p*-value was lower than the predefined α=0.05.

The underlying three factor polynomial models include linear, two-factor interactions as well as quadratic terms as depicted by Eq. D1. In this equation A, B and C represent the independent variables, i.e., the emulsion oil concentration with respect to total solids, the emulsification stirring speed and the spray drying inlet air temperature.

$$Y = \mathrm{a} + b_1\mathrm{A} + b_2\mathrm{B} + b_3\mathrm{C} + b_{12}\mathrm{AB} + b_{13}\mathrm{AC} + b_{23}\mathrm{BC} + c_1A^2 + c_2B^2 + c_3C^2 \qquad \text{(Eq. D1)}$$

The model coefficients (a, b_x and c_x) were estimated by multivariate linear regression and its significance assessed after performing the corresponding ANOVA (Table D1).

Table D1. Linear and interaction effects and respective significance levels (p) of the tested variables [factors: emulsion oil concentration with respect to total solids (A), emulsification stirring speed (B) and spray drying inlet air temperature (C)] and interactions on encapsulation yield and efficiency.

	Encapsulation yield		**Encapsulation efficiency**	
	Coeff. SC	p **value**	**Coeff. SC**	p **value**
Constant	42.4		41.4	
A	-12.7	1.76E-07	25.9	2.2E-08
B	2.7	0.052	-2.8	0.185
C	2.7	0.052	-2.5	0.239
AB			10.9	0.001

The contour plots fitted to the encapsulation yield and efficiency (Chapter 3 Part II Figure 1) can be described using a polynomial model as a function of emulsion oil concentration with respect to total solids (A), emulsification stirring speed (B) and spray drying inlet air temperature (C). In these response surface, the non-significant effects (Table D1) were removed from the complete model (Eq. D1) giving origin to the simplified models described in Eq. D2 and Eq. D3.

$$Encapsulation\ yield, wt.\% = 42.4 - 12.7\mathrm{A} + 2.7\mathrm{B} + 2.7\mathrm{C} \quad \text{(Eq. D2)}$$

$$Encapsulation\ efficiency, wt.\% = 41.4 + 25.9\mathrm{A} - 2.8\mathrm{B} - 2.5\mathrm{C} + 10.9AB \quad \text{(Eq. D3)}$$

Table D2. ANOVA analysis for encapsulation yield and efficiency obtained using different spray drying emulsion conditions.

Encapsulation yield	DF	SS	MS (variance)	F	*p*-value	SD
Total	17	33119.0	1948.2			
Constant	1	30409.5	30409.5			
Total corrected	16	2709.5	169.3			13.0
Regression	3	2421.9	807.3	36.5	0.000	28.4
Residual	13	287.7	22.1			4.7
Lack of Fit	11	287.0	26,1	78.3	0.013	5.1
(Model error)						
Pure error	2	0.7	0.3			0.6
(Replicate error)						
	N = 17	Q^2 =	0.798	Cond. no. =	1.1	
	DF = 13	R^2 =	0.894	RSD =	4.7	
		R^2 adj. =	0.869			

Encapsulation efficiency	DF	SS	MS (variance)	F	*p*-value	SD
Total	17	40179,4	2363.5			
Constant	1	29186,2	29186.2			
Total corrected	16	10993,2	687.1			26.2
Regression	4	10328,1	2582.0	46.6	0.000	50.8
Residual	12	665,094	55.4			7.4
Lack of Fit	10	569,978	57.0	1.2	0.538	7.5
(Model error)						
Pure error	2	95,1152	47.5			6.9
(Replicate error)						
	N = 17	Q^2 =	0.869	Cond. no. =	1.5	
	DF = 12	R^2 =	0.939	RSD =	7.4	
		R^2 adj. =	0.919			

The values for R^2 of these models suggest a good agreement between the experimental data and the values predicted by the model for the encapsulation yield and efficiency. About 87% and 92% of the observed overall variance concerning the encapsulation yield and efficiency respectively, are explained by these models (Table D2). The reproducibility of the model to the encapsulation yield and efficiency was 93% and 99% respectively, considering the center points.

Table D3. Summary of particle CIELab parameters.

Exp.	L*	a*	b*	C*	h*
N1	67.03 ± 0.04	15.75 ± 0.01	56.55 ± 0.04	58.70 ± 0.04	1.299 ± 0.001
N2	68.50 ± 0.02	12.93 ± 0.03	58.89 ± 0.04	60.29 ± 0.04	1.355 ± 0.001
N3	55.29 ± 0.12	18.23 ± 0.04	40.44 ± 0.16	44.36 ± 0.16	1.147 ± 0.001
N4	55.58 ± 0.10	18.39 ± 0.03	41.91 ± 0.15	45.77 ± 0.13	1.157 ± 0.002
N5	67.76 ± 0.01	12.97 ± 0.02	55.66 ± 0.04	57.15 ± 0.03	1.342 ± 0.001
N6	67.69 ± 0.04	13.53 ± 0.04	59.18 ± 0.06	60.70 ± 0.06	1.346 ± 0.001
N7	52.35 ± 0.06	17.93 ± 0.01	35.39 ± 0.09	39.68 ±0.08	1.102 ± 0.001
N8	53.52 ± 0.11	17.66 ± 0.06	38.07 ± 0.26	41.97 ±0.26	1.137 ± 0.002
N9	59.01 ± 0.07	17.60 ± 0.03	46.60 ± 0.01	49.81 ± 0.01	1.210 ± 0.001
N10	62.25 ± 0.07	16.53 ± 0.06	51.56 ± 0.14	54.14 ± 0.12	1.261 ± 0.002
N11	78.36 ± 0.10	4.97 ± 0.09	54.56 ± 0.06	54.78 ± 0.05	1.480 ± 0.002
N12	53.38 ± 0.05	17.97 ± 0.04	37.87 ± 0.07	41.92 ± 0.07	1.128 ± 0.001
N13	65.94 ± 0.04	13.68 ± 0.07	48.93 ± 0.03	50.81 ± 0.04	1.298 ± 0.001
N14	61.08 ± 0.04	16.80 ± 0.02	50.82 ± 0.06	53.53 ± 0.05	1.251 ± 0.001
N15	62.12 ± 0.12	16.30 ± 0.07	51.73 ± 0.20	54.24 ± 0.21	1.266 ± 0.001
N16	61.04 ± 0.06	15.96 ± 0.06	50.33 ± 0.07	52.80 ± 0.05	1.264 ± 0.001
N17	62.70 ± 0.03	16.14 ± 0.04	52.69 ±0.09	55.10 ± 0.10	1.274 ± 0.001

REFERENCES

[1] J.B. Friesen, G.F. Pauli, GUESSmix-guided optimization of elution-extrusion counter-current separations, J. Chromatogr. A. 1216 (2009) 4225–4231. https://doi.org/10.1016/j.chroma.2008.12.053.

[2] N. Fumat, A. Berthod, K. Faure, Effect of operating parameters on a centrifugal partition chromatography separation, J. Chromatogr. A. 1474 (2016) 47–58. https://doi.org/10.1016/j.chroma.2016.10.014.

[3] Y. Ito, Golden rules and pitfalls in selecting optimum conditions for high-speed counter-current chromatography, J. Chromatogr. A. 1065 (2005) 145–168. https://doi.org/10.1016/j.chroma.2004.12.044.

[4] A.N. Nunes, V. Ivasiv, F. Gouveia, J. Oliveira, M. Ros, A.A. Matias, J. Oliveira, M. Ros, Isolation of Bluish Anthocyanin-derived Pigments obtained from Blueberry Surplus using Centrifugal Partition Chromatography, J. Chromatogr. A. (2023). https://doi.org/10.1016/j.chroma.2023.464150.

[5] M. Kato, D. Kodama, T. Ono, M. Kokubo, Volumetric Properties of Carbon Dioxide + Ethanol at 313.15 K, J. Chem. Eng. Data. 54 (2009) 2953–2956.

[6] T. Zhu, H. Gong, M. Dong, Density and Viscosity of CO 2 + Ethanol Binary Systems Measured by a Capillary Viscometer from 308 . 15 to 338 . 15 K and 15 to 45 MPa, J. Chem. Eng. Data. 65 (2020) 3820–3833. https://doi.org/10.1021/acs.jced.0c00175.

[7] H. Pohler, E. Kiran, Volumetric Properties of Carbon Dioxide + Ethanol at High, J. Chem. Eng. Data. 42 (1997) 384–388.

ITQB NOVA, Avenida da República, 2780-157 Oeiras, Portugal | Tel +351 214 469 100 | itqb.unl.pt